SYNTHESIS AND STRUCTURE OF SOME COORDINATION POLYMERS OF SILVER(I), CERIUM(IV) AND MANGANESE(III)

A Thesis

Submitted for the Degree of

DOCTOR OF PHILOSOPHY

by

Sunkari Sailaja

School of Chemistry

University of Hyderabad

Hyderabad 500 046

INDIA

SEPTEMBER 2002

To

My Parents

CONTENTS

CHAPTER II   Coordination Polymers of Silver(I) with Aminomethyl-pyridines

CHAPTER III   Coordination Polymers of Cerium(IV) with Pyridine-2,6-dicarboxylic Acid

CHAPTER IV   Schiff Base Complexes of Manganese(III) And Iron(III).

Syntheses, Structure, Polymorphism, Spectral and Magnetic Studies of

$[Mn(Salpn)NCS]_2$, $[Mn(Salpn)NCS]_n$ and $Fe(Salpn)(CH_3OH)NCS$

CHAPTER V   Complexes of Silver(I) with Protonated Aminomethyl-pyridines

STATEMENT

I hereby declare that the matter embodied in this thesis is the result of investigations carried out by me in the School of Chemistry, University of Hyderabad, India under the supervision of Prof. M. V. Rajasekharan.

In keeping with the general practice of reporting scientific observations due acknowledgements have been made wherever the work described is based on the findings of other investigators.

S. Sailaja

Hyderabad

September 2002

CERTIFICATE

Certified that the work embodied in this thesis entitled *'SYNTHESIS AND STRUCTURE OF SOME COORDINATION POLYMERS OF SILVER(I), CERIUM(IV) AND MANGANESE(III)"* has been carried out by **Ms.** S. **Sailaja** under my supervision and the same has not been submitted elsewhere for any degree.

Hyderabad

M. V. RAJASEKHARAN

September 2002

(Thesis Supervisor)

DEAN

SCHOOL OF CHEMISTRY

ACKNOWLEDGEMENTS

I express my sincere thanks and gratitude to my guide Prof M. V. Rajasekharan, for his inspiring and tireless guidance. I have been fortunate enough to work with him and learnt a lot. His help and concern, both in academic and personal spheres are invaluable for me.

I thank the present and past Dean(s) of the School of Chemistry for extending all the facilities of the Department. My thanks are due to all the faculty members of the School, who are one of the best teachers I've come across.

I thank all the technical and non-teaching staff of the School of Chemistry and CIL for their help and cooperation. My special thanks to Mr. Raghavaiah for his help during X-ray data collection.

The magnetic studies on Mn(salpn)NCS were done in collaboration with the group of Prof. J.J. Girerd, Laboratories de Chimie Inorganique, Universite Paris-Sud, France.

I thank CSIR, New Delhi, for fellowship.

I thank my labmates Dr. Ramalakshmi, Ayub, Kishore Babu and Prasad for their help and cooperation.

I am thankful to my teacher, Dr. Sreeramarnoorthy, for his interesting lectures, which inspired me to choose the track of *Chemistry*. I acknowledge the help and invaluable guidance I have been receiving from him till now. Thanks to my college teachers Ms. Padmavathy, who assisted me financially to join my Ph. D. course and Dr. Saroja, for her guidance at various occasions.

My association with my friends Ramalakshmi, Sindhu, Aneetha, Vijju, Mangai, Madhavi, Satyen, Subbu, Sankaran, Praveen, Venu, Aparna, Sampath,

ABBREVIATIONS AND DEFINITIONS

acac	acetylacetonate
amp	aminomethylpyridine
dmp	2,9-dimethyl-1,10-phenanthroline
dmbp	6,6'-dimethyl-2,2'-bipyridine
d	Hydrogen to acceptor distance in A
D	Donor to acceptor distance in A
dbpe	bis(di-*ter*-butylphosphinoethane)
dipicH2	pyridine-2,6-dicarboxylic acid
hfac	hexafluoroacetylacetonate
NIT-R	alkyl substituted nitronyl oxide
Pc^{2-}	dianion of Phthalocyanine
pmaH	C-pyridylmethanaminium
pyz	pyrazine
SB	Schiff base
salen	N, N'-bis(salicylidene)-1,2-diaminoethane
salpn	N, N'-bis(salicylidene)-1,3-diaminopropane
TCB	1,3,5-tricyanobenzene
TTF	tetrathiafulvalene
TTM - TTP	2,5-bis-(4',5'-bis(methylthio)-1',3'-dithiol-2'-ylidene)-1,3,4,6-tetrathiapentalene

vi

$$R1 = \Sigma ||F_o| - |F_c|| \: / \: \Sigma |F_o|.$$

$$wR2 = [\Sigma w(F_o^2 - F_c^2)^2 / \: \Sigma(wF_o^4)]^{1/2}$$

$$w^{-1} = [\sigma^2(F_o)^2 + (AP)^2 + BP], \: P = [2F_c^2 + \text{Max}\,(F_o^2, 0)]/3$$

$$S = [\Sigma\{w(F_o^2 - F_c^2)^2\}/(n\text{-}p)]^{1/2}$$

$$U_{eq} = 1/3(U_{11}a^2a^{*2} + U_{22}b^2b^{*2} + U_{33}c^2c^{*2} + U_{23}b^*c^*bc\cos\alpha + U_{12}a^*b^*ab\cos\gamma + U_{13}a^*c^*ac\cos\beta)$$

PREFACE

The study of coordination polymers has gained momentum with the understanding of several non-covalent interactions leading to their clever manipulation. With the recognition of coordinate bond as a non-covalent bond, along with hydrogen bond, stacking interactions etc., this field is emerging rapidly. Though the number of factors to be controlled are higher when compared to organic systems, still the interest in the field arises from the large number of elements available in the periodic table along with their varying oxidation states and coordination geometries to play with, to generate novel and interesting solid state structures with desirable properties.

The thesis primarily discusses the synthesis and structure of the coordination polymers of (a) Ag^+ with the simple ligand (aminomethyl)pyridine and different anions, (b) mixed metal polymers of the rare earth Ce^{4+} and alkaline earth Sr^{2+} and Ba^{24} with the bridging ligand pyridine-2,6-dicarboxylic acid and (c) Schiff base complexes of Mn^{3+} and Fe^{3+}. Along with the polymers, the final chapter discusses the structural details of the Ag^+ complexes formed with protonated ligands, which are generally rarely observed.

As the thesis is focussed on coordination polymers, the first chapter gives a brief review of coordination polymers starting from their genesis, the forces that

hold them, the synthetic strategies involved, along with their expected applications which are the driving forces for their study.

The second chapter deals with the several coordination polymers formed between Ag^+ and the three isomers of (aminomethyl)pyridine. This chapter illustrates the role of ligand flexibility and counterion on the generation of interesting chains, networks and solid state packing patterns. Simple variation of the ligand from 2-amp to 3-amp, keeping the anion ($ClO_4"$) constant, led to the interesting synthetic triple helical infinite chain, the first one to be reported. Varying the ligand to 4-amp and keeping the same anion, led to chains which are assembled into a 3-connected 2-D network through Ag--Ag interactions. The structural variations observed when the anion is changed to $BF4"$ and PF_6^- are discussed in detail and compared.

The third chapter deals with mixed metal coordination polymers formed by Ce^{4+} and Sr^{2+}/Ba^{2+} ions with pyridine-2,6-dicarboxylic acid. The polymers include linear chain structures as well as layered structures. Different structures are seen with a small variation in the conditions of preparation.

The fourth chapter deals with the synthesis, structure and magnetic properties of the Schiff base complexes of Mn(III) and Fe(III). Mn(salpn)NCS shows an interesting polymorphism. The chain form is ferromagnetic, while the dimeric form has virtually no magnetic interactions. An interesting observation regarding the dimer is that, it forms chains of dimers held by weak $S \cdots \pi(phenyl)$ interactions which have not been seriously looked at before.

The fifth and the final chapter discusses the structural aspects of Ag^+ complexes formed with the protonated (aminomethyl)pyridines, which are rare examples of complexes with cationic ligands. An interesting observation in these systems is that, in spite of the existence of several hydrogen bonds, the anions are highly disordered.

The observation of several novel structures in apparently simple systems shows the great potential of the "mix and watch" approach in the field of coordination chains and networks. There is also scope for "design", for example, (i) addition of hydrophobic groups to amp, so as to make the complexes water insoluble which may then act as anion exchangers, (ii) replacement of Ce and Ca/Sr/Ba in the mixed metal-dipic/dipicH2 system by Gd^+ and a paramagnetic transition metal ion so as to obtain ferrimagnetic ordering....

Part of the work reported in this thesis has been published or communicated in a preliminary form.

1. One Dimensional Coordination Polymers of Silver(I) with Aminomethylpyridines. Example of a Triple Helical Infinite Chain. **S. Sailaja** and M. V. Rajasekharan. *Inorg. Chem.* **2000,** *39,* 4586.

2. Complexes of Ag(l) with Cationic Ligands: bis[(pyridylmethyl)ammonio]Silver(I) Salts. S. **Sailaja,** G. Swarnabala and M. V. Rajasekharan. *ActaCryst.* **2001,** *C57*, 1162.

3. A One-Dimensional Coordination Polymer with Alternating CeN_3O_6 and $SrNO_7$. S. **Sailaja** and M. V. Rajasekharan. *Ada Cryst.* **2001,** *E57,* **m341.**

4. Synthesis, Structure and Magnetic Properties of $[Mn^{III}(salpn)NCS]_n$, a Helical Polymer and the Dimer $[Mn^{III}(salpn)NCS]_2$. Weak Ferromagnetism in $[Mn^{III}(salpn)NCS]_n$ Related to the Strong Magnetic Magnetic Anisotropy in Jahn-Teller Mn(III) (salpnH2 = N,N'- bis(Salicylidene)-l,3-diaminopropane). **S. Sailaja,** K. Rajender Reddy, M. V. Rajasekharan, C. Hureau, E. Riviere, J. Cano, and J.-J. Girerd. (submitted to *Inorg. Chem.*).

5. Polymeric Coordination Compounds, **S. Sailaja** and M. V. Rajasekharan, *Proc. Symposium on Modern Trends in Inorganic Chemistry, Bangalore* (2000), P52.

CHAPTER I

Coordination Polymers - A Brief Review

1.1. Introduction

Classically, polymers were recognized as compounds with several repeat units connected to each other extending over a long range. Several polymers, both organic and inorganic in nature, were known since more than a century. The prominent examples include starch, cellulose, rubber, silica and minerals. The structures of naturally occurring silica, silicates and other minerals may all be considered as polymeric in nature in a broad sense, as they extend in all the three dimensions by the connectivity of the repeat units. Mimicking natural systems, the first polymers synthesized were primarily organic in nature, where the carbon atom formed the backbone of the chain. These organic polymers were built by a handful of elements like C, H, N, 0, S and halogens. The classical covalent bond functioned as the connecting link between the repeat units in all these polymeric systems. These organic polymers, typically polyethylene (PE) and polyvinylchloride (PVC) brought such a revolutionary change in the human life that they were recognized as new generation materials of the 20th century. The first organic polymers synthesized were polyvinyls first made in 1838, followed by polystyrene. Closely parallel to the research in organic polymer chemistry, the field of coordination chemistry developed with the pioneering work of the Swiss chemist Alfred Werner during 1866 - 1919. It was later realized that the coordination complexes can also be

connected to each other through bridging ligands. The metal - ligand bond was initially termed semi-polar bond by Lowry and later as coordinate covalent bond by Sidgwick.[1] Structures formed by the coordinative linking of the bridging ligands to the metal centers were termed as "coordination polymers" by Bailar.[2] In such cases, the coordinate bond acting as the connecting thread between the monomeric complex repeat units, was treated similar to the covalent bond. Hence, any structural entities with metal elements forming the polymeric backbone were traditionally treated as coordination polymers.[3-4] With research progressing rapidly, besides the coordinate bond, other forces like hydrogen bond, stacking interactions, atom - atom interactions and atom - π interactions, which are weak compared to the covalent bond, were also found to be capable of assembling the repeat units, thus giving rise to polymeric structures.[5] Being very weak in nature (usually < 40 kcal/mol), these forces were called non-covalent forces. As the energy of coordinate bond is nearly same as these weak forces and also it differs from the covalent bond in terms of electron pair contribution to the bond, the coordinate bond was later recognized as a non-covalent force along with others. Therefore, in modern terms the coordination polymers may be defined as *structural entities formed by a large number of repeat units made of coordination complexes connected intermolecularly through the operation of non-covalent forces.* The traditional polymers connected by covalent bond and the modern coordination polymers connected by non-covalent bonds are shown in Figure 1.1. The repeat units of these coordination polymers may be made of a single metal atom or often two (or more) metal atoms. The two metal atoms may be same or different giving rise to either homobimetallic or heterobimetallic coordination polymers. When the polymeric chain made of homo- or heterometallic repeat units extends in space in one dimension, one-dimensional (1-D) coordination polymers result, while extension of

while extension of repeat units in two or three dimensions gives rise to two or three dimensional (2- or 3-D) networks. Scheme 1.1 differentiates between covalent and coordination polymers.
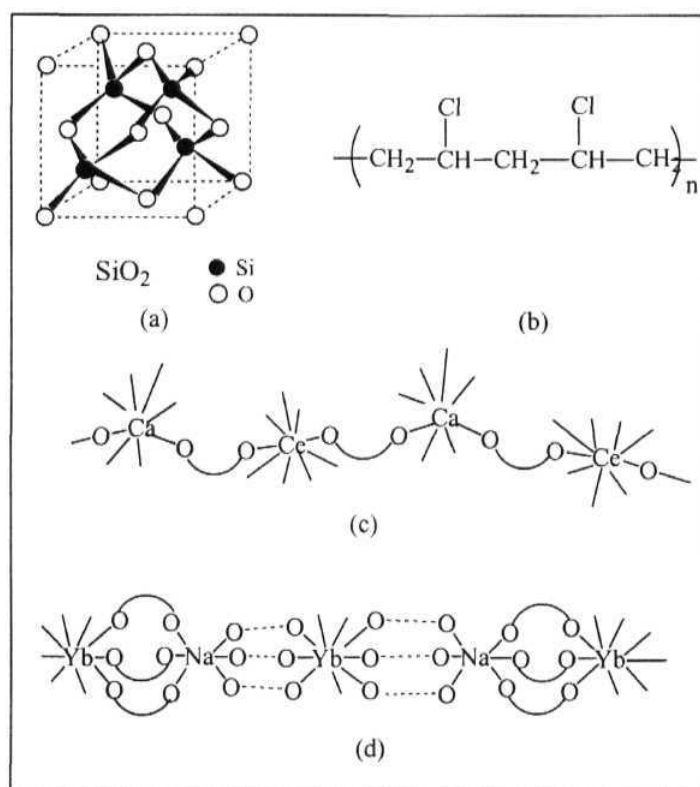
Figure 1.1 Schematic representation of covalently connected (a) silica and (b) polyvinyl chloride; (c) coordinatively connected coordination polymer in $Ce(dipic)_3Ca(dipicH_2)(OH_2)_3 \cdot 5H_2O$[6] and (d) alternating coordinate and hydrogen bonded polymer in $Na_3[Yb(dipic)_3] \cdot NaClO_4 \cdot 10H_2O$.[7]
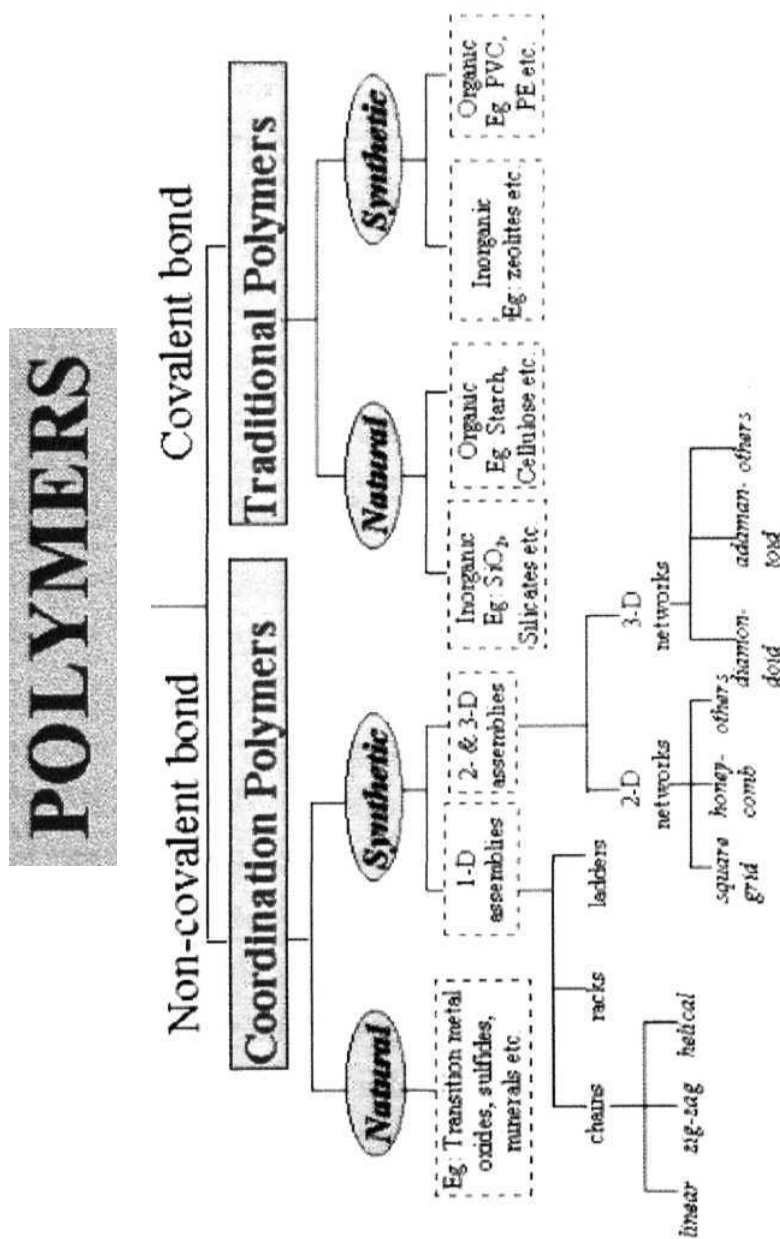
Scheme 1.1 Various kinds of polymers based on the type of bond present.

1.2. Definition of the non covalent forces

In decreasing order of energy, the weak forces are described as follows.[8,10]

(a) Coordinate Bond: This is the basic linkage involved in the formation of all coordination complexes and acts as a primary link in connecting the repeat units of coordination polymers. Though first treated as a *semi-polar bond* by Lowry due to the inequality of charge distribution that arises during the bond formation, the term "coordinate covalent bond" was given by Sidgwick for bonds of this type[1] as represented in Scheme 1.2. Energy of this bond lies approximately in the range 40 - 100 kcal/mo 1.

$$M^{m+} + nL: \longrightarrow \left[M:L_n \right]^{m+} \quad (or) \quad M \longleftarrow L$$
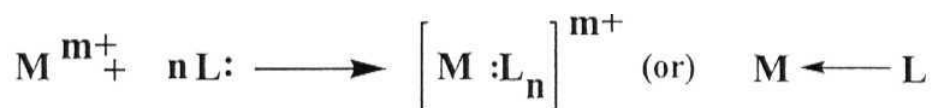
where M   is the metal ion; L is the ligand; m+ is the primary valency and n is the secondary valency of the metal ion.

Scheme 1.2 Pictorial representation of the coordinate bond.

(b) Ion - Ion Interactions: Weak attractive interactions existing between ions as in the crystal lattice of NaCl are known as ion - ion interactions. These are non - directional and purely electrostatic in nature. Energy of this interaction lies usually in the range 25 - 80 kcal/mol. A representation of the cation surrounded by the six nearest neighbour anions in NaCl crystal is shown in Figure 1.2.
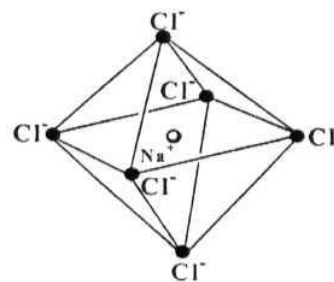
(c) **Hydrogen Bond:** This force comes next in the energy scale for non-covalent interactions and is often exploited for the deliberate design and synthesis of novel coordination polymers. Conventionally, hydrogen bond is a weak interaction operating between hydrogen atom covalently bonded to an electronegative atom (refened to as hydrogen bond donor, D) and another electronegative atom (referred to as hydrogen bond acceptor, A) and included all bonds like $O-H\cdots O$ in water and carboxylic acid dimers (Figure 1.3a) and $N-H\cdots O$ in DNA base pairs (Figure 1.3b). Later on, the interactions between less electronegative donors like C, and acceptors like O, Cl and the π cloud of phenyl ring were also recognized as weak non-conventional hydrogen bonds which include $C-H\cdots O$, $C-H\cdots X$ and $C-H\cdots\pi$ interactions (Figure 1.3c). The hydrogen bond energry ranges from 4 - 4 0 kcal/mol. for the "strong" type and less than about 4 kcal/mol. for the "weak" bonds.[11] Extensive literature discussing the nature, strength and importance of hydrogen bond as a design element,[11-17] its directional and metrical properties,[18-19] role in the directed structure formation[20-25] and its influence on the structure stabilization,[21,26-31] and the resulting properties[32,36] is available. The relevance of hydrogen bond in structural biology is well described by Jeffrey and Saenger.[37]
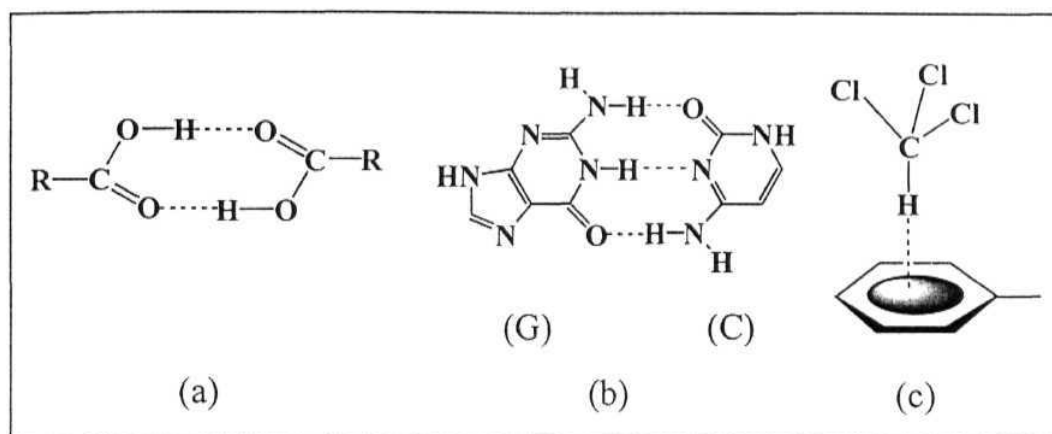
Figure 1.3 Schematic representation of commonly seen strong hydrogen bonds in (a) acid dimer (b) DNA base pairs Guanine(G) and Cytosine(C) and (c) the weak hydrogen bond seen in chloroform - phenyl interactions.[38]

(d) Ion - Dipole Interactions: The attractive interactions operating between an ion and a dipole may be regarded as ion - dipole interactions. These are directional interactions and fall off with distance as a function of $1/r^2$. This interaction is responsible for the solvation of ions (Figure 1.4), dissolution of ionic solids like NaCl in polar solvents like H_2O and attraction between M^{n+} and crown ethers. The interaction has energy in the range 12 - 50 kcal/mol.
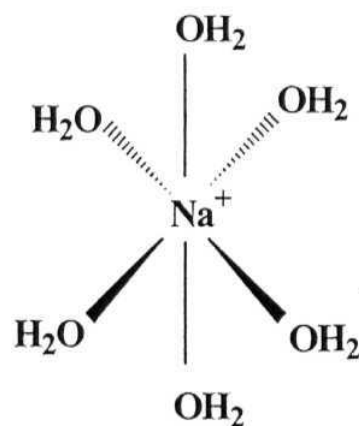
Figure 1.4

(e) **Dipole - Dipole Interactions:** These are the attractive forces arising from the alignment of dipoles relative to each other with energies in the range $1-12$ kcal/mol. These interactions may be operational in a head to tail arrangement of dipoles as shown in Figure 1.5a or in an antiparallel arrangement as shown in Figure 1.5b for the carbonyl dipole. These are weaker than the ion-dipole interactions and fall off rapidly with distance $(1/r^3)$. These interactions are also directional and are responsible for the association and structure of polar liquids.
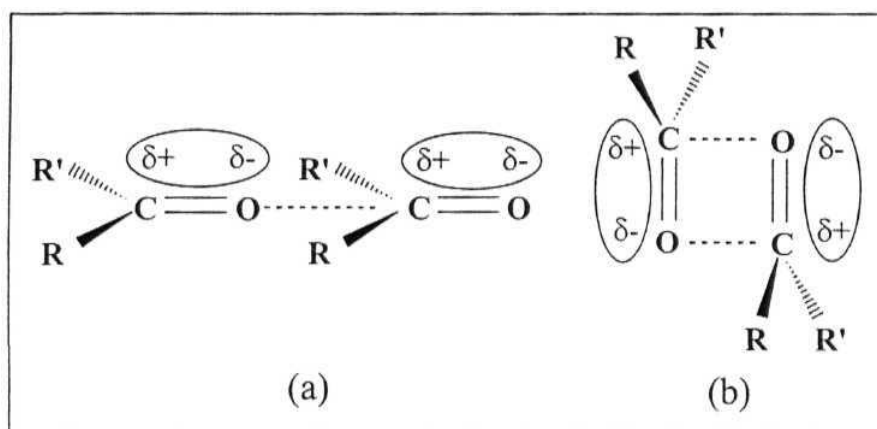
Figure 1.5 (a) Head-to-tail and (b) anti-parallel arrangment of dipoles in carbonyls.

(f) **Stacking ($\pi\cdots\pi$) Interactions:** This interaction is due to a weak attractive force operating between the *n* electron clouds of two aromatic rings. According to Sanders and Hunter,[39] this arises because of the attraction between the negatively charged *n* cloud of one molecule and the positively charged a C framework of its adjacent molecule (Figure 1.6a). There are perhaps no examples of perfect face to face stacking but offset face to face stacking (Figure 1.6b) is seen where one ring is slipped

relative to the second ring. This offset face to face stacking may be thought of as responsible for the slippery feel of graphite and its lubricant properties. Several intermediate geometries may also be present depending upon the steric requirements. The nature and role of this interaction in molecular recognition has been reviewed by Hunter.[40] There are several examples for the role and influence of this interaction in stabilizing structures and giving rise to specific properties.[41"54]
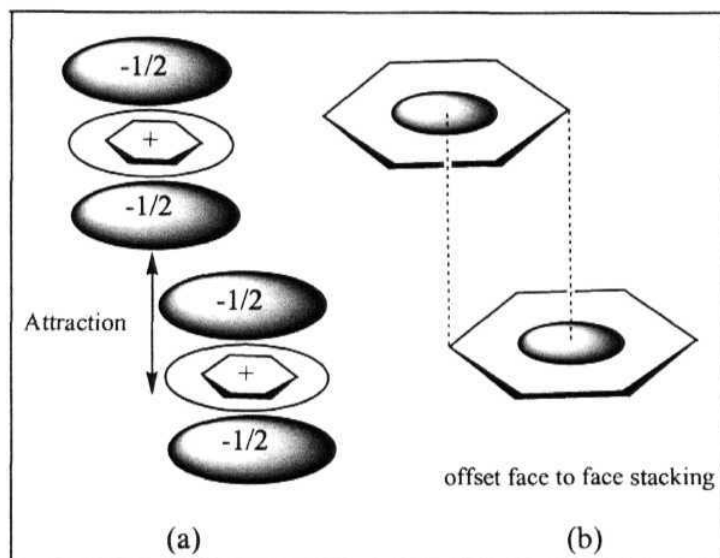
Figure 1.6 Aromatic *n* stacking: the attractive interactions operating between π cloud and σ framework of the aromatic ring (a) leading to an offset face to face π - π stacking (b).[39]

  (g) Atom - *n* Interaction: This is a similar type of interaction as stacking, but instead of operating between two *n* clouds, it operates between an atom or a cation and a

n cloud of an aromatic ring or double bond. Typical interactions of this kind are the ones operating between K^+ and benzene (Figure 1.7). It has been shown that this interaction has energy in the range 10-40 kcal/mol. in the case of simple ions like K^+, Na^+ etc. with benzene ring and in the range 10-20 kcal/mol in the case of alkylated ammonium ions and substituted benzenes. The nature of this interaction, a physical model for it and its presence in biological structures and synthetic systems has been reviewed recently by Ma and Dougherty.[55] The distance dependence is proposed to be $1/r^n$ (n < 2). In a recent report,

Figure 1.7 K^+ - benzene complex (gas phase) at its optimized geometry.[55]

Lindemann et al. examines the structural features of Ag···arene interaction.[56] Besides, this type of interaction observed between Ag^+ and toluene,[57] Cs^+ and imidazole,[58] there are examples of atom-π interaction like $S···\pi$[59,60] where S atom points normally to the center of the ring.

(h) **Atom - Atom Interactions:** Weak intermolecular attractive interactions operating between two identical or similar atoms may be termed as atom - atom interactions. This force may be thought of as mainly operating due to charge polarization, when the electron density around one nucleus is attracted by the second nucleus and vice-versa. There are several examples of solid state structures stabilized by
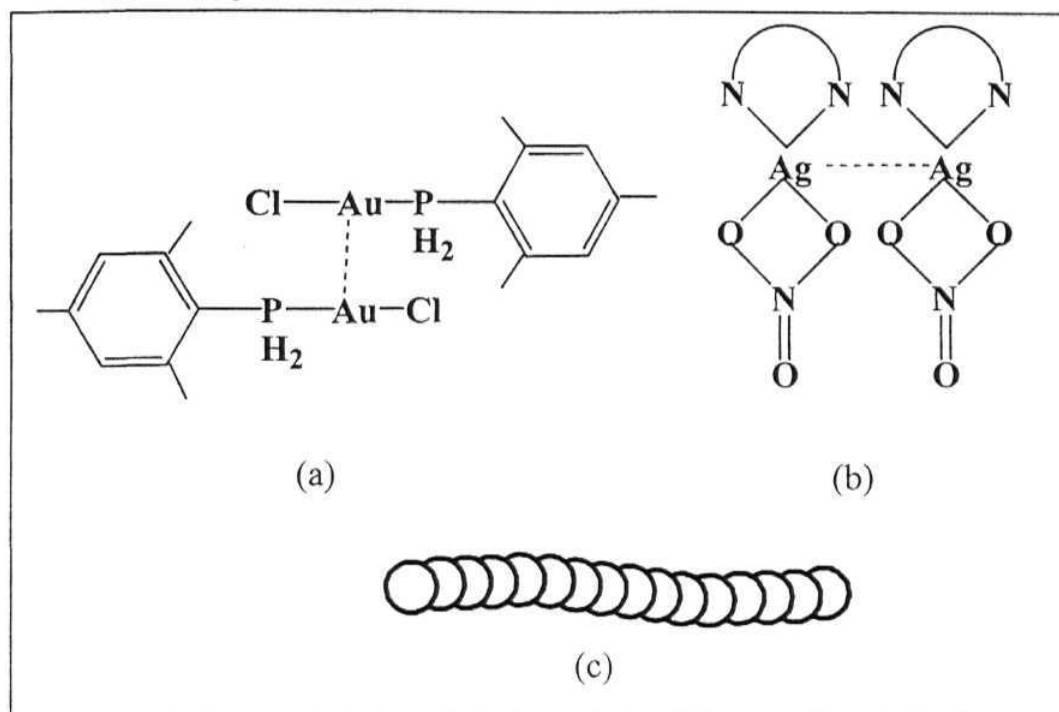
Figure 1.8 (a) Au$\cdots$Au interactions in $[2,4,6\text{-}(\text{t-Bu})_3\text{C}_6\text{H}_2\text{PH}_2\text{AuCl}]_2$[75] (b) Ag$\cdots$Ag interactions in Ag(dmbp)NO$_3$[76] (c) I$_8^{2-}$ chains formed by "normal" as well as weak I...I interactions in Mn(bpy)$_3$I$_8$.[77]

(i) Van der Waals Interactions: Forces arising out of the polarization of an electron cloud by an adjacent nucleus due to momentary imbalance in electron distribution resulting in weak electrostatic attraction may be termed as van der Waals interactions. Also known as London dispersion forces, these are the weakest of all known forces available to a chemist. These interactions operate only at very short distances and

fall off very rapidly $(1/r^6)$. These are non-directional and have energy < 1 kcal/mol. These weak interactions are responsible for the liquefaction of noble gases and the formation of inclusion compounds. Figure 1.9 shows the close packed structure of Ar in the crystal lattice.[78]

● = Ar
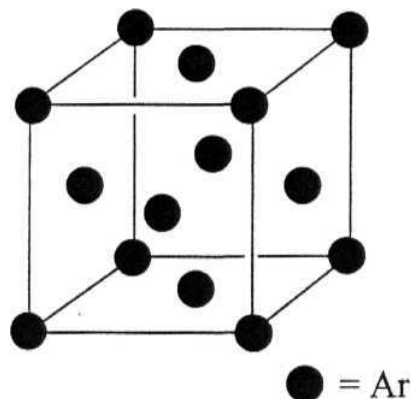
Figure 1.9

1.3. Synthetic Strategy

(a) **Self - Assembly Approach:** The main strategy for synthesizing coordination polymers or networks involves metal ion directed self assembly. In the present context, self-assembly may be defined[79] as the spontaneous association of either a few or many molecular components under equilibrium conditions resulting in stable, structurally well defined aggregates joined by non-covalent bonds. The components that undergo self - assembly are called tectons, tecton meaning builder in greek. These builder units may in all probability be the metal ions and ligands of the polymer chain repeat units. The spontaneous association takes place through the recognition of the complementary tectonic units under the control of the non-covalent interactions operating intermolecularly. For these tectons to associate, their reacting sites should have favorable spatial disposition such that their complementary sites can approach closely by recognition, which may lead to interaction without any steric inhibition. Self- assembly of an architecture is a multi - step process which involves reversibility of the connecting

events in order to achieve global energy minimum. The kinetic lability offers such recognition induced self - assembly systems, the abilty to undergo annealing and self - healing of defects. This is possible only because the forces involved in bond making and breaking in these systems are weak non - covalent interactions. Such a process is not seen in covalently linked systems involving relatively non - labile species and stronger bonds. The role of recognition and self - assembly in achieving various types of solid state structural entities like linear chains,[80-90] zig-zag chains,[57-86,91,98] helicates,[99,100] helical chains,[100-121] 1-D racks,[122-124] 1-D ladders,[31-47-64-125-127] supramolecular boxes,[128-129] capsules,[130] 2-D square networks,[131,135] 2-D honeycomb networks,[136-141] diamondoid networks,[142] adamantoid networks,[43-44-142,146] nanostructures,[147] and other possible structural motifs[148] have been reviewed. Some of the structural motifs are represented in Scheme 1.3.

(b) Hydrothermal **Synthesis:** While self-assembly from solutions under ambient conditions has been very fruitful for the synthesis of non-covalent structures, hydro(solvo)thermal procedures are sometimes employed. This method involves a one pot reaction at high pressures and temperatures. The best example for this type of reaction is the mineral formation in earth's crust, where temperatures above 100 °C and pressure above 1 bar are provided naturally. Mimicking these conditions this method was originally used by geologists and mineralogists to understand the geological processes that led to mineral formation. In industry, this method has been used extensively to prepare pure quartz crystals with sufficiently large size to study its properties for varied applications.

This method has the following advantages over the conventional chemical methods:

(a) To obtain compounds with elements in oxidation states that are otherwise difficult to obtain,

(b) to obtain low temperature phases,

(c) to obtain metastable compounds and

(d) for getting single crystals of new compounds which are otherwise difficult to obtain.

Application of this method for growing single crystals for various purposes and the role of hydro thermal synthesis in preparative chemistry have been reviewed .[149-152] In recent times, several polymeric coordination compounds were synthesized using this method as a preparative tool, which exhibit properties like magnetism,[153,155] luminescence,[84,125-156-157] nonlinear optical activity,[158,159] and microporosity.[160] A recent review by Feng and Xu[161] gives an overview of different materials being synthesized using this technique, while the review by Hagrman et al.,[151] illustrates use of this method in the preparation of organodiamine templated molybdenum oxides.
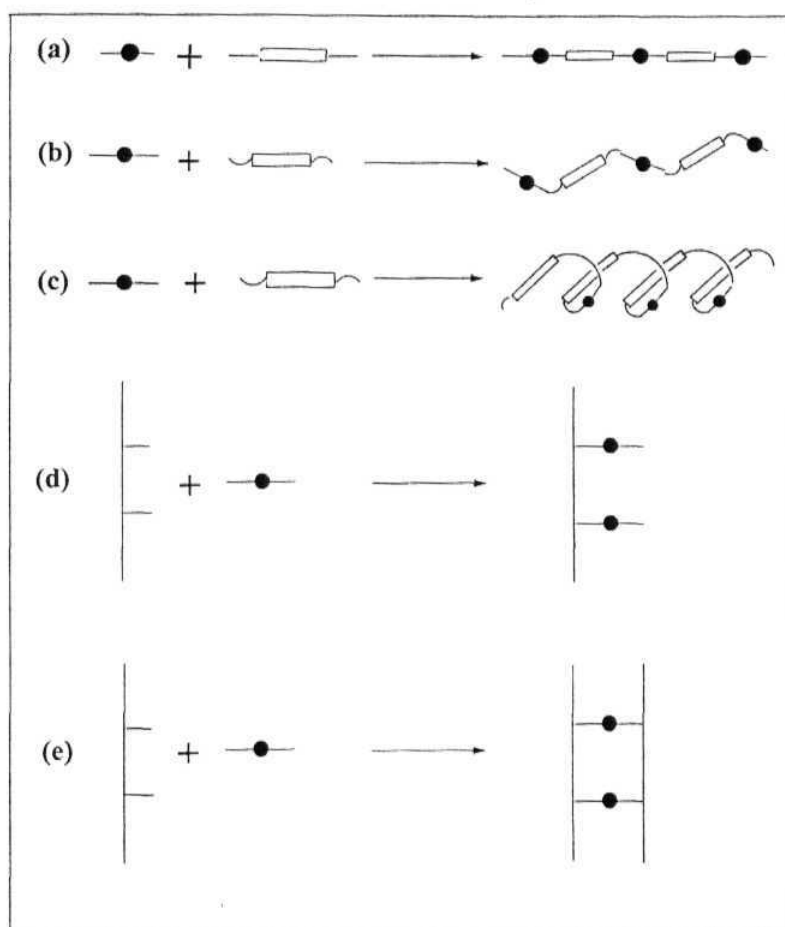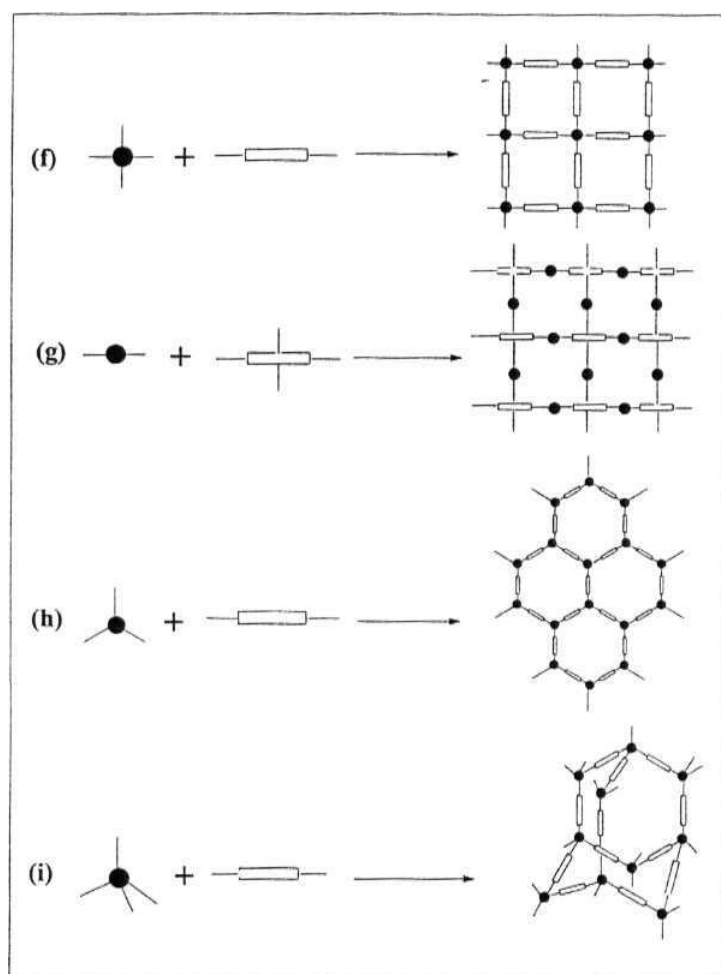
Scheme 1.3 (a) 1-D linear chain (b) 1-D zig-zag chain (c) 1-D helical chain (d) 1-D rack (e) 1-D ladder (0 & (g) 2-D square network (h) 2-D honeycomb network (i) 3-D adamantoid network. From (a) - (e) only two coordinate metal ions are shown. In principle, metal ions with other coordination numbers and geometry may also form these structures.

1.4. Factors Influencing Self-Assembly Process

Design of coordination networks takes into account the coordination characteristics *(viz.,* geometrical and ligand atom preferences) of the metal ion as well as the structural features *(viz.,* charge, multifunctionality, chelate and/or bridge forming ability) of the ligand.

The geometrical preference refers to the preferred coordination geometry (linear, trigonal planar, square planar etc.) of the metal ion in a complex under given set of conditions. Ligand atom preferences refer to the specific coordination of the metal ion to a specific atom of the ligand when there is a possibility of several atoms for binding. This tendency of coordination to a specific ligand atom is usually a consequence of the hard and soft acid-base nature of the ions.[162]

For a ligand, multifunctionality refers to the number of functional groups it possesses and thus the number of available sites for coordination. When a monofunctional ligand like pyridine with one coordinating site N, coordinates to a metal atom, complexation terminates there. But, for a ligand like aminomethylpyridine (amp) , along with the pyridine N atom, there is an amino N atom available for coordination. So, a single amp can bridge two metal centers by simultaneous coordination using both the N atoms. Hence, it can be understood that multifunctional ligands aid polymer or network formation. Besides these multifunctional ligands, there are examples of single atom bridges, mainly the halide and oxide bridges.[71,163-167]

Chelate or bridge forming ability refers to the ability of the ligand to function as a chelate or as a bridge between metal centers. Ligands like 1,10-phenanthroline and 2,2'-bipyridine can only function as chelates by coordinating to the adjacent *(cis)* sites of the

metal atom. Ligands like 2-amp can act as chelating as well as bridging ligand while its isomers 3-amp and 4-amp can act only as bridging ligands. The chelate formation is also influenced by the bite of the ligand and the ring dimensions. Though the ligand has adjacent coordinating sites which can give rise to chelate formation, the ring so formed will be stable only if it is not under strain. It has been observed that five membered rings are most stable as their geometry is optimum. Higher membered chelate rings are less stable and hence occur less frequently.

1.5. Applications of Coordination Polymers

Rapid growth in the field of coordination polymers and networks in recent times can be attributed to their expected role as new materials like molecular magnets, metallic and superconducting polymers, optical (luminescence/SHG) materials, ion-exchangers and microporous solids. Further, the novel solid state structures they generate are often quite appealing and aesthetically pleasing. Figure 1.10 schematically illustrates how an idea can be turned to a new material with desired properties. A brief discussion of the applications of the coordination polymers is presented in the following paragraphs.
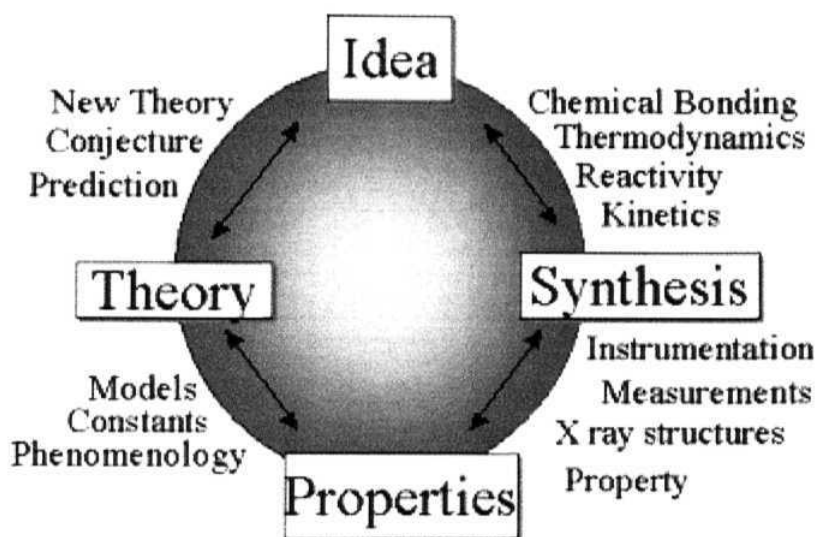
Figure 1.10 Pictorial representation of the inter-relationship between an idea and other factors to achieve the desired property (adapted from ref. 170).

(a) Molecular Magnets: Molecular magnetism deals with the synthesis and characterization of new materials with predictable magnetic properties followed by correlation of the results to the proposed theory. It plays an important role in the emerging field of *molecular electronics*, where molecular magnetic systems are used in digital display systems and in devising novel magnetic systems useful for information storage and processing.[168-170] Kahn, in his famous book, "Molecular Magnetism"[171] gives an excellent account of the theory and examples of molecular systems exhibiting magnetic interactions. The goal of all studies in this field is to have FM materials which exhibit magnetic ordering at RT. With an aim to develop materials exhibiting magnetism

at RT, several systems have been designed and their magnetic behavior studied which often showed good FM or AFM interactions. High T_c (315 K) molecualr magnet has been first realized in the prussian blue analog, $V[Cr(CN)_6]_{0.86} \cdot 2.8H_2O$.[172] This system is structurally similar to the prussian blue, except for the small variation in the geometry of V^{II}. As the stoichiometry of Cr^{III} to V^{II} (0.86/1) is less than 1, only 86% of the coordinating sites around V are occupied by the $[Cr(CN)_6]^{3-}$ ions. The remaining 14% sites is filled by the water molecules, which are coordinated to V through the oxygen atoms. The overall structure is similar to the rock salt structure of prussian blue with short range order (Figure 1.11). From the IR data, a - Cr^{III} - C = N -- (V^{II} / V^{III}) sequence has been ascertained. The antiparallel spins of Cr^{III} (3/2) and V^{II} (3/2) cancel each other. But the uncompensated antiparallel spins of Cr^{III} (3/2) and V^{III} (1) give rise to short range anti ferromagnetic interactions. The AFM interaction explains the low saturation magnetization at 10 K. The long range order of the uncompensated antiferromagnetically coupled spins makes this system a high T_c ferrimagnet.

While the above system is a high T_c moleuclar magnet, it is a non stoichiometric as well as a mixed oxidation state material. Following this observation, the groups of Girolami and Miller reported similar non - stoichiometric and mixed oxidation state V and Cr systems, characterized by powder X-ray and having a formula $KV^{II}[Cr^{III}(CN)_6] \cdot 2.8H_2O \cdot 0.1KOTf$ which has a T_c of 376 K[173] and $K_{0.058}V^{II/III}[Cr^{III}(CN)_6]_{0.79} \cdot (SO_4) \cdot 0.93H_2O$ with T_c of 372 K[174] respectively. The 3D ferrimagnetic order in these systems have been suggested as a promising route to other high T_c molecuclar magnets.

Other recent systems with promising magnetic properties (transition towards FM or AFM) include heterobimetallic polymers involving dicyanamide anion;[49138]

bimetallic systems consisting of transition metals and U^{IV} with schiff base ligands;[175] infinite networks and chains with polynitrile ligands;[143,176-180] azide bridged networks;[181-184] 3-D stacked honeycomb systems;[140,185] linear chains;[184,186-188] free-radical systems[34-189] and clusters.[190-195] Besides these, there are examples of systems synthesized under hydrothermal conditions[46-153] exhibiting interesting magnetic properties. Also, there is a recent report of optically active molecular magnet.[196]
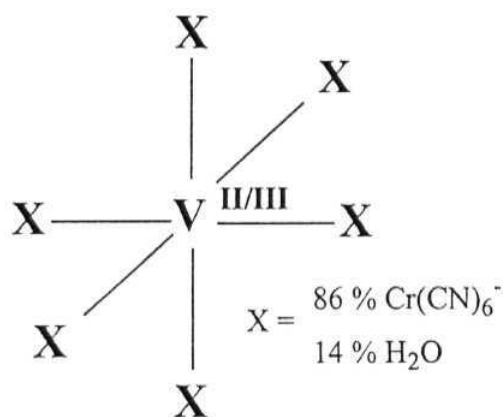
Figure 1.11 First high T_c ferrimagnet, $V[Cr(CN)_6]_{0.86} \cdot 2.8H_2O$.

(b) Metallic and Superconducting Polymers: The review by Chen and Suslick,[2] gives an overall view of various coordination polymeric systems showing conductivity similar to that of metals. These include stacked structures having $[Pt(CN)_4]^{2-}$ stacks, planar metal complexes like $Ni(Pc)(I_3)_{0.33}$, iodine doped polysiloxane polymers of phthalocyanine, $[M(Pc)X]$, (M = Si, Ge, Sn, Al, Ga, Cr; X = O, F) (Pc = the dianion of phthalocyanine), macroclyclic complexes linked by bridging ligands like $[M(Pc)(L-L)]\propto$ (L-L = pyrazine, bipyridine, tz, CN^-, N_3^- etc.). Also there are reports of metal coordinated

TTF systems[197200] showing good conducting properties when doped with iodine (5-7 orders of magnitude higher) than their undoped analogues. Extremely high metallic conductivity of the order 500 000 Scm^{-1} at 3.5 K and decreasing steadily with temperature, was found in the radical anion salt 2,5-Dimethyl-N,N'-dicyanoquinonediimine and Cu(I).[52] (Figure 1.12a). Iodine doped Ag(I) coordination polymer of TTM-TTP exhibiting good conductivity (RT conductivity 0.85 Scm^{-1})[69] was reported recently.

The well known high T_c ceramic based superconductors,[201] eg., $YBa_2Cu_3O_7$ (Figure. 1.12b) can be considered as examples of 3D networked coordination polymers.

(a)   (b)
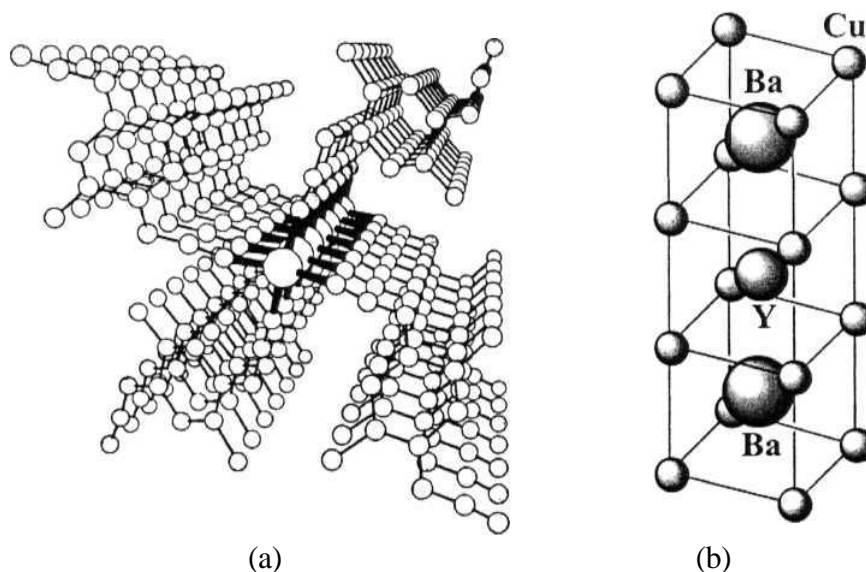
Figure 1.12 (a) *n* stacks responsible for metallic conductivity in the coordination polymer $[2,5\text{-DM-DCNQI}]_2Cu^{52}$ and (b) high T_c ceramic based superconductor $YBa_2Cu_3O_7$.[201]

(c) Optical (SHG/Luminescent) Materials: The two optical properties of coordination polymers studied extensively are second harmonic generation (SHG) and luminescence, for their possible use in information acquisition, processing, storage and transmission. The non - linear nature of light and its associated property like SHG have a large impact on fields like telecommunications, signalling etc. This property is best exhibited by inorganic salts like potassium titanyl phosphate (KTP), potassium dihydrogen phosphate (KDP) and lithium niobate ($LiNbO_3$). Other systems exhibiting good SHG response among coordination polymers include, a Ag coordination polymer,[202] 1-D helical chain made of heterobimetallic(La & Ag) clusters,[110] 1-D coordination polymer of Mn(hfac)2(NIT-R),[2] square networks of Zn(II) and Cd(II) with *m*-pyridine carboxylates,[158] (Figure 1.13a) diamondoid networks of Zn(II) and Cd(II) with *p*-pyrdine carboxylates,[159] and several π-conjugated organic systems.[2]

Besides exhibiting NLO activity, several self-assembled coordination polymers showing luminescence were reported. These luminescent compounds may find use in blue light emitting diode (LED) devices. Such systems include tetranuclear Cu(I) clusters,[203-204] 2-D layered polymers of Cu(I),[157] zinc coordination polymers assembled under hydrothermal conditions,[156] a tetranuclear Zn compound,[205] square grid compound of Zn(II) with norfloxacin,[206] unidimensional Ag polymer,[207] heterometallic dirhodium-silver chains,[208] neutral molecular rectangles of Re,[209] lanthanide coordination polymers,[84] and triple helical chain polymer of Hg.[106] A Pt(II) luminescent compound which detects aromatic hydrocarbon vapors has been reported recently.[210] (Figure 1.13b) This example throws light on their use as an "electronic nose" or as a detecting or emitting layer in a LED.

<center>(a)   (b)</center>
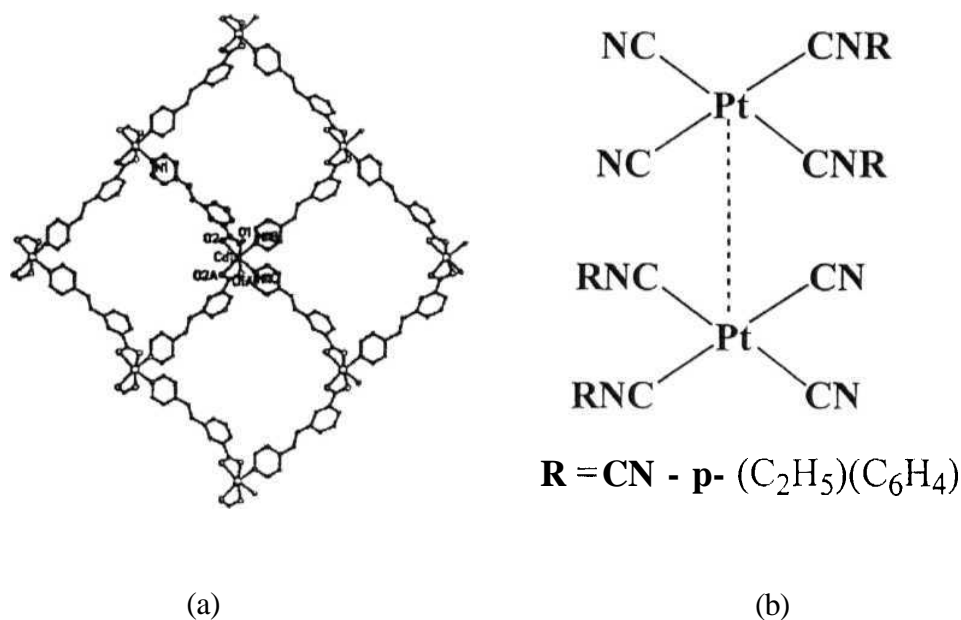
Figure   1.13   (a)   Square   network   of   Cd{3-[2-(4-pyridyl)ethenyl]benzoate}2, with SHG efficiency of ~ 12 times that of LiNbO$_3$[159] and (b) Pt - Pt interactions leading to the stacked structure in Pt[CN-p-(C$_2$H$_5$)C$_6$H$_4$]$_2$ (luminescence sensor for hydrocarbon vapours. (adapted from ref. 210).

(d) Ferroelectric Materials:[2] Ferroelectricity is analogous to ferromagnetism. This type of materials exhibit unusual electro-optical, photorefractive and pyroelectric properties and find use in electronic oscillators, high-frequency filters, electroacoustic converters, pyroelectric radiant energy receivers and non-linear capacitive elements. Though most ferroelectrics are metal oxides like BaTiO$_3$ and LiNbO$_3$ and some are

liquid-crystals, polymers of metalloporphyrins, for example, [Fe^{II}(TPP)(pyCN)] and [Fe^{III}(TPP)(pyCO$_2$)] have been suggested as ferroelectric materials (Figure 1.14). Similar to porphyrins, stacked systems without bridging ligands formed by bowl- or cone-shaped molecules with ferroelectric properties have been reported for lead phthalocyanines, metallocyclophanes and cyclotncatechylenes.
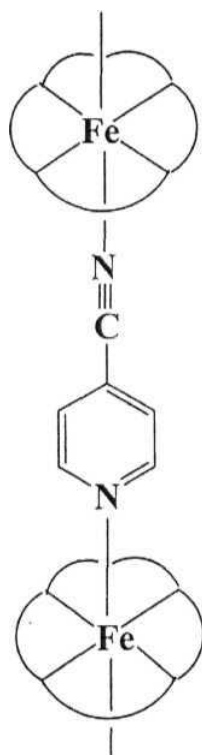
Figure 1.14 Infinite chain of [Fe^{II}(TPP)(pyCN)] connected by the bridging cyanopyridine, exhibiting ferro - electric properties (adapted fom ref. 2).

(e) Microporous Materials: Coordination polymers with open network structures can be fine tuned to generate cavities with desirable sizes which can act as ion-exchangers and also show microporosity for guest exchange. This property can be exploited to synthesize compounds that can function as substitutes to zeolites, besides their application in heterogeneous catalysis and adsorption. In this respect it is necessary to **maintain** the crystal integrity while being porous to the exchange of ions. Hence, strategies for having compounds which are thermally stable and porous to guest exchange are required. With a view to synthesize such open framework compounds with thermal stability, work by several groups resulted in basically three types of compounds. These are channels of (a) diamondoid type,[26,146,211] (b) open frameworks with rectangular,[212214] square,[133''135'215''217] and hexagonal type[137-218''220]   and (c) other network/layered solids.[53,85,132,141,160,221-229] Microporous materials crystallized from solvents are invariably obtained as solvates. The desolvated material obtained by heating or by applying vacuum may sometimes retain its crystallinity and porosity as judged from single crystal diffraction[230] or powder diffractograms.[228,231]   It has also been possible to conduct experiments on reversible desolvation / solvation cycles[231]   and guest exchange reactions.[53-132-139-141'218]   Insoluble porous solids containing anions inside cavities are known to exchange with other anions present in the solution.[146-213]

Engineering the networks by controlling the self-assembling features for functioning as zeolite substitutes in different types of solids have been reviewed by several groups.[142,232,233] Helical polymers with large chiral cavities [62,119,234] have been reported which represent a prototype of new chiral porous materials which may find applications in the field of stereospecific synthesis and enantioselective separations.
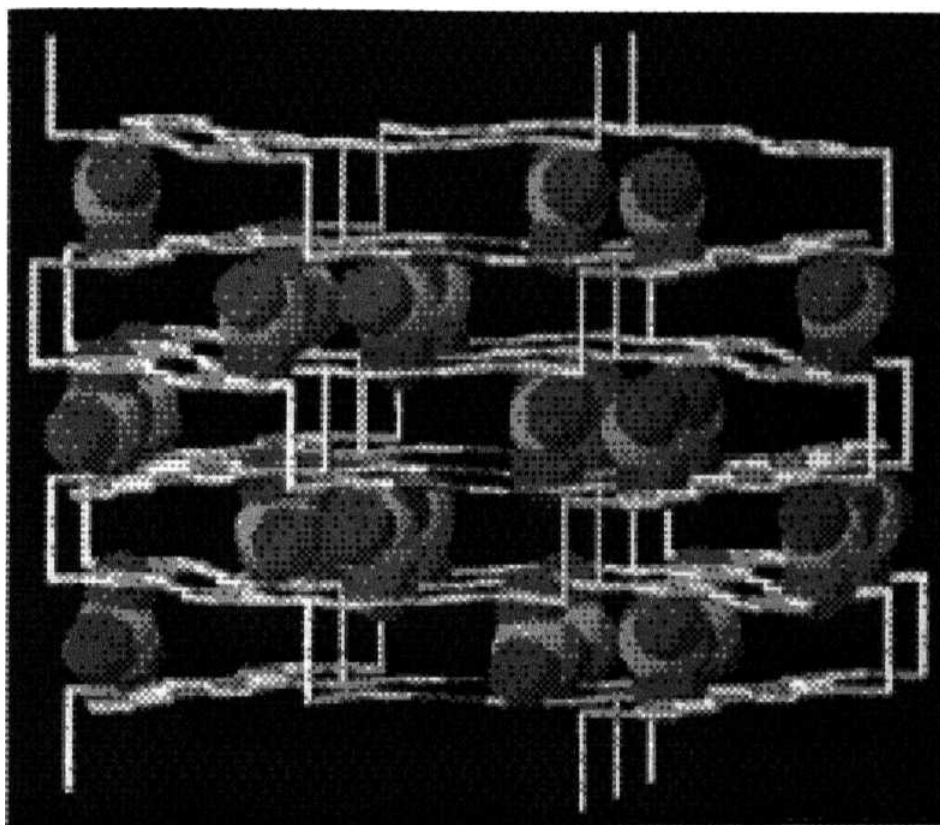
Figure 1.15 Structure of Ag(4,4'-bpy)NO$_3$ showing large channels containing (disordered) NO3" ions. The anions exchange readily with PF$_6^-$, BF$_4^-$, MoO$_4^{2-}$ and SO$_4^{2-}$, when the solid is suspended in an aqueous solution containing the anions.[213]

1.6. References

(1)   Moeller, T. *Inorganic Chemistry An advanced Textbook;* Asia Publishing House: Bombay, 1952, pp 193.

(2)   Chen, C.-T.; Suslick, K. S. *Coord. Chem. Rev.* 1993, *128, 293.*

(3)   Carraher, J. C. E. *J. Chem. Educ.* **1981,** *58,* 921.

(4)   Dey, A. K. *J. Indian Chem. Soc.* **1986,** *63,* 357.

(5)   Brunsveld, L.; Folmer, B. J. B.; Meijer, E. W.; Sijbesma, R. P. *Chem. Rev.* **2001,** *101*, 4071.

(6)   Swarnabala, G.; Rajasekharan, M. V. *Inorg. Chem.* **1998,** *37,* 1483.

(7)   Albertsson, J. *Acta. Chem. Scand.* **1972,** *26,* 1005.

(8)   Steed, J. W.; Atwood, J. L. *Supramolecular Chemistry*; John Wiley & Sons, Ltd.: England, 2000.

(9)   Ref. 1, Ch. 6.

(10) Hamill, W. H.; Williams, J., R. R.; MacKay, C. *Principles of Physical Chemistry; 2* ed.; Prentice-Hall of India Private Limited: New Delhi, 1968, pp 477.

(11) Desiraju, G. R.; Steiner, T. *The Weak Hydrogen Bond: In Structural Chemistry & Biology*; Oxford University Press Inc., New York: New York, 1999.

(12) Etter, M. C. *Acc. Chem. Res.* **1990,** *23,* 120.

(13) Aakeroy, C. B.; Seddon, K. R. *Chem. Soc. Rev.* **1993,** 397.

(14) Etter, M. C. *J. Phys. Chem.* **1991,** *95,* 4610.

(15) Braga, D.; Grepioni, F. *J. Chem. Soc, Dalton Trans* **1999,** 1.

(16) Alkorta, I.; Rozas, I.; Elguero, J. *Chem. Soc. Rev.* **1998,** *27,* 163.

(17) Raymo, F.; Bartberger, M. D.; Houk, K. N.; Stoddart, J. F. *J. Am. Chem. Soc.* **2001,** *123,* 9264.

(18) Bernstein, J.; Davis, R. E.; Shimoni, L.; Chang, N.-L. *Angew. Chem. Int. Ed. Engl.* **1995,** *34,* 1555.

(19) Steiner, T. *J. Chem, Soc, Chem. Commun.* **1994,** 2341.

(20) Subramanian, S.; Zaworotko, M. J. **1994,** *137,* 357.

(21) Burrows, A. D.; Chan, C.-W.; Chowdhry, M. M.; McGrady, J. E.; Mingos, D. M. P. *Chem. Soc. Rev.* 1995, *24,* 329.

(22) Felix, O.; Hosseini, M. W.; Cian, A. D.; Fischer, J. *Angew. Chem. Int. Ed Engl.* **1997,** *36,* 102.

(23) Marsh, A.; Silvestri, M.; Lehn, J.-M. *Chem. Commun.* **1996,** 1527.

(24) Burrows, A. D.; Mingos, D. M. P.; White, A. J. P.; Williams, D. J. *Chem. Commun.* 1996,97.

(25) Aakeröy, C. B.; Beatty, A. M.; Helfrich, B. A. *J. Chem. Soc, Dalton Trans.* **1998,** 1943.

(26) Munakata, M.; Wu, L. P.; Yamamoto, M.; Kuroda-Sowa, T.; Maekawa, M. *J. Am. Chem. Soc.* **1996,** *118,* 3117.

(27) Carlucci, L.; Ciani, G.; Proserpio, D. M.; Sironi, A. *J. Chem. Soc, Dalton Trans.* **1997,** 1801.

(28) Allen, M. T.; Burrows, A. D.; Mahon, M. F. *J. Chem. Soc. Dalton Trans* **1999,** 215.

(29) Chowdhry, M. M.; Mingos, D. M. P.; White, A. J. P.; Williams, D. J. *Chem. Commun.* **1996,** 899.

(30) Beijer, F. H.; Kooijman, H.; Spek, A. L.; Sijbesma, R. P.; Meijer, E. W. *Angew. Chem. Int. Ed.* 1998, 57, 75.

(31) Fromm, K. M.; Goesmann, H.; Bernardinelli, G. *Polyhedron* **2000,** *19,* 1783.

(32) Schauer, C. L.; Matwey, E.; Fowler, F. W.; Lauher, J. W. *J. Am. Chem. Soc.* **1997,** *119,* 10245.

(33) Bertelli, M.; Carlucci, L.; Ciani, G.; Proserpio, D. M.; Sironi, A. *J. Mater. Chem.* **1997,7,** 1271.

(34) Romero, F. M.; Ziessel, R.; Bonnet, M.; Pontillon, Y.; Ressouche, E.; Schweizer, J.; Delley, B.; Grand, A.; Paulsen, C. *J. Am. Chem. Soc.* **2000,** *122,* 1298.

(35) Chen-jie, F.; Chun-ying, D.; Cheng, H.; Qing-jin, M. *Chem. Commun.* **2000,** 1187.

(36)   Fan, E.; Yang, J.; Geib, S. J.; Stoner, T. C; Hopkins, M. D.; Hamilton, A. D. *J. Chem. Soc, Chem. Commun.* 1995, 1251.

(37)   Jeffrey, G. A.; Saenger, W. *Hydrogen Bonding in Biological Structures',* Springer-Verlag, Berlin: Germany, 1991.

(38)   Atwood, **J. L.; Bott, S.** G.; Jones, C; Raston, C. L. *J. Chem. Soc, Chem. Commun.* **1992,** 1349.

(39)   Hunter, C. A.; Sanders, J. K. M. *J. Am. Chem. Soc.* **1990,** *112,* 5525.

(40)   Hunter, C. A. *Chem. Soc. Rev.* **1994,** 101.

(41)   Chen, H.; Ogo, S.; Fish, R. H. *J. Am. Chem. Soc.* **1996,** *118,* 4993.

(42)   Stynes, D. V. *Inorg. Chem.* **1994,** *33,* 5022.

(43)   Blake, A. J.; Champness, N. R.; Khlobystov, A. N.; Lemenovskii, D. A.; Li, W.-S.; Schroder, M. *Chem. Commun.* **1997,** 1339.

(44)   Hirsch, K. A.; Wilson, S. R.; Moore, J. S. *Chem. Eur. J.* **1997,** *3,* 765.

(45)   Hartshorn, C. M.; Steel, P. J. *J. Chem. Soc.,Dalton Trans* **1998,** 3935.

(46)   Lawandy, M. A.; Huang, X.; Wang, R.-J.; Li, J.; Lu, J. Y.; Yuen, T.; Lin, C. L. *Inorg. Chem.* 1999, *38,* 5410.

(47)   Zhang, L.; Cheng, P.; Tang, L.-F.; Weng, L.-H.; Jiang, Z.-H.; Liao, D.-Z.; Yan, S.-P.; Wang, G.-L. *Chem. Commun.* **2000,** 717.

(48)   Long, D.-L.; Blake, A. J.; Champness, N. R.; Schroder, M. *Chem. Commun.* **2000,** 2273.

(49) Tanase, S.; Ferbinteanu, M.; Andruh, M.; Mathoniere, C; Strenger, I.; Rombaut, G. *Polyhedron* **2000,** *19,* 1967.

(50) Anderson, H. L.; Bashall, A.; Henrick, K.; McPartlin, M.; Sanders, J. K. M. *Angew. Chem. Int. Ed. Engl.* **1994,** *33,* 429.

(51) Hirsch, K. A.; Wilson, S. R.; Moore, J. S. *Inorg. Chem.* **1997,** *36,* 2960.

(52) Aumüller, A.; Erk, P.; Klebe, G.; Hiinig, S.; Schütz, J. U. v.; Werner, H.-P. *Angew. Chem. Int. Ed. Engl.* **1986,** *25,* 740.

(53) Yaghi, O. M.; Li, G.; Li, H. *Nature* **1995,** *378,* 703.

(54) Magistrato, A.; Pregosin, P. S.; Albinati, A.; Rothlisberger, U. *Organometallics* **2001,** *20,* 4178.

(55) Ma, J. C.; Dougherty, D. A. *Chem. Rev.* **1997,** 97, 1303.

(56) Lindemann, S. V.; Rathore, R.; Kochi, J. K. *Inorg. Chem.* **2000,** *39,* 5707.

(57) Wu, H.-P.; Janiak, C.; Rheinwald, G.; Lang, H. *J. Chem. Soc., Dalton Trans* **1999,** 183.

(58) Tadokoro, M.; Shiomi, T.; Isobe, K.; Naksuji, K. *Inorg. Chem.* **2001,** *40,* 5476.

(59) Mikuriya, M.; Yamato, Y.; Tokii, T. *Bull. Chem. Soc. Jpn.* **1992,** *64,* 1466.

(60) Sailaja, S.; Rajasekharan, M. V. *Unpublished results* .

(61) Withersby, M. A.; Blake, A. J.; Champness, N. R.; Hubberstey, P.; Li, W.-S.; Schroder, M. *Angew. Chem. Int. Ed. Engl.* **1997,** *36,* 2327.

(62) Sailaja, S.; Rajasekharan, M. V. *Inorg. Chem.* **2000,** *39,* 4586.

(63) Burrows, A. D.; Mahon, M. F.; Palmer, M. T. *J. Chem. Soc.,Dalton Trans.* **1998,** 1941.

(64) Kang, Y.; Lee, S. S.; Park, K.-M.; Lee, S. H.; Kang, S. O.; Ko, J. *Inorg. Chem.* 2001,40,7027.

(65) Kristiansson, O. *Inorg. Chem.* **2001,** *40,* 5058.

(66) Leznoff, D. B.; Xue, B.-Y.; Batchelor, R. J.; Einstein, F. W. B.; Patrick, B. O. *Inorg. Chem.* 2001, *40,* 6026.

(67) Dai, J.; Kuroda-Sowa, T.; Munakata, M.; Maekawa, M.; Suenaga, Y.; Ohno, Y. *J. Chem. Soc, Dalton Trans.* 1997, 2363.

(68) Sheng, T.; Wu, X.; Wang, Q.; Gao, X.; Lin, P. *Polyhedron* **1998,** *17,* 4519.

(69) Zhong, J. C.; Misaki, Y.; Munakata, M.; Kuroda-Sowa, T.; Maekawa, M.; Suenaga, Y.; Konaka, H. *Inorg. Chem.* **2001,** *40,* 7096.

(70) Desiraju, G. R. *Angew. Chem. Int. Ed. Engl,* **1995,** *34,* 2311.

(71) Stenzel, V.; Jeske, J.; du Mont, W.-W.; Jones, P. G. *Inorg. Chem.* **1997,** *36,* 443.

(72) Menon, S.; Balagopalakrishna, C.; Rajasekharan, M. V.; Ramakrishna, B. L. *Inorg. Chem.* 1994,35,950.

(73) Schmidbaur, H. *Chem. Soc. Rev.* **1995,** 391.

(74) Pyykko, P. *Chem. Rev.* **1999,** *97,* 597.

(75)   Huheey, J. E.; Keiter, E. A.; Keiter, R. L. *Inorganic Chemistry: Principles of Structure and Reactivity,* 4 ed.; Addison Wesley Longman(Singapore) Pte. Ltd.: New York, 2000, pp 883.

(76)   Venkatalakshmi, N.; Rajasekharan, M. V. *Transition Met. Chem.* **1992,** *17,* 455.

(77)   Ramalakshmi, D.; Reddy, K. R.; Padmavathy, D.; Rajasekharan, M. V.; Arulsamy, N.; Hodgson, D. J. *Inorg. Chim. Acta.* **1999,** *284, 158.*

(78)   Ref. 1, pp. 376.

(79)   Lehn, J.-M. *Supramolecular Chemistry Concepts and Perspectives*; VCH: Germany, 1995.

(80)   Boldog, I.; Rusanov, E. B.; Chernega, N.; Sieler, J.; Domasevitch, K. V. *Polyhedron* **2001,***20,* 887.

(81)   Kwak, C.-H.; Jeong, J.; Kim, J. *Inorg. Chem. Commun.* **2001,** *4,* 264.

(82)   Carballo, R.; Castiñeiras, A.; Covelo, B.; Vazquez-Lopez, E. M. *Polyhedron* **2001,** *20,* 899.

(83)   Dong, Y.-B.; Smith, M. D.; Loye, H.-C. z. *Inorg. Chem.* **2000,** *39, 1943.*

(84)   Ma, L.; Evans, O. R.; Foxman, B. M.; Lin, W. *Inorg. Chem.* 1999, *38, 5837.*

(85)   Reineke, T. M.; Eddaoudi, M.; O'Keeffe, M.; Yaghi, O. M. *Angew. Chem. Int. Ed.* **1999**, *38*, 2590.

(86)   Rivas, J. C. M.; Brammer, L. *Inorg. Chem.* **1998,** *37,* 4756.

(87) Ferbinteanu, M.; Marinescu, G.; Roesky, H. W.; Noltemeyer, M.; Schmidt, H-G.; Andruh, M. *Polyhedron* **1998**,*18*, 243.

(88) Lu, J.; Yu, C; Niu, T.; Paliwala, T.; Crisci, G.; Somosa, F.; Jacobson, A. J. *Inorg. Chem.* 1998,37,4637.

(89) Masciocchi, N.; Ardizzoia, G. A.; LaMonica, G.; Maspero, A.; Galli, S.; Sironi, A. *Inorg. Chem.* **2001**, *40*,6983.

(90) Kuang, S.-M.; Zhang, Z.-Z.; Wang, Q.-G.; Mak, T., C. W. *Chem. Commun.* 1998, 581.

(91) Bu, X.-H.; Liu, H.; Du, M.; Wong, K. M.-C; Yam, V. W.-W.; Shionoya, M. *Inorg. Chem.* **2001**, *40*, 4143.

(92) Goodgame, D. M. L.; Miiller, T. E.; Williams, D. J. *Polyhedron* 1992, 77, 1513.

(93) Hanton, L. R.; Richardson, C; Robinson, W. T.; Turnbull, J. M. *Chem. Commun.* 2000, 2465.

(94) Chen, C.-Y.; Lo, F.-R.; Kao, H.-M.; Lii, K.-H. *Chem. Commun.* 2000, 1061.

(95) Navarro, J. A. R.; Freisinger, E.; Lippert, B. *Inorg. Chem.* 2000, *39,* 1059.

(96) Shi, Z.; Zhang, L.; Gao, S.; Yang, G.; Hua, J.; Gao, L.; Feng, S. *Inorg. Chem.* 2000, *39,* 1990.

(97) Chiang, W.; Ho, D. M.; Engen, D. V.; Thompson, M. E. *Inorg. Chem.* 1993, *32,* 2886.

(98)   Chan, C.-W.; Mingos, D. M. P.; White, A. J. P.; Williams, D. J. *Chem. Commun.* 1996,81.

(99)   Conn, M. M.; Rebek, J. J. *Chem. Rev.* 1997, *97,* 1647.

(100) Piguet, C; Bernardinelli, G.; Hopfgartner, G. *Chem. Rev.* **1997,** *97,* 2005.

(101) Nakano, T.; Okamoto, Y. *Chem. Rev.* **2001,** *101,*4013.

(102) Jung, O.-S.; Kim, Y. J.; Lee, Y.-A.; Chae, H. K.; Jang, H. G.; Hong, J. *Inorg. Chem.* **2001,** *40,* 2105.

(103) Horikoshi, R.; Mochida, T.; Moriyama, H. *Inorg. Chem.* **2001,** *40,* 2430.

(104) Zhang, H.; Cai, J.; Feng, X.-L.; Liu, J.-Z.; Li, X.-Y.; Ji, L.-N. *Inorg. Chem. Commun.* 2001,4,241.

(105) Li, B.; Yin, G.; Cao, H.; Liu, Y.; Xu, Z. *Inorg. Chem. Commun.* **2001,** *4,* 451.

(106) Ciurtin, D. M.; Pschirer, N. G.; Smith, M. D.; Bunz, U. H. F.; Loye, H.-C. z. *Chem. Mater.* 2001, *13,* 2743.

(107) Schroder, U.; Beyer, L.; Sieler, J. *Inorg. Chem. Commun.* **2000,** *3,* 630.

(108) Shi, Z.; Feng, S.; Gao, S.; Zhang, L.; Yang, G.; Hua, J. *Angew. Chem. Int. Ed.* **2000,** *39,* 2325.

(109) Hong, M.; Su, W.; Cao, R.; Fujita, M.; Lu, J. *Chem. Eur. J.* **2000,** *6,* 427.

(110) Zhang, Q.-F.; Leung, W.-H.; Xin, X.-Q.; Fun, H.-K. *Inorg. Chem.* **2000,** *39,* 417.

(111) Carlucci, L.; Ciani, G.; Proserpio, D. M.; Sironi, A. *Inorg. Chem.* **1998,** *37,* 5941.

(112) Hirsch, K. A.; Wilson, S. R.; Moore, J. S. *J. Am. Chem. Soc.* **1997**, *119*, 10401.

(113) Batten, S. R.; Hoskins, B. F.; Robson, R. *Angew. Chem. Int. Ed.* **1997,** *36, 636.*

(114) Gelling, O. J.; Bolhuis, F. v.; Feringa, B. L. *J. Chem. Soc, Chem. Commun.* **1991,** 917.

(115) Carlucci, L.; Ciani, G.; Gudenberg, D. W. v.; Proserpio, D. M. *Inorg. Chem.* **1997,** 56,3812.

(116) Goodgame, D. M. L.; Hill, S. P. W.; Williams, D. J. *Polyhedron* **1992,** *11,* 1841.

(117) Wu, B.; Zhang, W.-J.; Yu, S.-Y.; Wu, X.-T. *J. Chem. Soc, Dalton Trans.* **1997,** 1795.

(118) Psillakis, E.; Jeffery, J. C; McCleverty, J. A.; Ward, M. D. *J. Chem. Soc, Dalton Trans.* **1997,** 1645.

(119) Biradha, K.; Seward, C; Zaworotko, M. J. *Angew. Chem. Int. Ed.* **1999,** *38, 492.*

(120) Hester, C. A.; Baughman, R. G.; Collier, H. L. *Polyhedron* **1997,** *16, 2893.*

(121) Tong, M.-L.; Chen, X.-M.; Ye, B.-H. *Inorg. Chem.* **1998,** *37, 5278.*

(122) Hanan, G. S.; Arana, C. R.; Lehn, J.-M.; Baum, G.; Fenske, D. *Chem. Eur. J.* 1996,2, 1292.

(123) Hayashi, M.; Miyamoto, Y.; Inoue, T.; Oguni, N. *J. Chem. Soc, Chem. Commun.* **1992**, 1752.

(124) Hanan, G. S.; Arana, C. R.; Lehn, J.-M.; Fenske, D. *Angew. Chem. Int. Ed. Engl.* **1995,** *34,* 1122.

(125) Persky, N. S.; Chow, J. M.; Poschmann, K. A.; Lacuesta, N. N.; Stoll, S. L.; Bott, S. G.; Obrey, S. *Inorg. Chem.* **2001,** *40,* 29.

(126) Tong, M.-L.; Chen, H.-J.; Chen, X.-M. *Inorg. Chem.* **2000,** *39,* 2235.

(127) Blake, A. J.; Li, W.-S.; Lippolis, V.; Schroder, M. *Chem. Commun.* **1997,** 1943.

(128) Hunter, C. A. *Angew. Chem. Int. Ed. Engl.* **1995,** *34,* 1079.

(129) Hannon, M. J.; Painting, C. L.; Errington, W. *Chem. Commun.* **1997,** 1805.

(130) Albrecht, M. *Chem. Rev.* **2001,** *101,* 3457.

(131) Tong, M.-L.; Zheng, S.-L.; Chen, X.-M. *Polyhedron* **2000,** *19,* 1809.

(132) Noro, S.-i.; Kitagawa, S.; Kondo, M.; Seki, K. *Angew. Chem. Int. Ed.* **2000,** *39,* 2082.

(133) Sharma, C. V. K.; Griffin, S. T.; Rogers, R. D. *Chem. Commun.* **1998,** 215.

(134) Suenaga, Y.; Yan, S. G.; Wu, L. P.; Ino, I.; Kuroda-Sowa, T.; Maekawa, M.; Munakata, M. *J. Chem. Soc., Dalton Trans.* **1998,** 1121.

(135) Fujita, M.; Kwon, Y. J.; Washizu, S.; Ogura, K. *J. Am. Chem. Soc.* **1994,** *116,* 1151.

(136) Braga, D.; Angeloni, A.; Grepioni, F.; Tagliavini, E. *Chem. Commun,* **1997,** 1447.

(137) Liu, Q.-D.; Li, J.-R.; Gao, S.; Ma, B.-Q.; Liao, F.-H.; Zhou, Q.-Z.; Yu, K.-B. *Inorg. Chem. Commun.* **2001,** *4,* 301.

(138) Batten, S. R.; Jensen, P.; Moubaraki, B.; Murray, K. S. *Chem. Commun.* **2000,** 2331.

(139) Gardner, G. B.; Venkataraman, D.; Moore, J. S.; Lee, S. *Nature* **1995,** *374,* 792.

(140) Goher, M. A. S.; Cano, J.; Journaux, Y.; Abu-Youssef, M. A. M.; Mautner, F. A.; Escuer, A.; Vicente, R. *Chem. Eur. J.* **2000,** *6,* 778.

(141) Venkataraman, D.; Gardner, G. B.; Lee, S.; Moore, J. S. *J. Am. Chem. Soc.* **1995,** 777, 11600.

(142) Zaworotko, M. J. *Chem. Soc. Rev.* **1994,** *25,* 283.

(143) Yeung, W.-F.; Man, W.-L.; Wong, W.-T.; Lau, T.-C.; Gao, S. *Angew. Chem. Int. Ed.* **2001,40,3031.**

(144) Ferlay, S.; Koenig, S.; Hosseini, M. W.; Pansanel, J.; Cian, A. D.; Kyritsakas, N. *Chem. Commun.* 2002, 218.

(145) Carlucci, L.; Ciani, G.; Proserpio, D. M.; Sironi, A. *Chem. Commun.* **1994,** 2755.

(146) Hoskins, B. F.; Robson, R. *J. Am. Chem. Soc.* **1990,** 772, 1546.

(147) Whitesides, G. M.; Mathias, J. P.; Seto, C. T. *Science* **1991,** *236,* 1312.

(148) Swiegers, G. F.; Malefetse, T. J. *Chem. Rev.* **2000,** *1 00,* 3483.

(149) Rebenau, A. *Angew. Chem. Int. Ed. Engl.* 1985, *24,* 1026.

(150) Laudise, R. A. *Prog. Inorg. Chem.* **1962,** *3,* 1.

(151) Hagrman, P. J.; Hagrman, D.; Zubieta, J. *Angew. Chem. Int, Ed.* **1999,** *38,* 2638.

(152) Shahriari, D. Y.; Barnabe, A.; Mason, T. O.; R., P. K. *Inorg. Chem.* **2001,** *40,* 5734.

(153) Gutschke, S. O. H.; Molinier, M.; Powell, A. K.; Winpenny, R. E. P.; Wood, P. T. *Chem. Commun.* 1996, 823.

(154) Kim, **Y.;** Jung, D.-Y. *Inorg. Chem.* **2000,** *39,* 1470.

(155) Bazan, B.; Mesa, J. L.; Pizarro, J. L.; Goni, A.; Lezama, L.; Arriortua, M. L.; Rojo, T. *Inorg. Chem.* **2001,** *40,* 5691.

(156) Tao, J.; Tong, M.-L.; Shi, J.-X.; Chen, X.-M.; Ng, S. W. *Chem. Commun.* **2000,** 2043.

(157) Zhang, J.; Xiong, R.-G.; Chen, X.-T.; Che, C.-M.; Xue, Z.; You, X.-Z. *Organometallics* 2001, *20,* 4118.

(158) Evans, O. R.; Lin, W. *Chem. Mater.* **2001,** 73, 3009.

(159) Evans, O. R.; Lin, W. *Chem. Mater.* **2001,** *13,* 2705.

(160) Ayyappan, P.; Evans, O. R.; Lin, W. *Inorg. Chem.* **2001,** *40,* 4627.

(161) Feng, S.; Xu, R. *Acc. Chem. Res.* **2001,** *34,* 239.

(162) Ref. 75, pp 352.

(163) Bernalte-García, A.; Diaz-Diez, M. A.; Garcia-Barros, F. J.; Higes-Rolando, F. J.; Pizarro-Galán, A. M.; Martin-Ramos, J. D.; Valenzuela-Calahorro, C. *Polyhedron* **1997,** *16*, 297.

(164) Bailey, R. D.; Pennington, W. T. *Polyhedron* **1997,** *16,* 417.

(165) Goher, M. A. S.; Mautner, F. A. *Polyhedron* **2000,** *19,* 601.

(166) Kawashima, T.; Takai, K.; Aso, H.; Manabe, T.; Takizawa, K.; Kachi-Terajima, C; Ishii, T.; Miyasaka, H.; Matsuzaka, H.; Yamashita, M.; Okamato, H.; Kitagawa, H.; Shiro, M.; Toriumi, K. *Inorg. Chem.* **2001,** *40,* 6651.

(167) Menon, S.; Rajasekharan, M. V.; Tuchagues, J.-P. *Inorg. Chem.* **1997,** *36,* 4341.

(168) Miller, J. S.; Epstein, A. J. *Angew. Chem. Int. Ed. Engl.* **1994,** *33,* 385.

(169) Kahn, O.; Martinez, C. J. *Science* **1998,** *279,* 44.

(170) Verdaguer, M. *Polyhedron* **2001,** *20,* 1115.

(171) Kahn, O. *Molecular Magnetism;* VCH: New York, 1993.

(172) Ferlay, S.; Mallah, T.; Ouahes, R.; Veillet, P.; Verdaguer, M. *Nature* **1995,** *378,* 701.

(173) Holmes, S. M.; Girolami, G. S. *J. Am. Chem. Soc.* **1999,** *121,* 5593.

(174) Miller, J. S. *Inorg. Chem.* **2000,** *39,* 4392.

(175) Borgne, T. L.; Riviere, E.; Marrot, J.; Thuery, P.; Girerd, J.-J.; Ephritikhine, M. *Chem. Eur. J.* 2002, *8,* 774.

(176) Triki, S.; Pala, J. S.; Decoster, M.; Molinie, P.; Toupet, L. *Angew. Chem. Int. Ed.* *1999,38,* 113.

(177) Zhang, S.-W.; Fu, D.-G.; Sun, W.-Y.; Hu, Z.; Yu, K.-B.; Tang, W.-X. *Inorg. Chem.* **2000,** *39,* 1142.

(178) Yan, B.; Wang, H.-D.; Chen, Z.-D. *Polyhedron* **2001,** *20,* 591.

(179) Miller, J. S.; Manson, J. L. *Acc. Chem. Res.* **2001,** *34,* 563.

(180) Kou, H.-Z.; Gao, S.; Jin, X. *Inorg. Chem.* **2001,** *40,* 6295.

(181) Monfort, M.; Resino, I.; Ribas, J.; Stoeckli-Evans, H. *Angew. Chem. Int. Ed.* **2000,** *39,* 191.

(182) De Munno, G.; Poerio, T.; Viau, G.; Julve, M.; Lloret, F. *Angew. Chem. Int. Ed. Engl.* **1997,36,** 1459.

(183) Hao, X.; Wei, Y.; Zhang, S. *Chem. Commun.* **2000,** 2271.

(184) Abu-Youssef, M. A. M.; Escuer, A.; Goher, M. A. S.; Mautner, F. A.; Reiß, G. J.; Vicente, R. *Angew. Chem. Int. Ed.* 2000, *39,* 1624.

(185) Goher, M. A. S.; Cano, J.; Journaux, Y.; Abu-Youssef, M. A. M.; Mautner, F. A.; Escuer, A.; Vicente, R. *Chem. Eur. J.* **2000,** *6,* 778.

(186) Tang, L.-F.; Zhang, L.; Li, L.-C; Cheng, P.; Wang, Z.-H.; Wang, J.-T. *Inorg. Chem.* **1999,** *38,* 6326.

(187) Li, L.; Liao, D.; Jiang, Z.; Yan, S. *Polyhedron* **2000,** *19,* 1575.

(188) Reddy, K. R.; Rajasekharan, M. V.; Tuchagues, J.-P. *Inorg. Chem.* **1998,37,** 5978.

(189) Mathevet, F.; Luneau, D. *J. Am. Chem. Soc.* **2001,** *123,* 7465.

(190) Sun, Z. M.; Ruiz, D.; Rumberger, E.; Incarvito, C. D.; Folting, K.; Rheingold, A. L.; Christou, G.; Hendrickson, D. N. *Inorg. Chem.* **1998,** *37,* 4758.

(191) Aubin, S. M. J.; Spagna, S.; Eppley, H. J.; Sager, R. E.; Christou, G.; Hendrickson, D. N. *Chem. Commun.* **1995,** 803.

(192) Eppley, H. J.; Tsai, H.-L.; de Vries, N.; Folting, K.; Christou, G.; Hendrickson, D. N. *J. Am. Chem. Soc.* **1995,** *117,* 301.

(193) Lis, T. *Acta Cryst.* **1980,** *B36,* 2042.

(194) Gatteschi, D.; Sessoli, R.; Cornia, A. *Chem. Commun.* **2000,** 725.

(195) Slageren, J. v.; Sessoli, R.; Gatteschi, D.; Smith, A. A.; Helliwell, M.; Winpenny, R. E. P.; Cornia, A.; Barra, A.-L.; Jansen, A. G. M.; Rentschler, E.; Timco, G. A. *Chem. Eur. J.* 2002, *8,* 277.

(196) Andres, R.; Brissard, M.; Gruselle, M.; Train, C; Vaissermann, J.; Malezieux, B.; Jamet, J.-P.; Verdaguer, M. *Inorg. Chem.* **2001,** *40,* 4633.

(197) Gan, X.; Munakata, M.; Kuroda-Sowa, T.; Maekawa, M. *Bull. Chem. Soc. Jpn.* **1994,** *67,* 3009.

(198) Gan, X.; Munakata, M.; Kuroda-Sowa, T.; Maekawa, M.; Yamamoto, M. *Polyhedron* 1995, *14,* 1647.

(199) Munakata, M.; Kuroda-Sowa, T.; Maekawa, M.; Hirota, A.; Kitagawa, S. *Inorg. Chem.* **1995,** *34,* 2705.

(200) Kuroda-Sowa, T.; Hirota, A.; Munakata, M.; Maekawa, M. *Mol. Cryst. Liq. Cryst.* **1996,** *285,* 69.

(201)   Shriver, D. F.; Atkins, P. W.; Langford, C. H. *Inorganic Chemistry;* Oxford
        University Press, Walton Street, Oxford 0X2 6DP, 1990, pp 588.

(202)   Janiak, C.; Scharmann, T. G.; Albrecht, P.; Marlow, F.; Macdonald, R. *J. Am.
        Chem. Soc.* 1996,775,6307.

(203)   Kyle, K. R.; Ryu, C. K.; DiBenedetto, J. A.; Ford, P, C. *J. Am. Chem. Soc.* **1991,**
        773,2954.

(204)   Ford, P. C.; Cariati, E.; Bourassa, J. *Chem. Rev.* **1999,** *99,* 3625.

(205)   Ma, Y.; Chao, H.-Y.; Wu, Y.; Lee, S. T.; Yu, W.-Y.; Che, C.-M. *Chem. Commun.*
        1998,2491.

(206)   Chen, Z.-F.; Xiong, R.-G.; Zhang, J.; Chen, X.-T.; Xue, Z.-L.; You, X.-Z. *Inorg.
        Chem.* 2001,40,4075.

(207)   Perreault, D.; Drouin, M.; Michel, A.; Harvey, P. D. *Inorg. Chem.* **1992,** *31,* 3688.

(208)   Heyduk, A. F.; Krodel, D. J.; Meyer, E. E.; Nocera, D. G. *Inorg. Chem. Commun.*
        2002, *41,* 634.

(209)   Rajendran, T.; Manimaran, B.; Lee, F.-Y.; Lee, G.-H.; Peng, S.-M.; Wang, C. M.;
        Lu, K.-L. *Inorg. Chem.* **2000,** *39,* 2016.

(210)   Buss, C. E.; Mann, K. R. *J. Am. Chem. Soc.* **2002,** *124,* 1031.

(211)   Kitazawa, T.; Nishikiori, S.-i.; Kuroda, R.; Iwamoto, T. *J. Chem. Soc, Dalton
        Trans.* **1994,** 1029.

(212)   Robinson, F.; Zaworotko, M. J. *J. Chem. Soc, Chem. Commun.* **1995,** 2413.

(213) **Yaghi,** O. M.; Li, H. *J. Am. Chem. Soc.* **1996,** *118,* 295.

(214) Kuehl, C. J.; Huang, S. D.; Stang, P. J. *J. Am. Chem. Soc.* **2001,***123, 9634.*

(215) Carlucci, L.; Ciani, G.; Proserpio, D. M.; Sironi, A. *Angew. Chem. Int. Ed. Engl.* 1995,34, 1895.

(216) Li, J.-M.; Zhang, Y.-G.; Chen, J.-H.; Rui, L.; Wang, Q.-M.; Wu, X.-T. *Polyhedron* 2000, *19,* 1117.

(217) Wang, R.; Hong, M.; Weng, J.; Su, W.; Cao, R. *Inorg. Chem. Commun.* **2000,** *3,* 486.

(218) Heo, J.; Kim, S.-Y.; Whang, D.; Kim, K. *Angew. Chem. Int. Ed.* **1999,** *38,* **641.**

(219) Lin, K.-J. *Angew. Chem. Int. Ed.* **1999,** *38,* 2730.

(220) Tadokoro, M.; Isobe, K.; Uekusa, H.; Ohashi, Y.; Toyoda, J.; Tashiro, K.; Nakasuji, K. *Angew. Chem. Int. Ed.* 1999, *38,* 95.

(221) Batten, S. R.; Hoskins, B. F.; Robson, R. *J. Am. Chem. Soc.* **1995,** *117,* 5385.

(222) Gardner, G. B.; Kiang, Y.-H.; Lee, S.; Asgaonkar, A.; Venkataraman, D. *J. Am. Chem. Soc.* **1996**, *118*, 6946.

(223) Eddaoudi, M.; Li, H.; Yaghi, 0. M. *J. Am. Chem. Soc.* **2000;** *122,* 1391.

(224) Batten, S. R.; Hoskins, B. F.; Robson, R. *Chem.Eur. J.* **2000,** *6,* 156.

(225) Kasai, K.; Aoyagi, ML; Fujita, K. *J. Am. Chem. Soc.* **2000,** *122,* 2140.

(226) Yuan, A.; Zou, J.; Li, B.; Zha, Z.; Duan, C; Liu, Y.; Xu, Z.; Keizer, S. *Chem. Commun.* **2000,** 1297.

(227) Choi, H. J.; Lee, T. S.; Suh, M. P. *Angew. Chem. Int. Ed.* **1999,** *38,* 1405.

(228) Kondo, M.; Okubo, T.; Asami, A.; Noro, S.-i.; Yoshitomi, T.; Kitagawa, S.; Ishii, T.; Matsuzaka, H.; Seki, K. *Angew. Chem. Int. Ed.* **1999,** *38,* 140.

(229) Kepert, C. J.; Rosseinsky, M. J. *Chem. Commun.* **1998,** 31.

(230) Brunet, P.; Simard, M.; Wuest, J. D. *J. Am. Chem. Soc.* **1997,** *119,* 2737.

(231) Carlucci, L.; Ciani, G.; Moret, M.; Proserpio, D. M.; Rizzato, S. *Angew. Chem. Int. Ed.* **2000,** *39,* 1506.

(232) Janiak, C. *Angew. Chem. Int. Ed. Engl.* 1997, *36,* 1431.

(233) Muller, A.; Reuter, H.; Dillinger, S. *Angew. Chem. Int. Ed Engl.* **1995,** *34,* 2328.

(234) Carlucci, L.; Ciani, G.; Proserpio, D. M.; Rizzato, S. *Chem. Commun.* **2000,** 1319.

Coordination Polymers of Silver(I) with Aminomethylpyridines

Ag^+ ion is well known for its two coordinate geometry, besides its tendency to show 3- and 4-coordination. The two coordination of Ag^+ helps formation of linear chains, when coordinated with suitable bridging ligands. The affinity of Ag^+ for N-donor ligands, especially pyridine and its derivatives is well known. Aminomethylpyridine is a ligand, which can act as bridging as well as chelating ligand depending on the orientation of the $-CH_2NH_2$ group relative to pyridine nitrogen position. 2-aminomethylpyridine (2-amp), which readily forms tris-chelates, is also known to bind in the bridging mode in a few compounds.[1-2] Its isomers, 3-aminomethylpyridine (3-amp) and 4-aminomethylpyridine (4-amp) can only act as bridging ligands. Our work with Ag^+ and amp resulted in various polymeric systems of Ag^+, where the chain formation is achieved by the coordination through the pyridine and amino nitrogens to different Ag(I) centers. The structural details of such polymeric Ag(I) complexes with the isomers of amp, *viz.,* 2-, 3- and 4-amp are presented in this chapter and comparisons are made based on the change in anion. The non-covalent forces that stabilize the packing patterns are highlighted.

2.1. Experimental

2.1.1. Synthesis

$AgClO_4.H_2O$ was prepared according to a reported procedure.[3] $AgBF_4$ and $AgPF_6$ were purchased from Acros Chemicals. 2-amp, 3-amp and 4-amp were purchased from Lancaster Chemicals.

Caution: Perchlorate salts are dangerous (especially if they are dry) and should be handled with care.

(a) Preparation of Ag(2-amp)ClO$_4$ (1): 2-amp (1.20 mL, 11.6 mmol) was added to a 5 mL aqueous solution of $AgClO_4 \cdot H_2O$ (2.255g, 10.01 mmol) and stirred for about 10-15 minutes. The white precipitate formed was filtered, washed with cold water and dried. Yield: 2.292g (7.27 mmol, 73 %). Single crystals suitable for X-ray analysis were obtained by slow concentration of aqueous solutions of the precipitate in a desiccator over con. H_2SO_4. Anal. Calcd. for $C_6H_8N_2O_4ClAg$ (MW: 315.465) C, 22.84; H, 2.56; N, 8.88. Found: C, 23.10; H, 2.54; N, 9.13. Characteristic IR peaks (KBr/cm[1]): 3325(b), 1595, 1477, 1437, 1087(b), 761, 626.

(b) Preparation of Ag(2-amp)BF$_4$ (2): 2-amp (0.65 mL, 6.3 mmol) was added to a 10 mL aqueous solution of $AgBF_4$ (1.283g, 6.59 mmol) and stirred for about 20 minutes. White precipitate formed was filtered, washed with cold water and dried. Yield: 1.520g (5.0 mmol, 79 %). Single crystals suitable for X-ray analysis were obtained by slow concentration of aqueous solutions of the precipitate in a desiccator over con. H2SO4. Anal. Calcd. for $C_6H_8N_2F_4BAg$ (MW 302.82): C, 23.80; H, 2.66; N, 9.25. Found, C, 23.77; H, 3.10; N, 8.61. Characteristic IR peaks (KBr/cm[1]): 3345, 1595, 1478, 1437, 1304, 1057(b), 762, 611.

(c) Preparation of $Ag_2(2\text{-amp})_3(PF_6)_2$ (3): 2-amp (0.2 mL, 1.9 mmol) was added to an aqueous solution of $AgPF_6$ (0.513g, 2.03 mmol) and stirred for about 1 hr. White precipitate formed was filtered, washed with cold water and dried. Yield: 0.560g.‡ Single crystals suitable for X-ray analysis were obtained by slow concentration of aqueous solutions of the precipitate in a desiccator over Con. H_2SO_4. Anal. Calcd. for $C_{18}H_{24}N_6F_{12}P_2Ag_2$ (MW 830.11) C, 26.05; H, 2.91; N, 10.12. Found: C, 26.26; H, 2.55; N, 9.86. Characteristic IR peaks (KBr/cm^{-1}): 3341, 1595, 1478, 1437, 1150, 841, 611, 559.

(d) Preparation of $Ag(3\text{-amp})ClO_4$ (4): 3-amp (1.00 mL, 9.82 mmol) was added to a 5 mL aqueous solution of $AgClO_4 \cdot H_2O$ (2.255g, 10.01 mmol) and stirred for about 10-15 minutes. The white precipitate formed was filtered, washed with cold water and dried. Yield: 3.003g (9.52 mmol, 97 %). Single crystals suitable for X-ray analysis were obtained by slow concentration of aqueous solutions of the precipitate in a desiccator over con. H_2SO_4. Anal. Calcd. for $C_6H_8N_2O_4ClAg$ (MW: 315.465) C, 22.84; H, 2.56; N, 8.88. Found: C, 23.03; H, 2.55; N, 8.11. Characteristic IR peaks (KBr/cm^{-1}): 3344, 1595, 1483,1431, 1087(b), 788,625.

(e) Preparation of $Ag(3\text{-amp})BF_4$ (5): 3-amp (0.52 mL, 5.1 mmol) was added to a 10 mL aqueous solution of $AgBF_4$ (1.071g, 5.50 mmol) and stirred for 30 minutes in an ice bath. The white precipitate formed was filtered, washed with cold water and dried. Yield: 0.857g (2.83 mmol, 55 %). Recrystallization of the precipitate from water yielded colorless crystals, which appear to loose crystallinity slowly and turn to pink color. Anal. Calcd. for $C_6H_8N_2F_4BAg$ (MW 302.82): C, 23.80; H, 2.66; N, 9.25. Found: C, 24.03; H, 2.60; N, 8.69. Due to poor quality of the crystals, single crystal x-ray data could not be

collected. Characteristic IR peaks (KBr/cm^{-1}): 3360, 1595, 1481, 1431, 1300, 1057(b), 790,710,639,520.

(f) Preparation of Ag$_2$(3-amp)$_3$(PF$_6$)$_2$ (6): 3-amp (0.28 mL, 2.7 mmol) was added to an aqueous solution of AgPF$_6$ (0.704g, 2.79 mmol) and stirred for about 1 hr. White precipitate formed was filtered, washed with cold H$_2$O and dried. Yield: 1.005g.J Single crystals **suitable** for X-ray analysis were obtained by slow concentration of aqueous solutions of the precipitate in a desiccator over con. H2SO4. Anal. Calcd. for C$_{18}$H$_{24}$N$_6$F$_{12}$P$_2$Ag$_2$ (MW 830.11) C, 26.05; H, 2.91; N, 10.12; Found: C, 26.07; H, 2.74; N, 9.46. Characteristic IR peaks (KBr/crn^1): 3414, 1615, 1483, 1431, 1397, 831, 710, 640, 559.

(g) **Preparation of Ag(4-amp)ClO$_4$·0.5H$_2$O** (7): 4-amp (1.00 mL, 9.8 mmol) was added to a 5 mL aqueous solution of AgClO$_4$·H$_2$O (2.260g, 10.03 mmol) and stirred for about 10 -15 minutes. The white precipitate formed was filtered, washed with cold water and dried. Yield: 2.557g (7.91 mmol, 81 %). Single crystals suitable for X-ray analysis were obtained by slow concentration of aqueous solutions of the precipitate in a desiccator over con. H$_2$SO$_4$. Anal. Calcd. for C$_6$H$_9$N$_2$O$_{4.5}$ClAg (MW 323.46): C, 22.21; H, 2.80; N, 8.63. Found: C, 22.97; H, 2.43; N, 8.98. Characteristic IR peaks (KBr/cm^{-1}): 3315(b), 1612, 1429, 1086(b), 806,625.

(h) Preparation of Ag(4-amp)BF$_4$·0.75CH$_3$CN (8): 4-amp (0.5 mL, 4.9 mmol) was added to a 3 mL aqueous solution of ·AgBF$_4$ (l.OlOg, 5.19 mmol) and stirred continuously for about 15-20 minutes. White precipitate formed was filtered, washed with cold H$_2$O and dried. Yield: 1.46g (4.4 mmol, 89 %). Single crystals suitable for X-ray analysis were obtained by recrystallization of the precipitate from CH3CN at RT. Anal. Calcd. for C$_{15}$H$_{20.5}$N$_{5.5}$F$_8$B$_2$Ag$_2$ (MW 667.23): C, 27.00; H, 3.10; N, 11.55. Found:

C, 27.09; H, 3.05; N, 11.50. Characteristic IR peaks (KBr/cm^{-1}): 3337, 1609, 1562, 1429, 1360, 1057, 926, 795, 631.

(i) Preparation of Ag(4-amp)PF$_6$ (9): 4-amp (0.21 mL, 2.1 mmol) was added to an aqueous solution of AgPF$_6$ (0.512g, 2.03 mmol) and stirred continuously for 1 hr. White precipitate formed was filtered, washed with cold H$_2$O and dried. Yield: 0.631g (1.75 mmol, 86 %). Single crystals suitable for X-ray analysis were obtained by slow concentration of aqueous solutions of the precipitate in a desiccator over Con. H2SO4. Anal. Calcd. for C$_6$H$_8$N$_2$F$_6$PAg (MW 360.98) C, 19.96; H, 2.23; N, 7.76. Found: C, 20.27; H, 2.02; N, 7.32. Characteristic IR peaks (KBr/cm^{-1}): 3356, 1618, 1595, 1562, 1468, 1433, 1366, 1233, 1130, 1069, 995, 831, 619, 557.

2.1.2. Physical Measurements: IR spectra were recorded on a Jasco 5300 FT/IR infrared spectrometer. C, H, N analysis was performed on a Perkin-Elmer 240C elemental analyzer for 1, 4, 7 and 8 at the University of Hyderabad, and on a Perkin Elmer 2400 CHNS/O analyzer for 2, 3, 5, 6 and 9 at CSMCRI, Bhavnagar. X-ray data were collected on an Enraf Nonius CAD-4 diffractometer for 1, 4, 7 and 8 at the University of Hyderabad and for 2, 3, 6 and 9 at IIT, Bombay. Powder diffractograms were measured using PW3710 model Philips Analytical X-ray diffractometer.

2.1.3. X-ray Crystallography: X-ray data were collected for colorless crystals with dimensions, 0.46 x 0.40 x 0.28 mm for 1; 0.32 x 0.28 x 0.24 mm for 2; 0.80 x 0.44 x 0.40 mm for 3; 0.76 x 0.24 x 0.16 mm for 4; 0.30 x 0.25 x 0.20 mm for 6; 0.32 x 0.14 x 0.14 mm for 7; 0.56 x 0.42 x 0.40 mm for 8 and 0.40 x 0.35 x 0.35 mm for 9 on an Enraf Nonius CAD-4 diffractometer using graphite monochromated Mo-Ka radiation. The data were corrected for Lorentz polarization effects and absorption.[4] The structures were solved by a combination of Patterson heavy atom method and direct methods (SHELXS-

97) and refined (over F^2) by least squares techniques (SHELXL-97).[5] Drawings were made using ORTEP-III[6] and Rasmol 2.6.[7]

1 crystallizes in the triclinic system, space group P 1̄ with 2 molecules in the unit cell. A total of 4332 reflections (4280 unique, 3524 with $F > 4\sigma F$) were collected in the θ range 1.83 to 27.48, with indices $0 < h < 9$, $-14 < k < 14$, $-14 < l < 14$. All the non-hydrogen atoms were refined anisotropically while the ring hydrogen atoms were included in the calculated positions using a riding model. Bond length constraints were applied to methylene and amine hydrogens after locating from difference maps. All hydrogens were assigned fixed U_{iso} values, equal to $1.2U_{eq}$ of the parent atom for ring atoms and $1.5U_{eq}$ for CH_2 and NH_2 hydrogen atoms. The final cycle of full matrix least squares refinement on F^2 converged with unweighted and weighted refinement factors of $R1 = 0.0463$ and $wR2 = 0.1130$ respectively. The goodness of the fit (S) is 1.094 for 4280 unique reflections and 278 parameters. The maximum and minimum residual electron density on the final fourier map corresponded to 2.04 and -1.90 e/A^{3} respectively.

2 crystallizes in the monoclinic system, space group $C2/c$, with 8 molecules in the unit cell. A total of 2362 reflections (2078 unique, 1843 with $F > 4\sigma F$) were collected in the θ range 2.52 to 27.47, with indices $-7 < h < 21$, $0 < k \leq 14$, $-14 < l < 12$. All the non-hydrogen atoms were refined anisotropically while the ring and methylene hydrogen atoms were included in the calculated positions using a riding model. Bond length constraints were applied to amine hydrogens after locating from difference maps. All hydrogens were assigned fixed U_{iso} values, equal to $1.2U_{eq}$ of the parent atom for ring and methylene hydrogens. The U_{iso} of amine hydrogens were refined. The final cycle of full matrix least squares refinement on F^2 converged with unweighted and weighted refinement factors of $R1 = 0.0195$ and $wR2 = 0.0478$ respectively. The goodness of the fit

(S) is 1.082 for 2078 unique reflections and 136 parameters. The maximum and minimum residual electron density on the final fourier map corresponded to 0.354 and -0.059 e/A"^{3} respectively.

3 crystallizes in the monoclinic system, space group $P2_1/a$, with 4 molecules in the unit cell. A total of 6735 reflections (6433 unique, 2981 with $F > 4\sigma F$) were collected in the θ range 1.47 to 27.47, with indices $0 < h < 13$, $0 < k < 26$, $-18 < l < 17$. All the non-hydrogen atoms were refined anisotropically while the ring and methylene hydrogen atoms were included in the calculated positions using a riding model. Bond length constraints were applied to amine hydrogens after locating from difference maps. All hydrogens were assigned fixed U_{iso} values, equal to $1.2U_{eq}$ of the parent atom for ring and methylene hydrogens and $1.5U_{eq}$ for the amine hydrogens. Among the two PF_6^- ions, one is disordered. The disorder is modeled by splitting each fluorine into two halves and their site occupation is tied with free variable (FVAR), which is refined. Bond length constraints were applied to P-F and F-F distances to fit an octahedron. The final cycle of full matrix least squares refinement on F^2 converged with unweighted and weighted refinement factors of $R\backslash = 0.0581$ and $wR2 = 0.1534$ respectively. The goodness of the fit (S) is 0.931 for 6433 unique reflections and 434 parameters. The maximum and minimum residual electron density on the final fourier map corresponded to 0.808 and -0.792 e/Å$^-$ respectively.

Crystallographic data for 1, 2 and 3 are presented in Table 2.1, atomic parameters for 1 are tabulated in Table 2.2, for 2 in Table 2.3 and for 3 in Table 2.4 respectively.

Table 2.1 Crystallographic data for Ag(2-amp)ClO$_4$ (1), Ag(2-amp)BF$_4$ (2) and Ag$_2$(2-amp)$_3$(PF$_6$)$_2$ (3).

	1	2	3
formula	C$_{12}$H$_{16}$Ag$_2$Cl$_2$N$_4$O$_8$	C$_6$H$_8$AgBF$_4$N$_2$	C$_{18}$H$_{24}$Ag$_2$F$_{12}$N$_6$P$_2$
formula weight	630.93	302.82	830.11
a *(A)*	7.672(6)	16.788(2)	10.029(7)
b (A)	11.1401(11)	11.5719(6)	20.291(12)
c (Å)	11.322(4)	11.3864(7)	13.907(6)
α (°)	91.207(14)	90	90
β (°)	105.52(4)	123.671(8)	95.38(5)
γ (°)	90.48(2)	90	90
V (Å^3)	932.1(8)	1840.9(3)	2818(3)
Z	2	**8**	**4**
Space group	$P\bar{1}$	*C2lc*	*P2\la*
T (K)	293(2)	293(2)	293(2)
λ (A)	0.71073	0.71073	0.71073
ρ_{calcd}(Mg/m^3)	2.248	2.185	1.957
//(mm^{-1})	2.438	2.210	1.604
$R1$	0.0463	0.0195	0.0581
$wR2$	0.1130	0.0478	0.1534

weighting scheme, **1**:$A = 0.0873$; $B = 0.0103$; **2**: $A = 0.0232$; $B = 1.5807$;

3: $A = 0.1059$; $B = 0.0000$ (see p. vi for definitions).

Table 2.2 Atomic parameters for Ag(2-amp)ClO$_4$ (1).

Atom	10^4x	10^4y	10^4z	10^3U_{eq}	Atom	10^4x	10^4y	10^4z	10^3U_{eq}
Ag1	5052(1)	4186(1)	2752(1)	42(1)	C9	8881(7)	6720(5)	6059(4)	49(1)
Ag2	3853(1)	9166(1)	1252(1)	44(1)	C10	8730(7)	5497(5)	6180(4)	47(1)
N1	2297(5)	217(3)	-226(3)	34(1)	CH	7633(6)	4843(4)	5228(4)	44(1)
N2	3257(4)	3283(3)	1174(3)	32(1)	C12	5674(6)	7029(4)	2885(4)	40(1)
N3	6682(5)	5345(3)	4186(3)	35(1)	CH	2259(1)	6163(1)	-311(1)	32(1)
N4	5524(5)	8330(3)	2855(3)	40(1)	01	2798(5)	5159(3)	-933(3)	55(1)
Cl	2142(5)	1415(4)	-102(3)	31(1)	02	1886(5)	5790(3)	799(3)	47(1)
C2	1051(6)	2073(4)	-1034(4)	38(1)	03	3713(4)	7045(3)	-30(3)	47(1)
C3	104(6)	1485(5)	-2107(4)	46(1)	04	680(4)	6698(3)	-1088(3)	48(1)
C4	258(7)	275(4)	-2229(4)	48(1)	Cl2	6630(1)	1311(1)	4265(1)	38(1)
C5	1371(6)	-334(4)	-1279(4)	43(1)	05	7917(6)	375(4)	4475(4)	67(1)
C6	3182(6)	1975(4)	1117(4)	35(1)	06	6743(6)	1948(3)	5400(3)	60(1)
C7	6816(5)	6531(4)	4068(3)	33(1)	07	7005(5)	2129(3)	3386(3)	58(1)
C8	7900(7)	7242(4)	4996(4)	47(1)	08	4838(5)	817(3)	3801(3)	57(1)

Table 2.3 Atomic parameters for Ag(2-amp)BF$_4$ (2).

Atom	10^4x	10^4y	10^4z	10^3U_{eq}	Atom	10^4x	10^4y	10^4z	10^3U_{eq}
Ag1	3859(1)	548(1)	1849(1)	41(1)	C6	3759(2)	1024(2)	-1005(2)	35(1)
N1	3787(1)	2139(2)	815(2)	36(1)	N2	3880(2)	1066(2)	-2185(2)	38(1)
Cl	3759(1)	2181(2)	-393(2)	33(1)	B1	3570(2)	-2190(2)	-380(2)	39(1)
C2	3719(2)	3227(2)	-1009(3)	49(1)	F1	4111(1)	-1643(1)	-812(2)	62(1)
C3	3705(2)	4244(2)	-389(3)	59(1)	F2	3109(1)	-3129(1)	-1252(2)	56(1)
C4	3719(2)	4203(2)	829(3)	59(1)	F3	2909(1)	-1417(1)	-468(2)	61(1)
C5	3763(2)	3139(2)	1401(3)	51(1)	F4	4187(1)	-2550(2)	998(2)	70(1)

Table 2.4 Atomic parameters for $Ag_2(2\text{-amp})_3(PF_6)_2$ (3).

Atom	10^4x	10^4y	10^4z	10^3U_{eq}	Atom	10^4x	10^4y	10^4z	10^3U_{eq}
Ag1	6357(1)	312(1)	1757(1)	81(1)	C17	3786(7)	-690(4)	3814(5)	71(2)
Ag2	4812(1)	724(1)	3461(1)	88(1)	C18	2493(8)	-325(4)	3562(7)	88(2)
N1	6598(5)	-816(3)	1934(4)	59(1)	N6	2645(6)	255(4)	3009(6)	99(2)
C1	7801(7)	-1014(3)	2277(5)	60(2)	P1	10282(2)	-1462(1)	5711(2)	76(1)
C2	8110(9)	-1678(4)	2376(6)	86(2)	F1A(0.50)	9030(2)	-1942(11)	5520(2)	104(8)
C3	7166(12)	-2135(4)	2122(7)	102(3)	F1B(0.50)	9040(2)	-1923(13)	5700(3)	142(13)
C4	5924(11)	-1935(4)	1764(6)	93(3)	F2A(0.50)	11110(2)	-2082(9)	6110(2)	141(11)
C5	5664(8)	-1280(4)	1686(5)	79(2)	F2B(0.50)	9410(3)	-836(11)	5730(3)	154(13)
C6	8846(8)	-502(4)	2562(6)	82(2)	F3A(0.50)	9420(3)	-893(12)	5230(2)	137(10)
N2	8596(7)	121(3)	2097(6)	87(2)	F3B(0.50)	11260(3)	-2051(10)	5750(3)	186(15)
N3	4770(6)	1019(3)	1327(4)	61(1)	F4A(0.50)	11591(19)	-1026(9)	5821(13)	113(9)
C7	3709(8)	805(4)	768(6)	81(2)	F4B(0.50)	11520(2)	-974(10)	5854(17)	157(14)
C8	2669(9)	1197(5)	438(6)	96(3)	F5A(0.50)	9830(2)	-1271(12)	6687(17)	120(7)
C9	2744(10)	1851(6)	669(7)	107(3)	F5B(0.50)	10470(4)	-1481(15)	6886(11)	154(11)
C10	3833(9)	2083(4)	1257(6)	86(2)	F6A(0.50)	10630(3)	-1607(12)	4652(14)	124(9)
C11	4823(7)	1665(3)	1576(5)	64(2)	F6B(0.50)	10180(4)	-1447(18)	4630(12)	183(14)
C12	6006(8)	1860(4)	2285(7)	87(2)	P2	-1593(2)	1129(1)	-456(2)	81(1)
N4	5748(7)	1686(3)	3274(5)	90(2)	F7	-2159(8)	1084(5)	-1525(4)	171(3)
N5	4928(6)	-338(3)	3929(4)	66(2)	F8	-2696(8)	642(3)	-171(6)	165(3)
C13	6053(8)	-660(5)	4228(5)	82(2)	F9	-2613(7)	1704(3)	-375(7)	164(3)
C14	6094(13)	-1311(6)	4422(7)	110(3)	F10	-1055(9)	1197(4)	646(5)	177(3)
C15	4941(16)	-1668(5)	4293(7)	120(4)	F11	-531(6)	1649(4)	-675(6)	168(3)
C16	3796(11)	-1363(5)	3995(7)	101(3)	F12	-600(9)	567(4)	-574(7)	203(4)

Site occupation factors of disordered sites are given after the respective atom labels.

4 crystallizes in the monoclinic system, space group *P2\lc* with 4 molecules in the unit cell. A total of 4905 reflections (4273 unique, 3111 with $F > 4\sigma F$) were collected in the θ range 1.58 to 27.45, with indices $-2 < h < 10$, $-4 < k \le 11$, $-33 < l < 33$. All the non-hydrogen atoms were refined anisotropically while the ring hydrogen atoms were included in the calculated positions using a riding model. Bond length constraints were applied to methylene and amine hydrogens after locating from difference maps. All hydrogens were assigned fixed U_{iso} values, equal to $1.2 U_{eq}$ of the parent atom for ring atoms and $1.5 U_{eq}$ for CH_2 and NH_2 hydrogen atoms. The final cycle of full matrix least squares refinement on F^2 converged with unweighted and weighted refinement factors of $R1 = 0.0600$ and $wR2 = 0.1505$ respectively. The goodness of the fit *(S)* is 1.085 for 4273 unique reflections and 277 parameters. The maximum and minimum residual electron density on the final fourier map corresponded to 1.129 and -1.227 e/A'^3 respectively.

6 crystallizes in the triclinic system, space group $P\bar{1}$, with 2 molecules in the unit cell. A total of 6890 reflections (6317 unique, 4086 with $F > 4a/^7$) were collected in the θ range 1.70 to 27.47, with indices $-4 \le h \le 13$, $-14 < k < 14$, $-15 < l < 15$. All the non-hydrogen atoms were refined anisotropically while the ring and methylene hydrogen atoms were included in the calculated positions using a riding model. Bond length constraints were applied to amine hydrogens after locating from difference maps. All hydrogens were assigned fixed U_{iso} values, equal to $1.2 U_{eq}$ of the parent atom for ring and methylene hydrogens and $1.5 U_{eq}$ for the amine hydrogens. Among the two PF_6^- ions, one is disordered. The disorder is modeled by splitting each fluorine into two halves and their site occupation is tied with free variable (FVAR), which is refined. Bond length constraints were applied to P-F and F-F distances to fit an octahedron. The final cycle of full matrix least squares refinement on F^2 converged with unweighted and weighted

refinement factors of R_1 = 0.0569 and $wR2$ = 0.1608 respectively. The goodness of the fit (5) is 1.038 for 6317 unique reflections and 434 parameters. The maximum and minimum residual electron density on the final fourier map corresponded to 0.801 and -1.188 e/Å^{-3} respectively.

Crystallographic data for 4 and 6 are presented in Table 2.5, atomic parameters for 4 are tabulated in Table 2.6 and for 6 in Table 2.7 respectively.

Table 2.5 Crystallographic data for Ag(3-amp)ClO$_4$ (4) and Ag$_2$(3-amp)$_3$(PF$_6$)$_2$ (6).

	4	6
formula	$C_{12}H_{16}Ag_2Cl_2N_4O_8$	$C_{18}H_{24}Ag_2F_{12}N_6P_2$
formula weight	630.93	830.11
a (Å)	8.345(4)	10.4482(7)
b (Å)	8.6748(7)	11.1468(9)
c (Å)	26.056(9)	12.2720(11)
α (°)	90	81.018(7)
β (°)	97.96(4)	80.868(6)
γ (°)	90	80.977(6)
V (Å^3)	1868.0(11)	1380.99(19)
Z	4	2
Space group	$P2_1/c$	$P\bar{1}$
T (K)	293(2)	293(2)
λ (A)	0.71073	0.71073
ρ_{calcd}(Mg/m^3)	2.243	1.996

Table 2.5 contd . . . . .

$\mu \ (\text{mm}^{-1})$	2.433	1.636
$R\backslash$	0.0600	0.0569
$wR2$	0.1505	0.1608

weighting scheme, 4: $A = 0.0904$; $B = 6.2536$; 6: $A = 0.1140$;

$B = 0.0000$; (see p. vi for definitions).

Table 2.6 Atomic parameters for $Ag(3\text{-}amp)ClO_4$ (4).

Atom	10^4x	10^4y	10^4z	10^3U_{eq}	Atom	10^4x	10^4y	10^4z	10^3U_{eq}
Ag1	1852(1)	8658(1)	1007(1)	45(1)	C10	3173(11)	15604(10)	238(3)	52(2)
Ag2	6779(1)	17207(1)	1532(1)	48(1)	C11	4332(10)	16429(9)	547(3)	41(2)
N1	1018(7)	6547(7)	1315(2)	35(1)	C12	3066(12)	12004(10)	1066(3)	49(2)
C1	1770(9)	5983(8)	1766(3)	36(2)	N4	2669(12)	10785(8)	691(3)	53(2)
C2	1274(8)	4661(8)	2001(3)	31(1)	Cl1	-3272(2)	4639(2)	2678(1)	38(1)
C3	-42(9)	3881(9)	1742(3)	40(2)	O1	-4247(7)	5847(8)	2417(3)	68(2)
C4	-814(9)	4407(9)	1282(3)	42(2)	O2	-4011(6)	4049(7)	3103(2)	44(1)
C5	-281(9)	5747(9)	1079(3)	42(2)	O3	-1690(7)	5214(8)	2874(3)	55(2)
C6	2277(9)	4154(10)	2504(4)	46(2)	O4	-3146(9)	3425(9)	2314(3)	65(2)
N2	1491(8)	3153(8)	2846(3)	43(2)	Cl2	7771(3)	10351(3)	682(1)	54(1)
N3	5083(7)	15872(7)	1001(2)	35(1)	O5	7910(18)	8848(10)	551(4)	135(5)
C1	4643(9)	14458(9)	1137(3)	36(2)	O6	6329(17)	10900(3)	493(8)	257(12)
C8	3483(9)	13555(8)	850(3)	35(2)	O7	8745(14)	11276(14)	388(5)	131(4)
C9	2740(11)	14163(10)	390(3)	49(2)	O8	8420(3)	10560(16)	1177(4)	220(10)

Table 2.7 Atomic parameters for $Ag_2(3\text{-amp})_3(PF_6)_2$ (6).

Atom	10^4x	10^4y	10^4z	10^3U_{eq}	Atom	10^4x	10^4y	10^4z	10^3U_{eq}
Ag1	1794(1)	1985(1)	4033(1)	83(1)	C17	-6197(5)	3955(5)	547(4)	57(1)
N1	2003(4)	1248(4)	2380(4)	68(1)	C18	-6209(7)	3917(6)	4011(5)	77(2)
C1	955(4)	1466(5)	1847(4)	60(1)	N6	-6580(5)	2752(5)	4586(4)	69(1)
C2	996(5)	1418(4)	721(5)	55(1)	P1	-8441(1)	4624(1)	-2571(1)	64(1)
C3	2217(6)	1130(6)	123(6)	79(2)	F1A(0.52)	-9566(12)	3964(17)	-1981(16)	156(8)
C4	3292(6)	877(7)	670(8)	97(2)	F1B(0.48)	-9414(15)	4714(18)	-1422(13)	166(8)
C5	3172(6)	945(6)	1779(7)	84(2)	F2A(0.52)	-7760(2)	4590(2)	-1611(13)	201(12)
C6	-247(5)	1679(6)	193(5)	68(1)	F2B(0.48)	-7490(14)	5080(2)	-1925(17)	150(9)
N2	-1077(5)	2784(5)	400(5)	81(2)	F3A(0.52)	-7556(14)	3479(16)	-2894(18)	165(7)
N3	-3187(4)	2585(5)	-1788(4)	66(1)	F3B(0.48)	-8040(3)	3278(13)	-2240(3)	300(2)
C7	-2088(5)	2348(7)	-2484(5)	78(2)	F4A(0.52)	-9402(11)	5810(13)	-2524(16)	131(6)
C8	-2003(6)	2167(8)	-3556(5)	87(2)	F4B(0.48)	-8820(3)	6061(13)	-2731(15)	158(10)
C9	-3191(8)	2256(10)	-3962(6)	116(3)	F5A(0.52)	-8990(2)	4712(17)	-3725(12)	172(9)
C10	-4299(7)	2464(10)	-3280(6)	115(3)	F5B(0.48)	-9500(2)	4350(3)	-3160(3)	280(2)
C11	-4298(5)	2635(7)	-2214(6)	85(2)	F6A(0.52)	-7375(17)	5390(2)	-3340(18)	192(9)
C12	-743(9)	1680(11)	-4184(7)	124(3)	F6B(0.48)	-7490(2)	4570(3)	-3585(11)	183(10)
N4	-288(9)	2463(11)	-4950(10)	210(7)	P2	-2903(1)	383(1)	3103(1)	60(1)
Ag2	-3134(1)	3092(1)	-70(1)	69(1)	F7	-3348(9)	-878(5)	3244(7)	197(3)
N5	-5057(4)	3655(4)	965(3)	55(1)	F8	-2375(7)	54(5)	4264(4)	151(2)
C13	-5095(5)	3680(5)	2062(4)	53(1)	F9	-2377(6)	1654(5)	2964(5)	136(2)
C14	-6232(5)	3988(5)	2774(4)	56(1)	F10	-4196(5)	1040(6)	3659(5)	149(2)
C15	-7404(5)	4301(5)	2293(5)	63(1)	F11	-3434(6)	745(6)	1956(4)	133(2)
C16	-7365(5)	4266(5)	1182(5)	65(1)	F12	-1569(5)	-214(5)	2477(4)	125(2)

Site occupation factors of disordered sites are given after the respective atom labels.

7 crystallizes in the hexagonal system, space group $P6_522$ with 12 molecules in the unit cell. A total of 5643 reflections (1718 unique, 995 with $F > 4\sigma F$) were collected in the θ range 2.52 to 24.93, with indices $0 < h < 11, -11 < k < 9, 0 < l < 46$. All the non-hydrogen atoms were refined anisotropically while the ring and methylene hydrogen atoms were included in the calculated positions using a riding model. Bond length constraints were applied to amine hydrogens after locating from difference maps. All hydrogens were assigned fixed U_{iso} values, equal to $1.2U_{eq}$ of the parent atom for ring atoms and $1.5U_{eq}$ for CH_2 and NH_2 hydrogen atoms. The final cycle of full matrix least squares refinement on F^2 converged with unweighted and weighted refinement factors of $R\backslash = 0.0579$ and $wR2 = 0.0981$ respectively. The goodness of the fit (S) is 1.032 for 1718 unique reflections and 139 parameters. The maximum and minimum residual electron density on the final fourier map corresponded to 0.441 and -0.417 $e/A^{"3}$ respectively.

8 crystallizes in the orthorhombic system, space group C222|, with 8 molecules in the unit cell. A total of 6323 reflections (6072 unique, 3944 with $F > 4\sigma F$) were collected in the θ range 2.52 to 30.01, with indices $-13 < h < 4, -22 < k < 22, -39 < l < 0$. All the non-hydrogen atoms, except for one disordered BF_4 unit and one solvent CH_3CN were refined anisotropically while the ring and methylene hydrogen atoms were included in the calculated positions using a riding model. Bond length constraints were applied to amine hydrogens after locating from difference maps. All hydrogens were assigned fixed U_{iso} values, equal to $1.2U_{eq}$ of the parent atom for ring and methylene hydrogens and $1.5U_{eq}$ for the amine hydrogens. One of the BF_4^- anion is highly disordered. The disorder is modeled by splitting each fluorine into two halves and their site occupation is tied with free variable (FVAR), which is refined. The disordered BF_4 unit is refined isotropically. Bond length constraints were applied to B-F and F-F distances to fit a tetrahedron.

Among the two solvent CH3CN molecules, only one molecule with half site occupation could be located fully. For the other CH3CN molecule with full site occupation, the methyl C atom could not be located. This may be due to the severe disorder in the anionic unit. Bond length constraints were applied to the -C≡N of the CH3CN molecule. The hydrogen atom positions of the methyl carbon (C14) of solvent CH3CN were initially located by geometrical considerations and their positions fixed as their geometry is going bad due to disorder in the parent C (C14) position. The final cycle of full matrix least squares refinement on F^2 converged with unweighted and weighted refinement factors of $R\backslash = 0.0766$ and $wR2 = 0.2064$ respectively. This high $R\backslash$ value is due to the severe disorder in one of the anionic unit. The goodness of the fit *(S)* is 1.067 for 6072 unique reflections and 285 parameters. The maximum and minimum residual electron density on the final fourier map corresponded to 1.356 and -1.378 e/Å^{-3} respectively.

9 crystallizes in the monoclinic system, space group $P2_1/m$, with 2 molecules in the unit cell. A total of 1426 reflections (1242 unique, 1145 with $F > 4\sigma F$) were collected in the θ range 2.83 to 27.46, with indices $-2 < h < 6$, $0 < k < 18$, $-9 < l < 9$. All the non-hydrogen atoms were refined anisotropically while the ring and methylene hydrogen atoms were included in the calculated positions using a riding model. Bond length constraints were applied to amine hydrogens after locating from difference maps. All hydrogens were assigned fixed U_{iso} values, equal to $1.2U_{eq}$ of the parent atom for ring and methylene hydrogens and $1.5U_{eq}$ for the amine hydrogens. The PF_6^- ion is found to be disordered. The disorder is modeled by splitting the equatorial fluorine atoms into two halves and their site occupation is tied with free variable (FVAR), which is refined. Bond length constraints were applied to P-F and F-F distances to fit an octahedron. The final cycle of full matrix least squares refinement on F^2 converged with unweighted and

weighted refinement factors of $R\backslash = 0.0474$ and $wR2 = 0.1241$ respectively. The goodness of the fit (S) is 1.079 for 1242 unique reflections and 104 parameters. The maximum and minimum residual electron density on the final fourier map corresponded to 1.794 and -1.230 e/A$^{"3}$ respectively.

Crystallographic data for 7, 8 and 9 are presented in Table 2.8, atomic parameters for 7 are tabulated in Table 2.9, for 8 in Table 2.10 and for 9 in Table 2.11 respectively.

Table 2.8 Crystallographic data for Ag(4-amp)ClO$_4$·0.5H$_2$O (7), Ag(4-amp)BF$_4$·0.75CH$_3$CN (8) and Ag(4-amp)PF$_6$ (9).

	7	8	9
formula	C$_6$H$_8$AgClN$_2$O$_{4.50}$	C$_{15}$H$_{20.50}$Ag$_2$B$_2$F$_8$N$_{5.50}$	C$_6$H$_8$AgF$_6$N$_2$P
formula weight	323.46	667.23	360.98
a (A)	9.3154(11)	9.272(2)	5.2089(7)
b (Å)	9.3154(11)	16.164(12)	14.3950(17)
c (Å)	39.313(5)	27.851(2)	7.0149(14)
α (°)	90	90	90
fin	90	90	96.538(14)
	120	90	90
γ (°)	2954.4(6)	4174(3)	522.6(13)
	12	8	2
z	$P6_522$	$C222_1$	$P2_1/m$
Space group	293(2)	293(2)	293(2)
T (K)	0.71073	0.71073	0.71073
λ (Å)			

Table 2.8 contd....

ρ_{calcd}(Mg/m^3)	2.182	2.123	2.294
μ (mm^{-1})	2.314	1.962	2.140
$R\backslash$	0.0579	0.0766	0.0474
$wR2$	0.0981	0.2064	0.1241

weighting scheme, 7: $A = 0.0400$; $B = 4.3428$; 8: $A = 0.1371$; $B = 3.5078$;

9: $A = 0.1069$; $B = 0.0000$ (see p. vi for definitions).

Table 2.9 Atomic parameters for Ag(4-amp)ClO$_4$·0.5H$_2$O (7).

Atom	10^4x	10^4y	10^4z	10^3U_{eq}	Atom	10^4x	10^4y	10^4z	10^3U_{eq}
Ag1	1121(1)	-29(1)	7835(1)	67(1)	N2	1009(15)	7651(12)	7745(3)	3(3)
N1	1272(13)	2324(11)	7915(2)	49(2)	CH	-2701(5)	-2701(5)	8333	77(1)
Cl	-93(16)	2434(15)	7927(3)	59(3)	01	-2250(2)	-1392(19)	8145(4)	245(9)
C2	-51(19)	3920(16)	7962(3)	66(4)	02	-3037(19)	-4019(18)	8143(4)	198(7)
C3	1394(16)	5371(12)	7979(3)	48(3)	Cl2	5380(3)	761(7)	7500	75(2)
C4	2795(14)	5258(14)	7966(3)	59(3)	03	4931(16)	1695(14)	7687(3)	154(5)
C5	2733(14)	3719(14)	7924(3)	55(3)	04	5663(17)	-228(19)	7714(3)	166(5)
C6	1508(16)	7029(15)	8035(3)	59(3)	OW	-2377(13)	5250(3)	7500	240(12)

Table 2.10 Atomic parameters for Ag(4-amp)BF$_4$·0.75CH$_3$CN (8).

Atom	10^4x	10^4y	10^4z	10^3U_{eq}	Atom	10^4x	10^4y	10^4z	10^3U_{eq}
Ag1	4581(1)	493(1)	3337(1)	59(1)	B1	5920(13)	2678(7)	3906(5)	70(4)
N1	2274(7)	559(6)	3242(3)	49(2)	F1	4731(10)	2438(10)	3653(4)	125(4)
Cl	1479(12)	-103(7)	3227(4)	56(3)	F2	6322(19)	2072(9)	4218(6)	189(8)
C2	-23(13)	-62(8)	3199(5)	63(3)	F3	7050(14)	2787(10)	3566(5)	167(7)
C3	-705(9)	679(8)	3163(4)	53(2)	F4	5741(19)	3376(7)	4152(7)	209(10)

Table 2.10 contd...

C4	148(11)	1387(7)	3172(4)	54(3)	B2	6790(2)	0	5000	72(5)
C5	1613(13)	1314(8)	3210(4)	61(3)	F5	7616(15)	-512(9)	4735(5)	198(8)
C6	-2332(12)	760(11)	3082(5)	78(4)	F6	6008(18)	451(9)	4688(5)	237(11)
N2	-3134(8)	479(9)	3491(4)	69(3)	B3	5000	-1351(15)	2500	124(12)
Ag2	3516(1)	-600(1)	4304(1)	65(1)	F7A(0.44)	3822(12)	-1875(14)	2420(10)	119(13)
N3	2265(9)	486(5)	4415(3)	44(2)	F8A(0.44)	5250(4)	-898(17)	2105(5)	480(8)
Cl	785(11)	462(7)	4436(4)	57(3)	F7B(0.56)	3795(11)	-832(14)	2509(13)	196(18)
C8	5(12)	1180(7)	4484(4)	58(3)	F8B(0.56)	4970(4)	-1800(16)	2093(4)	260(3)
C9	638(12)	1949(6)	4508(4)	48(2)	N5	5000	1455(11)	2500	78(5)
C10	2164(13)	1969(7)	4484(5)	60(3)	C13	5000	2100(16)	2500	99(8)
CH	2922(11)	1226(6)	4443(4)	49(2)	C14	5000	3049(16)	2500	260(4)
C12	-217(15)	2727(7)	4544(5)	68(3)	C15	2650(3)	-1520(17)	1467(9)	125(7)
N4	-320(12)	3268(6)	4175(4)	69(3)	N6	2500(4)	-1186(19)	1115(10)	179(10)

Site occupation factors of disordered sites are given after the respective atom labels.

Table 2.11 Atomic parameters for Ag(4-amp)PF$_6$ (9).

Atom	$10^4 x$	$10^4 y$	$10^4 z$	$10^3 U_{eq}$	Atom	$10^4 x$	$10^4 y$	$10^4 z$	$10^3 U_{eq}$
Ag	1531(1)	7500	1949(1)	40(1)	N1	-1438(10)	7500	3828(7)	39(1)
P	0	5000	10000	42(1)	Cl	-2362(8)	6705(3)	4453(6)	42(1)
F1	1425(6)	4014(2)	10108(5)	62(1)	C2	-4202(9)	6678(3)	5724(6)	43(1)
F2A(0.48)	-2270(3)	4569(11)	8680(4)	126(10)	C3	-5121(10)	7500	6409(7)	34(1)
F2B(0.52)	-2010(4)	4594(14)	8400(3)	125(9)	C4	-7054(11)	7500	7848(7)	37(1)
F3A(0.48)	1640(3)	5314(13)	8370(3)	127(11)	N2	-5772(9)	7500	9858(7)	38(1)
F3B(0.52)	1400(5)	5255(14)	8250(2)	153(14)					

Site occupation factors of disordered sites are given after the respective atom labels.

2.2. Results

2.2.1. Structure of Ag(2-amp)C104 (1): The asymmetric unit of 1 contains two Ag centers (Figure 2.1). The structure is a polymeric zig-zag chain made up from the coordination of Ag to the pyridine and amine N atoms from two different ligands. Agl is
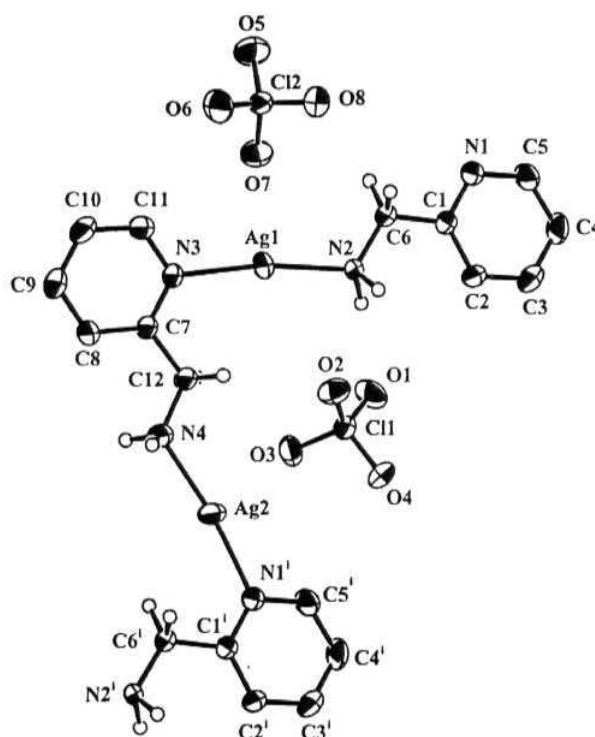
Figure 2.1 Ortep view of the molecular structure of 1 with atom labeling. Atoms are represented as 50% probability ellipsoids. Ring hydrogens have been omitted for clarity. Symmetry code: (i) x, $y + 1$, z.

coordinated to pyridine N (N3) of one ligand and an amine N (N2) of a different ligand with a linear geometry. The linear coordination of Ag2 is fulfilled by the coordination through a symmetry related pyridine N (Nl#l) and an amino nitrogen (N4) of two ligands (Table 2.12). The gross structure is similar to that of the previously reported nitrate analog,[2] except that the two Ag(2-amp) moieties that form the repeating unit in 1 are crystallographically different while in the nitrate salt they are related by symmetry.

Table 2.12 Bond lengths (A) and angles (°) and important stacking interactions for Ag(2-amp)ClO$_4$ (**1**).

Agl-N3	2.160(3)	Agl-N2	2.164(3)	Ag2-Nl#l	2.153(3)
Ag2-N4	2.156(3)	N3-Agl-N2	171.01(12)	Nl#l-Ag2-N4	172.62(13)

Cl1...N3#4	3.55(1)

#1 $x, y+1, z$ #4 $-x+1, -y+1, -z+1$

The crystal is made up of zigzag chains with the perchlorate ions occupying the voids formed between centrosymmetrically related chains (Figure 2.2). There is only very weak interaction between the Ag atoms and perchlorate 0 atoms (the shortest Ag···O distance is 2.732(3) A). The perchlorate ions are involved in hydrogen bonding with the amino groups.
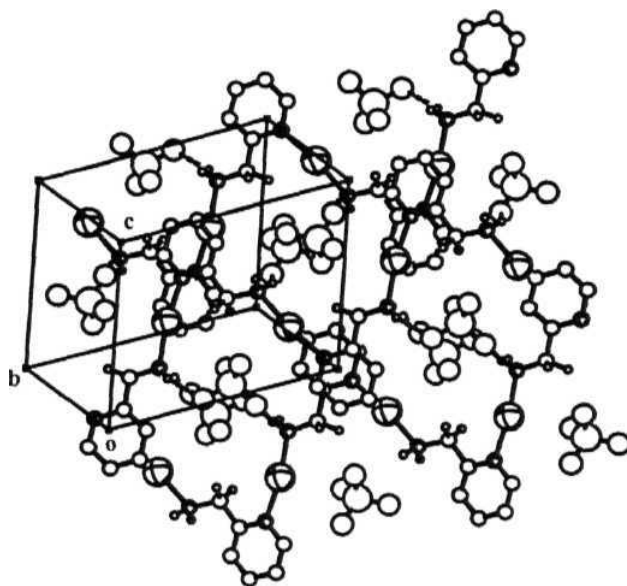
Figure 2.2 Packing diagram of 1. Large "footballs" represent silver atoms, and small "footballs" represent nitrogen atoms. Chlorine atoms are represented by large open circles.

2.2.2. Structure of Ag(2-amp)BF₄ (2): The polymeric chain of 2, has one Ag(2-amp)BF₄ in the asymmetric unit (Figure 2.3). The coordination geometry around Ag is linear (Table 2.13). The polymeric repeat unit is Ag-amp-Ag', where the neighboring silver centers in the chain are related by glide plane. Two such centrosymmetrically related chains are connected by weak Ag···Ag contacts, giving rise to a complex ladder like pattern. The anions are involved in hydrogen bonding with the amino group of the ligand (Figure 2.4).
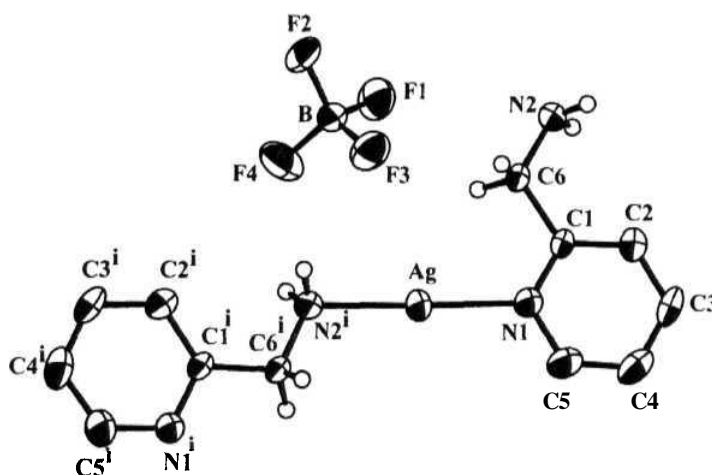
Figure 2.3 Ortep view of the molecular structure of 2 with atom labeling. Atoms are represented as 50% probability ellipsoids. Ring hydrogens have been omitted for clarity. Symmetry code: (i) x, $-y$, $z + 1/2$.

Table 2.13 Bond lengths (A) and angles (°), Ag$\cdots$Ag contacts and stacking interactions for Ag(2-amp)BF$_4$ (2).

Ag1-N1	2.1515(18)	Ag1-N2#1	2.1576(18)	N1-Ag1-N2#1	177.81(7)
Ag1...Ag1#2	3.2510(6)				
C5#4...C5#5	3.462(4)				

#1 x, $-y$, $z + 1/2$ #2 $-x + 1$, y, $z + 1/2$ #4 x, $-y$, $z + 3/2$ #5 $-x + 1$, $-y$, $-z + 2$
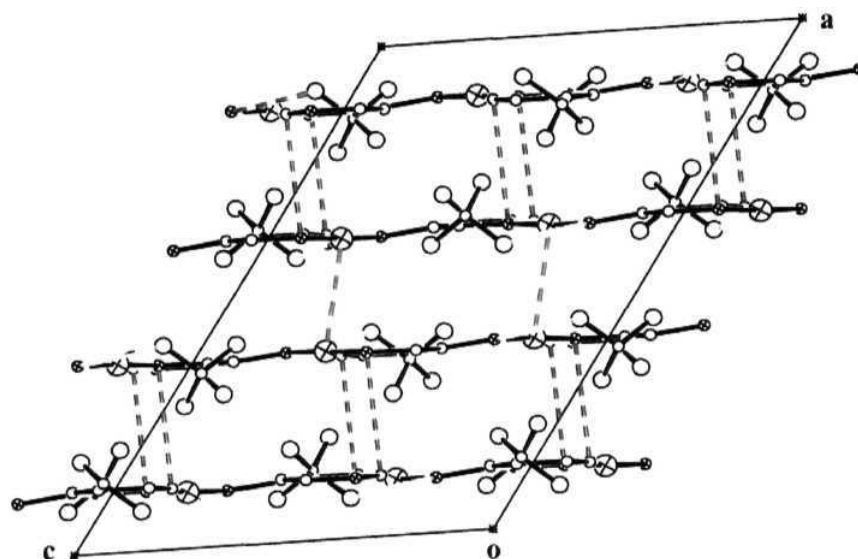
Figure 2.4 Packing diagram of 2. Large hatched circles represent Ag atoms and small hatched circles, the N atoms. Red lines indicate Ag· • • Ag interactions. Blue lines indicate ring stacking and yellow lines, the hydrogen bonding interactions.

2.2.3. Structure of $Ag_2(2\text{-}amp)_3(PF_6)_2$ (3): The structure of 3 is monomeric and dinuclear, and is different from 1 and 2. The asymmetric unit (Figure 2.5) contains two chemically inequivalent 3-coordinate Ag(I) centers. There are three ligands in the asymmetric unit. Two of them are acting as chelates with unsymmetrical Ag-N bonds. The third ligand bridges the two Ag(I) centers by coordinating through the amine (N4) and pyridine (N3) nitrogen atoms. The coordination around Ag1 is therefore, made up of two pyridine and amine nitrogen atoms. The bridging ligand binds more strongly with the Ag^+ ions with equal Ag-N distances (Table 2.14). Both Ag(I) centers have a distorted

trigonal planar coordination. Ag1 and Ag2 deviates by 0.073(4) and 0.042(4) A respectively from their coiTesponding coordination planes. The chelating angle around both the Ag atoms is acute [N2-Agl-Nl = 73.7(2)° and N5-Ag2-N6 = 73.6(2)°]. The short chelating angles along with unsymmetrical chelating Ag-N distances gives a distorted "Y" shaped geometry around both the Ag centers. The unsymmetrical nature of the chelation is more pronounced for Ag2 than Agl, as can be seen from the Ag-N distances.

(a)

(b)   (c)
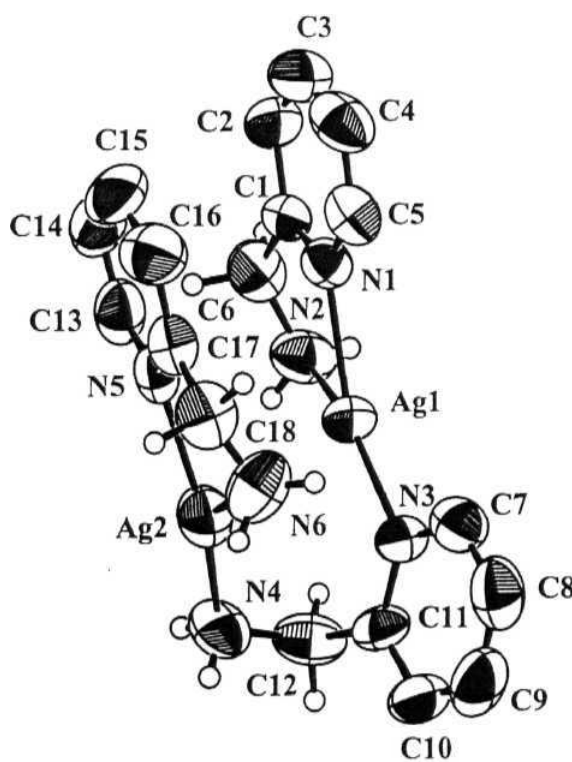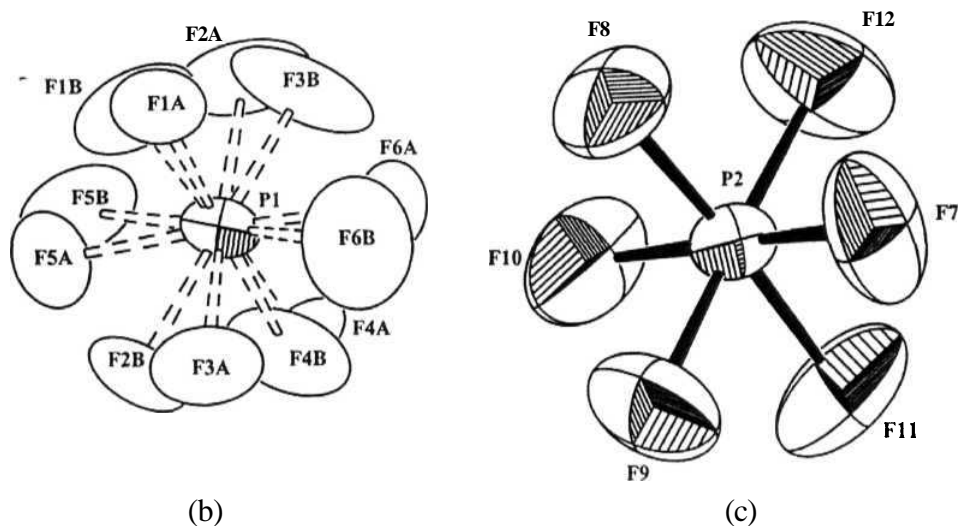
Figure 2.5 Ortep view of (a) cationic unit, (b) and (c) anionic units in 3 with atom labeling. Atoms are represented as 50% displacement ellipsoids for (a) and as 25% ellipsoids for (b) and (c). Ring hydrogens have been omitted for clarity. In (b), the disordered fluorine positions are indicated as open ellipses and bonds to them are shown as broken lines.

Table 2.14 Bond lengths (A) and angles (°), stacking interactions and Ag···Ag contacts for $Ag_2(2-amp)_3(PF_6)_2$ (**3**).

Ag1-N3	2.184(5)	Ag1-N2	2.284(7)	Ag1-N1	2.313(6)
Ag2-N4	2.193(7)	Ag2-N5	2.250(6)	Ag2-N6	2.401(7)
N3-Ag1-N2	147.7(2)	N3-Ag1-N1	138.2(2)	N2-Ag1-N1	73.7(2)
N4-Ag2-N5	151.1(2)	N4-Ag2-N6	135.1(3)	N5-Ag2-N6	73.6(2)

Table **2.14** contd. . . . .

N1...C13	3.302(9)	N1...N5	3.510(8)	C1...C13	3.442(11)
Ag1...Ag2	3.067(2)				

There is an intramolecular $Ag\cdots Ag$ interaction between the two Ag centers (Table 2.14). The distance of $Ag\cdots Ag$ separation falls in the range of $Ag\cdots Ag$ separation observed in other discrete molecules: (i) 2.88 A in dinuclear, 2-coordinate glycine silver(I) nitrate[8] (ii) 2.778 A and 2.834 A in dinuclear, 2- coordinate bis(3-hydroxy-4-phenyl-2,2,3-trimethylcyclohexane carboxylato)disilver(I) dihydrate[9] (iii) 3.38 - 3.49 A in dinuclear, 3- coordinate silver(I)-tricyclohexylarsine adduct[10] (iv) 3.177 A in hexanuclear, 2-coordinate Ag(I) imidazole perchlorate" (v) 3.085 A in dinuclear, 2-coordinate $Ag_2(dmp)_2(NO_3)_2$[12] and (vi) 3.087 A in dinuclear, 4- coordinate $Ag(dmbp)NO_3$.[13] Within the molecule, there are stacking interactions (Table 2.14). The unit cell has four independent molecules in which the cationic and anionic units are arranged in alternate layers (Figure 2.6). The anionic F's are involved in strong hydrogen bonding with the amine hydrogens, with $H\cdots A$ distances in the range 2.3 - 2.6 A. There is no Ag-F interaction present.
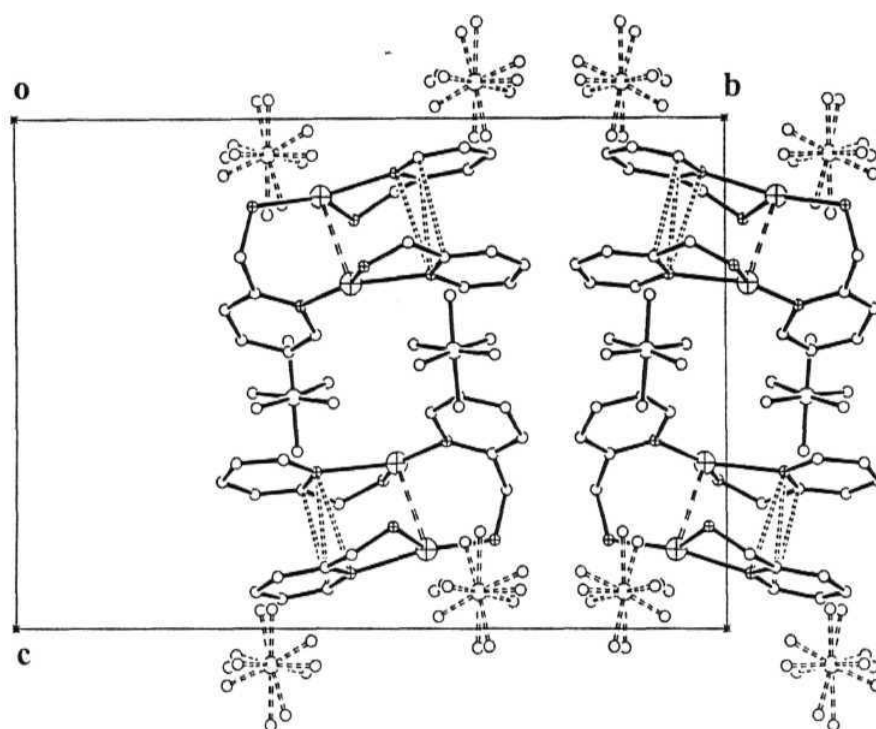
Figure 2.6 Packing diagram of 3. Large hatched circles represent Ag atoms and small hatched circles, N atoms. P atoms are shown as large open circles. Ring C and F atoms are shown as small open circles. Dashed lines indicate Ag⋯Ag interactions. Dotted lines indicate stacking interactions. The bonds from P to disordered F atoms are shown as broken lines.

2.2.4. Structure of Ag(3-amp)ClO₄ (4): The asymmetric unit of 4 (Figure 2.7), consists of two Ag(3-amp)ClO₄ sub units. As observed in 1, here also Ag1 and Ag2 have linear geometry. However, Ag1 is more linear than Ag2 (Table 2.15). Also, the linearity around Ag1 is more than in 1, while that around Ag2 is comparable to or same as in 1.
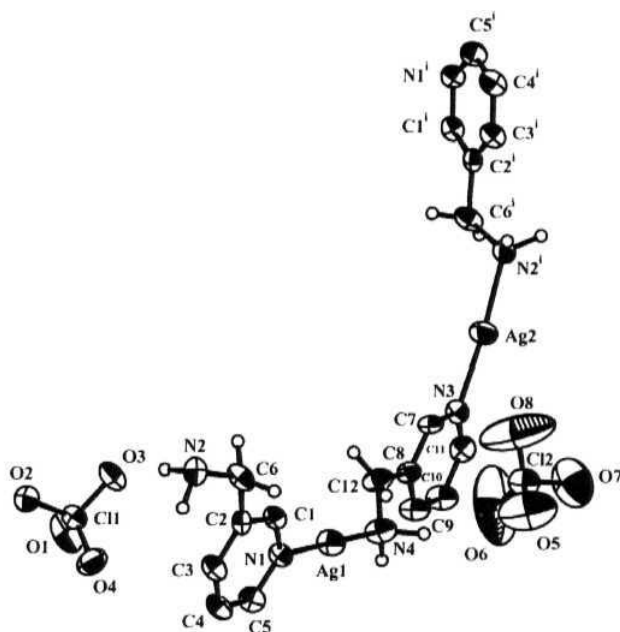
Figure 2.7 Ortep view of the molecular structure of 4 with atom labeling. Atoms are represented as 50% probability ellipsoids. Ring hydrogens have been omitted for clarity. Symmetry code: (i) -x + 1, y + 3/2, -z + 1/2.

Table 2.15 Selected bond lengths (A) and angles (°) and important stacking interactions for Ag(3-amp)ClO$_4$ (4).

Ag1-N1	2.153(6)	Ag1-N4	2.168(7)	Ag2-N2#l	2.177(7)
Ag2-N3	2.172(6)	N1-Ag1-N4	179.4(3)	N3-Ag2-N2#l	169.1(2)

C9...C5#2	3.57m

#1   -x + 1, -y 3/2, -z + 1/2   #2 x, y + 1, z

The polymeric chain of 4, is based on a repeating unit containing four Ag(3-amp) moieties. The chains assemble in the form of a triple helix (Figure 2.8). The helical repeat distance is 3 times the *b*-axis translation. There are two enantiomeric triple helices
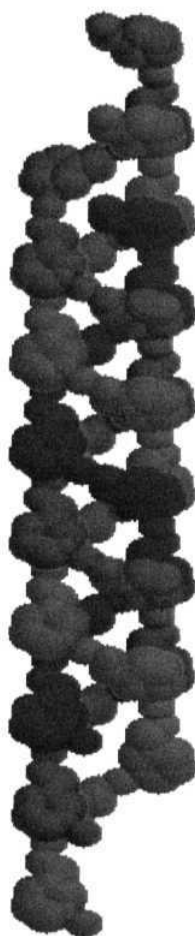
Figure 2.8 Space filling model of the triple helix in 4. The three strands are represented with three different colors.

running through the unit cell. This formation produces nearly 4A wide tunnels along the *b*-axis. Half the ClO_4^- ions are stacked inside these tunnels while the other half are stacked outside (Figure 2.9). Another unusual feature of the structure is that each triple helix is 'connected' by H-bonding of the ClO_4^- oxygen atoms from within the helix to the NH_2 groups of the adjacent helix, leading to the formation of a H-bonded string of triple helices along the *a*-axis (Figure 2.10).
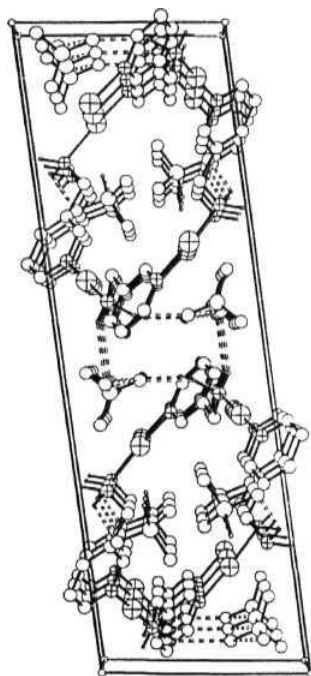
Figure 2.9 Packing diagram of 4. Large hatched atoms are silver atoms and small hatched atoms are nitrogen atoms. Hydrogen bonds are shown as broken lines.
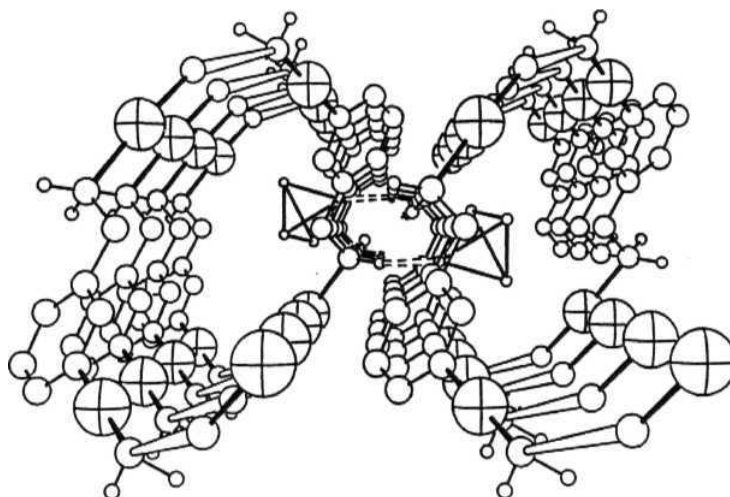
Figure 2.10 View showing the hydrogen bonded (broken lines) string of triple helices running along the *a*- axis in **4.**

2.2.5. Structure of Ag$_2$(3-amp)$_3$(PF$_6$)$_2$ (6): The asymmetric unit of 6 consists of two Ag(I) centers with 3- coordination (Figure 2.11). There are three ligands in the asymmetric unit, and all are acting as bridging ligands connecting the silver centers. Ag1 is coordinated to one pyridine and two amine N atoms from three different ligands. There are two short and one long Ag-N bonds. The N-Ag-N angles are close to 120°, thus giving a trigonal planar geometry to Ag1. However, the Ag1 atom deviates from the plane defined by its coordinating N atoms by 0.178(4) A. Coordination around Ag2 is completed by two pyridine and one amine nitrogen atom from three different ligands. There are one short Ag-N bond and two relatively longer Ag-N bonds. The asymmetry in

(a)

(b)

(c)
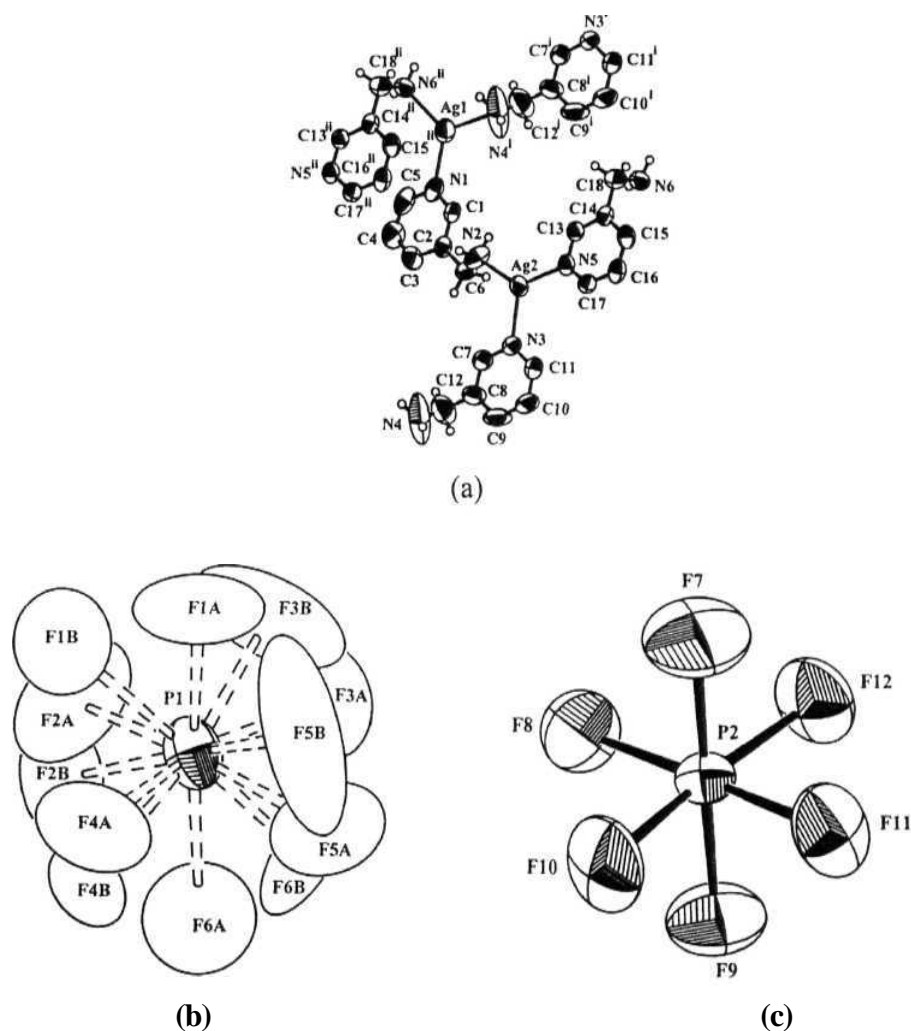
Figure 2.11 Ortep view of (a) cationic unit (b) and (c) anionic units in 6 with atom labeling. Atoms are represented as 50% displacement ellipsoids for (a) and as 25% ellipsoids for (b) and (c). Ring hydrogens have been omitted for clarity. In (b), the disordered fluorine positions are indicated as open ellipses and bonds to them are shown as broken lines. Symmetry codes: (i) $x, y, z + 1$; (ii) $x + 1, y, z$.

Table 2.16 Selected bond lengths (A) and angles (°) and important stacking interactions for $Ag_2(3\text{-}amp)_3(PF_6)_2$ (**6**).

Ag1-N1	2.271(5)	Ag1-N4#2	2.357(10)	Ag1-N6#1	2.255(5)
Ag2-N2	2.274(5)	Ag2-N3	2.277(4)	Ag2-N5	2.256(4)
N6#1-Ag1-N1	122.85(16)	N1-Ag1-N4#2	120.7(4)	N6#1-Ag1-N4#2	114.7(4)
N5-Ag2-N3	117.92(15)	N5-Ag2-N2	129.21(18)	N2-Ag2-N3	112.64(19)
C17#1...C4	3.530(10)	C17#1...C5	3.574(8)	C16#1...N1	3.572(7)
C15#1...N1	3.537(7)				

#1 $x +\backslash, y, z$ #2 $x, y, z + 1$

the Ag2-N bond distances are much less when compared to Ag1-N distances. The Ag2 atom lies more closely to the plane defined by its coordinating N atoms (deviation, 0.063(3) A). The angles around Ag2 are close to 120° and hence the geometry is trigonal planar. The amino nitrogens deviates (N2, 0.979(9) A; N4, 0.948(15) A; N6, 1.407(8) A) from the mean planes defined by their associated ring atoms.

      The structure is a 2-D network. The anions fit into the cavities formed by the cationic units (Figure 2.12) and are involved in strong hydrogen bonding with the amino groups, the H$\cdots$A distances ranging from 2.2-2.6 A. No Ag$\cdots$Ag contacts are observed, but stacking is present.
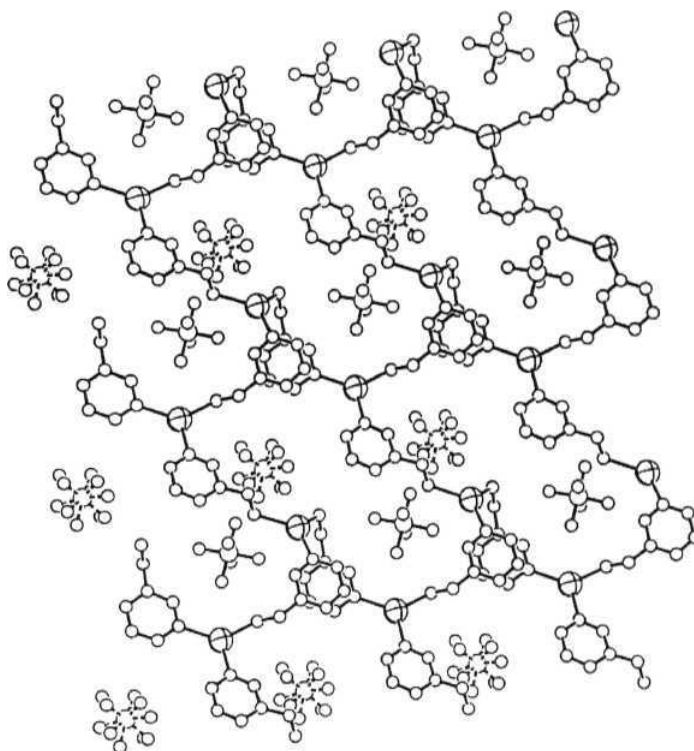
Figure 2.12 Packing diagram of 6. Ag atoms are shown as large footballs. N atoms are represented as small footballs, P atoms as large open circles and F atoms and ring C atoms as small open circles. The bonds from P to disordered F atoms are shown as broken lines.

2.2.6. Structure of Ag(4-amp)ClO$_4$·0.5H$_2$O (7): The polymeric chain of 7 has just one Ag(4-amp)]ClO$_4$ in its repeating unit (Figure 2.13). The coordination geometry around Ag is linear (Table 2.17). As expected from the ligand structure, the polymeric chain is more linear in this case. It has in fact a saw-tooth like appearance due to the sharp bend at

Figure 2.13 Ortep view of 6 with atom labeling. Atoms are represented as 50% probability ellipsoids. Ring hydrogens have been omitted for clarity. Symmetry codes: (i) $x,y - 1, z$; (ii) $y, x, -z + 7/6$; (iii) $-x+y + 1, y,$ $-z + 3/2$.

each $-CH_2$ group. Due to crystal symmetry, there are twelve polymeric chains in the lattice. Since all the chains run in the *xy-plane*, the structure may be viewed as made up of alternating layers of polymeric chains and anions (Figure 2.14). Lattice water is also found in the cation layer. The 6-fold screw symmetry coupled with weak Ag···Ag interaction cause the polymer chains to assemble into helical ladders (Figure 2.15).

Table **2.17** Selected bond lengths (A) and angles (°), stacking interactions and $Ag \cdots Ag$ contacts for Ag(4-amp)ClO$_4 \cdot$0.5H$_2$O (7).

Ag1-N1	2.149(9)	Ag1-N2#1	2.141(9)	N2#1-Ag1-N1	178.6(4)
N1...N1#2	3.27(1)	C1...N1#2	3.50(2)	C1...C5#2	3.53(2)
C5...N1#2	3.60(1)				
Ag...Ag#2	3.379(19)				

#1 $x, y- 1, z$ #2 $-x + y, y, z + 3/2$
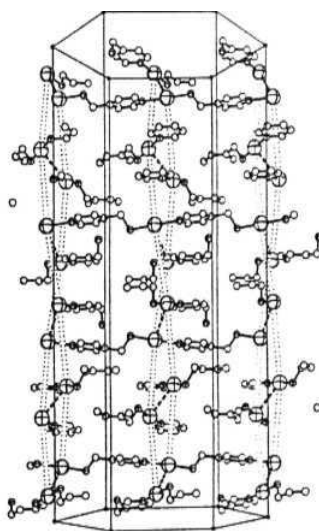
Figure 2.14 View showing the arrangement of symmetry related chains in the hexagonal cell. The dashed lines indicate $Ag \cdots Ag$ contacts. The

dotted lines are drawn only as an aid for the eye to visualize the helical packing and do not represent chemical bonds.
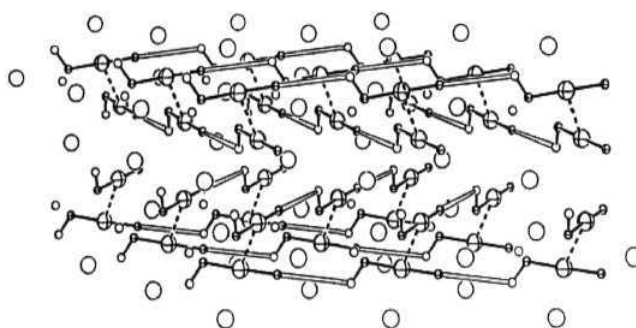
Figure 2.15 Stacking of the double layers viewed sideways to the hexagonal axis. The open circles represent the chlorine atoms of the perchlorate ions and lattice water molecules. The aromatic rings are reduced to double-line "bonds" connecting the nitrogen atoms, for clarity. Ag$\cdots$Ag long contacts (dashed bonds) connect the two layers rotated by 60° with respect to each other.

However, there is no bond along the helix. The rungs of the ladder are formed by the Ag$\cdots$Ag bonds. The projection in the *xy*-plane has hexagonal symmetry (Figure 2.16). The packing of the saw-tooth type chains in 7 is highly unusual in that there are twelve symmetry related polymers in the lattice. These chains are networked through Ag$\cdots$Ag interactions. The anions are involved in H-bonding with the NH_2 groups. The chains and anions pack in alternate layers in the unit cell.
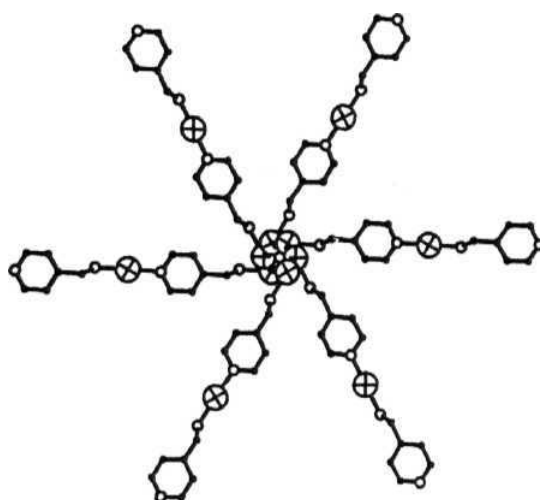
Figure 2.16 View showing the hexagonal symmetry of the twelve symmetry related chains in **7.**

2.2.7. Structure of Ag(4-amp)BF$_4$·0.75CH$_3$CN (8): The asymmetric unit (Figure 2.17) is made up of two Ag(4-amp)$^+$ moieties, two anions and CH$_3$CN solvent molecule. Ag1 and Ag2 are coordinated to a pyridine and an amine N atom from two different ligands, with a linear geometry. Bond lengths and angles are given in Table 2.20. The geometry around Ag2 is more linear than around Ag1. The Ag1-N distances are nearly equal, while Ag2 has two unequal Ag-N distances. As seen in 7, the polymeric linear chain has a sharp bend at the methylene group, thus giving rise to a saw-tooth type appearance to the chain. The gross structural features are same as observed in 7.
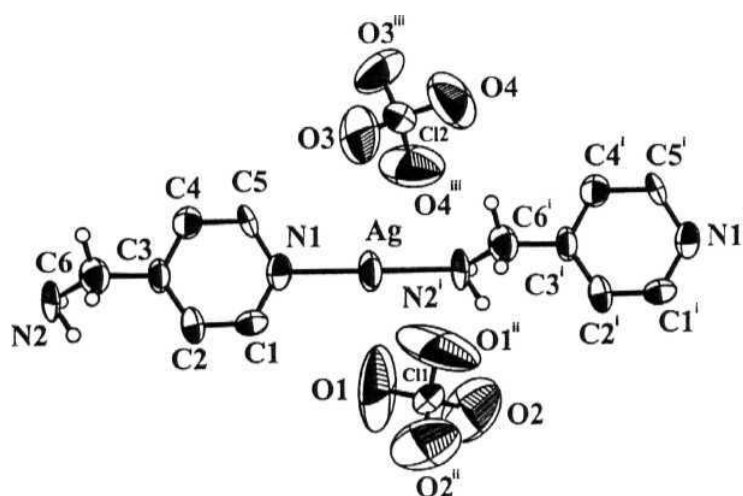
(a)

(b)
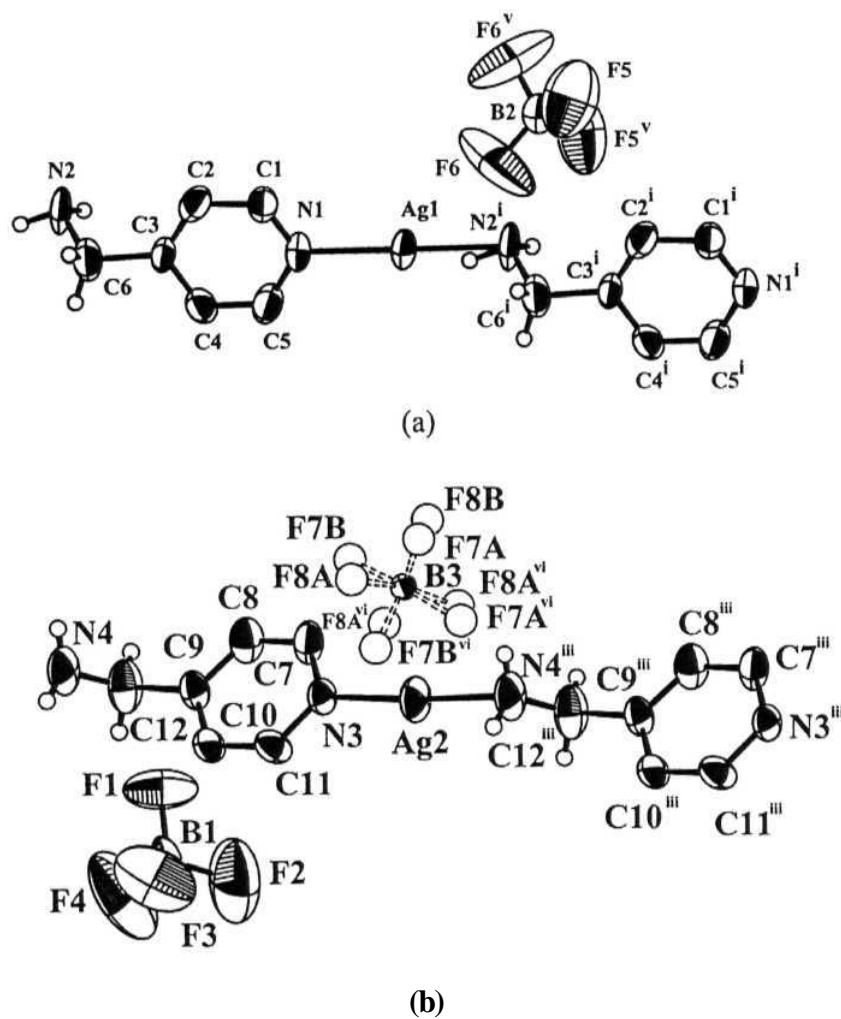
Figure 2.17 Ortep view of the molecular structure of **8** with atom labeling. Atoms are represented as 50% displacement ellipsoids. Ring hydrogens have been omitted for clarity. Symmetry codes: (i) $x + 1, y, z$; (iii) $x + 1/2, y - 1/2, z$; (v) $x, -y, -z + 1$; (vi) $-x + 1, y, -z + 1/2$. In (b), the disordered fluorine positions are indicated as open ellipses and bonds to them are shown as broken lines.

Table 2.20 Selected bond lengths (A) and angles (°) and **Ag· ·Ag** interactions for Ag(4-amp)BF$_4$·0.75CH$_3$CN (8).

Ag1-N1	2.158(7)	Ag1-N2#1	2.162(7)	Ag2-N3	2.128(7)
Ag2-N4#3	2.154(9)	N1-Ag1-N2#1	175.0(4)	N3-Ag2-N4#3	176.9(4)

Ag1...Ag2	3.3699(15)

#1 $x + 1, y, z$ #3 $x + 1/2, y - 1/2, z$

The unit cell has two different types of polymer chains. There are 8 chains corresponding to the symmetry positions of the space group (Figure 2.18). The repeat unit of this chain is one (Ag1-amp)$^+$. The second chain is built of (Ag2-amp-Ag2-amp)$^{2+}$ repeat units. In this repeat unit, the two silver centers are related by the *C*- centered symmetry of the unit cell. Because of the symmetry relation, the chains built of (Ag2-amp-Ag2-amp)$^{2+}$ are only 4 in the unit cell. Altogether, there are 12 chains in the unit cell. This is similar to the situation in 7, but there the 12 chains are all of the same kind. The anions sit within the cationic layers and strongly hydrogen bond to the amino groups. The two types of silver atoms, Ag1 and Ag2 are separated by 3.370(2) A, indicating the presence of a weak Ag···Ag interaction. This distance is nearly equal to what is present in 7.
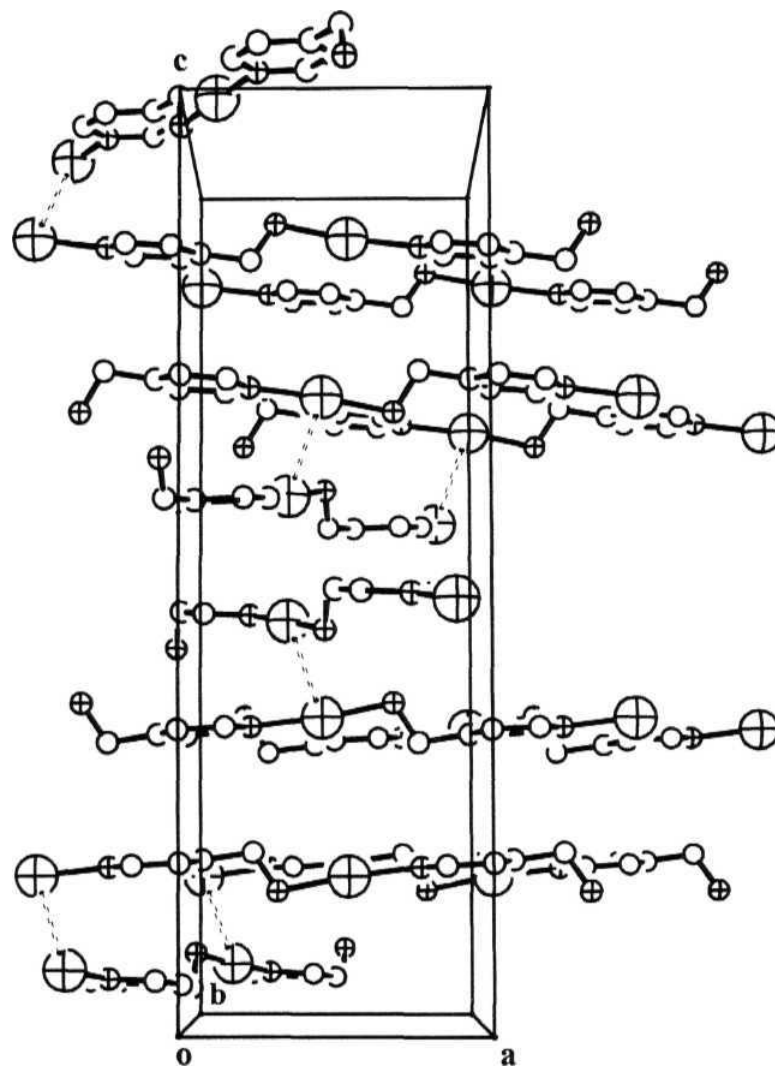
Figure 2.18 Packing of twelve symmetry related chains in 8. Broken lines represent the Ag· ·Ag interactions. Ag atoms are shown as large footballs and N atoms as small footballs. C atoms are shown as small open circles.

2.2.8. Structure of Ag(4-amp)PF₆ (9): This is the simplest of all the structures discussed. The asymmetric unit has one $Ag(4\text{-amp})PF_6$ (Figure 2.19). The polymer repeat unit is $Ag(4\text{-amp})^+$, which is situated on a mirror plane. The 2-coordination around Ag is completed by the coordination of a pyridine N and an amine N atom from a translationally related ligand. The geometry around Ag is near linear (Table 2.21).

Table 2.21 Selected bond lengths (A) and angles (°) and important stacking interactions for $Ag(4\text{-amp})PF_6$ (9).

Ag-N1	2.144(6)	Ag-N2#1	2.143(5)	N2#1-Ag-N1	174.84(16)		
N1#3...N2#1	3.379(7)						
C3#3...N1	3.571(10)	C4#3...N1	3.421(8)	C2#4...N2#3	3.319(6)		

#1 $x + 1, y, z - 1$ #3 $x + 1, y, z$ #4 $x + 1, -y + 3/2, z$
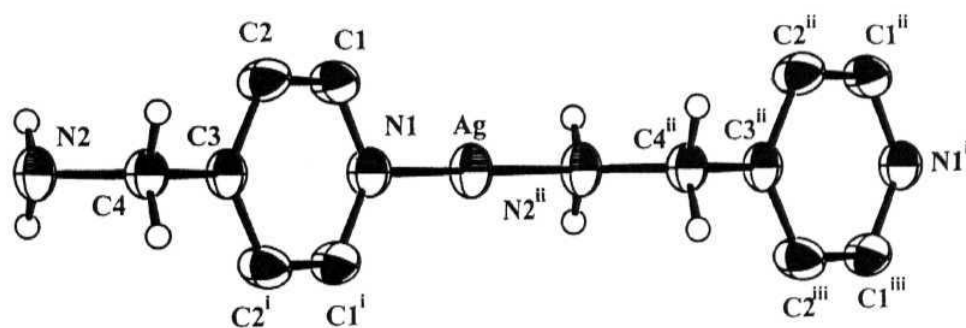
(a)
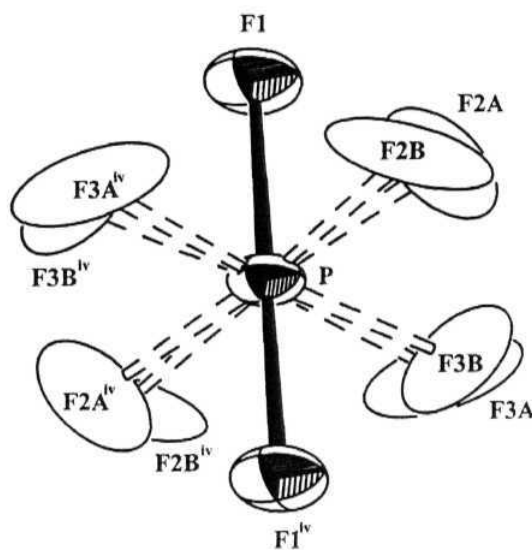
(b)

Figure 2.19 Ortep view of (a) cation and (b) anion in 9 with atom labeling. Atoms are represented as 50% probability ellipsoids in (a) and as 25% probability ellipsoids in (b). Ring hydrogens have been omitted for clarity. Symmetry codes: (i) x, $-y + 3/2$, z; (ii) $x + 1$, y, z-\; (iii) $x + 1$, $-v + 3/2$, $z - 1$; (iv) -x, $-y + 1$, -z + 2. In (b), the disordered fluorine positions are indicated as open ellipses and bonds to them are shown as broken lines.

There are two polymeric chains in the unit cell. As in 7 and 8, the chains have saw-tooth type appearance due to the ligand geometry. The cationic chains and anions are arranged in alternate layers in the unit cell (Figure 2.20). The anions are involved in

hydrogen bond with the amino groups. Ring stacking is observed. However, there is no Ag···Ag interaction.
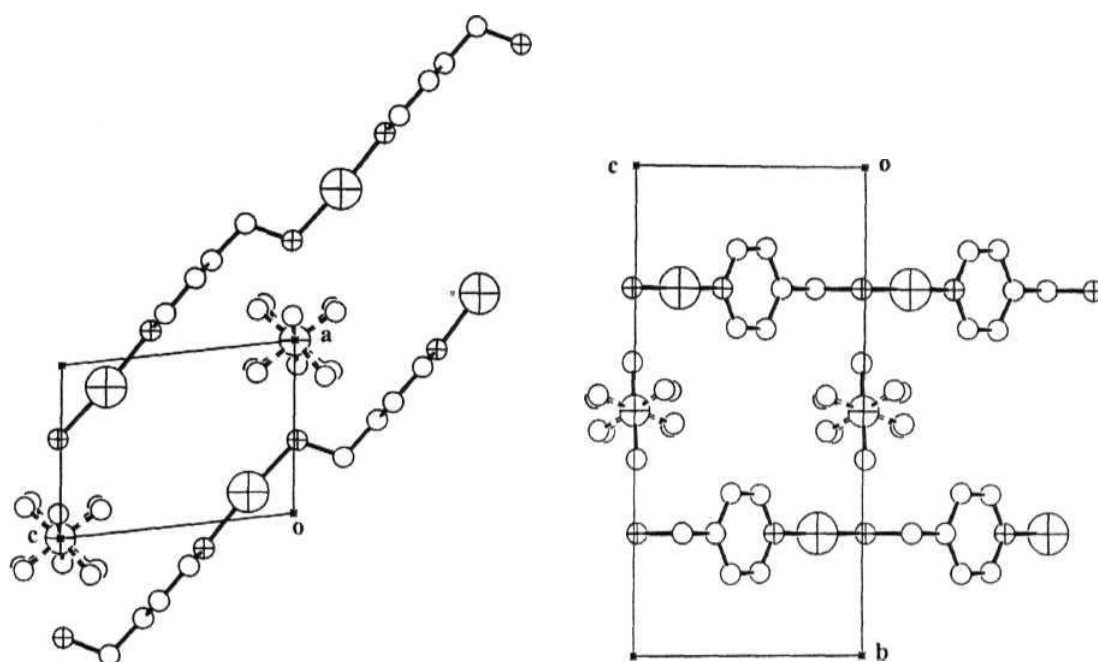
Figure 2.20 Two views showing the packing of cationic chains **and** anions in the unit cell of 9. (a) ac plane (b) bc plane. Ag atoms are shown as large footballs, P atoms as medium footballs and N atoms as small footballs. C atoms and F atoms are shown as open circles. The bonds from P to disordered F atoms are shown as broken lines.
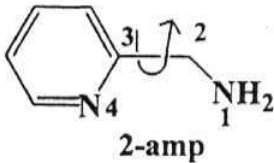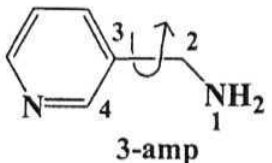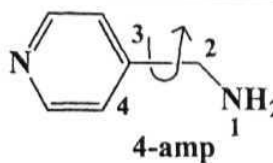
2.3. Discussion

2.3.1. Synthesis: Formation of 1:1 complexes in all the cases, except for 3 and 6 is in accordance with the ratios of starting materials taken. The bulk precipitate formed when the ligand and Ag(I) salts are mixed is the same as the crystals obtained by recrystallization. This fact is proved by the agreement of the IR of the precipitate and the single crystals. Also, the experimental powder pattern of the precipitate and the powder pattern calculated based on the crystal structure[14] are same. However, in the case of 3 and 6 there are differences in the IR of the precipitate and the crystals as well as the X-ray powder patterns of the precipitate and the calculated powder pattern. This observation suggests that the precipitate formed in case of 3 and 6 is probably a 1:1 complex, as observed in all other cases, but recrystallization from water leads to reorganization to a 2:3 compound. It is to be noted that both the initial preparation and the recrystallization result in (near) quantitative yields. The crystals are analytically pure 2:3 complexes. However, the exact nature of the precipitate is not certain.

2.3.2. Ligand and anion control on structure formation: The two main factors that control the structure formed in all the complexes discussed are the conformational flexibility of the ligand and role of anion in influencing the structure packing.

Unlike ligands like pyrazine, where there is no flexibility in the ligand, the amp ligands have a flexible $-CH_2NH_2$ group in which the torsion about the C-N bond, may vary in the range 0-180°. Further, in the case of 2-amp, depending on the torsion angles, the ligand can bind in either the bridging or the chelating mode. Both these modes have been noted previously.[15-18] The torsion angles observed for the various structures are given in Table 2.22.

Table 2.22 Torsion angles'

	2-amp	3-amp	4-amp
NO_3^-	180		
ClO_4^-	−170,−168	−158, 145	−112
BF_4^-	170		−68, 109
PF_6^-	23, −30, 80	−51, 111,90	−90

t The torsion angle (x) is defined for the atom sequence 1,2,3,4 and follows the convention of Allen and Rogers. Allen, F. H. and Rogers, D. *Ada Cryst.* 1969, *B25,* 1326.

The variation in the anion size and shape has a marked influence on the crystal packing. The van der Waals radii of BF_4^- and ClO_4^- are nearly same (2.78 A) while that of PF_6^- is much larger (2.98 A). The PF_6^- salts show greatest deviation in the present series of structures. In the case of 2-amp, it results in a chelated dinuclear complex, while in the

case of 3-amp, it forms a planar 3-connected network. On the other hand, in the case of 4-amp, the planar network formed by Ag⋯Ag bonds in BF_4^- and ClO_4^- salts is broken to form a simple chain structure in the PF_6^- salt. The shift from the smaller tetrahedral ClO_4^- and BF_4^- to larger octahedral PF_6^- resulted in the structural change from simple chains to 3-connected networks. The weak interaction between **Ag$^+$** and anions as well as its tendency towards d^{10}-d^{10} affinity also contributes to the packing. It is generally observed that these two types of interactions operate in the absence of each other.

2.3.3. Comparisons Among the Ag(2-amp)X Chain Systems (X = NO$_3^-$, ClO$_4^-$, BF$_4^-$):

The chains of Ag(2-amp)NO$_3$,[2] Ag(2-amp)ClO$_4$ (1) and Ag(2-amp)BF$_4$ (2) have a wave like appearance. In all the three cases, the centrosymmetrically related chains have a phase difference. Besides, the phase difference, chains of 1 and Ag(2-amp)NO$_3$ also have a lateral displacement. As seen from Figure 2.21, in 1 and Ag(2-amp)NO$_3$, due to the lateral displacement of the chains there are sufficiently large voids, which can accommodate the anions. Whereas, in the case of Ag(2-amp)BF$_4$, the chains have only phase difference but are not displaced laterally. The absence of lateral displacement of chains, coupled with weak Ag⋯Ag interactions generate cavities which are very small. This makes the anions to sit along the chain edges instead of being filled in the cavities.

An interesting feature of 2 is that the presence of weak Ag⋯Ag interactions gives a complicated ladder type appearance for centrosymmetrically related chains(Figure 2.22). The ligand structure combined with the glide symmetry which connects the chain repeat units and the weak Ag⋯Ag interactions appear to be the responsible factors for this type of ladder formation. This arrangement differs from a regular staircase, in that the adjacent 'steps' are on opposite sides.
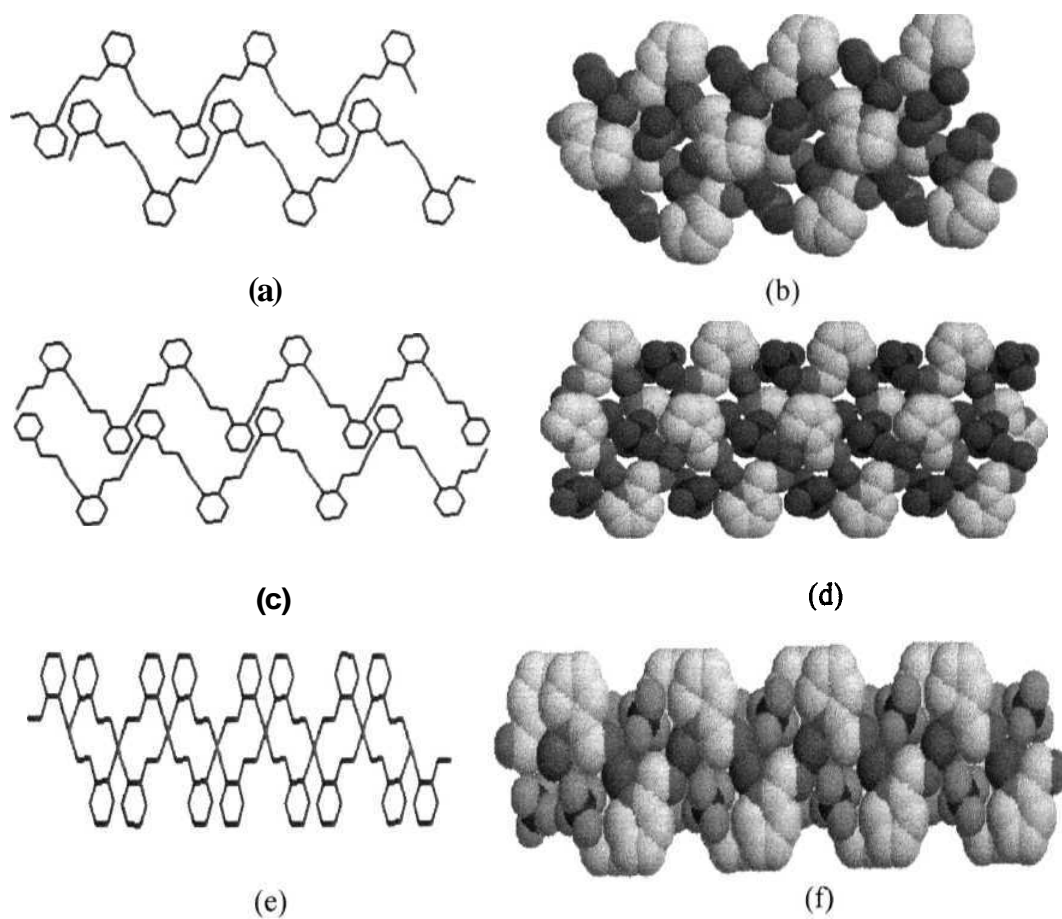
Figure 2.21 Stick representations showing the channels and space filling models showing packing of anions respectively for $Ag(2\text{-amp})NO_3$ (a and b); $Ag(2\text{-amp})ClO_4$ (c and d) and $Ag(2\text{-amp})BF_4$ (e and f).
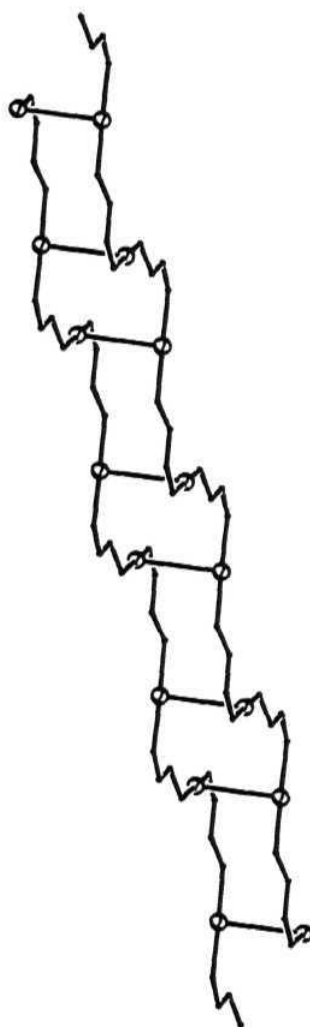
Figure 2.22 View showing the ladder type arrangement of chains in 2. Ligand is shown as a simple chain by omitting some of the ring atoms.

2.3.4. $Ag_2(2\text{-amp})_3(PF_6)_2$ - 3-coordinate Ag(I) with Chelating Ligands: The fact that chelation is possible in 2-amp is seen in the structure of 3. While 2- and 4- coordination is a commonly observed geometry for Ag(I), 3- coordination is also observed in several systems which often exhibit network structure. Though most such systems are polymeric,[19"28] discrete systems with 3- coordinate Ag(I) are also reported.[10,13,29,30] The present example is a simple monomeric structure. The absence of a network structure can be attributed to the chelating nature of the ligand, as opposed to bridging mode observed in 1 and 2. Though the chelation of the ligand is not a favorable geometry, intramolecular $Ag\cdots Ag$ interactions and hydrogen bonding may be responsible for the stabilization of such a strained chelate geometry.

The change in the anion geometry from tetrahedral in 1 and 2 to octahedral in 3 along with the larger anion size appear to favor the formation of a dinuclear chelate. It may be noted that the cation and anion sizes are comparable resulting in an efficient packing in alternate layers (Figure 2.6).

2.3.5. $Ag(3\text{-amp})ClO_4$ - The First Synthetic Triple Helix: The structure of $Ag(3\text{-amp})ClO_4$ provides an example of synthetic triple helical structures which are intriguing. Several helical coordination polymers are known, even though they are less numerous than the (finite length) helicates.[31,32] Examples exist for single,[33-46] and double,[47-49] helical infinite chains. In the case of double and higher order helices, it is necessary to distinguish between two possibilities. (i) The strands of the helix are independent infinite chains held together by non-covalent forces other than the coordinate bond, quite analogous to the situation in DNA. This can be readily realized only for linear two-coordinate metal ions. $Ag(CF_3SO_3)\{1,3\text{-bis(4-pyridyl)propane}\}$[47] is a double helical complex of this type, where the two strands are held by $Ag\cdots Ag$ interaction. Another

example of a Ag(I) double helix is reported where the strands are held together by van der Waals interactions.[48] (ii) The strands are not independent, but are attached through coordinate bonds to a column of metal atoms which form the axis of the helix.[50] While there are no examples of true coordination polymers of this type, an interesting case of a dinuclear Cu(I) complex which stack together to give the appearance of an infinite double helix has been reported.[51]   To our knowledge, 4 is the first triple helical infinite chain coordination polymer and it belongs to type (i) discussed above. The helical coil in 4 is unique in generating a tunnel space large enough to accommodate 50% of the anions. Since the repeat unit is made up of four complex moieties, when projected down its axis the helix reduces to a squarate (in appearance) as shown in Figure 2.23. It is noteworthy that all the NH_2 groups are arranged on the outside of the 'square'. This *exo*-orientation of the NH_2 groups is complementary to the *endo*-orientation of the CH_2 groups. As a result, the anions within a helical coil will have to form H-bonds only with the NH2 groups of the adjacent coil. The volume of the tunnel space generated is almost the same for the alternative (*exo*-CH_2, *endo*-NH_2) arrangement, even though the shape of the space is modified. The main reason for preferring the former conformation appears to be that it allows the anions which are outside the tunnels also to participate in H-bonding.

Helical structure in which anions are packed inside as well as outside the coils would lead to high electrostatic stabilization. The triple helical coils are further stabilized by π stacking interactions of the phenyl rings (Figure 2.24).
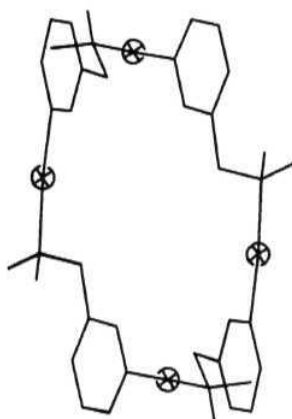
Figure 2.23 Squarate appearance of helical strand in **4.**
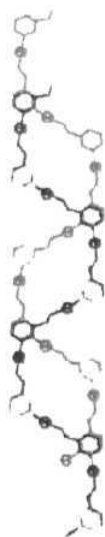
Figure 2.24 View showing the *n* stacking of phenyl rings in the triple helix of 4.

There are two recent reports of other triple helical infinite chains based on 4-coordinate $Hg(II)^{52}$ and 6- coordinate $Mn(III).^{53}$ The triple helical chains in 4-coordinated Hg(II) complex, $HgX_2(C_{31}H_{24}N_2) \cdot CH_2Cl_2$ (X = Cl, Br) belongs to the type (i) discussed above and exhibit luminescent properties in the solid state. As observed in 4, coordinative linkage between the repeat units (Hg-L) leads to the formation of helical strands. Three independent strands, coiled around each other form the triple helix which propagates along the *b*-axis direction. The voids formed appear to be filled by the ligand groups, unlike in 4, where uncoordinated anions occupy the voids.

The second reported triple helix is based on Mn(III) and differs from the triple helix in 4 and the helix based on Hg(II) in the following aspects. In this case, complexation of $Mn(NCS)_2$ with 4,4'-bipyridine (L) and 4,4'-azobispyridine (L') gives rise to the triple helical structure with a helical repeat unit of (2L'-Mn-L-Mn). The main difference is in the strand and helix formation. Here, the helical strands are built by linking of the repeat units with hydrogen bonds, which propagate along the *b*-axis direction. The triple helix cannot be resolved into three independent strands, as it is formed by the interpenetration of three parallel 2-D networks. The large rhombic channels (19 x 9 A) appear to be occupied by the coordinated anions.

It may be noted that a naturally occurring triple helix is found in the protein collagen.[54]

2.3.6. $Ag_2(3\text{-amp})_3(PF_6)_2$ - 2D Network of 3-Coordinate Ag(I): While 3 has a monomeric structure with 3-coordinate Ag(I), 6 shows a network structure, commonly observed in other 3-coordinate Ag(I) systems. There are examples of triconnected silver(I) giving rise to either 2-D[19,21] or 3-D[19,22,23,55,56] network or framework structures.

Among the 2-D networks of 3-coordinate Ag(I), $Ag_2(pyz)_3(BF_4)_2$[19] shows a 2-D sheet structure and $Ag(TCB)CF_3SO_3$[21] shows a honeycomb type layer arrangement which is homeotypic with CaCuP structure. The geometry of Ag1 and Ag2 is more planar in the present case, than in $Ag_2(pyz)_3(BF_4)_2$ or $Ag(TCB)CF_3SO_3$. The unsymmetrical Ag-N distances are comparable to that observed in above examples.

The structure is a 3-connected 2-D network. The layers have a step appearance due to the rising in the ligand around Ag1 as shown in Figure 2.25. The packing of layers generate channels which are occupied by the anions (Figure 2.26). These channels are made up of three Ag1 and three Ag2 centers with the coordinated ligands. However, the space between the layers is filled alternately with the ordered and disordered anions (Figure 2.27).
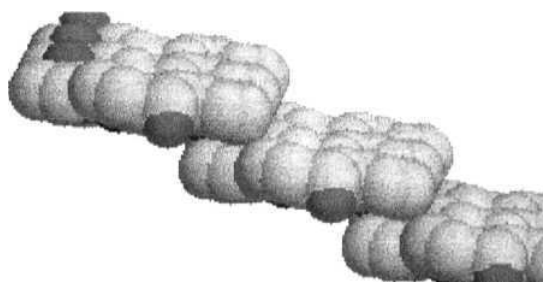
Figure 2.25 Space filling model showing the terraced appearance of a single layer in 6.

(a)   **(b)**
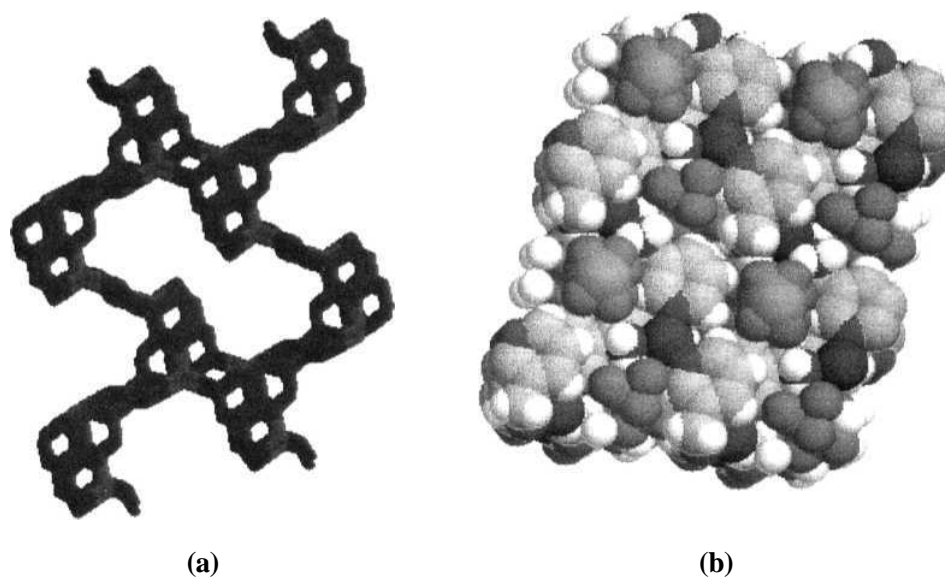
Figure 2.26 (a) Stick representation of the channels and (b) space filling model showing the anions in the channels in **6.**

(a)   (b)
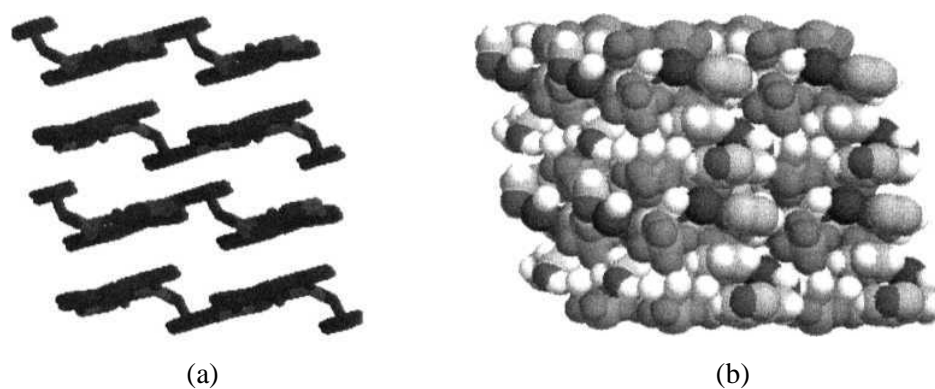
Figure 2.27 (a) Stick representation showing channels between the layers and (b) space filling model showing the ordered and **disordered** anions sitting in the channels in 6.

The network structure is analogous to the 3-connected hexagonal plane nets formed by elements of the V group. Structure of certain binary compounds A_2X_3, for example, As_2S_3[57] also has the same topology. The present network may be represented as ABX_3 where $A = Ag1$, $B = Ag2$ and $X = $ 3-amp. The network generates large channels (3 x 6 A^2) big enough to accommodate the PF_6^- ions.

2.3.7, Ag(4-amp)X - Anion Control of Packing Symmetry: The primary polymeric form in all the three complexes ($X = ClO_4^-$, BF_4^- and PF_6^-) is a saw-tooth type one dimensional chain. The simplest packing of the chains is observed in the PF_6^- salt. A groove is formed next to the '-CH_2 bends' of adjacent chains. The anions are accommodated in the grooves (Figure 2.28a). The space filling model shows that this packing leaves narrow (2 x 2 A^2) unoccupied microchannels (Figure 2.28b). There are no solvents or Ag··Ag bonds in this structure.

The packing in ClO_4^- and BF_4 salts are closely related (Figure 2.28c and d). Both structures contain Ag···Ag bonds which organize the chains into 3-connected 2-D networks (Figure 2.29). In the ClO_4^- salt each layer is rotated by 60° with respect to its adjacent layer. Six such layers alternating with anion layers make up one unit cell. In the BF_4^- salt there are only four layers and there is no rotation between adjacent layers. The *b*-axis length of the orthorhombic cell is approximately 3 times the *a*-axis length. This cell therefore results from a distortion of the hexagonal cell towards lower symmetry. The orthorhombic packing results from flattening the hexagonal packing by about 33% and spreading it in the *ab* plane along with a rotation of adjacent chains to correspond to orthorhombic symmetry.

(a)

(b)

(c)

(d)
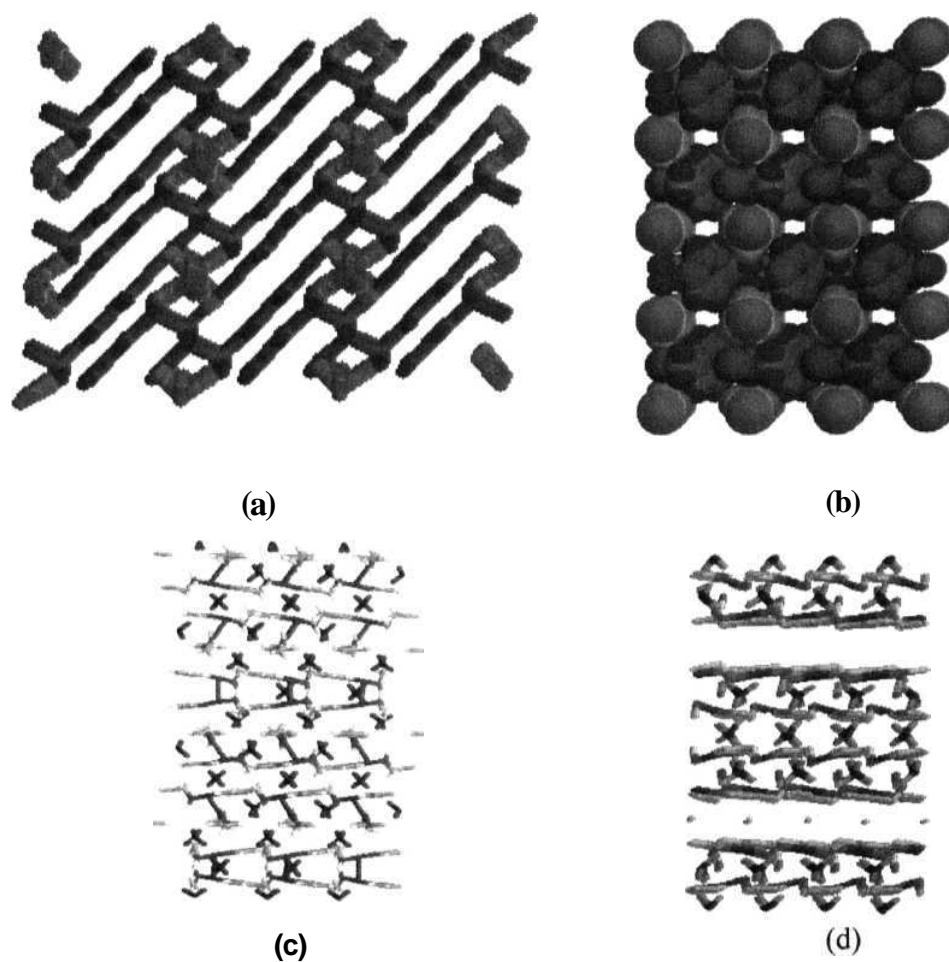
Figure 2.28 Stick representation of the packing of cationic chains and anions in the unit cell of (a) $Ag(4\text{-}amp)PF_6$ (c) $Ag(4\text{-}amp)ClO_4 \cdot 0.5H_2O$ (d) $Ag(4\text{-}amp)BF_4 \cdot 0.75CH_3CN$ and (b) space filling model showing micro channels in $Ag(4\text{-}amp)PF_6$.

(a)   (b)
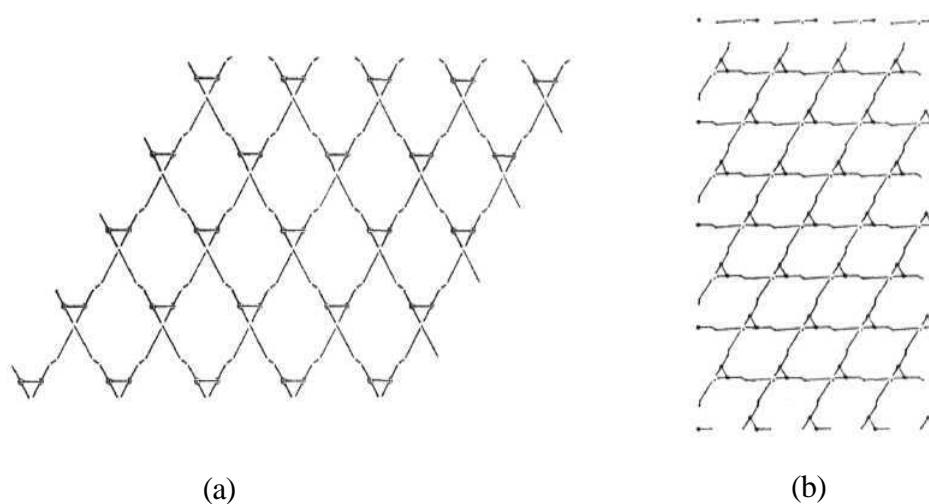
Figure 2.29 View showing 2-D networks in (a) $Ag(4\text{-amp})ClO_4\cdot0.5H_2O$ and (b) $Ag(4\text{-amp})BF_4\cdot0.75CH_3CN$

The formation of chiral crystals from non-chiral starting materials is an intriguing problem in crystal chemistry. There are not many polymeric chain compounds crystallizing in $P6_522$ space group.[58] However, this is the preferred space group for urea inclusion compounds.[59]

2.4. Conclusions

The ligands used in the present study are rather simple, but generate interesting structures in combination with different silver salts. While bridging mode of coordination is common for all the three ligands, 2-amp also shows the chelating mode in its complex with $AgPF_6$.

The size and shape of the anion have a large influence on the structure formation. While polymeric chains are observed with the tetrahedral ions of near equal size (BF_4^- and ClO_4^-), shift to the larger, octahedral ion PF_6^- resulted in either chelate or network structure. However, in the case of 4-amp, chains are seen with all anions. The polymeric chains either remain as simple chains (1 and 9) or pack into ladders (2) or a triple helix with large tunnel space (4) and generate networks (6, 7 and 8) with the weak interactions offering the stabilizing forces.

The examples shown illustrate that simple starting materials lead to novel and interesting structures with the aid of non-covalent interactions. However, the doubts regarding the nature of the precursor precipitate in two cases (3 and 6) may be cleared by a better characterization of the precipitates. There is ample scope for the extension of this series. Only two (very different) structures are now available for the Ag - 3-amp system. Additional compounds especially the BF_4^- and NO3" salts need to be crystallized. Another more ambitious project would be to modify the ligand to make the complexes water-insoluble. The resulting tunnel or layer structures may be investigated for their anion exchange properties.

2.5. Notes and References

‡ The precipitate is the precursor of the crystalline product and its composition is at present not ascertained (see section 2.3.1)

(1)   Crawford, C. A.; Day, E. F.; Streib, W. E.; Huffman, J. C; Christou, G. *Polyhedron* **1994,73,2933.**

(2)   Swarnabala, G.; Rajasekharan, M. V. *Polyhedron* **1997,** 76, 921.

(3)   Hill, A. E. *J. Am. Chem, Soc.* **1921,** *43,* 254.

(4)   North, A. C. T.; Phillips, D. C; Mathews, F. S. *Acta Cryst.* **1968,** *A24,* 351.

(5) Sheldrick, G. M. *SHELXS-97 and SHELXL-97*; University of Gottingen: Germany, 1997.

(6)   Burnett, M. N.; Johnson, C. K. *ORTEP-III: Oak Ridge Thermal Ellipsoid Plot Program for Crystal Structure Illustrations;* Oak Ridge National Laboratory Report ORNL-6895: Tennessee, USA, 1996.

(7)   Sayle, R. *RasMol V2.6*; 2.6 ed.: Stevenage, Hertfordshire, U.K., 1995.

(8)   Mohana Rao, J. K.; Viswamitra, M. A. *Acta Cryst.* **1972,** *B28,* 1484.

(9)   Coggon, P.; McPhail, A. T. *J. Chem. Soc. Chem. Commun.* **1972,** 91.

(10) Bowmaker, G. A.; Effendy; Junk, P. C; White, A. H. *J. Chem. Soc, Dalton Trans.* 1998,2131.

(11) Eastland, G. W.; Mazid, M. A.; Russell, D. R.; Symons, M. C. R. *J. Chem. Soc. Dalton Trans.* 1980, 1682.

(12) Swarnabala, G.; Rajasekharan, M. V. *Polyhedron* **1996,**15, 3197.

(13) Venkatalakshmi, N.; Rajasekharan, M. V. *Transition Met Chem.* **1992,** *17,* 455.

(14) Kraus, W.; Nolze, G. *Powder Cell for Windows version 2.3;* Federal Institute **for** Materials Research and Testing: Berlin, Germany, 1999.

(15) Michelsen, K. *Acta Chem. Scand,* **1970,** *24,* 2003.

(16) Hodgson, D. J.; Michelsen, K.; Pedersen, E. *Acta Chem. Scand.* **1990,** *44,* 1002.

(17) Katz, B. A.; Strouse, C. E. *Inorg. Chem.* **1980,** *19,* 658.

(18) Mikami-Kido, M.; Y., S. *Acta Cryst.* **1982,** *B38,* 452.

(19) Carlucci, L.; Ciani, G.; Proserpio, D. M.; Sironi, A.../. *Am. Chem. Soc.* **1995,** *117,* 4562.

(20) Venkataraman, D.; Gardner, G. B.; Lee, S.; Moore, J. S. *J. Am. Chem. Soc.* **1995,** *117,* 11600.

(21) Gardner, G. B.; Venkataraman, D.; Moore, J. S.; Lee, S. *Nature* **1995,** *374,* 792.

(22) Aakeroy, C. B.; Beatty, A. M.; Helfrich, B. A. *J. Chem. Soc, Dalton Trans.* **1998,** 1943.

(23) Carlucci, L.; Ciani, G.; Proserpio, D. M.; Sironi, A. *Inorg. Chem.* **1997,** *36,* 1736.

(24) Hirsch, K. A.; Wilson, S. R.; Moore, J. S. *J. Am. Chem. Soc.* **1997,** *119,* 10401.

(25) Carlucci, L.; Ciani, G.; Proserpio, D. M.; Sironi, A. *Chem. Commun.* **1996,** 1393.

(26) Kuang, S.-M.; Zhang, Z.-Z.; Wang, Q.-G.; Mak, T., C. W. *Chem. Commun.* **1998,** 581.

(27) Smith, G.; Sagatys, D. S.; Campbell, C. A.; Lynch, D. E.; Kennard, C. H. L. *Aust. J. Chem.* **1990,43,** 1707.

(28) Sagatys, D. S.; Bott, R. C; Smith, G. *Polyhedron* **1992**, *11*, 49.

(29) Lancashire, R. J. *Comprehensive Coordination Chemistry;* Wilkinson, G.; Gillard, R. D. and McCleverty, J. A., Ed.; Pergamon Press: Oxford, 1987; Vol. 5, pp 784.

(30) Damayanthi, Y. *M. Phil. Dissertation;* University of Hyderabad: Hyderabad, India, 1991.

(31) Piguet, C.; Bernardinelli, G.; Hopfgartner, G. *Chem. Rev.* **1997,** *97,* 2005.

(32) Andre, N.; Scopelliti, R.; Hopfgartner, G.; Piguet, C; Bünzli, J.-C. G. *Chem. Commun.* 2002,214.

(33) Tong, M.-L.; Chen, X.-M.; Ye, B.-H. *Inorg. Chem.* **1998,** *37,* 5278.

(34) Reddy, K. R.; Rajasekharan, M. V.; Tuchagues, J.-P. *Inorg. Chetti.* **1998,** *37,* 5978.

(35) Kaes, C; Hosseini, M. W.; Rickard, C. E. F.; Skelton, B. W.; White, A. H. *Angew. Chem. Int. Ed.* 1998, *37,* 920.

(36) Hester, C. A.; Baughman, R. G.; Collier, H. L. *Polyhedron* **1997,** *16,* 2893.

(37) Biradha, K.; Seward, C; Zaworotko, M. J. *Angew. Chem. Int. Ed.* **1999,** *38,* 492.

(38) Suzuki, T.; Kotsuki, H.; Isobe, K.; Moriya, N.; Nakagawa, Y.; Ochi, M. *Inorg. Chem.* **1995,** *34,* 530.

(39) Batten, S. R.; Hoskins, B. F.; Robson, R. *Angew. Chem. Int. Ed.* 1997, *36,* 636.

(40) Doyle, G. A.; Goodgame, D. M. L.; Sinden, A.; Williams, D. J. *J. Chem. Soc., Chem. Commun.* **1993,** 1170.

(41) Jung, O.-S.; Kim, Y. J.; Lee, Y.-A.; Chae, H. K.; Jang, H. G.; Hong, J. *Inorg. Chem.* 2001,40,2105.

(42) Kang, Y.; Lee, S. S.; Park, K.-M.; Lee, S. H.; Kang, S. O.; Ko, J. *Inorg. Chem.* **2001,** *40,* 7027.

(43) Yang, S.-P.; Zhu, H.-L.; Yin, X.-H.; Chen, X.-M.; Ji, L.-N. *Polyhedron* 2000, *19,* 2237.

(44) Maggard, P. A.; Stern, C. L.; Poeppelmeier, K. R. *J. Am. Chem. Soc.* 2001, *123,* 7742.

(45) Zhang, H.; Cai, J.; Feng, X.-L.; Liu, J.-Z.; Li, X.-Y.; Ji, L.-N. *Inorg. Chem. Commun.* **2001,** *4,* 241.

(46) Erxleben, A. *Inorg. Chem.* 2001, *40,* 412.

(47) Carlucci, L.; Ciani, G.; Gudenberg, D. W. v.; Proserpio, D. M. *Inorg. Chem.* 1997, *36,* 3812.

(48) Mamula, O.; Zelewsky, A. v.; Bark, T.; Bernardinelli, G. *Angew. Chem. Int. Ed.* 1999, *38,* 2945.

(49) Lu, C.-Z.; Wu, C.-D.; Lu, S.-F.; Liu, J.-C.; Wu, Q.-J.; Zhuang, H.-H.; Huang, J.-S. *Chem. Commun.* **2002, 152.**

(50) Goodgame, D. M. L.; Hill, S. P. W.; Williams, D. J. *J. Chem. Soc., Chem. Commun.* **1993,** 1019.

(51) Carina, R. F.; Bernardinelli, G.; Williams, A. F. *Angew. Chem. Int. Ed. Engl.* **1993,** *32,* 1463.

(52) Ciurtin, D. M.; Pschirer, N. G.; Smith, M. D.; Bunz, U. H. F.; Loye, H.-C. z. *Chem. Mater.* 2001,73,2743.

(53) Li, B.; Yin, G.; Cao, H.; Liu, Y.; Xu, Z. *Inorg. Chem. Commun.* **2001,** *4,* 451.

(54) Ramachandran, G. N. and Kartha, G. *Nature.* **1954,***174,* 269. Quoted in Bansal, M. *Resonance* 2001, *6,* 38.

(55) Soma, T.; Yuge, H.; Iwamoto, T. *Angew. Chem. Int. Ed. Engl.* **1994,** *33,* 1665.

(56) Bu, W.-M.; Ye, L.; Fan, Y.-G. *Inorg. Chem. Commun.* **2000,** 3, 194.

(57) Wells, A. F. *Structural Inorganic Chemistry;* 4 ed.; Oxford University Press: London, 1979, pp 723.

(58) Withersby, M. A.; Blake, A. J.; Champness, N. R.; Hubberstey, P.; Li, W.-S.; Schroder, M. *Angew. Chem. Int. Ed. Engl.* 1997, *36,* 2327.

(59) Harris, K. D. M. *Chem. Soc. Rev.* **1997,** *26,* 279.

CHAPTER III

Coordination Polymers of Cerium(IV) with Pyridine-2,6-dicarboxylic acid

While coordination polymers with single metal atoms are largely seen, polymers with mixed metal atoms are also known. These systems are observed when both the metal atoms are connected by proper bridging ligands. In literature, there are reports of mixed metal polymers connected by appropriate bridging ligands.[1*5] DipicH$_2$, a multifunctional ligand is one of such bridging ligands which can act as a bridging as well as a chelating ligand. Several modes of coordination are known for dipicH$_2$: O-unidentate[6] dipicH$_2$; O,N-bidentate[7-9] dipicH"; O,N,O-tridentate[6,8,10-26] dipicH$_2$, dipicH" and dipic^{2-}; (O,N)O-bidentate bridging[27-28] dipic^{2-}; (O,N,O)O- and O,N,μ-O-tridentate bridging[20,21,29-36] dipic^{2-} (Scheme 3.1). In the early 1970s, several complexes of this ligand containing a trivalent lanthanide ion and Na$^+$ have been reported by Albertsson[29-32] which have shown mononulcear and three dimensional networks. A linear chain structure of alternating coordinate and hydrogen bond bridges was found for Na$_3$Yb(dipic)$_3$·NaClO$_4$·10H$_2$O.[31] However, fully coordinatively bridged infinite chain with dipicH$_2$, have been reported, viz., Ag[Gd(dipic)$_2$(H$_2$O)$_3$]·3H$_2$O[1] and [Ca(dipicH$_2$)(OH$_2$)$_3$][Ce(dipic)$_3$]·5H$_2$O.[2] Similar to the previously reported Ce-Ca alternating chain polymer, our efforts with other alkaline earth ions in this series, viz., Sr^{2+} and Ba^{2+} resulted in the formation of novel structures with Ce^{4+}, Ba^{2+} and dipicH$_2$. The structural details are presented in this chapter.
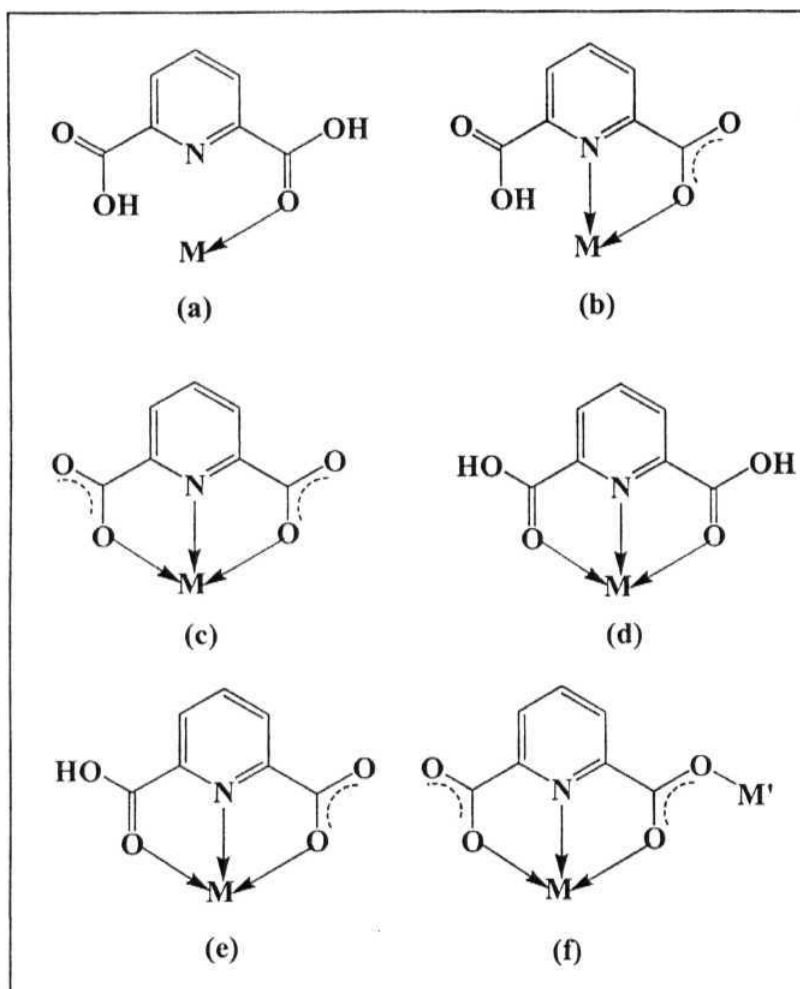
Scheme 3.1 Different coordination modes of dipicH$_2$. (a) O-unidentate dipicH$_2$ (b) O,N-bidentate dipicH' (c) O,N,O-tridentate dipic^{2-} (d) O,N,O-tridentate dipicH$_2$ (e) O,N,O-tridentate dipicH" and (f) O,N,O-tridentate (μ-O)-M' dipic^{2-}.

3.1. Experimental

3.1.1. Synthesis

$SrCl_2 \cdot 6H_2O$, $BaCl_2 \cdot 2H_2O$ and $(NH_4)_2Ce(NO_3)_6$ were purchased from Ranbaxy Chemicals. $DipicH_2$ was purchased from Lancaster Chemicals.

(a) Preparation of $Ce(dipic)_3Sr(dipicH_2)(OH_2)_3 \cdot 6H_2O$ (1): To a 5 mL aqueous solution of $SrCl_2 \cdot 6H_2O$ (0.267g, 1.00 mmol) and $(NH_4)_2Ce(NO_3)_6$ (0.550g, 1.00 mmol), 40 mL methanolic solution of $dipicH_2$ (0.668g, 4.00 mmol) was added slowly while stirring. As the methanolic solution was being added, the color changed from deep red to orange to pale yellow. After stirring for about 5 minutes, the precipitate formed was separated by filtration. The clear filtrate gave yellow crystalline material. Yield: 0.696g (0.66 mmol, 66 %). Recrystallization from hot water yielded pale yellow single crystals of 1 suitable for X-ray data collection. Anal. Calcd. for $C_{28}H_{32}CeN_4O_{25}Sr$ (MW: 1052.32) C, 31.96; H, 3.07; N, 5.32. Found: C, 31.86; H, 3.02; N, 5.41. Characteristic IR peaks (KBr/cm^{-1}): 3484, 1640, 1427, 1370, 1267, 1184, 1076, 1024, 924, 891, 768, 735, 691, 666.

(b) Preparation of $Ce(dipic)_3Ba(dipicH_2)(OH_2)_4 \cdot 5H_2O$ (2): To a 5 mL aqueous solution of $BaCl_2 \cdot 2H_2O$ (0.245g, 1.00 mmol) and $(NH_4)_2Ce(NO_3)_6$ (0.549g, 1.00 mmol), 40 mL methanolic solution of $dipicH_2$ (0.668g, 4.00 mmol) was added slowly while stirring. As the methanolic solution was being added, the color changed from deep red to orange to pale yellow. After stirring for about 5 minutes, the precipitate formed was separated by filtration. The clear filtrate gave yellow crystalline material. Yield: 0.701g (0.64 mmol, 64 %). Recrystallization from hot water yielded pale yellow single crystals of 2 suitable for X-ray data collection. Anal. Calcd. for $C_{28}H_{32}BaCeN_4O_{25}$ (MW

1102.04): C, 30.52; H, 2.93; N, 5.08. Found, C, 31.30; H, 1.91; N, 5.44. Characteristic IR peaks (KBr/cm^{-1}): 3428, 1607, 1568, 1441, 1375, 1275, 1188, 1082, 1018, 916, 727, 682.

(c) Preparation of Ce(dipic)$_3$Ba(OH$_2$)$_6$ (3): To a 10 mL aqueous solution of BaCl$_2$·2H$_2$O (0.489g, 2.00 mmol) and (NH$_4$)$_2$Ce(NO$_3$)$_6$ (1.104g, 2.01 mmol), 60 mL methanolic solution of dipicH$_2$ (1.005g, 6.01 mmol) was added slowly while stirring. As the methanolic solution was being added, the color changed from deep red to orange to pale yellow. After stirring continuously for 3 hr. pale yellow precipitate formed was separated by filtration, washed with cold methanol and dried. Recrystallization from hot water yielded yellow-orange prisms of 3 suitable for X-ray data collection. Yield: 0.786g (0.88 mmol, 88 %) Anal. Calcd. for C$_{21}$H$_{21}$BaCeN$_3$O$_{18}$ (MW 880.86) C, 28.63; H, 2.40; N, 4.77; Found: C, 29.14; H, 2.50; N, 4.29. Characteristic IR peaks (KBr/cm^{-1}): 3437, 1618,1427, 1338, 1186, 1080,1024,920,770,731,667.

(d) Preparation of Ce(dipic)$_3$Ba(OH$_2$)$_6$·2H$_2$O (4): The experimental procedure is the same as that of 3. After separating the crystals of 3 from the solution, the remaining solution yielded orange crystalline material. Recrystallization of the orange crystalline material from hot water yielded orange blocks of 4. Yield: 0.420g (0.46 mmol, 46 %). The combined yield of 3 and 4 from one preparation is 67 %. Anal. Calcd. for C$_{21}$H$_{25}$ BaCeN$_3$O$_{20}$ (MW: 916.86) C, 27.51; H, 2.75; N, 4.58. Found: C, 28.55; H, 2.013; N, 6.11. Characteristic IR peaks (KBr/cm-^{1}): 3382, 1632, 1427, 1362, 1265, 1179, 1074, 1024,922,856,826,768,735.

3.1.2. Physical Measurements: IR spectra were recorded on a Jasco 5300 FT/IR infrared spectrometer. C, H, N analysis was performed on a Perkin-Elmer 240C elemental analyzer. X-ray data were collected on an Enraf Nonius CAD-4 diffractometer. Powder

diffractograms were measured using PW3710 model Philips Analytical X-ray diffractometer.

3.1.3. X-ray Crystallography: X-ray data were collected for pale yellow crystals with dimensions, 0.40 x 0.40 x 0.10 mm for 1; 0.61 x 0.37 x 0.20 mm for 2; 0.50 x 0.30 x 0.28 mm for 3 and orange crystals with dimensions 0.34 x 0.30 x 0.28 mm for 4 on an Enraf Nonius CAD-4 diffractometer using graphite monochromated Mo-Kα radiation. The data were corrected for Lorentz polarization effects and absorption.[37]-[38] The structures were solved by a combination of Patterson heavy atom method and direct methods (SHELXS-97) and refined (over F^2) by least squares techniques SHELXL-93/SHELXL-97.[39,40] Drawings were made using ORTEP-III[41] and Rasmol 2.6.[42]

1 crystallizes in the triclinic system, space group $P\bar{1}$ with 2 molecules in the unit cell. A total of 7320 reflections (7217 unique, 5483 with $F > 4\sigma F$) were collected in the θ range 1.77 to 25.37, with indices $-13 < h < 12$, $-15 < k < 15$, $0 < l < 19$. All the non-hydrogen atoms were refined anisotropically while the ring hydrogen atoms were included in the calculated positions using a riding model. Among the eight water sites, six (OW6, OW7, OW8, OW9, OW10 and OW11) were refined with partial site occupation factors. Hydrogen atoms of water molecules could not be located. All hydrogens were assigned fixed U_{iso} values, equal to $1.2U_{eq}$ of the parent atom for ring atoms and $1.5U_{eq}$ for –COOH hydrogen atoms. The final cycle of full matrix least squares refinement on F^2 converged with unweighted and weighted refinement factors of $R\backslash = 0.0673$ and $wR2 = 0.1774$ respectively. The goodness of the fit (S) is 1.06 for 7217 unique reflections and 552 parameters. The maximum and minimum residual electron density on the final fourier map corresponded to 1.67 and -3.20 $e/Å^{-3}$ respectively.

2 crystallizes in the triclinic system, space group $P\,\overline{1}$, with 2 molecules in the unit cell. A total of 7449 reflections (7302 unique, 5734 with $F > 4\sigma F$) were collected in the θ range 1.75 to 25.13, with indices $-13 < h < 12$, $-15 < k < 15$, $0 < l < 19$. All the non-hydrogen atoms were refined anisotropically except the solvent water molecules, which were refined isotropically. Among the four coordinated water molecules, one (OW4) is disordered. The disorder was modeled by splitting it into two halves whose site occupation was refined by free variable (FVAR) refinement. Among the eight solvent water sites, seven (OW5, OW6, OW7, OW8, OW9, OW11 and OW12) were refined with partial site occupation. The hydrogens of only one water molecule (OW1) could be located from difference maps and bond length constraints were applied. The hydrogens of carboxylic groups were also located from difference maps. All hydrogens were assigned fixed U_{iso} values, equal to $1.2U_{eq}$ of the parent atom for ring and 1.3 for carboxylic hydrogens and water hydrogens. The final cycle of full matrix least squares refinement on F^2 converged with unweighted and weighted refinement factors of $R\backslash = 0.0595$ and $wR2 = 0.1587$ respectively. The goodness of the fit (S) is 1.048 for 7302 unique reflections and 541 parameters. The maximum and minimum residual electron density on the final fourier map corresponded to 2.795 and -3.761 $e/Å^{-3}$ respectively.

3 crystallizes in the trigonal system, space group $P31c$, with 6 molecules in the unit cell. A total of 6316 reflections (1108 unique, 1084 with $F > 4\sigma F$) were collected in the θ range 1.80 to 27.51, with indices $-16 \le h \le \backslash 6, -\backslash 6 < k < 16$, $0 < l < 11$. All the non-hydrogen atoms were refined anisotropically while the ring hydrogen atoms were included in the calculated positions using a riding model. Bond length constraints were applied to water hydrogens after locating from difference maps. All hydrogens were assigned fixed U_{iso} values, equal to $1.2U_{eq}$ of the parent atom for ring hydrogens and

$1.5U_{eq}$ for the water hydrogens. The final cycle of full matrix least squares refinement on F^2 converged with unweighted and weighted refinement factors of $R\backslash = 0.0178$ and $wR2$ = 0.0362 respectively. The goodness of the fit (*S*) is 1.138 for 1108 unique reflections and 146 parameters. The maximum and minimum residual electron density on the final fourier map corresponded to 0.566 and -0.777 e/A''^3 respectively. The structure is refined as a racemic twin.

4 crystallizes in the monoclinic system, space group *P2/n,* with 4 molecules in the unit cell. A total of 6803 reflections (3160 unique, 3029 with $F > 4\sigma F$) were collected in the θ range 1.86 to 27.37, with indices $-14 < h < 14$, $-14 < k < 0$, $-14 < l < 14$. All the non-hydrogen atoms were refined anisotropically while the ring hydrogen atoms were included in the calculated positions using a riding model. Among the three coordinated water molecules, for only two water molecules (OW1 and OW4), the hydrogens could be located. Bond length constraints were applied to water hydrogens after locating from difference maps. All hydrogens were assigned fixed U_{iso} values, equal to $1.2U_{eq}$ of the parent atom for ring hydrogens and $1.3U_{eq}$ for the water hydrogens. The final cycle of full matrix least squares refinement on F^2 converged with unweighted and weighted refinement factors of $R\backslash = 0.0383$ and $wR2 = 0.0879$ respectively. The goodness of the fit (*S*) is 1.124 for 3157 unique reflections and 223 parameters. The maximum and minimum residual electron density on the final fourier map corresponded to 2.115 and -2.132 e/A' respectively.

Crystallographic data for 1, 2, 3 and 4 are presented in Table 3.1 and atomic parameters for 1, 2, 3 and 4 are tabulated in Table 3.2, Table 3.3, Table 3.4 and Table 3.5 respectively.

Table 3.1 Crystallographic data for Ce(dipic)$_3$Sr(dipicH$_2$)(OH$_2$)$_3$·6H$_2$O (1), Ce(dipic)$_3$Ba(dipicH$_2$)(OH$_2$)$_4$·5H$_2$O (2), Ce(dipic)$_3$Ba(OH$_2$)$_6$ (3) and Ce(dipic)$_3$Ba(OH$_2$)$_6$·2H$_2$O (4)

	1	2	3	4
formula	C$_{28}$H$_{32}$Sr CeN$_4$O$_{25}$	C$_{28}$H$_{32}$Ba CeN$_4$O$_{25}$	C$_7$H$_7$Ba$_{0.33}$ Ce$_{0.33}$NO$_6$	C$_{10.50}$H$_{12.50}$Ba$_{0.50}$ Ce$_{0.50}$N$_{1.50}$O$_{10}$
formula weight	1052.32	1102.04	880.86	916.86
a *(Å)*	11.206(4)	11.050(6)	13.0370(11)	11.2287(7)
b (Å)	12.811(2)	12.940(4)	13.0370(11)	10.9693(10)
c (Å)	16.208(4)	16.4970(17)	9.1886(6)	11.3137(8)
α (°)	96.032(17)	96.926(16)	90	90
β (°)	103.54(2)	103.57(2)	90	92.322(6)
γ (°)	113.191(16)	112.25(3)	120	90
V (Å^3)	2028.0(9)	2063.9(13)	1352.5(2)	1392.38(18)
Z	2	2	6	4
Space group	$P\bar{1}$	$P\bar{1}$	*P*3$1c$	*P2/n*
T (K)	293(2)	293(2)	293(2)	293(2)
λ (Å)	0.71073	0.71073	0.71073	0.71073
ρ_{calcd}(Mg/m^3)	1.723	1.747	2.163	2.187
μ (mm^{-1})	2.518	2.129	3.201	3.119
R\	0.0673	0.0595	0.0178	0.0383
$wR2$	0.1774	0.1587	0.0362	0.0879

weighting scheme, 1; A = 0.1388; B = 0.5844; 2: A = 0945; B = 13.8724;

3: *A* = 0.0226; *B* = 0.3459 and 4: *A* = 0.0367; *B* = 0.8631 (see p. vi for definitions).

Table 3.2 Atomic parameters for $Ce(dipic)_3Sr(dipicH_2)(OH_2)_3 \cdot 6H_2O$ (1)

Atom	10^4x	10^4y	10^4z	10^3U_{eq}	Atom	10^4x	10^4y	10^4z	10^3U_{eq}
Ce	6125(1)	2696(1)	7421(1)	26(1)	C7	7318(11)	2023(9)	9240(7)	48(2)
Sr	10407(1)	7649(1)	7060(1)	34(1)	C8	7232(9)	1149(7)	6321(6)	39(2)
O1	7898(6)	4275(5)	7162(4)	35(1)	C9	6459(8)	1464(7)	5579(6)	33(2)
O2	9951(7)	5786(6)	7610(5)	56(2)	C10	6330(10)	1119(8)	4714(6)	44(2)
O3	6286(6)	1792(5)	8616(4)	42(2)	CH	5557(12)	1445(9)	4114(6)	52(3)
O4	7337(10)	1544(8)	9868(5)	83(3)	C12	4935(10)	2113(9)	4373(6)	46(2)
O5	7215(7)	1568(5)	7066(4)	43(2)	C13	5132(9)	2443(7)	5248(6)	35(2)
O6	7816(8)	542(7)	6188(5)	63(2)	C14	4551(9)	3180(7)	5631(6)	35(2)
O7	4842(6)	3372(5)	6464(4)	38(1)	C15	5489(10)	4461(8)	8672(6)	39(2)
O8	3865(8)	3557(6)	5154(5)	54(2)	C16	4160(9)	3360(8)	8483(6)	35(2)
O9	6379(6)	4326(5)	8366(4)	39(2)	C17	3071(10)	3265(9)	8779(6)	46(2)
O10	5650(8)	5369(6)	9133(5)	59(2)	C18	1957(12)	2200(9)	8549(7)	53(3)
O11	4236(6)	872(5)	6909(4)	38(1)	C19	1900(9)	1251(8)	8003(6)	38(2)
O12	2268(7)	-492(5)	6922(4)	46(2)	C20	3016(8)	1424(7)	7712(5)	30(2)
O13	11493(7)	6548(6)	6245(4)	45(2)	C21	3160(9)	505(7)	7140(5)	31(2)
O14	11693(8)	5763(6)	5038(5)	51(2)	C22	11247(10)	6358(7)	5467(7)	40(2)
O15	9144(7)	8780(6)	6250(4)	43(2)	C23	10408(9)	6826(7)	4902(6)	35(2)
O16	8281(8)	9274(6)	5051(5)	53(2)	C24	10095(11)	6598(9)	4026(7)	48(2)
OW1	12506(10)	8192(9)	8348(6)	109(4)	C25	9309(14)	7103(11)	3574(7)	64(3)
OW2	9714(11)	8467(9)	8291(7)	94(3)	C26	8932(12)	7805(10)	4023(7)	56(3)
OW3	7816(8)	6227(7)	6421(5)	67(2)	C27	9284(10)	7970(7)	4911(6)	35(2)
N1	8427(7)	3472(6)	8542(4)	33(2)	C28	8911(9)	8725(8)	5494(7)	38(2)
N2	5871(7)	2118(5)	5835(4)	30(2)	OW4	6640(10)	4769(8)	4002(7)	84(3)
N3	4121(7)	2464(6)	7947(4)	28(1)	OW5	5936(9)	3508(9)	563(7)	89(3)
N4	9986(7)	7485(6)	5349(5)	31(2)	OW6	7036(17)	4313(14)	2391(8)	101(5)
Cl	9095(10)	4871(7)	7682(6)	36(2)	OW7	5650(14)	8877(13)	167(10)	97(5)
C2	9485(9)	4375(7)	8443(6)	33(2)	OW8	8501(17)	9880(13)	117(9)	99(5)

Table 3.2 contd......

C3	10780(10)	4792(8)	9021(6)	42(2)	OW9	7706(17)	7504(12)	9061(12)	92(5)
C4	10967(11)	4264(10)	9709(6)	51(3)	OW10	1684(18)	9865(17)	1906(13)	128(7)
C5	9875(10)	3337(9)	9814(6)	47(2)	OW11	4813(17)	791(13)	1659(12)	107(7)
C6	8611(10)	2976(8)	9209(6)	41(2)					

Table 3.3 Atomic parameters for $Ce(dipic)_3Ba(dipicH_2)(OH_2)_4 \cdot 5H_2O$ (2)

Atom	10^4x	10^4y	10^4z	10^3U_{eq}	Atom	10^4x	10^4y	10^4z	10^3U_{eq}
Ce	6174(1)	2712(1)	7423(1)	37(1)	C17	4984(10)	2073(9)	4415(6)	62(3)
N1	4157(6)	2519(5)	7920(4)	39(1)	C18	5602(11)	1395(9)	4174(6)	66(3)
N2	8477(7)	3477(6)	8547(4)	43(2)	C19	6375(11)	1080(8)	4770(6)	60(3)
N3	5923(7)	2102(6)	5858(4)	43(2)	C20	6501(8)	1449(7)	5619(6)	47(2)
O1	4303(6)	940(5)	6919(4)	50(1)	C21	7289(9)	1151(8)	6354(6)	53(2)
O2	2365(7)	-394(6)	6960(5)	64(2)	Ba	10483(1)	7682(1)	7201(1)	56(1)
O3	6415(6)	4347(5)	8350(4)	50(1)	N4	10039(7)	7495(5)	5388(4)	40(2)
O4	5656(8)	5383(6)	9091(5)	75(2)	O13	9144(8)	8789(6)	6268(5)	67(2)
O5	7968(6)	4224(5)	7173(4)	48(1)	O14	8330(9)	9288(7)	5098(6)	75(2)
O6	10036(8)	5662(7)	7591(6)	83(2)	O15	11567(8)	6570(6)	6268(5)	65(2)
O7	6301(7)	1855(6)	8606(4)	59(2)	O16	11755(8)	5771(7)	5066(6)	69(2)
O8	7357(11)	1598(10)	9841(6)	114(4)	C22	8920(10)	8722(8)	5530(7)	53(2)
O9	4907(6)	3377(5)	6470(4)	51(2)	C23	9288(9)	7949(8)	4953(6)	49(2)
O10	3925(8)	3553(7)	5177(5)	73(2)	C24	8952(13)	7774(11)	4091(8)	76(3)
O11	7301(7)	1580(6)	7094(4)	57(2)	C25	9308(15)	7054(13)	3638(8)	88(4)
O12	7867(9)	522(7)	6230(6)	81(2)	C26	10099(12)	6559(9)	4088(7)	65(3)
C1	3207(9)	585(7)	7147(5)	46(2)	C27	10445(8)	6820(7)	4956(5)	40(2)
C2	3051(8)	1526(7)	7686(5)	42(2)	C28	11316(9)	6366(7)	5501(6)	46(2)
C3	1935(10)	1401(9)	7943(6)	55(2)	OW1	7761(10)	6050(8)	6281(6)	97(3)
C4	1954(10)	2325(9)	8446(7)	62(3)	OW2	12946(13)	7881(12)	8278(9)	156(6)
C5	3101(10)	3349(9)	8711(6)	58(2)	OW3	11395(17)	9167(12)	8837(8)	157(5)
C6	4185(9)	3417(7)	8432(5)	42(2)	OW4A(0.74)	8370(2)	7630(2)	7817(14)	180(12)
C7	5513(9)	4486(8)	8645(6)	48(2)	OW4B(0.26)	8500(3)	6750(3)	8204(17)	66(12)

Table 3.3 contd......

C8	9174(9)	4793(7)	7697(6)	49(2)	OW5	5882(13)	3438(11)	464(8)	84(3)
C9	9534(8)	4347(8)	8453(6)	49(2)	OW6	2346(17)	2425(14)	689(11)	79(4)
C10	10833(9)	4765(9)	9046(7)	62(3)	OW7	6959(17)	4393(14)	2346(11)	118(5)
CH	11006(10)	4277(10)	9729(7)	65(3)	OW8	1850(2)	224(18)	2174(14)	110(6)
C12	9898(11)	3377(10)	9819(7)	68(3)	OW9	5670(2)	9051(18)	354(14)	130(7)
C13	8654(9)	3010(8)	9208(6)	49(2)	OW10	6555(11)	4760(9)	3964(7)	108(3)
C14	7345(12)	2095(11)	9236(7)	71(3)	OW11	4410(2)	730(2)	1788(15)	122(7)
C15	4616(9)	3175(8)	5648(6)	51(2)	OW12	9810(3)	9480(2)	584(18)	144(9)
C16	5171(9)	2414(7)	5278(5)	46(2)					

Site occupation factors of disordered sites are given after the respective atom labels.

Table 3.4 Atomic parameters for $Ce(dipic)_3Ba(OH_2)_6$ (3)

Atom	10^4x	10^4y	10^4z	10^3U_{eq}	Atom	10^4x	10^4y	10^4z	10^3U_{eq}
Ce	3333	6667	2500(1)	16(1)	C3	-784(3)	4275(3)	1728(4)	27(1)
N1	1112(2)	5762(2)	2549(3)	18(1)	C4	-1309(3)	4722(3)	2652(5)	31(1)
01	2272(2)	5128(2)	853(3)	30(1)	C5	-613(3)	5697(3)	3515(4)	27(1)
02	628(3)	3547(3)	30(4)	37(1)	C6	607(3)	6193(3)	3431(4)	20(1)
03	2547(2)	7449(2)	4226(3)	27(1)	C7	1490(3)	7232(3)	4325(4)	22(1)
04	1152(3)	7775(3)	5111(4)	39(1)	Ba	0	0	2907(1)	19(1)
Cl	1149(3)	4452(3)	775(4)	23(1)	OW1	2356(3)	651(3)	2539(4)	41(1)
C2	444(3)	4831(3)	1708(4)	20(1)	OW2	1554(2)	1063(2)	5495(3)	29(1)

Table 3.5 Atomic parameters for $Ce(dipic)_3Ba(OH_2)_6·2H_2O$ (4)

Atom	10^4x	10^4y	10^4z	10^3U_{eq}	Atom	10^4x	10^4y	10^4z	10^3U_{eq}
Ce	7500	7483(1)	2500	22(1)	C7	9176(3)	9767(3)	1665(3)	28(1)
Ba	7500	5943(1)	7500	31(1)	N2	7500	5195(3)	2500	30(1)
N1	9311(2)	8537(2)	3400(3)	25(1)	05	9217(2)	6543(2)	1797(3)	36(1)
01	8130(2)	6856(2)	4413(3)	35(1)	06	10414(2)	4952(3)	1545(3)	45(1)

Table 3.5 contd......

02	9276(2)	6938(3)	6066(3)	46(1)	C8	8460(3)	4597(3)	2162(3)	31(1)
03	8289(2)	9085(2)	1384(3)	33(1)	C9	8494(3)	3326(3)	2153(4)	39(1)
04	9480(3)	10688(2)	1122(3)	42(1)	C10	7500	2702(4)	2500	44(1)
Cl	9794(3)	8154(3)	4422(3)	28(1)	C11	9462(3)	5391(3)	1797(3)	32(1)
C2	10870(3)	8595(3)	4883(4)	35(1)	OW1	8459(3)	7883(3)	8836(3)	48(1)
C3	11451(3)	9474(3)	4248(4)	38(1)	OW2	7984(12)	3507(12)	6806(16)	255(7)
C4	10932(3)	9903(3)	3191(4)	33(1)	OW3	8038(6)	4331(6)	5685(8)	115(2)
C5	9854(3)	9402(3)	2786(3)	27(1)	OW4	8728(4)	2341(4)	9237(5)	72(1)
C6	9030(3)	7237(3)	5042(3)	30(1)					

3.2. Results and Discussion

3.2.1 Synthesis: In all cases mixing the ligand and the metal ions leads to immediate formation of a precipitate. In the case of 1 and 2, this is a minor product and is discarded. The actual compounds are isolated from the mother liquor. However, in the case of 3 and 4, the initial precipitate was stirred in the solution for several hours and the precipitate is obtained as the major product. The nature of the initial precipitate in the case of 1 and 2 and the species remaining in solution in the case of 3 and 4 were not characterized. It may be noted that 3 and 4 are pseudo polymorphs, but as shown later they have very different structures. The X-ray powder pattern of the crystals were in agreement with the calculated diffractograms,[43] thereby establishing that the crystal X-rayed in each case is same as the bulk product.

3.2.2. Structure of **Ce(dipic)$_3$Sr(dipicH$_2$)(OH$_2$)$_3$·6H$_2$O** (1): The asymmetric unit of 1 consists of alternating nine coordinate Ce^{4+} (Figure 3.1a) and eight coordinate Sr^{2+} (Figure 3.1b), connected by the bridging carboxylate groups of dipic^{2-} thus assembling

into a one dimensional chain (Figure 3.2). Three tridentate dipic^{2-} ligands coordinate to Ce^{4+} in a slightly distorted tricapped trigonal prismatic mode. One tridentate dipicH$_2$ and three water molecules are coordinated to Sr^{2+}. Eight coordination around Sr^{2+} is achieved by the sharing of the carboxylate 0 atoms from two dipic$^{2"}$ ligands of adjacent [Ce(dipic)$_3$]$^{2-}$ units. This results in a distorted square antiprismatic geometry for the Sr^{2+} unit. Along the chain, the Ce$\cdots$Sr distances alternate between 6.462(2) and 6.929(2) A.

The cerium coordination polyhedron is essentially the same as that found in the calcium analog.[2] As expected, the Sr-(O,N) distances are longer (by about 0.1 A) than the Ca-(O,N) distances (Table 3.6). In both the structures, six out of the total eight solvent water sites have partial site occupation factors. Refinement suggests the present compound to be a hexahydrate, while the calcium stmcture was a pentahydrate.

(a)   (b)
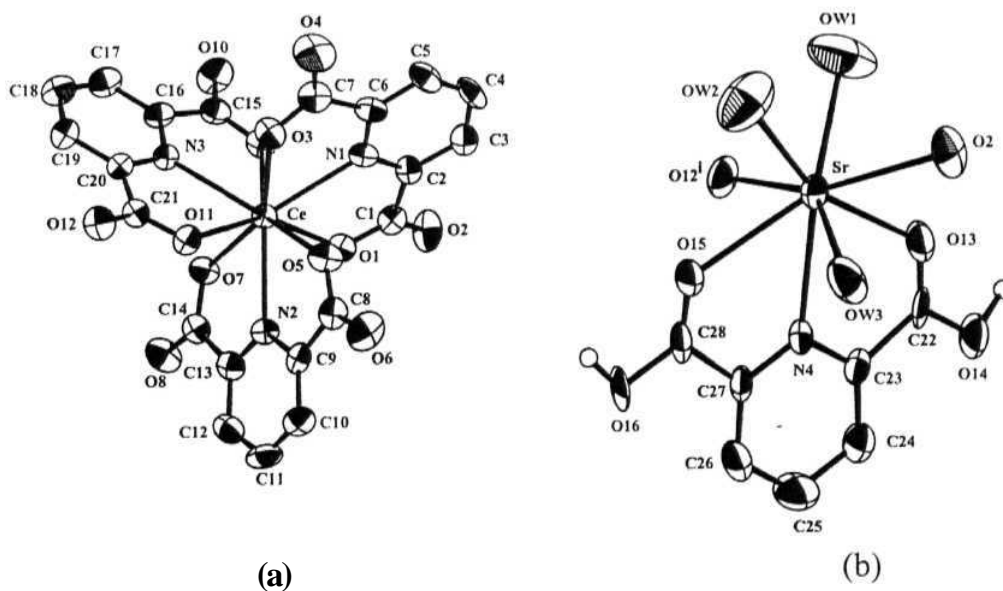
Figure 3.1 Ortep view of the coordination environment of (a) Ce^{4+} and (b) Sr^{2+} in 1. Atoms are represented as 50% displacement ellipsoids.

Ring hydrogens have been omitted for clarity. Symmetry code: (i) $x + 1$ $y + 1, z$.
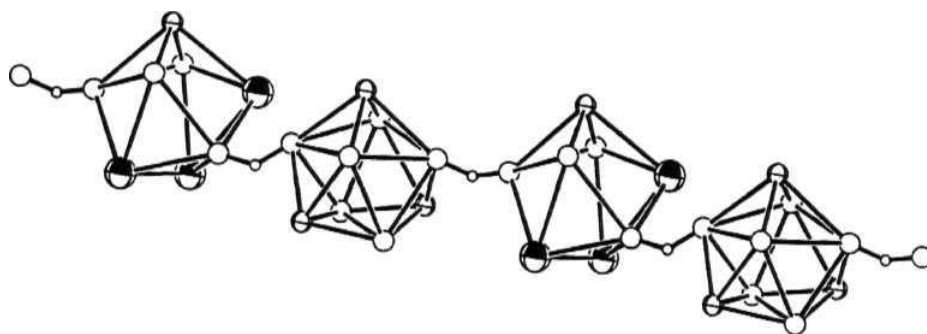
Figure 3.2 Perspective view of a segment of the polymeric chain formed by the linking of coordination polyhedra in 1. Three dipic$^{2"}$ nitrogen atoms (footballs) cap the trigonal prism formed by carboxylate oxygen atoms (large open circles) around Ce. The square antiprism around Sr is formed by three water molecules (large shaded footballs), one dipicH$_2$ nitrogen atom, and four carboxylate oxygen atoms. The alternating SrNO$_7$ and CeN$_3$O$_6$ polyhedra are linked by carboxylate groups (C1 and C21, small open circles). The Sr and Ce atoms are not shown.

Table 3.6 Bond lengths (A) and angles (°) for Ce(dipic)$_3$Sr(dipicH$_2$)(OH$_2$)$_3$·6H$_2$O (1).

Ce-O7	2.333(6)	Ce-N3	2.507(7)	Sr-OW2	2.571(9)
Ce-O9	2.334(6)	Ce-N2	2.515(7)	Sr-OW3	2.617(8)
Ce-O5	2.336(6)	Ce-N1	2.520(7)	Sr-O13	2.632(6)
Ce-O11	2.346(6)	Sr-02	2.540(7)	Sr-O15	2.640(6)
Ce-O3	2.366(6)	Sr-OW1	2.545(9)	Sr-N4	2.673(7)

Table 3.6 contd.....

Ce-O1	2.371(6)	Sr-O12#1	2.547(6)	O7-Ce-O9	80.2(2)
O7-Ce-O5	127.1(2)	O9-Ce-N2	137.0(2)	OW1-Sr-OW3	142.8(3)
O9-Ce-O5	144.5(2)	O5-Ce-N2	63.1(2)	O12#1-Sr-OW3	143.7(2)
O7-Ce-O11	86.3(2)	O11-Ce-N2	74.7(2)	OW2-Sr-OW3	85.0(3)
O9-Ce-O11	128.1(2)	O3-Ce-N2	134.5(2)	O2-Sr-O13	74.2(2)
O5-Ce-O11	80.9(2)	O1-Ce-N2	75.4(2)	OW1-Sr-O13	84.6(3)
O7-Ce-O3	147.0(2)	N3-Ce-N2	121.9(2)	O12#1-Sr-O13	85.7(2)
O9-Ce-O3	88.5(2)	O7-Ce-N1	139.0(2)	OW2-Sr-O13	160.0(3)
O5-Ce-O3	78.2(2)	O9-Ce-N1	72.6(2)	OW3-Sr-O13	101.3(3)
O11-Ce-O3	76.6(2)	O5-Ce-N1	71.9(2)	O2-Sr-O15	141.8(2)
O7-Ce-O1	80.0(2)	O11-Ce-N1	134.7(2)	OW1-Sr-O15	135.9(3)
O9-Ce-O1	75.7(2)	O3-Ce-N1	62.9(2)	O12#1-Sr-O15	74.0(2)
O5-Ce-O1	86.4(2)	O1-Ce-N1	64.1(2)	OW2-Sr-O15	79.0(3)
O11-Ce-O1	150.1(2)	N3-Ce-N1	117.8(2)	OW3-Sr-O15	71.9(2)
O3-Ce-O1	127.1(2)	N2-Ce-N1	120.2(2)	O13-Sr-O15	120.9(2)
O7-Ce-N3	74.2(2)	O2-Sr-OW1	76.0(3)	O2-Sr-N4	117.4(2)
O9-Ce-N3	64.3(2)	O2-Sr-O12#1	144.2(2)	OW1-Sr-N4	133.9(3)
O5-Ce-N3	138.4(2)	OW1-Sr-O12#1	72.8(3)	O12#1-Sr-N4	74.9(2)
O11-Ce-N3	63.8(2)	O2-Sr-OW2	90.4(3)	OW2-Sr-N4	139.1(3)
O3-Ce-N3	73.0(2)	OW1-Sr-OW2	79.3(4)	OW3-Sr-N4	77.7(2)
O1-Ce-N3	135.1(2)	O12#1-Sr-OW2	100.5(3)	O13-Sr-N4	60.8(2)
O7-Ce-N2	64.0(2)	O2-Sr-OW3	70.6(2)	O15-Sr-N4	60.4(2)

#1 $x + 1, y + 1, z$

3.2.3. Structure of Ce(dipic)₃Ba(dipicH₂)(OH₂)₄·5H₂O (2): The structure of **2** is similar as that observed in the previously reported $Ce(dipic)_3Ca(dipicH_2)(OH_2)_3·5H_2O^2$ and that in 1. The coordination around Ce^{4+} and Ba^{2+} is shown in Figure 3.3. The coordination environment around Ce^{4+} is distorted tricapped trigonal prismatic and the same as observed **in that** of **1.** Ba^{2+} is also nine coordinate with distorted tricapped trigonal prismatic geometry. The Ba^{2+} coordination polyhedron is made up of one dipicH2, four water molecules and two bridging carboxylate oxygen atoms from neighboring Ce^{4+} units. The resulting structure is a one dimensional chain of alternating nine coordinate Ce^{4+} and nine coordinate Ba^{2+} polyhedra (Figure 3.4). Along the chain, the Ce···Ba distances alternate between 6.509(3) and 7.027(4) A. Selected bond lengths and angles are tabulated in Table 3.7.

(a)   (b)
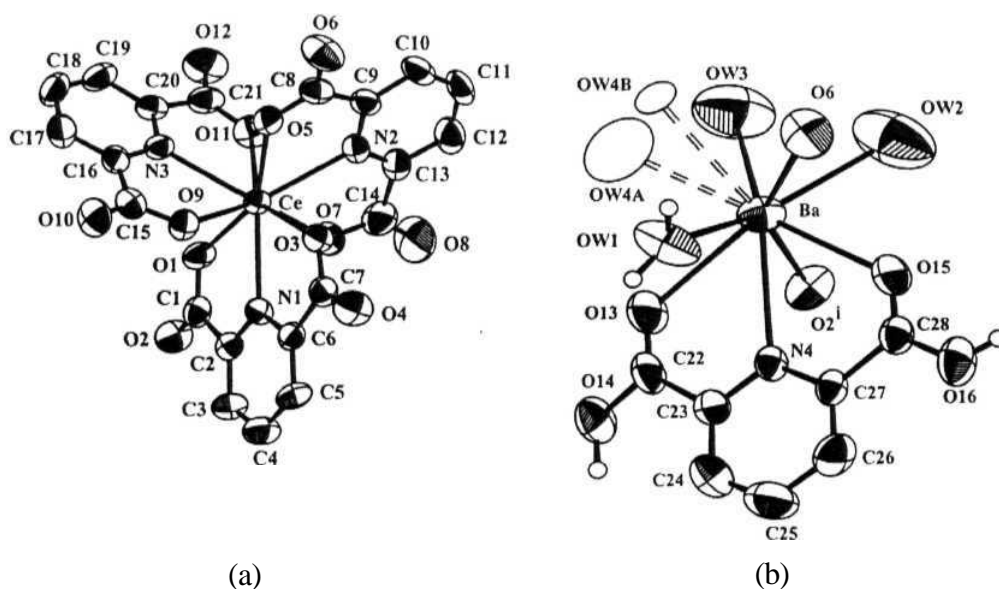
Figure 3.3 Ortep view of the coordination environment of (a) Ce   and (b) Ba^{2+} in **2.** Atoms are represented as 50% displacement ellipsoids.

Ring hydrogens have been omitted for clarity. Symmetry code: (i) $x + 1$, $y + 1$, z. In (b), the disordered $OW4$ positions are indicated as open ellipses and bonds to them are shown as broken lines.
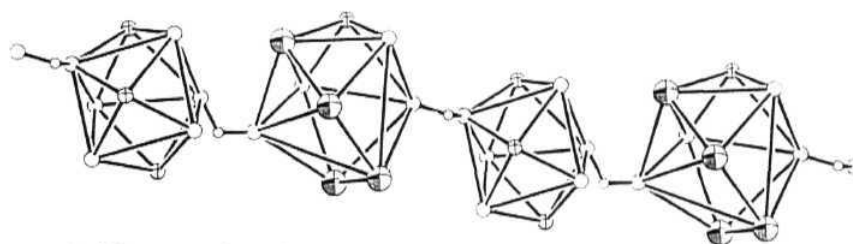
Figure 3.4 Perspective view of a segment of the polymeric chain formed by the linking of coordination polyhedra in 2. Three $dipic^2$ nitrogen atoms (footballs) cap the trigonal prism formed by carboxylate oxygen atoms (large open circles) around Ce. The trigonal prism around Ba is formed by four water molecules (large shaded footballs), one $dipicH_2$ nitrogen atom, and four carboxylate oxygen atoms. The alternating $BaNO_g$ and CeN_3O_6 polyhedra are linked by carboxylate groups ($C1$ and $C21$, small open circles). The Ba and Ce atoms are not shown.

Table 3.7 Bond lengths (A) and angles (°) for $Ce(dipic)_3Ba(dipicH_2)(OH_2)_4 \cdot 5H_2O$ (2).

Ce-O1	2.316(6)	Ce-N1	2.487(6)	Ba-OW2	2.779(13)
Ce-O9	2.318(6)	Ce-N2	2.516(7)	Ba-OW3	2.829(13)
Ce-O3	2.342(6)	Ce-N3	2.525(7)	Ba-OW1	2.843(9)
Ce-O11	2.345(6)	Ba-O2#2	2.717(7)	Ba-N4	2.878(7)
Ce-O5	2.359(6)	Ba-O13	2.770(7)	Ba-OW4A	2.74(2)
Ce-O7	2.360(6)	Ba-O15	2.740(7)	Ba-OW4B	3.03(2)

Table 3.7 contd.....

O1-Ce-O9	86.8(2)	O1-Ce-N3	74.4(2)	O15-Ba-OW3	136.3(4)
O1-Ce-O3	128.2(2)	O9-Ce-N3	63.6(2)	O13-Ba-OW3	98.6(3)
O9-Ce-O3	80.2(2)	O3-Ce-N3	137.0(2)	OW2-Ba-OW3	65.0(5)
O1-Ce-O11	81.0(2)	O11-Ce-N3	63.5(2)	O6-Ba-OW1	69.7(3)
O9-Ce-O11	127.0(2)	O5-Ce-N3	75.3(2)	O2#2-Ba-OW1	136.4(2)
O3-Ce-O11	144.1(2)	O7-Ce-N3	135.1(2)	0W4A-Ba-0W1	60.8(6)
O1-Ce-O5	149.7(2)	N1-Ce-N3	121.6(2)	O15-Ba-OW1	91.7(3)
O9-Ce-O5	79.9(2)	N2-Ce-N3	120.9(2)	O13-Ba-OW1	71.8(3)
O3-Ce-O5	76.3(2)	C8-O6-Ba	144.8(7)	0W2-Ba-0W1	142.1(3)
O11-Ce-O5	85.5(2)	O6-Ba-O2#2	145.4(2)	0W3-Ba-0W1	127.4(4)
O1-Ce-O7	76.4(2)	O6-Ba-OW4A	86.5(7)	O6-Ba-N4	111.3(2)
O9-Ce-O7	146.7(2)	O2#2-Ba-OW4A	124.2(6)	O2#2-Ba-N4	71.2(2)
O3-Ce-O7	87.8(2)	O6-Ba-O15	71.1(2)	OW4A-Ba-N4	117.4(5)
O11-Ce-O7	78.9(2)	O2#2-Ba-O15	84.0(2)	O15-Ba-N4	56.95(19)
O5-Ce-O7	127.3(2)	OW4A-Ba-O15	149.7(6)	O13-Ba-N4	56.82(19)
O1-Ce-N1	63.9(2)	O6-Ba-O13	141.3(2)	OW2-Ba-N4	121.3(4)
O9-Ce-N1	74.7(2)	O2#2-Ba-O13	70.5(2)	OW3-Ba-N4	146.5(3)
O3-Ce-N1	64.3(2)	OW4A-Ba-O13	72.0(6)	0W1-Ba-N4	70.3(2)
O11-Ce-N1	138.5(2)	O15-Ba-O13	113.5(2)	O6-Ba-OW4B	59.8(6)
O5-Ce-N1	135.8(2)	O6-Ba-OW2	72.6(3)	O2#2-Ba-OW4B	145.3(6)
O7-Ce-N1	72.1(2)	O2#2-Ba-OW2	77.1(3)	OW4A-Ba-OW4B	27.7(7)
01-Ce-N2	134.4(2)	OW4A-Ba-OW2	121.3(6)	O15-Ba-OW4B	129.4(6)
O9-Ce-N2	138.8(2)	O15-Ba-OW2	71.9(4)	O13-Ba-OW4B	98.6(6)
O3-Ce-N2	72.4(2)	O13-Ba-OW2	146.1(3)	OW2-Ba-OW4B	102.4(6)
O11-Ce-N2	71.9(2)	O6-Ba-OW3	102.0(3)	OW3-Ba-OW4B	69.5(7)

Table 3.7 contd. . . . . .

O5-Ce-N2	64.2(2)	O2#2-Ba-OW3	79.5(4)	OW1-Ba-0W4B	61.7(6)
O7-Ce-N2	63.1(2)	OW4A-Ba-OW3	67.0(6)	N4-Ba-OW4B	131.2(6)
N1-Ce-N2	117.4(2)				

#2	$x + 1, y + 1, z$

3.2.4. Structure of Ce(dipic)$_3$Ba(OH$_2$)$_6$ (3): The structure of 3 is rather different from 1 and 2. While the Ce coordination environment (Figure 3.5a) is the same as that observed in 1 and 2, Ba coordination environment is made of water molecules only (Figure 3.5b). Ce^{4+} is situated on a three fold axis and is coordinated to three symmetry related ligands resulting in a distorted tricapped trigonal coordination as observed in 1 and 2. Ba^{2+} is also situated on a three fold axis and coordinated to nine water molecules, with a tricapped trigonal prismatic geometry. Among the nine water molecules, three lie in the basal plane and the other six are shared with neighboring Ba^{2+} units lying above and below the basal plane forming a chain (Figure 3.6a). Ba-OW distances are slightly longer (about 0.1 A) than the distances in 2 (Table 3.8). In the unit cell, the Ce(dipic)$_3$$^{2-}$ units pack in a trigonal fashion (Figure 3.6b). The Ba(OH$_2$)$_6$$^{2+}$ polymer chain passes through the trigonal channels created by the anionic units (Figure 3.7). Along the chain, the Ba atoms are separated by 9.189(1) A. The coordinated waters are involved in hydrogen bonding with the carboxylate O atoms of the Ce(dipic)$_3$$^{2-}$ units, with H$\cdots$A distances in the range 1.7 - 2.6 A.

The polymer chain of Ba(OH$_2$)$_6$$^{2+}$ is similar to the polymer chain structure observed in SrCl$_2$·6H$_2$O.[44] This type of chain structure is observed in all the hexahydrates of Ca and Sr halides. However, such a hydrate is not known for BaCl$_2$, while BaI$_2$·6H$_2$O shows the same structure as the other hexahydrates mentioned above.

(a)   **(b)**
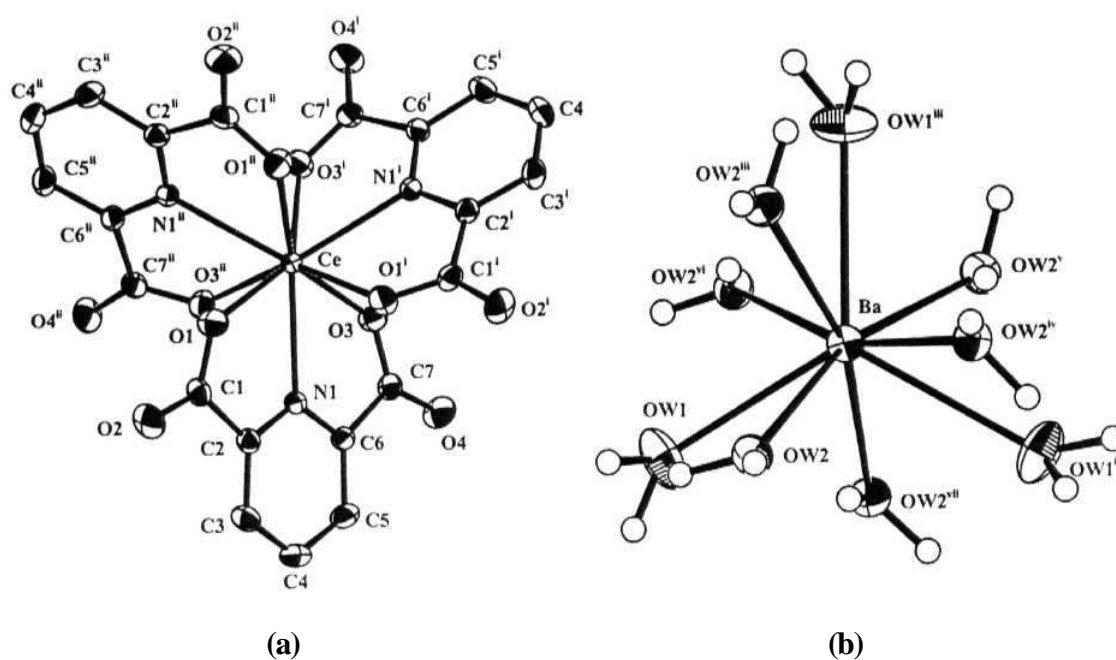
Figure 3.5 Ortep view of the coordination environment of (a) Ce^{4+} and (b) Ba^{2+} in 3. Atoms are represented as 50% displacement ellipsoids. Ring hydrogens have been omitted for clarity. Symmetry code: (i) $-x + y$, $-y + 1$, z; (ii) $-y + 1$, $x - y$, z; (iii) $-x + y$, $-x$, z; (iv) $-y$, $x - y$, z; (v) $-x$, $-x + y$, $z - 1/2$; (vi) $x - y$, $-y$, $z - 1/2$ and (vii) y, x, $z - 1/2$.

(a) **(b)**
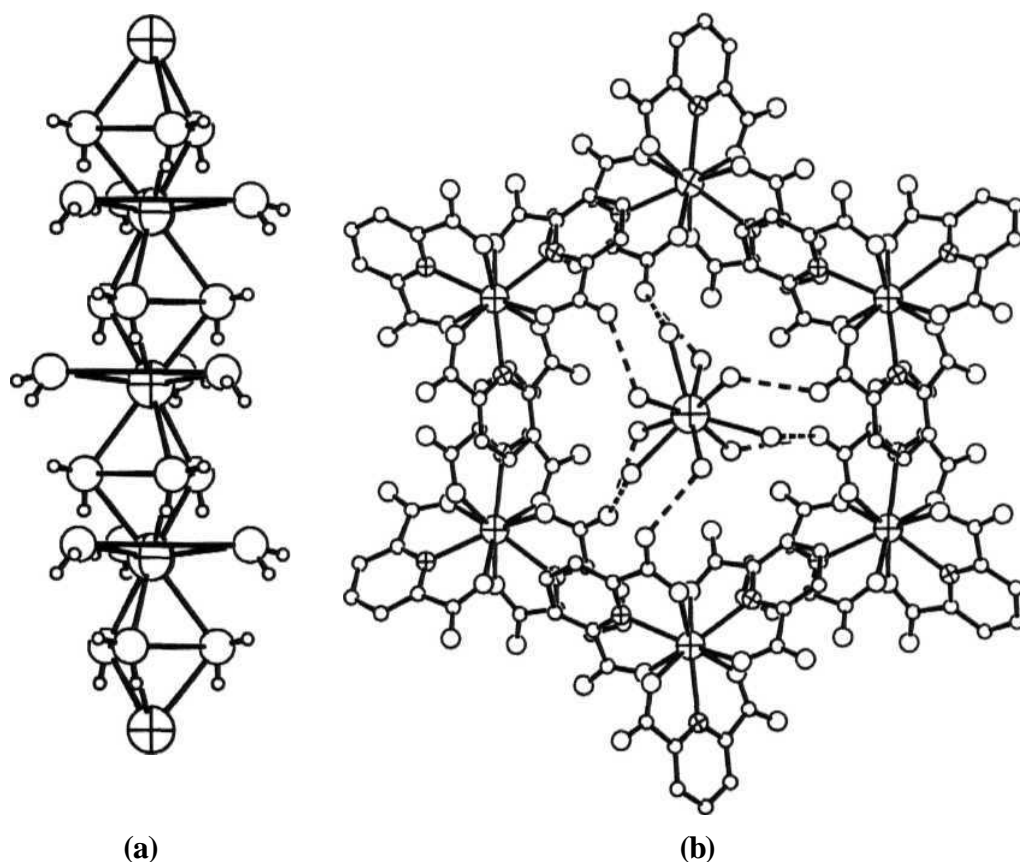
Figure 3.6 View showing (a) the polymeric chain of $Ba(OH_2)_6$ units in 3. Ba atoms are shown as footballs. Water oxygens are represented as open circles. (b) the trigonal arrangement of $Ce(dipic)3^{2-}$ units. The $Ba(OH_2)_6$ unit is sitting in the trigonal channel. Ba, Ce, and N atoms are shown as footballs in the decreasing order of size. C and carboxylate O atoms are shown as open circles. Hydrogen bonds between carboxylate oxygens and water molecules are shown in broken lines.

Figure 3.7 Stick representation of 3 showing the polymer chain of $Ba(OH_2)_6{}^{2+}$ passing through the trigonal channels of $Ce(dipic)_3{}^{2-}$. The polymer chain is shown in red color and the chelate rings in green and blue colors are in two different planes.

Table 3.8 Bond lengths (A) and angles (°) for $Ce(dipic)_3Ba(OH_2)_6$ (3).

Ce-O1#1	2.335(3)	Ce-N1	2.523(3)	Ba-OW2#5	2.851(3)
Ce-O1	2.335(3)	Ce-N1#1	2.523(3)	Ba-OW2#6	2.851(3)
Ce-O1#2	2.335(3)	Ce-N1#2	2.523(3)	Ba-OW2#7	2.851(3)
Ce-O3	2.377(2)	Ba-OW1#3	2.768(3)	Ba-OW2	2.979(3)
Ce-O3#1	2.377(2)	Ba-0W1#4	2.768(3)	Ba-OW2#4	2.979(3)
Ce-O3#2	2.377(2)	Ba-OW1	2.768(3)	Ba-OW2#3	2.979(3)
O1#1-Ce-O1	82.54(11)	O3-Ce-N1#1	71.80(9)	OW1-Ba-OW2#7	67.48(9)
O1#1-Ce-O1#2	82.54(11)	O3#1-Ce-N1#1	63.16(8)	OW2#5-Ba-OW2#7	66.03(9)
O1-Ce-O1#2	82.54(11)	O3#2-Ce-N1#1	136.78(10)	OW2#6-Ba-OW2#7	66.03(9)
O1#1-Ce-O3	83.01(9)	N1-Ce-N1#1	119.972(4)	OW1#3-Ba-OW2	126.56(9)
O1-Ce-O3	127.13(9)	O1#1-Ce-N1#2	140.21(11)	OW1#4-Ba-OW2	97.71(9)
O1#2-Ce-O3	144.60(9)	O1-Ce-N1#2	72.81(9)	OW1-Ba-OW2	64.04(9)
O1#1-Ce-O3#1	127.13(9)	O1#2-Ce-N1#2	63.98(9)	OW2#5-Ba-OW2	165.19(10)
O1-Ce-O3#1	144.59(9)	O3-Ce-N1#2	136.78(10)	OW2#6-Ba-OW2	125.49(10)
O1#2-Ce-O3#1	83.01(9)	O3#1-Ce-N1#2	71.80(9)	OW2#7-Ba-OW2	108.31(8)
O3-Ce-O3#1	80.35(10)	O3#2-Ce-N1#2	63.15(8)	OW1#3-Ba-OW2#4	97.71(9)
O1#1-Ce-O3#2	144.60(9)	N1-Ce-N1#2	119.968(4)	OW1#4-Ba-OW2#4	64.04(9)
O1-Ce-O3#2	83.01(10)	N1#1-Ce-N1#2	119.968(5)	OW1-Ba-OW2#4	126.56(9)
O1#2-Ce-O3#2	127.13(8)	OW1#3-Ba-OW1#4	118.53(3)	OW2#5-Ba-OW2#4	108.31(8)
O3-Ce-O3#2	80.35(10)	OW1#3-Ba-OW1	118.53(3)	OW2#6-Ba-OW2#4	165.19(10)
O3#1-Ce-O3#2	80.35(10)	OW1#4-Ba-OW1	118.53(3)	OW2#7-Ba-OW2#4	125.49(10)
O1#1-Ce-N1	72.81(9)	OW1#3-Ba-OW2#5	64.50(9)	OW2-Ba-OW2#4	62.88(8)
O1-Ce-N1	63.98(9)	OW1#4-Ba-OW2#5	67.48(9)	OW1#3-Ba-OW2#3	64.04(9)
O1#2-Ce-N1	140.21(11)	OW1-Ba-OW2#5	121.94(9)	OW1#4-Ba-OW2#3	126.56(9)

Table 3.8 contd......

O3-Ce-N1	63.16(8)	OW1#3-Ba-OW2#6	67.48(9)	OW1-Ba-OW2#3	97.71(9)
O3#1-Ce-N1	136.78(10)	OW1#4-Ba-OW2#6	121.94(9)	OW2#5-Ba-OW2#3	125.49(10)
O3#2-Ce-N1	71.80(9)	OW1-Ba-OW2#6	64.50(9)	OW2#6-Ba-OW2#3	108.31(8)
O1#1-Ce-N1#1	63.98(9)	OW2#5-Ba-OW2#6	66.03(9)	OW2#7-Ba-OW2#3	165.19(10)
O1-Ce-N1#1	140.21(11)	OW1#3-Ba-OW2#7	121.94(9)	OW2-Ba-OW2#3	62.88(8)
O1#2-Ce-N1#1	72.81(9)	OW1#4-Ba-OW2#7	64.50(9)	OW2#4-Ba-OW2#3	62.88(8)

#1 $-x + y, -x + 1, z$ #2 $-y + 1, x - y$ 1,2   #3 $-x + y, -x, z$ #4 $-y, x - y, z$
#5 $-x, -x+ y, z - 1/2$ #6 $x - y, -y, z - 1/2$ #7 $y, x, z - 1/2$

3.2.5. Structure of **Ce(dipic)$_3$Ba(OH$_2$)$_6$·2H$_2$O** (4): In 4 also, the coordination of Ce^{4+} is the same as observed in the above three cases. The coordination environment around Ce^{4+} and Ba^{2+} is shown in Figure 3.8. Three dipic^{2-} ligands coordinate in a tridentate fashion, giving a distorted tricapped trigonal prismatic geometry around Ce^{4+}. As opposed to the above three cases, here Ba^{2+} is ten coordinate. Such a coordination of ten for Ba^{2+} has been previously observed.[45] Ba is coordinated to six water molecules and four carboxylate oxygens from neighboring Ce(dipic)$_3{}^{2-}$ units giving a distorted bicapped square antiprismatic geometry (Figure 3.8c). The Ce-O,N and Ba-OW distances are same as those observed in 2 and 3 (Table 3.9). Each Ce is surrounded by four Ba units. All the five atoms are arranged in a square pyramidal geometry with Ce^{4+} at the apex and the four Ba^{2+} atoms in the basal plane. The Ce^{4+} deviates by 2.72 A from the mean plane defined by its surrounding Ba^{2+}. Similarly, each Ba^{2+} is surrounded by four Ce^{4+} in a distorted tetrahedral fashion. Ba^{2+} deviates by 1.03 A from the mean plane defined by the surrounding Ce^{4+}. This type of coordination around Ce^{4+} and Ba^{2+} units, give rise to a corrugated sheet structure (Figure 3.9). These sheets assemble as layers in the crystal .

The water molecules are involved in strong hydrogen bonding with the carboxylate oxygens, the $H \cdots A$ distances lying in the range 1.9 - 2.5 A and connect the layers (Figure 3.10). Different views of packing of the cationic and anionic units in the unit cell are shown in Figure 3.11.

The layer structure observed in the present case may be related to the (4,4) nets of AX type, seen in the structure of PbO.[46] In the present structure, it may be treated as A $= Ba^{2+}$ and $X = Ce^{4+}$.

(a)

(b)

(c)
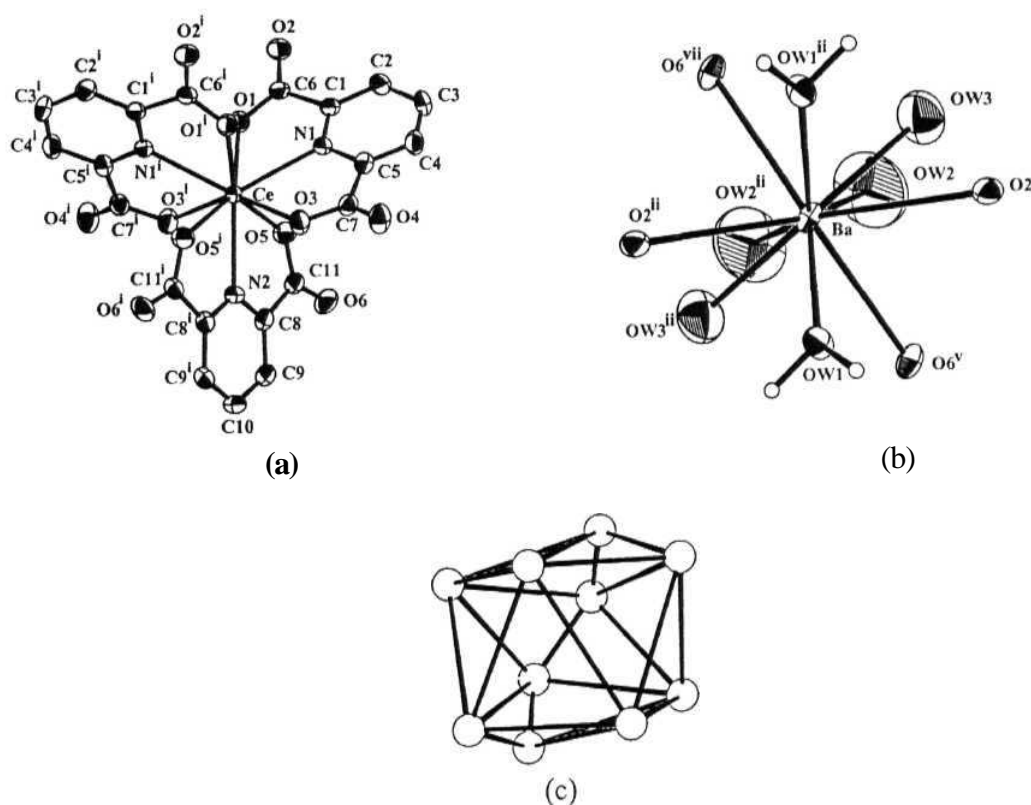
Figure 3.8 Ortep view of the coordination environment of (a) Ce^{4+}; (b) Ba^{2+} and (c) polyhedral drawing showing the bicapped square

antiprismatic geometry around Ba $^+$ in 4. Atoms are represented as 50% displacement ellipsoids in (a) and (b). Ring hydrogens have been omitted for clarity. Symmetry code: (i) -x + 3/2, y, ~z + 1/2; (ii) -x + 3/2, y, -z + 3/2; (v) -x + 2, -y + 1, -z + 1 and (vii) x - 1/2, -y + 1, z + 1/2.
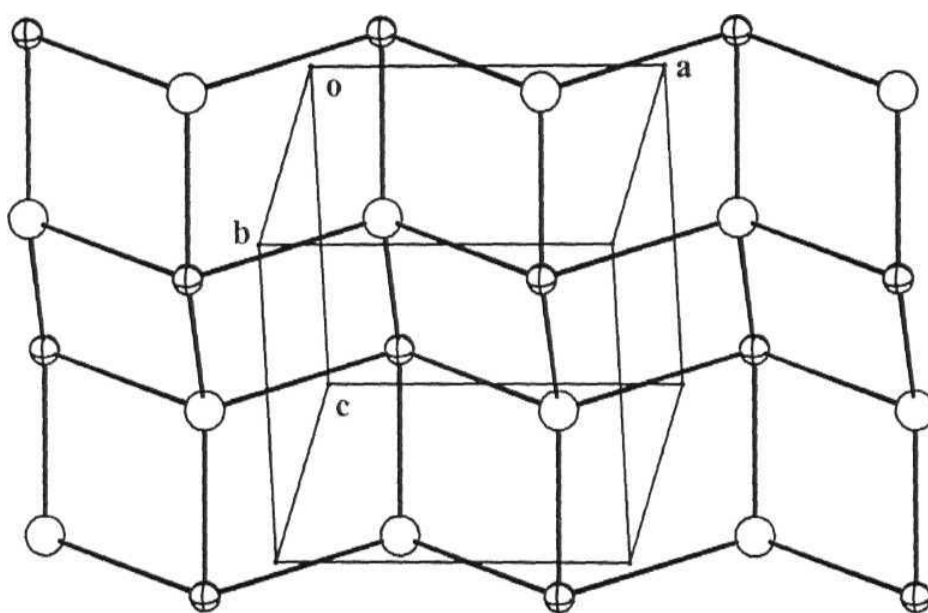
Figure 3.9 Corrugated sheet structure made of $Ce^{4"}$ and Ba^{2+} ions in 4. Footballs represent Ce atoms and open circles Ba atoms.
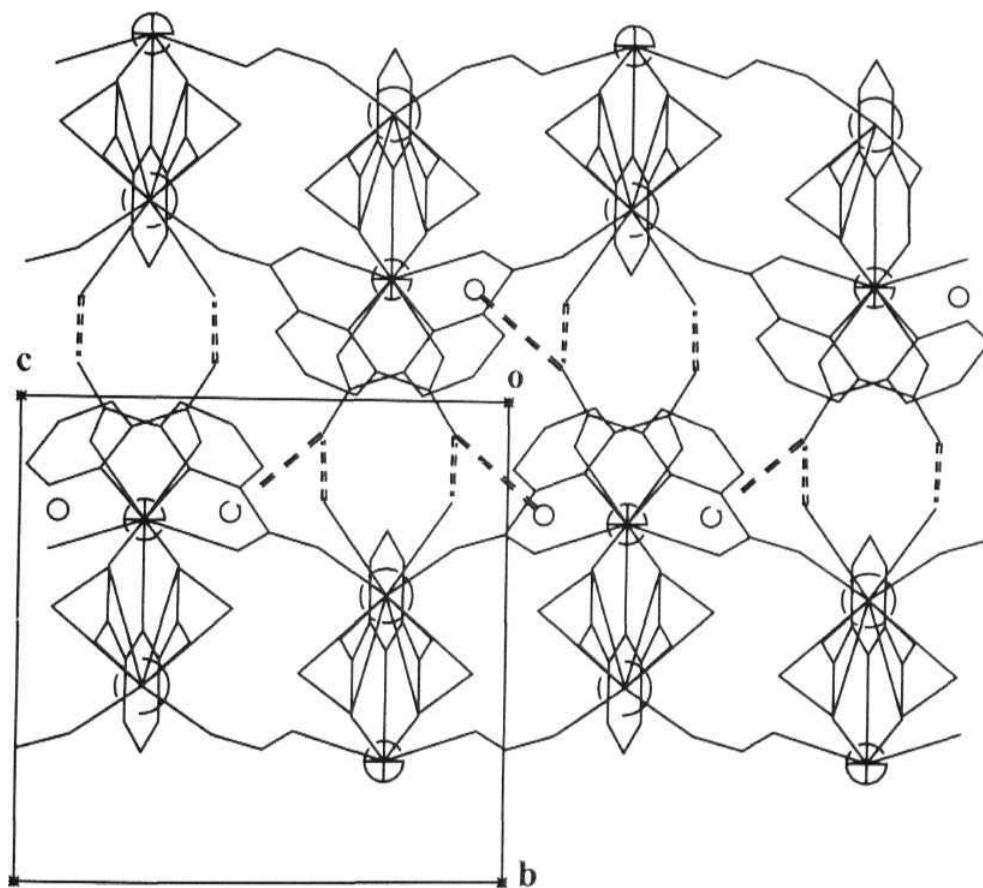
Figure 3.10 Skeletal drawing showing the hydrogen bond (broken lines) connected layers in 4. Footballs represent Ce atoms and large open circles, the Ba atoms. Small open circles represent the solvent water O atoms.

(a)   (b)

(c)
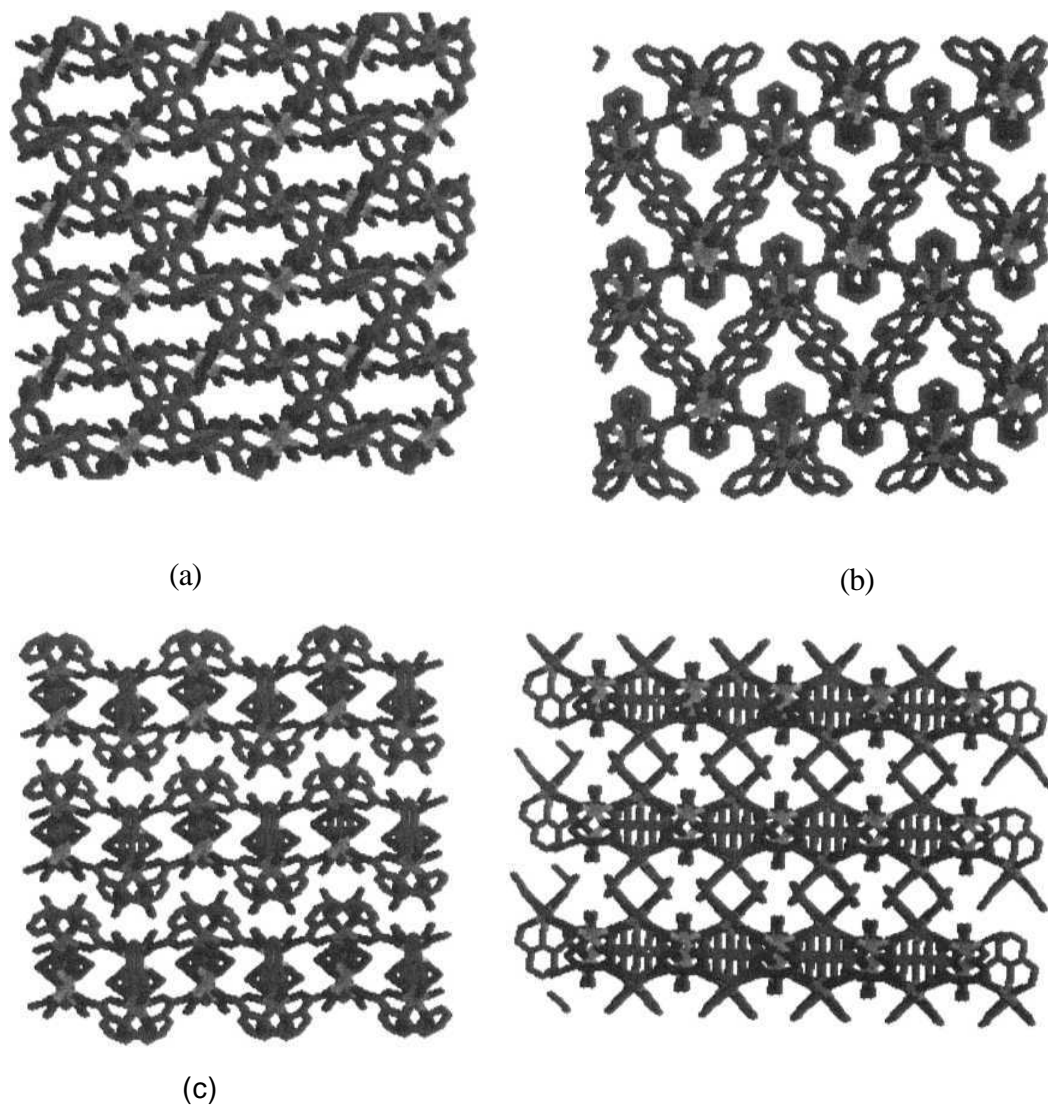
Figure 3.11 Different views of the packing in 4. (a) *ac* plane; (b) *ab* plane; (c) *bc* plane and (d) view down the diagonal of *ac* plane.

Table 3.9 Bond lengths (A) and angles (°) for $Ce(dipic)_3Ba(OH_2)_6 \cdot H_2O$ (4).

Ce-O1#1	2.352(3)	Ce-N1	2.518(3)	Ba-OW1	2.800(3)
Ce-O1	**2.352(3)**	Ce-N1#1	2.518(3)	Ba-OW1#4	2.800(3)
Ce-O5#1	**2.353(2)**	Ba-O6#2	2.722(3)	Ba-02	2.839(3)
Ce-O5	**2.353(2)**	Ba-O6#3	2.722(3)	Ba-O2#4	2.839(3)
Ce-O3#1	**2.357(2)**	Ba-0W3	2.795(7)	Ba-OW2	2.844(12)
Ce-O3	2.357(2)	Ba-OW3#4	2.795(7)	Ba-OW2#4	2.844(12)
Ce-N2	2.510(4)	N2-Ce-N1	117.33(6)	OW3#4-Ba-O2	147.23(15)
O1#1-Ce-O1	146.00(12)	O1#1-Ce-N1#1	63.52(9)	OW1-Ba-O2	75.70(9)
O1#1-Ce-O5#1	87.88(10)	O1-Ce-N1#1	135.59(9)	OW1#4-Ba-O2	70.30(9)
O1-Ce-O5#1	77.34(10)	O5#1-Ce-N1#1	71.26(9)	O6#2-Ba-O2#4	75.68(9)
O1#1-Ce-O5	77.34(10)	O5-Ce-N1#1	136.34(10)	O6#3-Ba-O2#4	121.65(10)
O1-Ce-O5	87.88(10)	O3#1-Ce-N1#1	63.87(9)	OW3-Ba-O2#4	147.23(15)
O5#1-Ce-O5	128.04(12)	O3-Ce-N1#1	75.88(9)	OW3#4-Ba-O2#4	69.23(16)
O1#1-Ce-O3#1	127.23(9)	N2-Ce-N1#1	117.32(6)	OW1-Ba-O2#4	70.30(9)
O1-Ce-O3#1	80.26(9)	N1-Ce-N1#1	125.35(12)	OW1#4-Ba-O2#4	75.70(9)
O5#1-Ce-O3#1	79.31(9)	O6#2-Ba-O6#3	137.70(13)	O2-Ba-O2#4	134.80(14)
O5-Ce-O3#1	146.99(9)	O6#2-Ba-OW3	71.84(16)	O6#2-Ba-OW2	73.9(3)
O1#1-Ce-O3	80.26(9)	O6#3-Ba-OW3	81.67(18)	O6#3-Ba-OW2	66.4(3)
O1-Ce-O3	127.23(9)	O6#2-Ba-OW3#4	81.67(19)	OW3-Ba-OW2	32.1(4)
O5#1-Ce-O3	146.99(9)	O6#3-Ba-OW3#4	71.84(16)	OW3#4-Ba-OW2	70.0(4)
O5-Ce-O3	79.31(9)	OW3-Ba-OW3#4	101.5(3)	OW1-Ba-OW2	142.2(3)
O3#1-Ce-O3	83.61(13)	O6#2-Ba-OW1	142.57(10)	OW1#4-Ba-OW2	129.7(4)
O1#1-Ce-N2	73.00(6)	O6#3-Ba-OW1	75.77(10)	O2-Ba-OW2	93.3(3)
01-Ce-N2	73.00(6)	0W3-Ba-0W1	141.98(15)	O2#4-Ba-OW2	131.7(3)

Table 3.9 contd.

O5#1-Ce-N2	64.02(6)	OW3#4-Ba-OW1	100.0(2)	O6#2-Ba-OW2#4	66.4(3)
O5-Ce-N2	64.02(6)	O6#2-Ba-OW1#4	75.77(10)	O6#3-Ba-OW2#4	73.9(3)
O3#1-Ce-N2	138.19(7)	O6#3-Ba-OW1#4	142.57(10)	OW3-Ba-OW2#4	70.0(4)
O3-Ce-N2	138.19(7)	OW3-Ba-OW1#4	100.0(2)	OW3#4-Ba-OW2#4	32.1(4)
O1#1-Ce-N1	135.59(9)	OW3#4-Ba-OW1#4	141.98(15)	OW1-Ba-OW2#4	129.7(4)
O1-Ce-N1	63.52(9)	OW1-Ba-OW1#4	81.09(15)	OW1#4-Ba-OW2#4	142.2(3)
O5#1-Ce-N1	136.34(10)	O6#2-Ba-O2	121.65(10)	O2-Ba-OW2#4	131.7(3)
O5-Ce-N1	71.26(9)	O6#3-Ba-O2	75.68(9)	O2#4-Ba-OW2#4	93.3(3)
O3#1-Ce-N1	75.88(9)	OW3-Ba-O2	69.23(16)	OW2-Ba-OW2#4	40.0(7)
O3-Ce-N1	63.87(9)				

#1 $-x + 3/2$, y, $-z + 1/2$ #2 $x - 1/2, -y + 1, z + 1/2$ #3 $-x + 2, -y + 1, -z + 1$

#4 $-x + 3/2$, y, $-z + 3/2$

3.3. Conclusions

The formation of compounds with different crystal structures in case of Ce^{4+}, Ba^+ and dipicH$_2$ is in part due to the different amounts of the starting materials and is highly dependent on the crystallization conditions. The formation of a tris-chelate with Ce^+ and a linear chain of Ba^{2+} with coordinated water molecules, in the absence of excess ligand is in accordance with the natural tendency of Ce^{4+} to form tris-chelates and Ba^+ for O atoms. The formation of such a polymeric structure with coordinated water molecules for Ba^{2+} may be correlated with the reversal of relative sizes of Ce^{4+} and alkaline earth ions while moving from Ca^{2+} to Ba^{2+}. Ba^{2+} is even much larger than the nine coordinated Ce^{4+}. Also, the increase in ionic size from Ca^{2+} to Ba^{2+} allows larger

coordination numbers which may lead to the formation of different structures in association with appropriate complementary units.

The chain structure observed with $Ba(OH_2)_6^{2+}$ in 3 suggests that same kind of reactions with Ca and Sr^+ may also give rise to similar chain structures analogous to the previously reported hexahydrates of Ca^{2+} and Sr^{2+} halides. Hence, the present work can be extended to synthesize Ca^{24} and Sr^{2+} complexes with three equivalents of ligand and determine the crystal structures. Also, the possibility of pseudo-polymorphism could be studied as seen in 3 and 4.

The crystallization of $Ba(OH_2)_6^{2+}$ polymer chain in 3, in a chiral space group, starting from non-chiral starting materials gives further scope to this work in isolating the single component and studying the possible electrical and optical properties.

3.4. References

(1)   Goodgame, D. M. L.; Muller, T. E.; Williams, D. J. *Polyhedron* **1992,** *11*, 1513.

(2)   Swarnabala, G.; Rajasekharan, M. V. *Inorg. Chem.* **1998,** *37,* 1483.

(3)   Mao, J.-G.; Song, L.; Huang, X.-Y.; Huang, J.-S. *Polyhedron* **1997,** *16,* 963.

(4)   Dong, Y.-B.; Smith, M. D.; Loye, H.-C. z. *Inorg. Chem.* **2000,** *39,* 1943.

(5)   Navarro, J. A. R.; Freisinger, E.; Lippert, B. *Inorg. Chem,* **2000,** *39,* 1059.

(6)   Lainé, P.; Gourdon, A.; Launay, J.-P. *Inorg. Chem.* **1995,** *34,* 5129.

(7)   Ventur, D.; Wieghardt, K.; Weiss, J. *Z. Anorg. Allg. Chem.* **1985,** *524,* 40.

(8)   Zhou, X.-Y.; Kostic, M. *Inorg. Chem.* 1988, *27,* 4402.

(9)   Herring, A. M.; Hcnling, I,.; Labringer, J. A.; Bcrcaw, J. E. *Inorg. Chem.* 1991, *30,* 851.

(10) Drew, M. G. B.; Fowles, G. W. A.; Mathews, R. W.; Walton, R. A. *J. Am. Chem. Soc.* 1969, 97, 7769.

(11) Drew, M. G. B.; Mathews, R. W.; Walton, R. A. *J. Chem. Soc. A* **1970,** 1405.

(12) Casellato, V.; Vigato, P. A. *Coord. Chem. Rev.* **1978,** *26,* 85.

(13) Sarchet, P. C; Loiseleur, H. *Acta Crystallogr.* **1993,** *B29,* 1345.

(14) Marangoni, G.; Degetto, S.; Graziani, R.; Bombieri, G.; Forsellini, E. *J. Inorg. Nucl. Chem.* **1974,** *36,* 1787.

(15) Bcrsted, B. H.; Belford, R. L.; Paul, I. C. *Inorg. Chem.* **1968,** 7, 1557.

(16) Gaw, H.; Robinson, W. R.; Walton, R. A. *Inorg. Nucl. Chem. Lett.* **1971,** 7, 695.

(17) Quaglieri, P. P.; Lo seleur, H.; Thomas, G. *Acta Crystallogr.* 1972, *B28,* 2583.

(18) Degetto, S.; Baracco, R.; Graziani, R.; Celon, E. *Transition Met. Chem.* **1978,** 3, 351.

(19) Baracco, R.; Bombieri, G.; Degetto, S.; Fosellini, E.; Graziani, R.; Marangoni, G. *Inorg. Nucl. Chem. Lett.* **1974,** *10*, 1045.

(20) Laine, P.; Gourdon, A.; Launay, J.-P.; Tuchagues, J.-P. *Inorg. Chem.* **1995,** *34*, 5150.

(21) Laine, P.; Gourdon, A.; Launay, J.-P. *Inorg. Chem.* **1995,** *34,* 5138.

(22) Laine, P.; Gourdon, A.; Launay, J.-P. *Inorg. Chem.* **1995,** *34*, 5156.

(23) Furst, W.; Gouzerh, P.; Jeannin, Y. *J. Coord. Chem.* **1979,** *8,* 237.

(24) Du Preez, J. G. H.; Rohwer, H. E.; van Brecht, B. J. A. M. *Inorg. Chim. Acta* **1983,** *73,* 67.

(25) Bresciani-Pahor, N.; Nardin, G.; Bonomo, R. P.; Purrello, R. *Transition Met. Chem.* **1985,** 70,316.

(26) du Preez, J. G. H.; van Brecht, B. J. A. M. *J. Chem. Soc.,Dalton Trans.* **1989,** 253.

(27) Chessa, G.; Marangoni, G.; Pilteri, B.; Bertoissi, V.; Gilli, G.; Ferritti, V. *Inorg. Chim. Acta* **1991,** 755,201.

(28) Espinet, P.; Miguel, J. A.; Garcia-Granda, S.; Miguel, D. *Inorg. Chem.* **1996,** *35,* 2287.

(29) Albertsson, J. *Acta Chem. Scand.* **1970,** *24,* 1213.

(30) Albertsson, J. *Acta Chem. Scand.* **1972,** *26,* 985.

(31) Albertsson, J. *Acta Chem. Scand.* **1972,** *26,* 1005.

(32) Albertsson, J. *Acta Chem. Scand.* **1972,** *26,* 1023.

(33) Strahs, G.; Dickerson, R. E. *Acta Crystallogr.* **1968,** *B24*, 571.

(34) **Palmer,** K. J.; Wong, R. Y.; Lewis, J. C. *Acta Oystallogr.* **1972,** *B28,* 223.

(35) Beveridge, K. A.; Bushnell, G. W. *Can. J. Chem.* **1979,** *57,* 2498.

(36) Nardin, G.; Randaccio, L.; Bonomo, R. P.; Rizzarelli, E. *J. Chem. Soc, Dalton Trans.* 1980,369.

(37) North, A. C. T.; Phillips, D. C; Mathews, F. S. *Acta Cryst.* **1968,** *A24,* 351.

(38) Walker, N.; Stuart, D. *Acta Gystallogr.* 1983, *A39,* 153.

(39) Sheldrick, G. M. *SHELXL-93*; University of Gottingen: Germany, 1993.

(40) Sheldrick, G. M. *SHELXS-97 and SHELXL-97;* University of Gottingen: Germany, 1997.

(41) Burnett, M. N.; Johnson, C. K. *ORTEP-III: Oak Ridge Thermal Ellipsoid Plot Program for Crystal Structure Illustrations*; Oak Ridge National Laboratory Report ORNL-6895: Tennessee, USA, 1996.

(42) Sayle, R. *RasMol V2.6*: Stevenage, Hertfordshire, U.K., 1995.

(43) Kraus, W.; Nolze, G. *Powder Cell/or Windows version 2.3;* Federal Institute for Materials Research and Testing: Berlin, Germany, 1999.

(44) Wells, A. F. *Structural Inorganic Chemistry;* 4 ed.; Oxford University Press: Oxford, 1979, pp 556.

(45) Pan, L.; Frydel, T.; Sander, M. B.; Huang, X.; Li, J. *Inorg. Chem.* **2001,** *40,* 1271.

(46) Ref. 44, pp 100.

CHAPTER IV

Schiff Base Complexes of Manganese(III) and Iron(lII). Syntheses, Structure, Polymorphism, Spectral and Magnetic Studies of [Mn(Salpn)NCS]$_2$, [Mn(SaIpn)NCS]$_n$ and Fe(Salpn)(CH$_3$OH)NCS

The combination of a pseudo-halide ion and a tetradentate Schiff base (SB) ligand is suitable for making neutral M(III) complexes of the type M(SB)X. The pseudo-halide ions, N3", NCS", NCO" have been studied extensively for their ability to bridge paramagnetic moieties into dimers, polymers and clusters.[1] These ions, especially N$_3^-$ exhibit different bridging modes, viz., μ-(1,3),[2-5] μ-(1,1),[6-9] and rarely μ-(1,1,1).[10] In the case of N3", the latter two modes are found to lead to ferromagnetic interactions. There are very few structurally characterized complexes of M(1I) with pseudo halide bridges, where M = Mn(III),[5,11-13] Fe(III),[9,12] and Cr(III)[14] . Mn(acac)$_2$X is found to have a linear chain structure when X is azide or thiocyanate.[5,15] Mn(salen)X is also believed to have a similar structure based on spectral and magnetic studies,[16] but there is no crystallographic data available for these complexes. Mn(salen)NCS which has been structurally characterized before, has a monomeric structure.[17] Being more flexible than salen, salpn allows both equatorial and cis-octahedral modes of ligation. The structure and magnetic properties of Mn(salpn)N3 and Fe(salpn)N3 have been previously reported.[12] A compound with empirical formula Mn(salpn)NCS and its hydrate have been previously prepared but not crystallographically characterized.[18] Further, the catalytic

efficiency of this compound towards epoxidation of alkenes has been investigated.[19] A recent paper by Miyasaka et al.,[20] reports magnetic and crystallographic characteristics of several substituted SB complexes of Mn(III) with halides and pseudohalides. The crystallographic characterization of Mn(salpn)NCS has been done in our laboratory previously.[21] While working with these thiocyanate complexes of Mn(III) with salpn, polymorphism has also been observed. Now, the polymorphism has been studied in detail along with its spectral and magnetic properties. Similar observations are noted with Fe(III) also. In this chapter, for the sake of completeness in the discussion, the structural details of the two polymorphic forms of Mn(salpn)NCS are presented and the results of polymorphism, spectral and magnetic studies are discussed in detail. Attempts to prepare analogous Fe(III) complexes led to the formation of Fe(salpn)(CH$_3$OH)NCS. Its crystal structure and spectral properties are presented.

4.1. Experimental

4.1.1. Synthesis

(a) [Mn(salpn)NCS]2 (1): In a beaker open to the atmosphere, salicylaldehyde (0.229g 1.88 mmol) and 1,3-diaminopropane (0.071g, 0.96 mmol) were stirred into 40 mL of ethanol. Mn(CH$_3$CO$_2$)$_2$·4H$_2$O (0.245g, 1.00 mmol) was added, and the stirring continued for about 1 h. To the resulting solution, KNCS (0.200g, 2.06 mmol) dissolved in a minimum amount of water was added. The solution was allowed to stand for about 3 h to complete the air oxidation of Mn(II). The filtered solution was then kept aside at room temperature (~35 °C) for 2-3 days over which time dark green crystals deposited. Yield: 0.330g (0.84 mmol, 89 %). Anal. Calcd. for MnC$_{18}$H$_{16}$N$_3$O$_2$S: C, 54.96; H, 4.10; N, 10.68. Found: C, 54.48; H, 4.13; N, 10.70. Important IR absorptions (cm^{-1}): 2043, 1601,

1543, 1468, 1443, 1396, 1310, 1148, 1124, 1076, 1030, 977, 895, 804, 754, 613, 463. When the ambient temperature was lower (18-20 °C, for example in winter) the solution affords small amounts of the polymeric form along with the dimer. Recrystallization from acetonitrile gives pure dimer over a wide range of temperatures (5-30 °C).

(b) [Mn(salpn)NCS]$_n$ (2): The procedure is the same as that for the dimer described above, except that the final solution was kept in a refrigerator (5 °C) for 8-10 days. The yield of dark green crystals of the polymer in a typical experiment was 85%. Anal. Calcd. for MnC$_{18}$H$_{16}$N$_3$O$_2$S: C, 54.96; H, 4.10; N, 10.68. Found: C, 54.63; H, 4.38; N, 10.65. Important IR absorptions (cm^1): 2068, 1609, 1541, 1466, 1400, 1300, 1150, 1 126, 1067, 1028, 968, 903, 804, 750, 615, 459.

(c) Preparation of Fe(salpn)(CH$_3$OH)NCS (3): In a beaker open to the atmosphere, salicylaldehyde (0.229g, 1.88 mmol) and 1,3-diaminopropane (0.071 g, 0.96 mmol) were stirred into 40 mL of methanol. Fe(ClO$_4$)$_3$·H$_2$O (0.355g, 1.00 mmol) in 17 mL methanol was added, and the stirring continued for about 15 minutes. To the resulting solution, KNCS (0.195g, 2.01 mmol) dissolved in 15 mL methanol was added and stirring continued for further 15 minutes. The final solution was filtered and refrigerated. Dark brown crystals separated after about two weeks. Yield: 0.285g (0.67 mmol, 71 %). Anal. Calcd. for FeC$_{19}$H$_{20}$N$_3$O$_3$S: C, 53.53; H, 4.73; N, 9.86. Found: C, 52.59; H, 4.05; N, 9.61. Important IR absorptions (KBr/cm^{-1}): 2043, 1609, 1545, 1470, 1443, 1400, 1290, 1205, 1150, 1126, 1069,1020,897,799,756,604. "

(d) Polymorphism: To study the effect of solvent, the dimer (1), obtained from the reaction in ethanol at RT, was recrystallized from various solvents, *viz.,* acetonitrile, dichloromethane, acetone, tetrahydrofuran, methanol and ethanol. In each case, crystallizations were done at two temperatures *viz.,* 35 °C and 5 °C. The crystalline

products obtained after 8-10 days were identified as dimer, polymer or as a mixture of the two using IR spectroscopy *(vide supra).* Similarly, 3 was also recrystallized from solvents as mentioned above at both RT and LT. Differences in IR spectra show the presence of polymorphism, but as good quality single crystals are not obtained no stmctural work was undertaken.

4.1.2. Physical Measurements: IR spectra were obtained as KBr pellets using Shimadzu FT-IR 8000 spectrometer. C, H, N analysis of 1 and 2 were performed on a Perkin-Elmer 240C elemental analyzer at the University of Hyderabad, while for 3, the analysis was performed on a Perkin-Elmer 2400, CHNS/O analyzer at CSMCRI, Bhavnagar. Reflectance spectra of powder samples were measured using Shimadzu UV-3100 spectrometer equipped with ISR-3100 integrating sphere attachment. Absorption spectra in ACN were measured on a Shimadzu UV-3100 PC spectrometer. Single crystal X-ray data were collected on an Enraf - Nonius CAD4 diffractometer using graphite monochromated Mo Ka radiation for 1 and 2 at 1IT, Madras and for 3 at 1IT, Bombay. Powder diffractograms were measured using PW3710 model Philips Analytical X-ray diffractometer.

4.1.3. X-ray Crystallography: X-ray data were collected for dark colored crystals with dimensions, 0.35 x 0.30 x 0.10 mm for 1; 0.25 x 0.20 x 0.20 mm for 2; and 0.40 x 0.25 x 0.15 mm for 3 on an Enraf-Nonius CAD4 diffractometer at room temperature using graphite monochromated Mo Ka radiation. The data were corrected for Lorentz polarization effects and absorption.[22-23] The structures were solved by a combination of heavy atom and direct methods using SHELX-86[24] for 1 and 2 and SHELXS-97[25] for 3 and refined using SHELXL-93/SHELXL-97.[25] 2 was refined as a racemic twin. Drawings were made using ORTEP-III[26] and Rasmol 2.6.[27]

1 crystallizes in the orthorhombic system, space group *Pbca*, with 8 molecules in the unit cell. A total of 2906 reflections (2906 unique, 1741 with $F > 4\sigma F$) were collected in the θ range 2.16 to 24.95, with indices $0 < h \leq 14$, $0 < k \leq 16$, $0 < l < 22$. All the non hydrogen atoms were refined anisotropically while the ring hydrogen atoms were included in the calculated positions using a riding model. All the hydrogens were assigned fixed U_{iso} values, equal to $1.2U_{eq}$ of the parent atom. The final cycle of full matrix least squares refinement on F^2 converged with unweighted and weighted refinement factors of $R\backslash = 0.0523$ and $wR2 = 0.1303$ respectively. The goodness of fit (S) is 1.012 for 2906 unique reflections and 228 parameters. The maximum and minimum residual electron density on the final fourier map corresponded to 0.758 and -0.507 e/A"^{3} respectively.

2 crystallizes in the orthorhombic system, space group *Pna2*$_1$, with 4 molecules in the unit cell. A total of 3021 reflections (1551 unique, 1480 with $F > 4\sigma F$) were collected in the θ range 2.40 to 24.98, with indices $-14 < h < 14$, $0 < k < 13$, $0 < l < 13$. All the non hydrogen atoms were refined anisotropically while the ring hydrogen atoms were included in the calculated positions using a riding model. All the hydrogens were assigned fixed U_{iso} values, equal to $1.2U_{eq}$ of the parent atom. The final cycle of full matrix least squares refinement on F^2 converged with unweighted and weighted refinement factors of $R1 = 0.0219$ and $wR2 = 0.0563$ respectively. The goodness of fit (5) is 1.053 for 1543 unique reflections and 227 parameters. The maximum and minimum residual electron density on the final fourier map corresponded to 0.304 and -0.248 e/Å^{-3} respectively.

3 crystallizes in the monoclinic system, space group *C2/c*, with 8 molecules in the unit cell. A total of 4672 reflections (4382 unique, 2272 with $F > 4\sigma F$) were collected

in the grange 2.56 to 27.46, with indices $-3 < h < 21$, $-1 < k < 1$, $-34 < l < 33$. All the non hydrogen atoms were refined anisotropically while the ring hydrogen atoms were included in the calculated positions using a riding model. All the hydrogen atoms were assigned fixed U_{iso} values, equal to $1.2U_{eq}$ of the parent atom. C9 was found to be disordered and the disorder was modeled by splitting it into two halves and refined by free variable (FVAR) refinement. The final cycle of full matrix least squares refinement on F^2 converged with unweighted and weighted refinement factors of $R1 = 0.0513$ and $wR2 = 0.1136$ respectively. The goodness of fit (S) is 0.911 for 4382 unique reflections and 259 parameters. The maximum and minimum residual electron density on the final fourier map corresponded to 0.477 and -0.514 e/A$^{"3}$ respectively.

　　Crystallographic data for 1, 2 and 3 are presented in Table 4.1, atomic parameters for 1 are tabulated in Table 4.2, for 2 in Table 4.3 and for 3 in Table 4.4 respectively.

Table 4.1 Crystallographic data for $[Mn(salpn)NCS]_2$ (1), $[Mn(salpn)NCS]_n$ (2) and $Fe(salpn)(CH_3OH)NCS$ (3).

	1	2	3
formula	$C_{18}H_{16}MnN_3O_2S$	$C_{18}H_{16}MnN_3O_2S$	$C_{19}H_{20}FeN_3O_3S$
formula weight	393.34	393.34	426.29
a (Å)	12.573(3)	12.5277(14)	16.431(3)
b (Å)	13.970(7)	11.576(2)	9.1571(13)
c (Å)	18.891(9)	11.513(2)	26.335(5)
α (°)	90	90	90
$PC)$	90	90	104.631(14)
γ (°)	90	90	90
	3318(2)	1669.6(4)	3833.8(11)
Z	8	4	8
Space group	*Pbca*	*Pna2*	*C2/c*
T (K)	293 (2)	293 (2)	293 (2)
λ (A)	0.71073	0.71073	0.71073
ρ_{calcd}(Mg/m`)	1.575	1.565	1.477
μ (mm^{-1})	0.938	0.933	0.920
$R1$	0.0523	0.0219	0.0513
$wR2$	0.1303	0.0563	0.1136

weighting scheme, **1**: $A = 0.0912$; $B = 0.0000$; *2:* $A = 0.0411$; $B = 0.1457$;

3: $A = 0.0639$; $B \sim 0.0000$ (see p. vi for definitions).

Table 4.2 Atomic parameters for [Mn(salpn)NCS]2 (1).

Atom	10^4x	10^4y	10^4z	10^3U_{eq}	Atom	10^4x	10^4y	10^4z	10^3U_{eq}
Mn	1280(1)	4958(1)	320(1)	24(1)	C7	2395(4)	3162(3)	37(3)	32(1)
S	4527(1)	5908(1)	1455(1)	52(1)	C8	2210(6)	3354(5)	1257(3)	74(2)
O1	1813(2)	4973(2)	-589(2)	31(1)	C9	1530(6)	3667(6)	1821(4)	81(2)
O2	350(2)	5989(2)	53(2)	28(1)	C10	455(4)	4039(4)	1657(3)	48(2)
N1	2026(3)	3707(3)	532(2)	28(1)	CH	189(3)	5723(3)	1553(3)	31(1)
N2	533(3)	4952(3)	1269(2)	28(1)	C12	137(3)	6643(3)	1221(3)	32(1)
N3	2560(3)	5770(3)	783(2)	46(1)	C13	-97(4)	7459(4)	1646(3)	41(1)
Cl	2230(3)	4267(4)	-986(3)	32(1)	C14	-235(5)	8342(4)	1332(3)	51(2)
Cl	2421(4)	4427(4)	-1707(2)	43(1)	C15	-171(5)	8421(4)	620(4)	52(2)
C3	2795(4)	3683(5)	-2124(3)	52(2)	C16	37(4)	7657(3)	185(3)	32(1)
C4	3036(4)	2792(5)	-1855(3)	54(2)	C17	194(3)	6755(3)	489(3)	27(1)
C5	2870(4)	2634(4)	-1157(3)	46(1)	C18	3375(4)	5812(3)	1076(3)	37(1)
C6	2464(3)	3341(3)	-700(3)	35(1)					

Table 4.3 Atomic parameters for [Mn(salpn)NCS]$_n$ (2).

Atom	10^4x	10^4y	10^4z	10^3U_{eq}	Atom	10^4x	10^4y	10^4z	10^3U_{eq}
Mn1	153(1)	1089(1)	23(1)	25(1)	C7	-526(2)	-1177(2)	874(3)	31(1)
S1	-734(1)	-1789(1)	-2762(1)	39(1)	C8	-1712(2)	222(3)	1556(3)	34(1)
O1	1308(1)	53(2)	-20(3)	38(1)	C9	-2382(2)	1128(2)	955(3)	35(1)
O2	1076(1)	2119(2)	-774(2)	35(1)	C10	-1854(2)	2309(2)	925(3)	34(1)
N1	-759(2)	-103(2)	874(2)	25(1)	CH	-972(2)	3249(2)	-594(3)	32(1)
N2	-967(2)	2363(2)	78(2)	27(1)	C12	-141(2)	3597(3)	-1384(3)	33(1)
N3	-584(2)	334(2)	-1610(2)	39(1)	C13	-302(3)	4603(3)	-2061(4)	45(1)
Cl	1268(2)	-1086(2)	-59(3)	31(1)	C14	497(3)	5050(3)	-2739(3)	50(1)
Cl	2145(3)	-1698(3)	-498(3)	43(1)	C15	1487(3)	4503(3)	-2747(3)	46(1)

Table 4.3 contd......

C3	2123(3)	-2888(3)	-557(3)	50(1)	C16	1670(2)	3520(3)	-2102(3)	39(1)
C4	1248(3)	-3508(3)	-159(4)	52(1)	C17	864(2)	3039(2)	-1405(3)	31(1)
C5	399(3)	-2930(3)	291(3)	46(1)	CIS	-654(2)	-538(3)	-2095(3)	32(1)
C6	394(2)	-1721(2)	349(3)	32(1)					

Table 4.4 Atomic parameters for Fe(salpn)(CH$_3$OH)NCS (3).

| Atom	10^4x	10^4y	10^4z	10^3U_{eq}	Atom	10^4x	10^4y	10^4z	10^3U_{eq}
Fe	97(1)	2421(1)	1483(1)	34(1)	CH	-1652(3)	2240(6)	588(2)	68(1)
S1	2240(1)	1357(2)	627(1)	94(1)	C9A(0.66)	-1820(4)	971(8)	914(3)	53(3)
01	539(2)	4360(3)	1515(1)	43(1)	C9B(0.34)	-1394(10)	602(19)	590(6)	71(7)
02	819(2)	1844(3)	2158(1)	37(1)	C10	-1195(3)	-209(5)	1041(2)	65(1)
N1	-886(2)	3104(4)	821(1)	43(1)	CH	-45(2)	-813(4)	1720(2)	**41(1)**
N2	-417(2)	246(3)	1439(1)	39(1)	C12	730(2)	-769(4)	2133(1)	34(1)
N3	870(2)	1704(4)	1042(1)	52(1)	C13	1070(3)	-2086(4)	2361(2)	46(1)
C1	471(2)	5374(4)	1149(2)	40(1)	C14	1800(2)	-2133(4)	2747(2)	47(1)
C2	1078(3)	6480(4)	1206(2)	49(1)	C15	2232(2)	-855(5)	2910(2)	48(1)
C3	996(3)	7594(5)	851(2)	59(1)	C16	1901(2)	477(4)	2708(2)	42(1)
C4	300(3)	7660(5)	419(2)	63(1)	C17	1139(2)	537(4)	2318(1)	33(1)
C5	-283(3)	6589(5)	347(2)	58(1)	C18	1448(2)	1557(5)	874(2)	45(1)
C6	**-215(2)**	**5411(4)**	701(1)	42(1)	03	-762(2)	3074(3)	1928(1)	41(1)
C7	-848(3)	4306(5)	**584(2)**	48(1)	C19	-1187(3)	4417(5)	1916(2)	70(1)

Site occupation factors of disordered atoms are given after the respective atom labels.

4.1.4. Magnetic Measurements: The two polymorphs 1 and 2 obtained from the reaction in ethanol were used for magnetic measurements. The purity of the polymorphs used for

magnetic studies were checked using IR and by comparing their X-ray powder diffraction patterns with those calculated[28] based on crystal structure. The samples were ground and pressed into pellets to avoid orientation effects. Magnetic data were recorded on a MPMS5 magnetometer (Quantum design Inc.) at Université Paris-Sud, France. The calibration was made at 298 K using a palladium reference sample furnished by Quantum design Inc. The magnetic susceptibility data were collected over a temperature range of 2-300 K a t a magnetic field of 2000 G for the [Mn(salpn)NCS]$_n$ and 500 G for the [Mn(salpn)NCS]2 and were corrected for diamagnetism using Pascal's constants. In the case of [Mn(salpn)NCS]$_n$, the $\chi_M T$ versus T curve was fitted using the classical *S = 2* chain law.[29] RT susceptibility of 3 was measured on a Sherwood scientific magnetic susceptibility balance. Calibration was made using $Hg[Co(NCS)_4]$ as standard at 300 K. Diamagnetic corrections were done using Pascal's constants.[30]

4.2. Results and Discussion

4.2.1. Structure of [Mn(salpn)NCS]$_n$ (2): The asymmetric unit of 2 is shown in Figure 4.1. The structure is analogous to that of the azide complex.[12] The salpn binds in the equatorial mode and thiocyanate acts as an end to end bridge. Each monomeric unit is related to its adjacent ones by a 2-fold screw axis, leading to a helix propagating along the crystallographic *c*-axis (Figure 4.2). While the gross structure is similar to that of the azide, there are significant differences in the coordination geometry. The two in-plane Mn-N distances in the azide complex were unequal which was attributed to the strain involved in the spiral formation (Table 2.1). In contrast, the thiocyanate has equal in-plane Mn-N distances. The long Mn-S bond apparently relieves any strain in the polymer
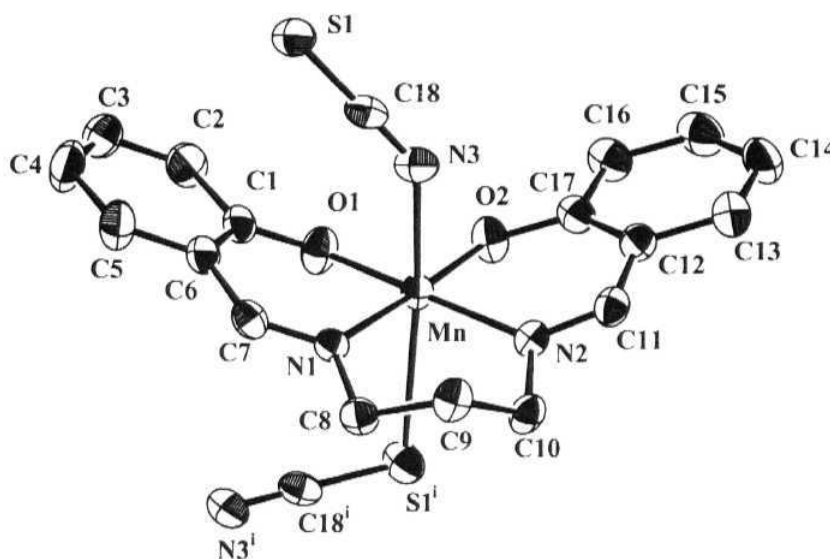
Figure 4.1 ORTEP view of one complex cation and its two bonded thiocyanate anions along the 1D chains of [Mn(salpn)NCS]$_n$ in 2. Hydrogen atoms have been omitted for clarity. Thermal ellipsoids are represented at 50% probability level. Symmetry labels: (i) -*x*, -*y*, *z* + 1/2.

Table 4.5 Selected bond lengths (A) and angles (°) in [Mn(salpn)NCS]$_n$ (2)

Mn-O1	1.880(2)	Mn-N2	2.037(2)	Mn-N3	2.270(3)
Mn-O2	1.897(2)	Mn-N1	2.042(2)	Mn-Sl#l	2.7737(11)
O1-Mn-O2	85.37(9)	N2-Mn-Nl	95.10(9)	O1-Mn-S1#1	90.47(9)
O1-Mn-N2	173.20(8)	O1-Mn-N3	92.63(11)	O2-Mn-S1#1	95.80(8)
O2-Mn-N2	88.83(9)	O2-Mn-N3	95.13(10)	N2-Mn-Sl#l	86.57(8)

Table 4.5 contd.

O1-Mn-N1	90.70(9)	N2-Mn-N3	91.43(10)	Nl-Mn-Sl#l	84.41(7)
O2-Mn-N1	176.06(8)	Nl-Mn-N3	84.84(10)	N3-Mn-Sl#l	168.84(7)

#1 -*x*, -*y*, *z* + 1/2
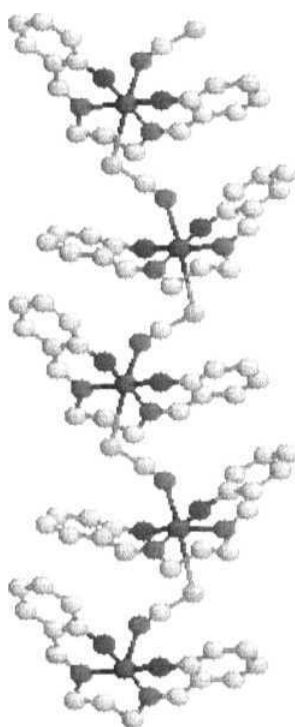
Figure 4.2 Perspective view of helical polynieric chains in 2. Colour
code for atoms: blue, N; red, O; yellow, S; grey, C; dark grey, Mn.

chain formation. The Jahn - Teller axis around Mn(III) corresponds to the N3-Mn-S
bond. The impact of this distortion on the magnetic properties is discussed later. The

inclination between the mean planes of the two halves of the SB ligand (excluding the methylene groups) is now 37.2(1)° as against 44.0(1)° in the azide complex..

4.2.2. Structure of **[Mn(salpn)NCS]₂** (1): The asymmetric unit of the dimer is shown in Figure 4.3. Here also, the salpn ligands adopt the equatorial coordination mode, however, the two halves of each salpn are now more coplanar than in the helical chain, the interplanar angle being 10.2(1)°. The thiocyanate ions remain terminal and N-bonded.

Figure 4.3 ORTEP view of the Mn(salpn)NCS dinuclear complex molecule in 1. Hydrogen atoms are omitted for clarity, and the thermal ellipsoids are represented at the 50% probability level. Symmetry labels:

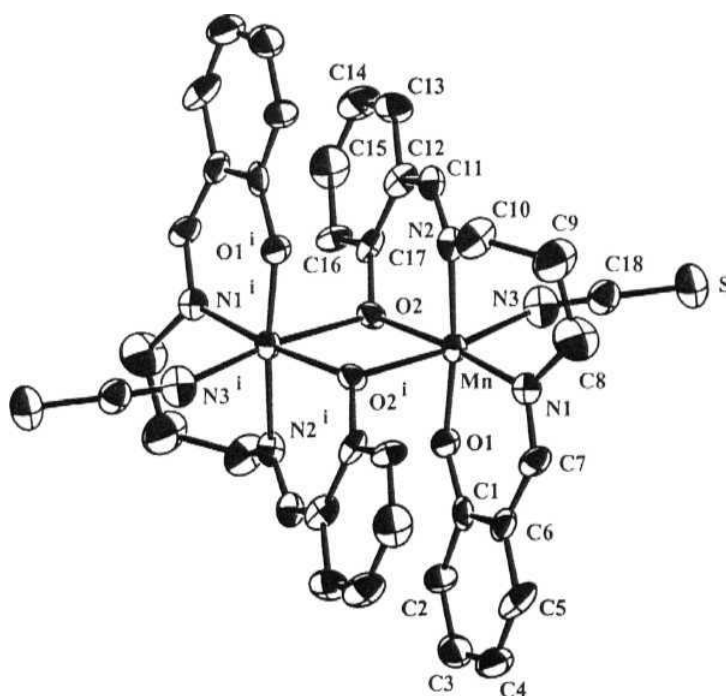Six coordination around the manganese atoms is completed by two highly unsymmetrical (Mn-0 1.923(3), 2.539(3) A) phenoxide bridges. The two halves of the dimer are related by a crystallographic inversion center. SCN-Mn-Obridge appears to be the Jahn-Teller elongation axis, even though the terminal thiocyanate ion is more strongly bound compared to the bridging thiocyanate in the polymer. The bridge angle $Mn-O_{bridge}-Mn'$ is 100.00(11)°, while the Mn-Mn' distance is 3.4406(11) A. The plane defining the MnO2Mn'O2' bridge makes an angle of 85.0(1)° with the equatorial coordination plane defined by the atoms, Mn, N1, N2, 01, and 02.

Table 4.6 Selected bond lengths and angles in $[Mn(salpn)NCS]_2$ (1).

Mn-O1	1.844(3)	Mn-02	1.923(3)	Mn-N1	2.024(4)
Mn-N2	2.025(4)	Mn-N3	2.154(5)	Mn-O2#1	2.539(3)
O1-Mn-N1	91.47(15)	O2-Mn-N1	168.77(14)	O1-Mn-O2	88.22(13)
O2-Mn-N2	87.31(14)	N1-Mn-N2	92.04(15)	O1-Mn-N2	173.67(14)
O2-Mn-N3	99.58(15)	N1-Mn-N3	91.61(16)	O1-Mn-N3	95.82(16)
N2-Mn-N3	89.35(16)	O1-Mn-O2#1	92.33(12)	O2-Mn-O2#1	80.01(12)
N1-Mn-02#1	88.79(12)	N2-Mn-O2#1	82.48(13)	N3-Mn-O2#1	171.83(14)

#1 $-x, -y + \1, -z$

The uncoordinated S has a significant role in stabilizing the crystal structure. The most remarkable feature is the S - π(phenyl) interactions which connect the dimers into one dimensional chains running along the crystallographic *a*-axis (Figure 4.4). The

distance between the S atom and the centroid of the phenyl ring is 3.66 A, while the C-centroid-S angle is 90 ± 11° for the six ring C atoms. A search in the Cambridge Crystallographic Data base for metal complexes having N-coordinated NCS" ion interacting with the π-cloud of phenyl rings resulted in 57 hits. Restricting the C-centroid-S angle to 90 ± 2° reduces the number of structures to 14. As expected, S - *n* (phenyl) interaction is a "soft bond" being influenced by other crystal packing considerations. The four symmetry related chains are linked into a three dimensional network through C-H⋯S interaction, the S ⋯H distance being in the range 3.0-3.4 A.
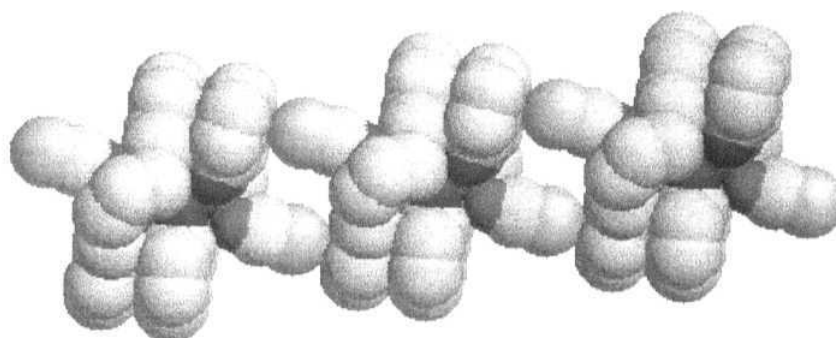
Figure 4.4 1-D chain of dimers linked by S⋯π(ring) interaction along the *a*- axis in 1. Colour code for atoms: blue, N; red, O; yellow, S; grey, C. The manganese atoms are hidden in this view.

4.2.3. Structure of Fe(salpn)(CH₃OH)NCS (3): The asymmetric unit is shown in Figure 4.5. In this case also, the salpn ligands adopt the equatorial coordination mode. Six coordination around Fe(III) is achieved by the coordination of NCS" ion and one solvent

CH3OH at the axial sites. The NCS" ion is terminal and N-bonded. The equatorial atoms Fe, N1, N2, 01 and 02 are nearly coplanar (rms devaiton, 0.09 A), the planarity being less than the that in $Fe(salpn)N_3$.[12] In $Fe(salpn)N_3$ the N3" ion is acting as μ-(1,1) bridge with the salpn ligand *cis*-octahedrally coordinated to Fe(III). The two halves of the ligand, excluding the methylene groups are also individually planar (rms deviation, 0.05 A), with the Fe atom deviating by 0.38 A and 0.51 A respectively. The angle between the two ligand planes is 28.75(10)° and is less than that in 2. The two Fe-O1 and Fe-O2
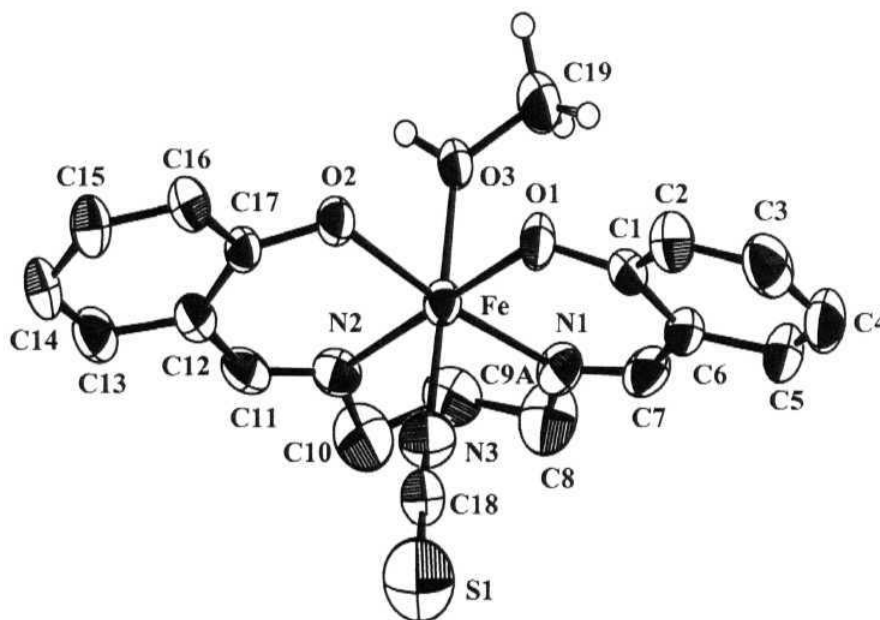
Figure 4.5 Ortep view of 3 with atom labeling. Atoms are shown as 50% thermal ellipsoids. Ring hydrogens have been omitted for clarity. Only one of the disordered C9 atom is shown.

distances are equal as in 1. In contrast to 1 and 2, the two Fe-N equatorial distances are also equal and shorter than the axial Fe-N bond (Table 4.7). However, the axial Fe-N distance is comparable to that observed in Fe(salpn)N$_3$. The uncoordinated S has a weak interaction with the C of the -C=N (S$\cdots$C7 = 3.686(4) A) which connects the monomeric units into a polymeric chain (Figure 4.6). The methanolic hydrogen is involved in hydrogen bonding with a symmetry related phenoxide 02 (03 $\bullet\bullet$ O2#2 = 2.681 (4) A).

Table 4.7 Selected bond lengths and angles for Fe(salpn)(CH$_3$OH)NCS (3).

Fe-O1	1.912(3)	Fe-N3	2.034(4)	Fe-N1	2.149(3)
Fe-02	1.944(2)	Fe-03	2.136(3)	Fe-N2	2.155(3)
O1-Fe-O2	94.31(10)	N3-Fe-O3	176.73(12)	O1-Fe-N2	179.14(10)
O1-Fe-N3	92.31(13)	O1-Fe-N1	87.97(12)	O2-Fe-N2	86.49(11)
O2-Fe-N3	96.32(12)	O2-Fe-N1	168.72(11)	N3-Fe-N2	87.93(13)
O1-Fe-O3	90.66(11)	N3-Fe-N1	94.63(13)	O3-Fe-N2	89.09(11)
O2-Fe-O3	84.82(11)	O3-Fe-N1	84.10(11)	N1-Fe-N2	91.19(13)
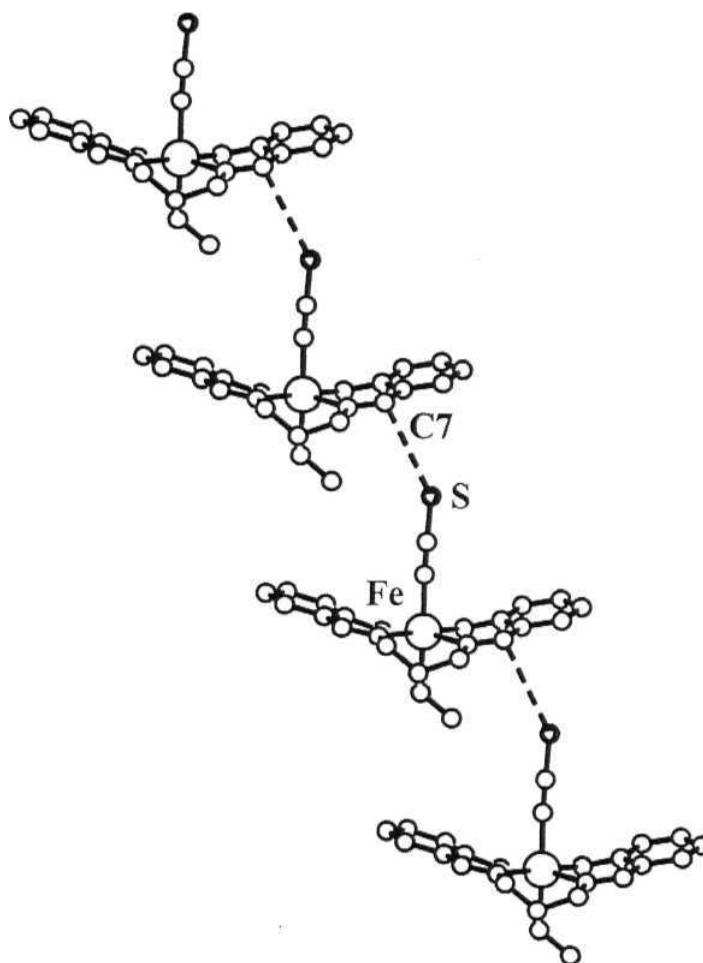
Figure 4.6   1-D Chain of monomeric 3 connected by weak S···C interactions (dotted lines).

4.3. Polymorphism and Optical Spectra: In case of 1 and 2 crystallization leads to one or the other polymorph or a mixture of the two depending upon the solvent and temperature. Acetonitrile and dichloromethane give only the dimer at both room temperature (RT) and low temperature (LT). The situation is similar in tetrahydrofuran, except that a small amount of polymer is also obtained at RT along with the dimer. Acetone produces a mixture at both temperatures, the amount of polymer being more at LT. Both methanol and ethanol give the dimer at RT and the polymer at LT. In the case of ethanol the LT product is contaminated with a small amount of the dimer. It turns out that the dimer is the preferred form at RT in all the solvents studied. Pure polymer is obtained only from methanol at LT. It is to be noted that even after complete evaporation of the solvent, there is no noticeable amount of dimer in the product obtained at LT from methanol, implying that dimer is kinetically not favoured at this temperature in this solvent. The two polymorphs 1 and 2 can be readily distinguished based on the IR absorption frequency corresponding to the N-C stretching vibration of the thiocyanate ion: 2043 cm^{-1} for dimer and 2068 cm^{-1} for polymer. The rest of the IR region (3000 - 400 cm^{-1}) is virtually identical for the two compounds (Figure 4.7). This is consistent with the general observation that the N-bonded thiocyanate ions have a lower N-C stretching frequency than the bridging thiocyanate.[31]
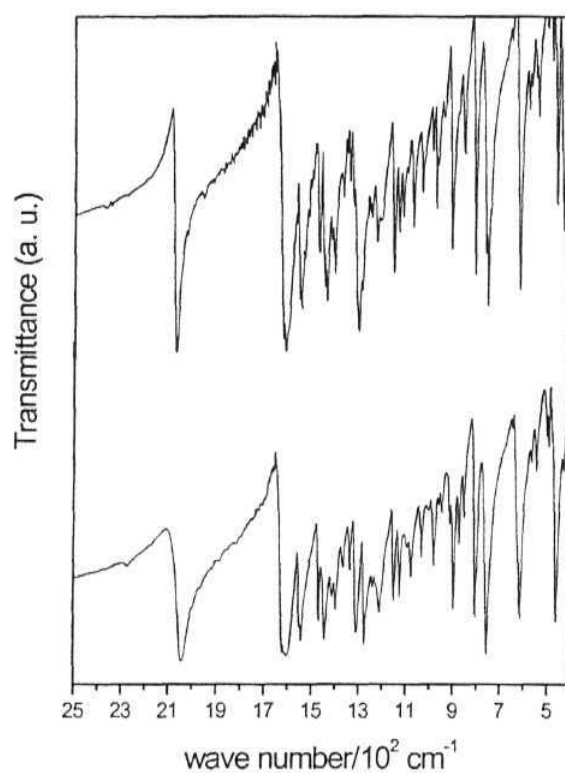
Figure 4.7 IR spectra of 1 (bottom) and 2 (top).

The **different** coordination environments in the two compounds is also reflected in the *d-d* absorption region: band maxima at 15690 cm'' and 16710 cm''' for 1; 16750 cm''' for 2(Figure 4.8a). The powder diffuse reflectance spectrum of 3 is presented in Figure 4.8b.

The solution spectra of the two polymorphs of Mn(III) in acetonitrile (Figure 4.9a) has several features and agree closely with the previously reported spectrum in aqueous solution:[32] 16750(220), 21100(1200), 25640(5000), 36100(17600) cm^{-1} ($Lmol^{-1}cm^{-1}$). The species present in solution is in all probability, solvent perturbed Mn(salpn)NCS. The bands at 21100 and 25640 cm^{-1} are probably due to ligand to metal charge transfer transition. The weak band at 16750 cm^{-1} is assigned to *d-d* transitions and probably includes in its envelope the transition from the split components of the ^5E state. The splitting is more prominent in the reflectance spectrum of 1 which has only weak axial interaction with the phenolate oxygen atoms. The solution spectra of 3 in acetonitrile (Figure 4.9b) also shows several features: 20200(1600), 31350(3700), 33900(3500), 38610(9100), 42730(15700), 46730(13900) cm^{-1}($Lmol^{-1}cm^{-1}$).

(a)   (b)
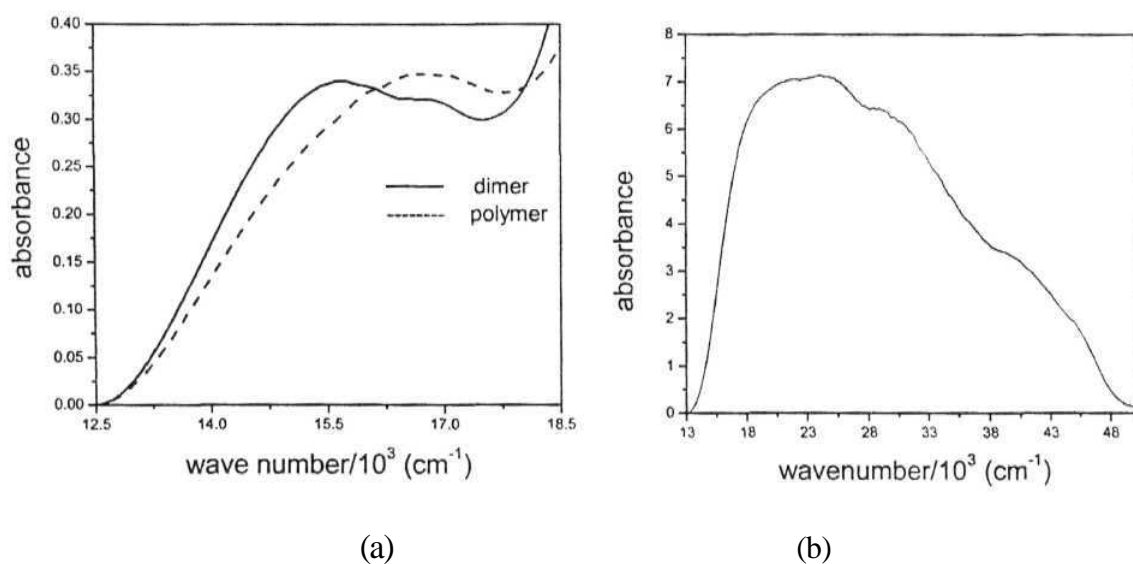
Figure 4.8 Powder diffuse reflectance spectra of (a) dimeric and polymeric Mn(salpn)NCS and (b) monomeric Fe(salpn)(CH$_3$OH)NCS.

(a)   **(b)**
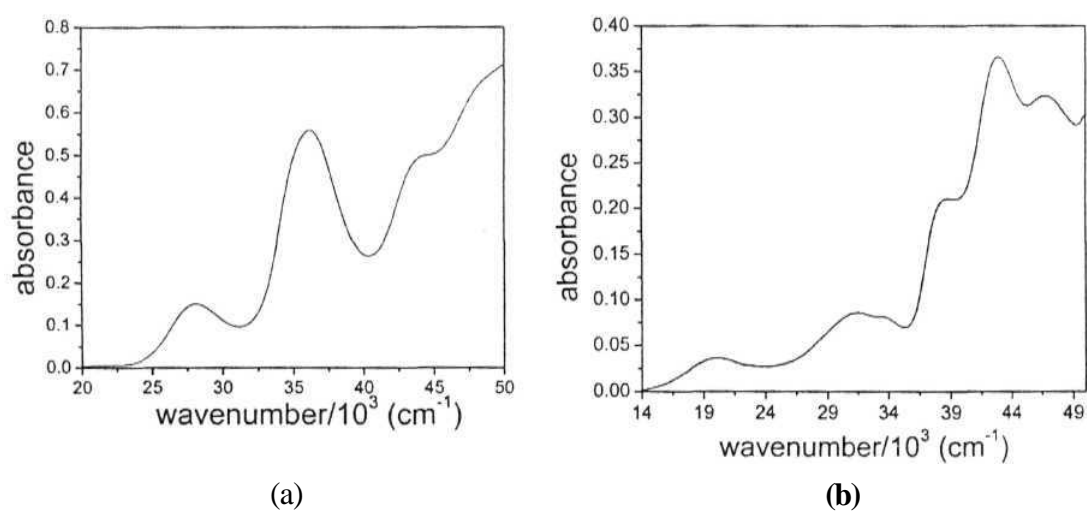
Figure 4.9 Solution spectra of (a) **2** and (b) **3** in ACN.

4.4. **Magnetic Properties:** Magnetic susceptibility of 2 was measured between 300 K and 2 K. The results are represented in Figure 4.10 as the product $\chi_M T$ per Mn as a function of T. At 300 K, $\chi_M T = 2.82$ cm^{3}mol^{-1}K. By itself this value which is lower than that for one isolated high spin Mn(III) indicates the presence of an antiferromagnetic coupling in the chain. This is confmned by the decrease of $\chi_M T$ as T decreases. At low temperature, an anomaly is observed in the $\chi_M T$ (see below). The data above 15 K are well fitted by the law for a chain of classical spins $S = 2$ with $J = -3.2$ cm^{-1} and g = 1.99. (The J is defined in such a way that the singlet to triplet excitation energy for an antiferromagnetically coupled pair of $S = 1/2$ ions is $-J$).
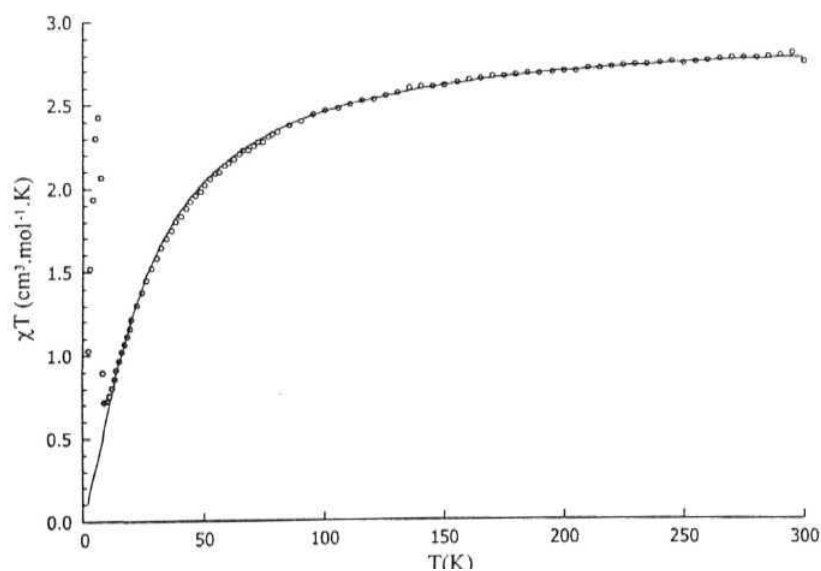
Figure 4.10 Product of the magnetic susceptibility per mole of manganese and temperature for the chain compound [Mn(salpn)NCS]$_n$

(dotted line). Solid line corresponds to the classical spin *S - 2* chain model with $g = 1.99$, $J = -3.2$ cm^{-1} using data above 15 K.

The anomaly in $\chi_M T$ was found in fact to be related to a spin ordering phenomenon. First when we recorded the magnetization at 2 K versus magnetic field we obtained a curve (Figure 4.11) exhibiting two regimes. At low field, magnetization increases steeply with magnetic field; at higher field magnetization increases at a slower
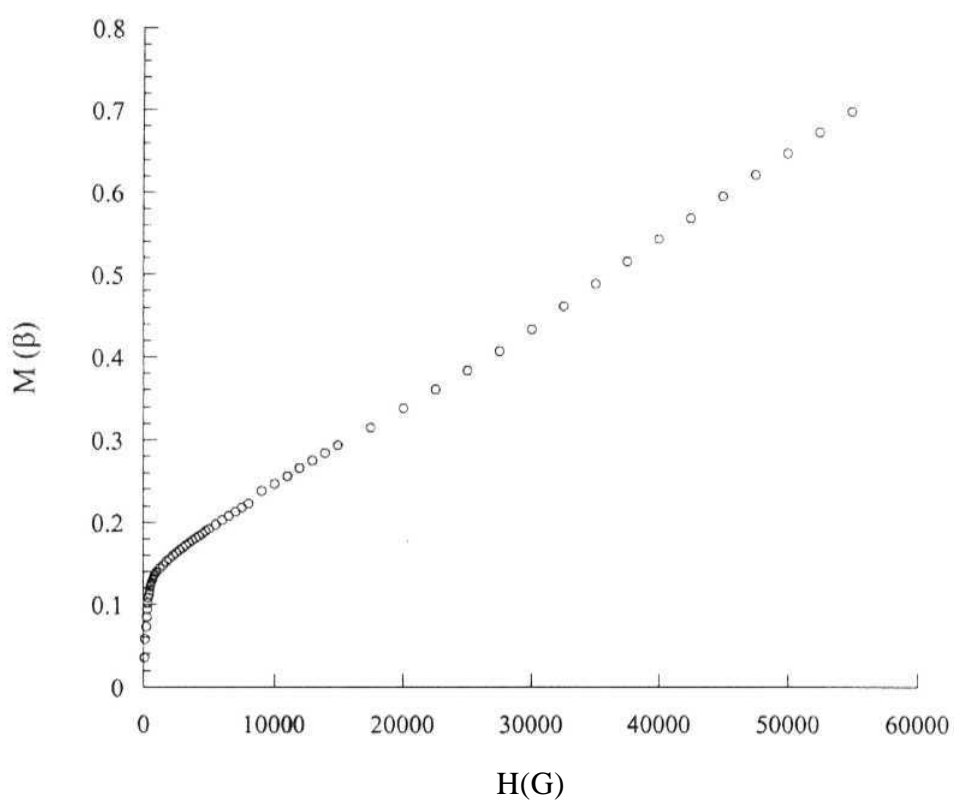
Figure 4.11 Magnetization per mole of manganese for 2 as a function of the magnetic field.

rate and in an almost linear fashion. This is strongly reminiscent of weak ferromagnetism.[33,34] An hysteresis (Figure 4.12) was detected in the ordered phase at 2 K with a coercive field of 2500 Oe.
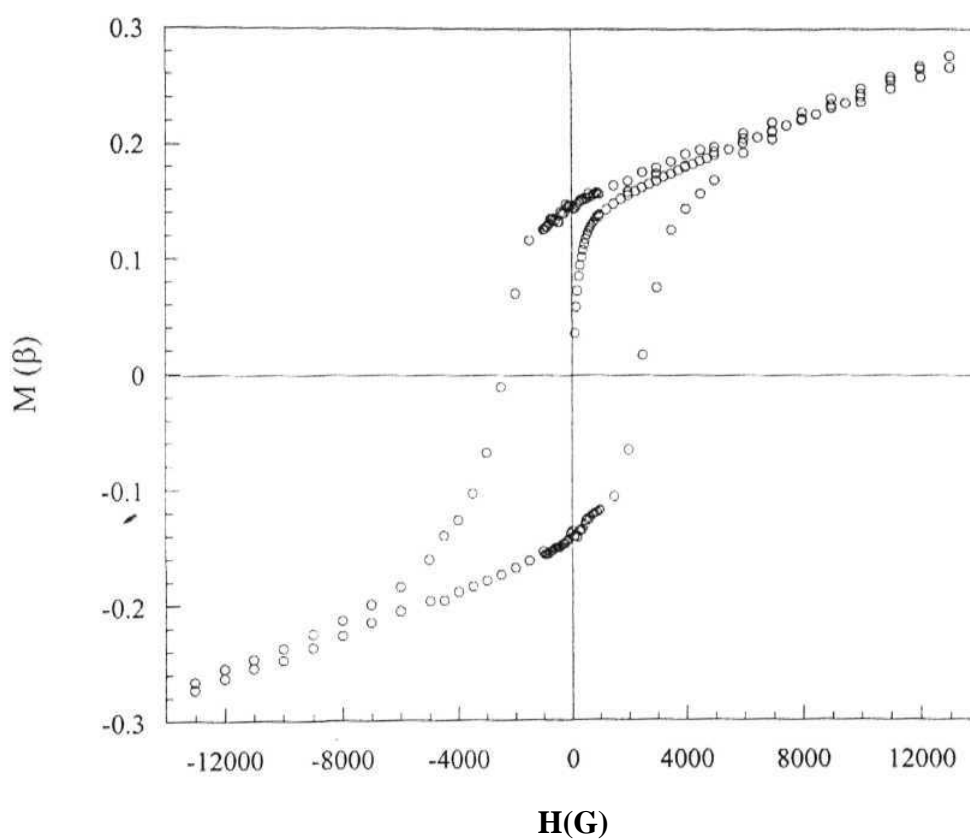
Figure 4.12 Hysteresis in the ordered phase of the chain compound [Mn(salpn)NCS]$_n$ at 2 K.

The phenomenology of the spin ordering was explored in detail (Figure 4.13) by measuring the zero field cooled (ZFC) and field cooled (FC) magnetization. The sample was cooled under zero field down to 4.5 K; at this temperature the field was set to 30 G and T was increased to 10 K. The sample was then cooled again under 30 G down to 4.5 K to get FC magnetization. As expected the FC curve is above the ZFC curve. The
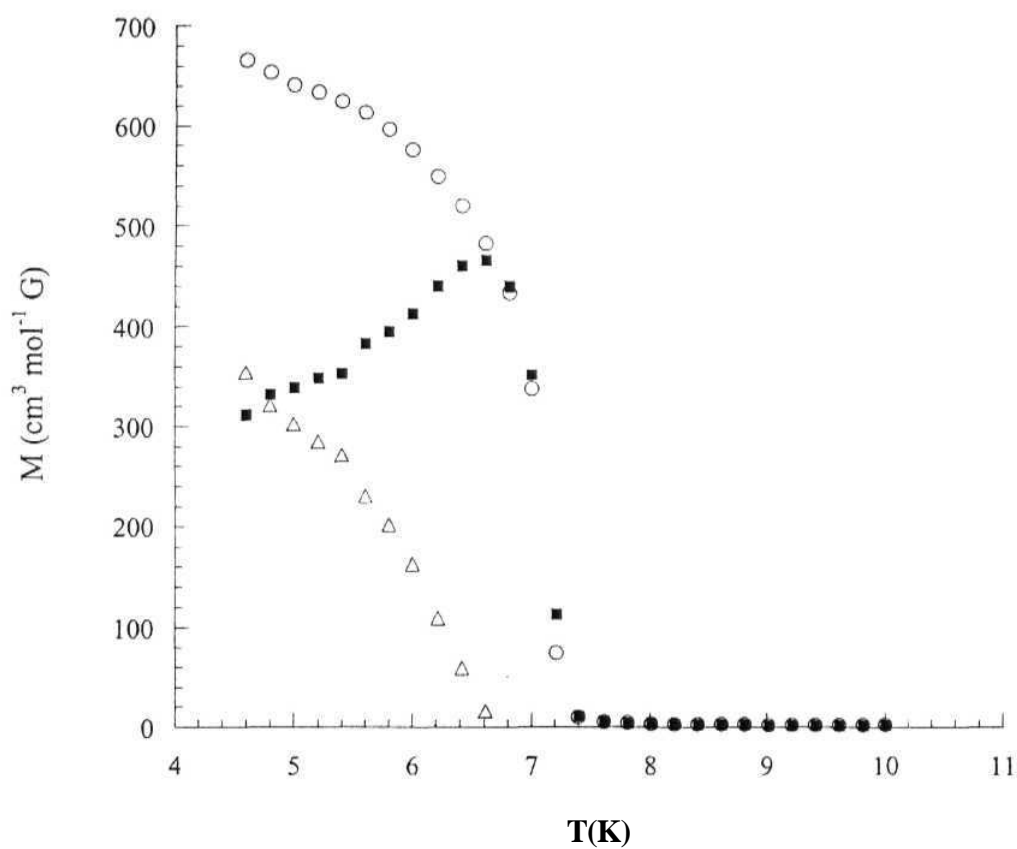
Figure **4.13** Temperature dependence of the magnetization per mole of manganese for the chain compound $[Mn(salpn)NCS]_n$ within a field of

30 G: (•) ZFC; (O) FC. The remnant magnetization was calculated as
FC - ZFC (A).

difference is indicative of the remnant magnetization which is found to vanish at T_c = 6.8 K. It has to be noted that the saturation magnetization is only a fraction of the magnetization of a high spin Mn(III) (4 (3) as expected for weak ferromagnetism.

Magnetic susceptibility of 1 was measured between 300 K and 2 K. The results are represented in Figure 4.14 as the product $\chi_M T$ as a function of T. At 300 K the product $\chi_M T$ was found to be equal to 6.01 cm^{3}mol^{-1}K corresponding to the expected value for two isolated high spin Mn(Ill). No exchange coupling is detected from these data, the drop in $\chi_M T$ below ~5 K being due to zero field splitting.
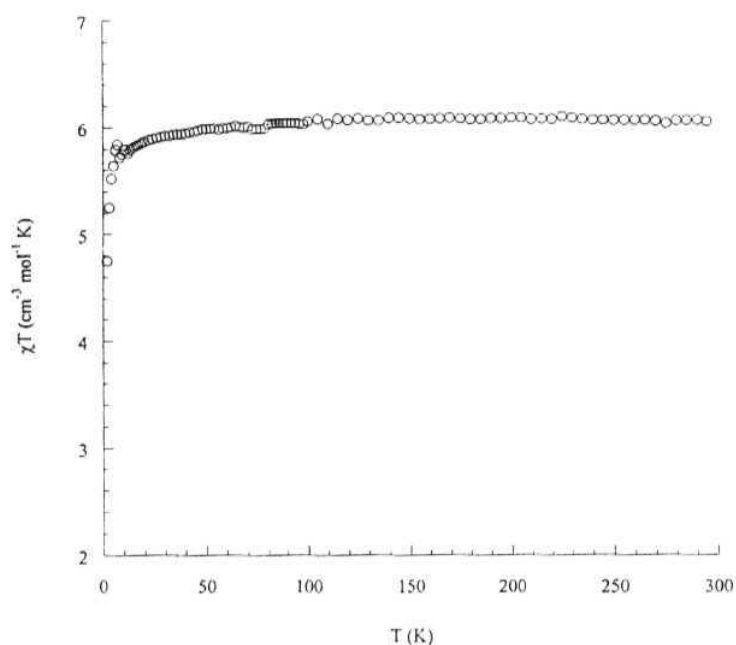
Figure 4.14 Product of the magnetic susceptibility per mole of manganese and temperature for the dimer compound [Mn(salpn)NCS]$_2$.

3 shows a room temperature magnetic moment of 6.26 BM, corresponding to high spin Fe(III). Variable temperature susceptibility studies are to be done.

4.5. Origin of the Weak Ferromagnetism of the Chain Compound: The anti ferromagnetic nature of the NCS* mediated coupling in the chain compound is quite clear from above. It is also well known that Mn(III) complexes exhibit a large anisotropy (typically D = -4 cm^{-1} for an elongation).[35]-[36] From the crystal structure it was observed that the Mn(III) ions are in an elongated environment with the Jahn-Teller (JT) elongation axis oriented towards the NCS" anion. The fourth unpaired electron is then in a d_z^2 orbital with the z-axis along the JT axis. As a consequence the axial anisotropy energy

component must be negative which means the spins will tend to orient along the JT axis.[36]

It has to be remarked that the JT axis is tilted relative to the chain axis by 23° if we take the $Mn_nMn_{n+2}S_n$ angle, and by 34° if we take $Mn_nMn_{n+2}N_n$ angle. The canting angle *i.e.,* the angle between two successive spins S, and S_2 along the chain is calculated as follows. S_1 and S_2 are assumed to be along the respective bisecting vectors. The vectors are defined as,

$$\vec{u} = 0.5(\overrightarrow{Mn_1S_1} + \overrightarrow{N_1Mn_1})$$
$$\vec{v} = 0.5(\overrightarrow{Mn_2S_2} + \overrightarrow{N_2Mn_2})$$

where, S_1, Mn_1, N_1 and S_2, Mn_2, N_2 belong to adjacent (screw related) units in Figure 4. 2.

From the X-ray structure it is determined that,

$$(\vec{u}, \vec{v}) = 55°.$$

As a consequence, the uncompensated moment per Mn can be estimated as

$$M_s = M_0 \sin[(\vec{u}, v)/2] = 4\beta \sin(55/2) = 1.84\beta.$$

This is almost 10 times larger than the saturation moment which can be estimated from measurements at 2 K (Figure 4.11). It is assumed that the low value observed is due to a combination of antiferromagnetic coupling between chains with a canting effect. This would need further studies to be ascertained.

4.6. Conclusions

Two factors related to the formation of helical chain are the flexibility of the salpn ligand which allows considerable deviation from co-planarity of the two halves of this ligand (inclination angle, 37° in the thiocyanate complex, 44° in the azide complex[12]) and the Jahn-Teller elongation along the pseudohalide bridge. In the case of the present thiocyanate complex, a third factor comes into play, *viz.,* the expected low affinity of Mn(III) for coordination with S. This factor would contribute to the relative stability of the dimer in spite of the highly unsymmetrical nature of the phenolate bridges. An important feature of the dimer is the interaction between the phenyl ring and the free S atom of the thiocyanate ion. While such interactions are present in other crystal structures as shown by the data base search, the importance of this non-covalent interaction has not yet been fully appreciated. Although the preferred crystallization of the dimer from most solvents is certainly related to the above factors, it is not clear why the polymer is the kinetically preferred product from methanol and ethanol.

The thiocyanate mediated exchange along the helical chain is weakly antiferromagnetic. However, below 7 K a magnetic ordering with weak ferromagnetic coupling sets in. A magnetic anomaly was also observed in the Mn(III) azide chain complex although a different interpretation was given.[12] It is shown that, in the present case, the weak ferromagnetism arises through large magnetic anisotropy in Mn(III) and resultant spin-canting with respect to the chain direction.

The structure and magnetic properties of the dimer are at variance with the recently observed trends in phenolate bridged Mn(III) dimers of salen type Schiff base ligands. In the salen series[20] it was observed that, (i) in $Mn_2^{III}(SB)X_2$, when X = NCS" or Cl⁻ the *trans* Mn⋯O_{bridge} is long (3.44 - 3.76 A), whereas when X = OH_2, the Mn⋯

O_{bridge} is short (2.43 - 2.66 A) and (ii) short bridges result in stronger ferromagnetic interaction (y ~ 3.0 cm^{-1}). In $Mn_2(salpn)_2(NCS)_2$, the $Mn \cdots O_{bridge}$ is short, but J ~0. There is no doubt that the $Mn \cdots O_{bridge}$ distance in the observed range is to some extent influenced by crystal packing considerations. However, the disagreement of the present dimer with the observed magneto-structural con-elation in the salen series is more difficult to explain. The net exchange parameter has contributions from several exchange pathways involving the four magnetic orbitals on each d^4 ion and these may be influenced by terminal ligands as well as bridge geometry. More phenolate bridged systems need to be studied to establish the correlations.

The formation of a monomeric complex with Fe(III) is contrary to the observations with Mn(III). As Fe(III) does not undergo Jahn-Teller distortion, salpn ligand in spite of being flexible could not stabilize a polymeric chain of Fe(III) as in the case of Mn(III). Also, the low affinity of Fe(III) towards S could not lead to a SCN" bridged dimer, thus forming only the monomeric complex. These observations are supported by the spectral studies where only one species is observed. The polymorphism seen in preliminary studies need to be investigated by finding the proper conditions for crystallization

4.7. References

(1) Vrieze, K.; van Koten, G. *Comprehensive Coordination Chemistry*; Wilkinson, G., Gillard, R. D. and McCleverty, J. A., Ed.; Pergamon Press: Oxford: England, 1987; Vol. 2, pp 225.

(2) Ribas, J.; Monfort, M.; Ghosh, B. K.; Cortes, R.; Solans, X.; Font-Bardia, M. *Inorg. Chem.* 1996, *35,* 864.

(3) Tuczek, F.; Bensch, W. *Inorg. Chem.* 1995, *34,* 1482.

(4) Escuer, A.; Vicente, R.; Goher, M. A. S.; Mautner, F. A. *Inorg. Chem.* 1995, *34,* 5707.

(5) Stults, B. R.; Marianelli, R. S.; Day, V. W. *Inorg. Chem.* 1975, *14*, 722.

(6) Ribas, J.; Monfort, M.; Diaz, C; Bastos, C; Solans, X. *Inorg. Chem.* 1994, *33,* 484.

(7) Mautner, A. F.; Goher, M. A. S. *Polyhedron* 1996, *15,* 1133.

(8) Cortes, R.; Pizarro, J. L.; Lezama, L.; Arriortua, M. I.; Rojo, T. *Inorg. Chem.* 1994, *33,* 2697.

(9) De Munno, D.; Poerio, T.; Viau, G.; Julve, M.; Lloret, F. *Angew. Chem. Int. Ed. Engl.* 1997, *36,* 1459.

(10) Wemple, M. W.; Adams, D. M.; Hagen, K. S.; Folting, K.; Hendrickson, D. N.; Christou, G. J. *Chem. Soc, Chem. Commun.* 1995, 1591.

(11) Li, H.; Zhong, Z. J.; Duan, C.-Y.; You, X.-Z.; Mak, T. C. W.; Wu, B. *Inorg. Chim. Acta.* **1998**, *271*, 99.

(12) Reddy, K. R.; Rajasekharan, M. V.; Tuchagues, J.-P. *Inorg. Chem.* 1998, *37,* 5978.

(13) Shen, H.-Y.; Liao, D.-Z.; Jiang, Z.-H.; Yan, S.-P.; Sun, B.-W.; Wang, G.-L.; Yao, X.-K.; Wang, H.-G. *Chem. Lett.* **1998,** 469.

(14) Zhang, K.-L.; Chen, W.; Xu, Y.; Wang, Z.; Zhong, Z. J.; You, X.-Z. *Polyhedron* **2001,** *20,* 2033.

(15) Gregson, A. K.; Moxon, N. T. *Jnorg. Chem.* **1982,** *21,* 586.

(16) Kennedy, B. J.; Murray, K. S. *Inorg. Chem.* **1985,** *24,* 1552.

(17) Mikuriya, M.; Yamato, Y.; Tokii, T. *Bull. Chem. Soc. Jpn.* **1992,** *65,* 1466.

(18) Kolawole, G. A. *Synth. React. Inorg. Met.-Org. Chem.* **1993,** *23,* 907.

(19) Agarwal, D. D.; Bhatnagar, R. P.; Jain, R.; Srivastava, S. *J. Chem. Soc, Perkin Trans.* 2 **1990,989.**

(20) Miyasaka, H.; Clerac, R.; Ishii, T.; Chang, H.-C.; Kitagawa, S.; Yamashita, M. *J. Chem. Soc, Dalton Trans.* **2002,** 1528.

(21) Reddy, K. R. *Research Report: C. S. 1. R. Associateship:* Hyderabad, 1996.

(22) North, A. C. T.; Phillips, D. C; Mathews, F. S. *Acta Cryst.* **1968,** *A24,* 351.

(23) Walker, N.; Stuart, D. *Acta Crystallogr.* **1983,** *A39,* 153.

(24) Sheldrick, G. M. *Ada Crystallogr.* **1990,** *A46,* 467.

(25) Sheldrick, G. M. *SHELXS97 and SHELXL 97;* University of Gottingen: Germany, 1997.

(26) Burnett, M. N.; Johnson, C. K. *ORTEP-III: Oak Ridge Thermal Ellipsoid Plot Program for Crystal Structure Illustrations*; Oak Ridge National Laboratory Report ORNL-6895: Tennessee, USA, 1996.

(27) Sayle, R. *RasMol V2.6*: Stevenage, Hertfordshire, U.K., 1995.

(28) Kraus, W.; Nolze, G. *Powder Cell for Windows version 2.3;* Federal Institute for Materials Research and Testing: Berlin, Germany, 1999.

(29) Fisher, M. E. *Am. J. Phys.* **1964,** *32,* 343.

(30) Datta, R. L.; Syamal, A. *Elements of Magnetochemistry;* S. Chand Co. Ltd.: New Delhi (India), 1982.

(31) Nakamoto, K. *Infrared and Raman Spectra of Inorganic and Coordination Compounds;* 3 ed.; John Wiley & Sons, Inc.: New York, 1977, pp 270.

(32) Ashmawy, F. M; Mc Auliffe, C. A.; Parish, R. V.; Tames, J. *Inorg. Chim. Acta.* **1985,** *103,* 133.

(33) Carlin, R. L.; Van Duyneveldt, A. J. *Magnetic Properties of Transition Metal Compounds;* Springer-Verlag, Inc.: New York, 1977; Vol. 2, pp 184.

(34) Bakalbassis, E.; Bergerat, P.; Kahn, O.; Jeannin, S.; Jeannin, Y.; Dromzee, Y.; Guillot, M. *Inorg. Chem.* **1992,** *31,* 625.

(35) Barra, A.-L.; Gatteschi, D.; Sessoli, R.; Abbati, G. L.; Cornia, A.; Fabretti, A. C; Uytterhoeven, M. G. *Angew. Chem. Int. Ed. Engl.* **1997,** *36,* 2329.

(36) Gerritsen, H. J.; Sabisky, E. S. *Phys. Rev.* **1963,** *132,* 1507.

CHAPTER V

Complexes of Silver(I) with Protonated Aminomethylpyridines

Complexes formed with cationic ligands are much less numerous than anionic or neutral ligands. Examples of structurally characterized metal complexes belong to four categories: (i) the well known tropylium cation,[1] (ii) thiamine substituted ligands,[2] (iii) the quaternary ammonium ion, $N(CH_2CH_2)_3NH^+$,[3] and (iv) the protonated phosphinoalkyl amine $(Ph_2PCH_2CH_2)_3NH^+$.[4] Protonation of the primary amine side chain of an N-heterocyclic ligand leads to another class of such ligands. The ligand aminomethylpyridine (amp) provides an example for this class of ligands, where the amino side chain can be protonated and still it can complex to metal ions through the pyridine N atom. Existence of $pmaH^+$ has been observed in the solution studies of Ag/amp systems[5] and its crystallographic characterization as $Ag(2\text{-}pmaH)_2(NO_3)_3$[6] has been recently reported from our laboratory. Complexes of these ligands are expected to have added stability due to hydrogen bonding with anions. Continuing with the above protonated system, our efforts with polymeric Ag(I) complexes of 3-amp and 4-amp have resulted in the isolation of two more protonated amp systems, whose structural details are presented in this chapter.

5.1. Experimental

5.1.1. Synthesis

(a) Preparation of Ag$_2$(3-pmaH)$_3$(OH$_2$)(ClO$_4$)$_5$ (1): Compound 1 was synthesized as follows. Polymeric Ag(3-amp)ClO$_4$[7] (0.830g, 2.63 mmol) was dissolved in 40 mL 0.1N HClO$_4$ and concentrated on a water bath until the final volume reduced to half the initial. The solution was then filtered and desiccated, which yielded white crystalline material after about 10 days. Recrystallization of the crystalline material from 10 mL 0.1N HClO$_4$ at 4 °C gave suitable single crystals for X-ray analysis. Yield: 0.485g (0.46 mmol, 52 %). Anal. Calcd. for C$_{18}$H$_{29}$N$_6$O$_{21}$Cl$_5$Ag$_2$ (MW: 1058.46) C, 20.43; H, 2.76; N, 7.94. Found, C, 23.49; H, 2.74, N, 8.21. Characteristic IR peaks (KBr/cm^{-1}): 3072(br), 1606(w), 1389(w), 1074(br), 860(s), 806(s), 708(s), 673(s), 629(s).

(b) Preparation of Ag$_2$(4-pmaH)$_4$(ClO$_4$)$_6$·2H$_2$O (2): Compound 2 was obtained as detailed. Polymeric Ag(4-amp)ClO$_4$[7] (0.500g, 1.55 mmol) was dissolved in 30 mL 0.1N HClO$_4$ and concentrated on a water bath until the final volume reduced to half the initial. The solution was then filtered and desiccated which yielded white crystalline material after about 10 days Recrystallization of the crystalline material from 10 mL 0.1N HClO$_4$ at 4 °C gave single crystals suitable for X-ray analysis. Yield: 0.410g (0.32 mmol, 82 %). Anal. Calcd. for C$_{18}$H$_{29}$N$_6$O$_{21}$Cl$_5$Ag$_2$ (MW: 1285.08) C, 22.43; H, 3.14; N, 8.72. Found, C, 21.72; H, 3.08; N, 7.87. Characteristic IR peaks (KBr/cm^{-1}): 3052(br), 1615(w), 1501(w), 1391(w), 1088(br), 774(w), 625(s).

(c) Attempted Preparation of Ag(2-pmaH)$_2$(ClO$_4$)$_3$ (3): Compound 3 was attempted to prepare following the procedure adopted for 1 and 2. When a solution of polymeric Ag(2-amp)ClO$_4$[7] in 0.1N HClO$_4$ is evaporated, white crystalline material is obtained. Repeated recrystallization of the crystalline material at 4 °C always gave

crystalline solid only. When the recrystallization is tried at RT, colorless single crystals are obtained. On the basis of C, H, N analysis and absence of silver in the crystals they are confirmed as NH_4ClO_4. Anal. Calcd. for H_4NO_4Cl (MW: 117.49) H, 3.43; N, 11.92. Found, H, 3.05; N, 10.51.

5.1.2. Physical Measurements: IR spectra were recorded on a Jasco 5300 FT/IR infrared spectrometer. C, H, N analysis was performed on a Perkin-Elmer 240C elemental analyzer. X-ray data were collected on an Enraf Nonius CAD-4 diffractometer.

5.1.3. X-ray Crystallography: X-ray data were collected for colorless crystals of 1 with dimensions 0.56 x 0.38 x 0.30 mm and of 2 with dimensions 0.44 x 0.44 x 0.32 mm on an Enraf Nonius CAD-4 diffractometer using graphite monochromated Mo-$K\alpha$ radiation. The data were corrected for Lorentz polarization effects and absorption.[8] The structures were solved by a combination of Patterson heavy atom method and direct methods (SHELXS) and refined (over F^2) by least squares techniques (SHELXL).[9] Drawings were made using ORTEP-III.[10]

1 crystallizes in the triclinic system, space group $P\bar{1}$, with 2 molecules in the unit cell. A total of 4610 reflections (4532 unique, 3740 with $F > 4\sigma F$) were collected in the θ range 1.94 to 24.93, with indices $-2 < h < 10$, $-12 < k < 13$, $-19 < l < 18$. The collected data is only 76% of the total data, as some of the data could not be collected due to instrumental problem. All the non-hydrogen atoms were refined anisotropically while the ring hydrogen atoms were included in the calculated positions using a riding model. Bond length constraints were applied to water and ammonio hydrogens. All hydrogens were assigned fixed U_{iso} values, equal to $1.2U_{eq}$ of the parent atom for ring atoms and $1.5U_{eq}$ for CH_2, NH_3^+ and H_2O hydrogen atoms. The final cycle of full matrix least squares refinement on F^2 converged with unweighted and weighted refinement factors of $R1 = 0.0388$ and $wR2 = 0.0949$ respectively. The goodness of the fit (S) is 1.032 for 4532 unique reflections and 499

parameters. The maximum and minimum residual electron density on the final fourier map corresponded to 0.700 and -0.973 e/A ^{3} respectively.

2 crystallizes in the triclinic system, space group $P\overline{1}$, with 2 molecules in the unit cell. A total of 8140 reflections (7941 unique, 5117 with $F > 4\sigma F$) were collected in the θ range 1.82 to 25.03, with indices $-4 < h < 13$, $-16 < k \leq 17$, $-17 < l < 17$. All the non-hydrogen atoms were refined anisotropically while the ring hydrogen atoms and **ammonio** hydrogen atoms were included in the calculated positions using a riding model. The U_{iso} values for ammonio hydrogen atoms were refined. Water hydrogens were located from difference maps and bond length constraints were applied. Except ammonio hydrogens, all hydrogens were assigned fixed U_{iso} values, equal to $1.2U_{eq}$ of the parent ring atoms and $1.5U_{eq}$ for CH_2 and H_2O hydrogen atoms. Ammonio group hydrogen thermal parameters were refined. The perchlorate oxygens were found to be disordered. The disorder is modeled by splitting each oxygen into two halves, which were refined isotropically by free variable (FVAR) refinement. The final cycle of full matrix least squares refinement on F^2 converged with unweighted and weighted refinement factors of $R\backslash = 0.0628$ and $wR2 = 0.1617$ respectively. The goodness of fit $(S) = 1.044$ for 7939 unique reflections and 605 parameters. The maximum and minimum residual electron density on the final fourier map corresponded to 0.780 and -0.582 e/A$^{'3}$ respectively.

Crystallographic data for 1 and 2 are presented in Table 5.1, and atomic parameters for 1 are tabulated in Table 5.2, and for 2 in Table 5.3 respectively.

Table 5.1 Crystallographic data for $Ag_2(3\text{-pmaH})_3(OH_2)(ClO_4)_5$ (1) and $Ag_2(4\text{-pmaH})_4(ClO_4)_6 \cdot 2H_2O$ (2).

	1	2
formula	$C_{18}H_{29}Ag_2Cl_5N_6O_{21}$	$C_{24}H_{40}Ag_2Cl_6N_8O_{26}$
formula weight	1058.46	1285.08
a (Å)	9.6868(7)	11.3358(7)
b (Å)	11.4840(8)	14.5436(10)
c (Å)	17.0637(13)	14.6015(17)
α (°)	102.288(6)	77.700(8)
β (°)	100.965(8)	89.519(6)
γ (°)	107.214(5)	74.421(6)
V (Å^3)	1705.2(2)	2262.5(3)
Z	2	2
Space group	$P\bar{1}$	$P\bar{1}$
T (K)	293(2)	293(2)
λ (Å)	0.71073	0.71073
ρ_{calcd} (Mg/m^3)	2.061	1.886
μ (mm^{-1})	1.634	1.316
$R1$	0.0388	0.0628
$wR2$	0.0949	0.1617

weighting scheme, **1**: $A = 0.0510$; $B = 4.3726$; **2**: $A = 0.1016$;

$B = 1.3280$ (see p. vi for definitions).

Table 5.2 Atomic parameters for Ag_2(3-pmaH)$_3$(OH$_2$)(ClO$_4$)$_5$ (1).

Atom	10^4x	10^4y	10^4z	10^3U_{eq}	Atom	10^4x	10^4y	10^4z	10^3U_{eq}
Ag1	2311(1)	4952(1)	1365(1)	57(1)	OW	-121(7)	5708(7)	6351(5)	136(3)
N1	4711(5)	5649(4)	1864(3)	40(1)	CH	-3668(2)	1612(1)	2256(1)	41(1)
C1	5479(6)	6887(5)	2253(3)	39(1)	O1	-4451(5)	1777(4)	1513(3)	57(1)
C2	6987(5)	7353(5)	2663(3)	32(1)	O2	-2177(5)	1700(5)	2231(3)	79(2)
C3	7744(6)	6512(5)	2665(3)	40(1)	O3	-4463(6)	392(4)	2329(3)	71(1)
C4	6966(6)	5246(5)	2252(3)	42(1)	O4	-3607(4)	2570(4)	2975(3)	54(1)
C5	5461(6)	4845(5)	1874(3)	41(1)	Cl2	1356(2)	8150(1)	5162(1)	49(1)
C6	7753(6)	8749(5)	3117(3)	40(1)	O5	2887(5)	8896(5)	5380(3)	73(1)
N2	8594(5)	9468(4)	2628(3)	41(1)	O6	1187(9)	6856(5)	4872(5)	130(3)
N3	-91(5)	4176(4)	849(3)	38(1)	O7	784(5)	8328(4)	5861(3)	74(1)
C7	-763(6)	2907(5)	549(3)	36(1)	O8	605(7)	8468(9)	4528(4)	140(3)
C8	-2257(5)	2329(5)	122(3)	32(1)	C13	2188(2)	7935(1)	2681(1)	39(1)
C9	-3106(6)	3098(5)	28(3)	42(1)	O9	3627(4)	8511(4)	3278(2)	52(1)
C10	-2415(7)	4397(5)	354(4)	45(1)	O10	2383(5)	7714(4)	1859(2)	55(1)
C11	-934(6)	4891(5)	754(3)	41(1)	O11	1396(5)	6757(4)	2795(3)	68(1)
C12	-2948(7)	907(5)	-206(4)	51(2)	O12	1379(5)	8791(4)	2783(3)	70(1)
N4	-2370(6)	386(4)	-899(3)	46(1)	C14	2212(2)	1999(1)	-434(1)	46(1)
Ag2	1551(1)	5163(1)	5799(1)	88(1)	O13	1114(5)	2179(4)	-1025(3)	61(1)
N5	3303(5)	4378(4)	5629(3)	43(1)	O14	3004(4)	1301(4)	-847(3)	52(1)
Cl3	3015(6)	3202(5)	5136(3)	42(1)	O15	1443(8)	1259(6)	30(4)	110(2)
C14	4085(6)	2644(5)	5110(3)	35(1)	O16	3225(7)	3187(5)	94(4)	118(3)
C15	5516(7)	3333(6)	5614(4)	48(2)	C15	1573(1)	2014(1)	2362(1)	36(1)
C16	5819(7)	4544(6)	6111(4)	55(2)	O17	1422(5)	3183(4)	2287(3)	65(1)
C17	4718(5)	5013(4)	6106(3)	46(2)	O18	3052(5)	2038(5)	2355(3)	71(1)
C18	3661(5)	1295(4)	4577(3)	50(2)	O19	501(4)	973(4)	1698(2)	53(1)
N6	4298(6)	1243(4)	3841(3)	44(1)	O20	1335(5)	1851(4)	3140(2)	59(1)

Table 5.3 Atomic parameters for $Ag_2(4\text{-}pmaH)_4(ClO_4)_6 \cdot 2H_2O$ (2).

Atom	10^4x	10^4y	10^4z	10^3U_{eq}	Atom	10^4x	10^4y	10^4z	10^3U_{eq}
Ag1	0	5000	5000	85(1)	O5B(0.30)	-5440(3)	5260(3)	3380(2)	118(10)
N1	-1868(5)	5931(4)	4932(3)	51(1)	O6A(0.70)	-4644(9)	6384(7)	2055(9)	79(3)
N2	-5952(5)	7920(4)	3451(4)	54(1)	O6B(0.30)	-4642(15)	6479(12)	2401(15)	49(5)
C1	-2098(6)	6888(5)	4779(5)	54(2)	O7A(0.70)	-5288(9)	4995(8)	2023(6)	67(3)
C2	-3247(6)	7497(5)	4629(5)	52(2)	O7B(0.30)	-5575(19)	5392(19)	1814(15)	65(6)
C3	-4253(5)	7137(4)	4639(4)	41(1)	O8A(0.70)	-3802(9)	4848(7)	3188(9)	82(3)
C4	-4002(6)	6134(5)	4860(5)	54(2)	O8B(0.30)	-3573(17)	4942(13)	2721(17)	67(6)
C5	-2846(7)	5551(5)	4995(5)	54(2)	C13	2414(2)	819(1)	3583(1)	62(1)
C6	-5534(6)	7794(6)	4425(5)	67(2)	O9A(0.65)	2700(7)	1593(6)	2968(6)	70(3)
Ag2	3817(1)	3340(1)	2858(1)	84(1)	O9B(0.35)	1389(15)	1261(12)	2779(11)	78(5)
N3	1989(5)	4269(5)	2766(4)	57(2)	O10A(0.65)	1606(10)	1171(7)	4278(7)	96(3)
N4	-2177(5)	6323(4)	1630(4)	51(1)	O10B(0.35)	3410(2)	149(16)	3227(16)	119(8)
N5	5591(5)	2322(4)	3040(4)	58(2)	O11A(0.65)	2130(12)	141(9)	3247(10)	122(4)
N6	9544(5)	-253(4)	2973(4)	52(1)	O11B(0.35)	2740(2)	1311(18)	4056(17)	126(8)
Cl	1759(6)	5237(5)	2594(5)	60(2)	O12A(0.65)	3546(13)	339(11)	4199(10)	139(5)
C8	618(6)	5853(5)	2549(5)	49(2)	O12B(0.35)	2070(2)	-32(16)	4044(16)	112(7)
C9	-380(5)	5469(4)	2685(4)	40(1)	CI4	1691(2)	8594(1)	1306(1)	55(1)
CIO	-150(6)	4466(5)	2891(5)	55(2)	O13A(0.65)	1958(10)	9045(6)	2057(7)	55(3)
CH	1018(7)	3896(5)	2913(5)	65(2)	O13B(0.35)	2360(3)	8980(17)	1824(19)	98(8)
C12	-1657(5)	6129(5)	2604(4)	51(2)	O14A(0.65)	371(10)	8758(10)	1312(10)	78(3)
C13	5707(6)	1377(6)	3386(6)	67(2)	O14B(0.35)	533(18)	8461(18)	1625(17)	75(6)
C14	6818(7)	703(5)	3619(5)	61(2)	O15A(0.65)	1989(13)	9086(9)	439(7)	81(4)
C15	7883(5)	972(5)	3490(4)	44(1)	O15B(0.35)	1440(2)	9420(17)	438(13)	81(7)
C16	7738(6)	1949(5)	3101(6)	64(2)	O16A(0.65)	2415(12)	7583(9)	1533(12)	99(4)
C17	6616(7)	2595(5)	2898(6)	72(2)	O16B(0.35)	2100(2)	7689(15)	1070(2)	91(8)
C18	9100(6)	267(6)	3747(5)	62(2)	C15	3378(2)	1020(1)	-2001(1)	60(1)
Ag3	5000	5000	0	76(1)	O17A(0.57)	2343(11)	1343(8)	-2700(10)	74(4)
N7	5531(5)	6334(4)	-334(4)	53(1)	O17B(0.43)	2172(14)	1398(11)	-2371(13)	69(5)
N8	7872(7)	8923(5)	-1006(6)	85(2)	O18A(0.57)	4351(17)	537(15)	-2508(13)	119(7)
C19	6617(7)	6359(5)	-657(4)	55(2)	O18B(0.43)	4369(17)	883(16)	-2595(13)	85(6)
C20	7009(6)	7200(5)	-859(4)	49(2)	O19A(0.57)	3304(12)	112(11)	-1447(10)	104(5)
C21	6243(6)	8057(4)	-709(4)	44(1)	O19B(0.43)	3476(18)	452(16)	-1109(16)	116(7)
C22	5100(7)	8036(5)	-383(5)	61(2)	O20A(0.57)	3497(12)	1681(9)	-1455(10)	98(5)
C23	4787(7)	7166(5)	-199(5)	62(2)	O20B(0.43)	3881(15)	1868(11)	-2026(13)	91(6)

Table 5.3 contd......

C24	6569(7)	9014(5)	-892(5)	65(2)	C16	1358(3)	6194(2)	-734(2)	97(1)
CH	1181(2)	7403(1)	4498(2)	65(1)	O21A(0.57)	198(16)	6839(12)	-1196(12)	116(6)
O1A (0.66)	1423(7)	8316(6)	4499(7)	66(2)	O21B(0.43)	600(3)	5470(2)	-540(18)	174(11)
O1B (0.34)	1549(17)	8186(14)	4023(15)	85(6)	O22A(0.57)	2212(12)	5595(9)	-1234(8)	87(4)
O2A(0.66)	151(8)	7624(6)	3788(6)	72(3)	O22B(0.43)	1630(3)	5299(16)	-944(16)	131(8)
O2B(0.34)	690(2)	6773(17)	4190(15)	111(8)	O23A(0.57)	1120(15)	6023(11)	224(11)	125(6)
O3A(0.66)	2209(9)	6831(7)	4053(7)	94(3)	O23B(0.43)	1830(2)	6254(16)	114(16)	136(8)
O3B(0.34)	2340(2)	6772(16)	5149(16)	116(8)	O24A(0.57)	2194(16)	6876(13)	-824(12)	159(7)
O4A(0.66)	955(9)	6849(8)	5284(7)	98(4)	O24B(0.43)	593(19)	6965(14)	-1439(14)	97(6)
O4B(0.34)	350(2)	7767(18)	5284(16)	120(8)	OW1	9206(5)	7545(5)	596(4)	73(2)
C12	-4857(2)	5517(1)	2608(1)	60(1)	OW2	9463(5)	1054(4)	1235(4)	75(2)
O5A(0.70)	-5775(7)	5832(7)	3268(5)	57(3)					

The site occupation factors of disordered sites are given after the respective atom labels.

5.2. Results and Discussion

5.2.1. Synthesis: The C,H,N analysis results do not correspond to the given formula for 1. Repeated analysis results always matched with a formula $Ag(3\text{-pmaH})_2(ClO_4)_3$ as opposed to the formula corresponding to 1. This might be due to the fact, that the bulk sample corresponds to the formula, $Ag(3\text{-pmaH})_2(ClO_4)_3$, while a minor fraction corresponds $Ag_2(3\text{-pmaH})_3OH_2(ClO_4)_5$, which has two protonated ligands around Ag1 and one protonated ligand and one water molecule around Ag2. The single crystal chosen for X-ray measurements probably is the one corresponding to a minor fraction of the sample.

5.2.2. Structure of $Ag_2(3\text{-pmaH})_3(OH_2)(ClO_4)_5$ (1): The asymmetric unit of 1 contains two silver centers, *viz.*, $[Ag(3\text{-pmaH})_2]^{3+}$ and $[Ag(3\text{-pmaH})(OH_2)]^{2+}$ (Figure 5.1). The coordination environment of Ag1 and Ag2 are shown in Figure 5.1 (a) and (b) respectively. Ag1 is coordinated to two protonated ligands and has a linear

geometry. Ag2 is coordinated to one protonated ligand and one water molecule. Bond lengths and angles are presented in Table 5.4. The geometry around Ag2 is bent. The

Table 5.4 Bond lengths (A) and angles (°) for $Ag_2(3\text{-pmaH})_3(OH_2)(ClO_4)_5$ (1).

Ag1-N1	2.150(4)	Ag1-N3	2.155(4)	N1-Ag1-N3	177.66(16)
Ag2-N5	2.182(4)	Ag2-OW	2.198(6)	N5-Ag2-OW	160.0(3)

geometry around Ag1 is more linear than in the previously reported Ag(2-pmaH)$_2$(NO$_3$)$_3$,[6] while the coordination geometry of Ag2 is similar to that of Ag(2-pmaH)$_2$(NO$_3$)$_3$. The bent geometry around Ag2 in 1 could be attributed to the coordination of OH$_2$ to Ag2, which is involved in hydrogen bonding with the anions, whereas, in the previous case of Ag(2-pmaH)$_2$(NO$_3$)$_3$, the bent geometry around Ag was attributed to the coordination of NO$_3^-$ oxygen to Ag. Comparing with the geometry of Ag(3-pmaH)$_2^{3+}$ in the same crystal, it is seen that coordination by OH$_2$
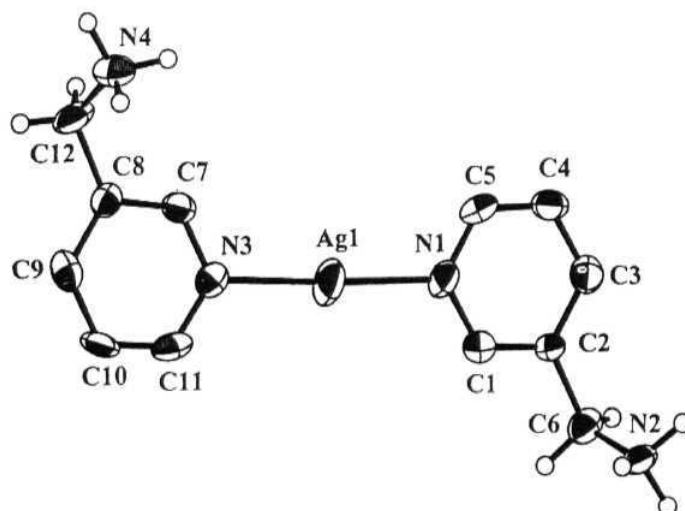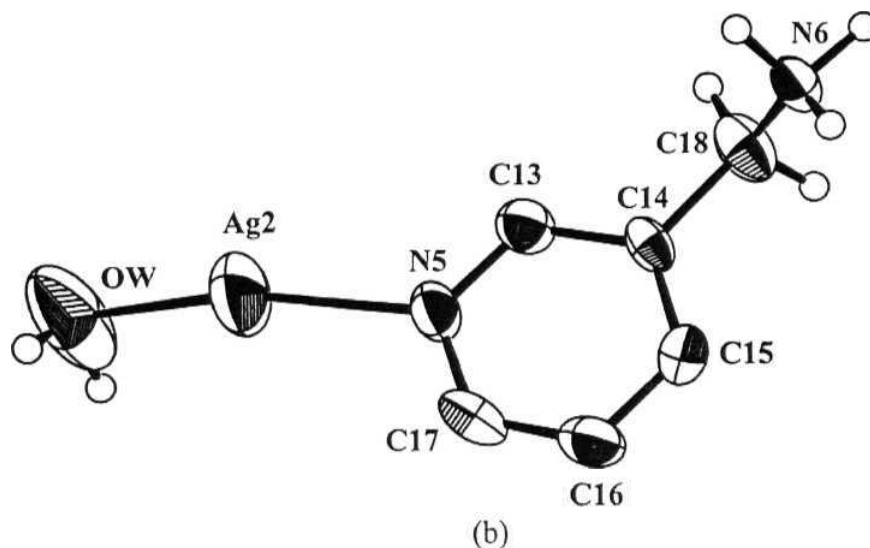

(a)

Figure 5.1 Ortep view of the cationic units in 1. (a) coordination environment of Ag1 and (b) coordination environment of Ag2 with atom labeling. Atoms are drawn as 50% probability ellipsoids. Anions and ring hydrogens are omitted for clarity.

has caused a lengthening of the *trans* Ag-N bond [Ag2-N5 = 2.182 (4) A while Ag1-N1 = 2.150 (4) A and Agl-N3 = 2.155 (4) A], Complexes where there is a direct coordination between water oxygen and silver are much less in number, compared to those with other donor atoms. In such complexes Ag is found to be with 3-coordination,[11-17] 4-coordination [18-20] or 5-coordination.[2024] Two coordinate Ag with one water ligand is found only in [Ag$_2$(dbpe)(H$_2$O)$_2$](BF$_4$)$_2$[25] in which the coordination is more linear [P-Ag-0 = 169.8 (1)°], than in 1. It has been proposed that the *trans* influence of the water ligand causes a shortening (0.06 A) of the Ag-P bond in this structure. This is in contrast to what is observed in 1, where a lengthening (0.03 A) of the Ag2-N5 bond is seen. Both linear and bifurcated 3 center hydrogen

bonds are found in 1, with $H\cdots A$ distances in the range 1.99 (3) A - 2.57 (5) A (Figure 5.2, Table 5.4).
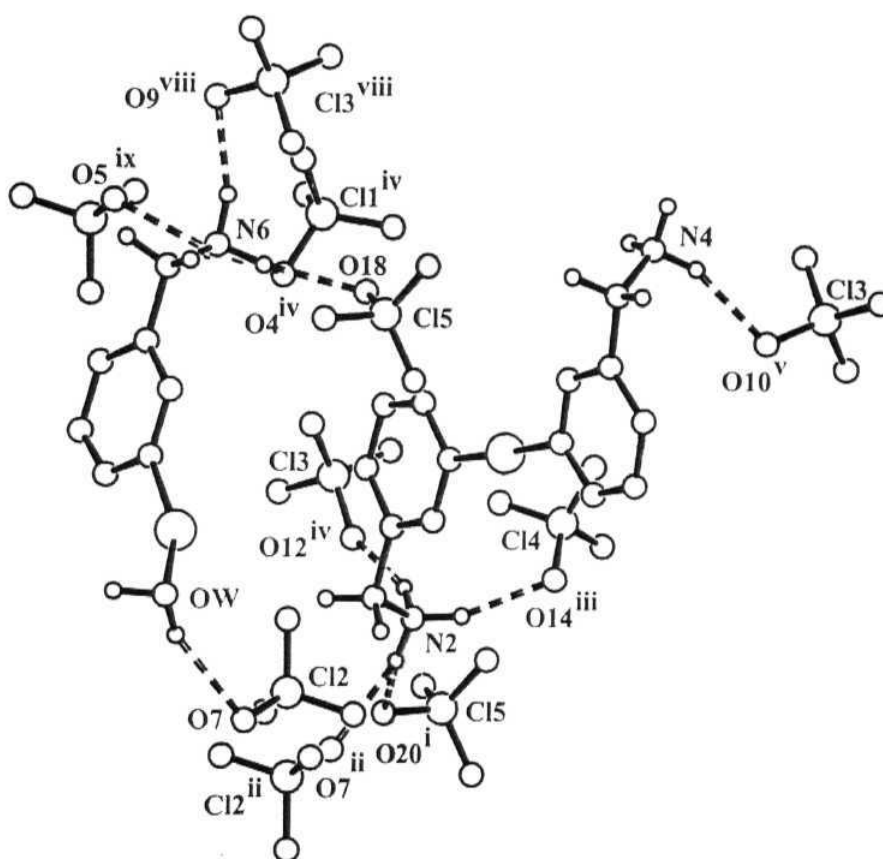
Figure 5.2 View of the hydrogen bonding (broken lines) present in 1. Only important hydrogen bonds are shown. Symmetry codes: (i) *x* + 1,*y* + 1,z;(ii) -*x* + 1, -*y* + 2, -z + 1; (iii) -*x* + 1, -*y*+ 1,-z;(iv).v + 1, *y*, z; (v) -*x*, -*y* + 1, -*z*; (viii) *x, y* - 1, z; (ix) -*x* + 1, -*y* + 1, -z + 1.

It appears from Figure 5.2 that hydrogen bonding has an influence on the coordination geometry around Ag2 in the aquo complex. Such influence of weak

interactions within the crystal lattice on the coordination geometry of Ag(I) complexes has been reported before.[26]

Table 5.4 Hydrogen bonding in $Ag_2(3\text{-pmaH})_3(OH_2)(ClO_4)_5$ (**1**).

D-H...A	d(A)	D(A)	θ(°)	D-H...A	d(A)	D(A)	G(°)
N2-HN21...O20#1	2.19(4)	3.017(6)	142(5)	N4-HN43...O15	2.53(3)	3.473(9)	166(5)
N2-HN21...O7#2	2.25(4)	3.025(6)	136(5)	N6-HN61...O9#8	1.96(3)	2.908(6)	162(5)
N2-HN22...O14#3	1.99(3)	2.945(6)	162(5)	N6-HN61...O12#8	2.57(5)	3.220(7)	123(4)
N2-HN23...O12#4	2.07(3)	3.002(6)	160(5)	N6-HN62...O4#4	2.25(5)	2.982(6)	131(5)
N2-HN23...O13#3	2.58(6)	3.090(6)	113(4)	N6-HN62...O5#9	2.26(5)	2.863(7)	119(4)
N4-HN41...O10#5	2.06(3)	2.995(6)	158(5)	N6-HN63...O18	2.06(2)	3.032(7)	169(5)
N4-HN42...O18#6	2.31(4)	3.115(7)	139(5)	N6-HN63...O20	2.52(5)	3.224(7)	129(5)
N4-HN42...O1#7	2.40(5)	3.145(7)	133(5)	0W-HW1...O7	2.28(6)	3.211(11)	156(12)
N4-HN43...O19#6	2.52(6)	3.046(6)	114(4)				

#1 $x + 1, y + 1, z$ #2 $-x+\backslash, -y + 2, -z+ 1$ #3 $-x + 1, -y +1, -z$

#4 $x + 1, y, z$ #5 $-x, -y + 1, -z$ #6 $-x, -y, -z$

#7 $-x - 1, -y, -z$ #8 $x, y- \backslash, z$ #9 $\sim x+ 1, -y 1, -z + 1$

5.2.3. Structure of $Ag_2(4\text{-pmaH})_4(ClO_4)_6 \cdot 2H_2O$ (2):

The asymmetric unit of **2** contains three silver atoms. Ag1 and Ag3 are situated on inversion centers and coordinated to two protonated ligands (Figure 5.3(a) & (c)), whereas Ag2 is coordinated to two crystallographically independent protonated ligands (Figure 5.3(b)), with a linear geometry. Bond lengths and angles are presented in Table 5.5. The geometry around Ag2 is comparable to that of Ag1 in **1**, but is more linear than in the previously reported $Ag(2\text{-pmaH})_2(NO_3)_3$.[6] There are six anions in the unit cell and all are found to be disordered. In this case, a network of hydrogen bonds are found with 3 different types of geometries, with H···A distances in the range 1.63(3) A to 2.65(8) A (Table 5.6). Besides, the normal 2-center hydrogen bond and

bifurcated 3-center hydrogen bond, a rarely observed 4-center hydrogen bond is also seen. The 4-center bond is present between HN21 and the acceptors O13A''', O11A''' and O1B'''. The solvent water molecules 0W1 and 0W2 participates in hydrogen bonding as donors as well as acceptors. It is noteworthy that the hydrogen bond network persists inspite of the positional disorder of the perchlorate O atoms.

Table 5.5 Bond lengths (A) and angles (°) for $Ag_2(4\text{-pmaH})_4(ClO_4)_6\cdot2H_2O$ (2).

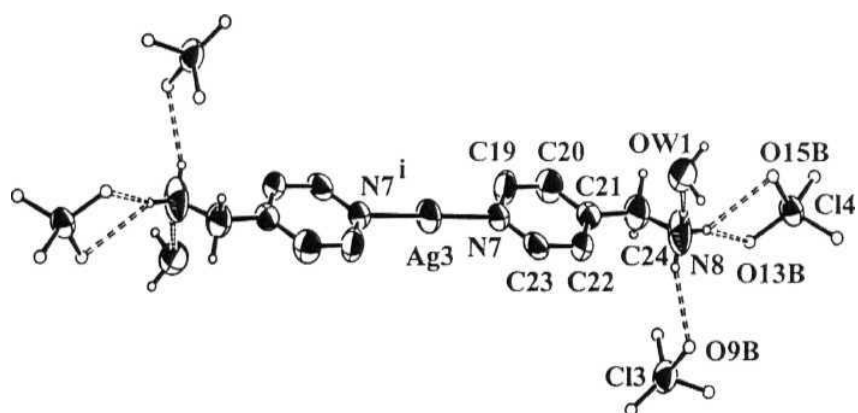| Ag1-N1#1	2.175(5)	Ag2-N3	2.136(5)	Ag3-N7#2	2.142(5)
Ag1-N1	2.175(5)	Ag2-N5	2.133(5)	Ag3-N7	2.142(5)
N1#1-Ag1-N1	180.0	N5-Ag2-N3	175.0(2)	N7-Ag3-N7#2	180.0

#1 -*x*, -*y* + 1, -z + 1   #2 -*x* + 1, ⇒• + 1, -z
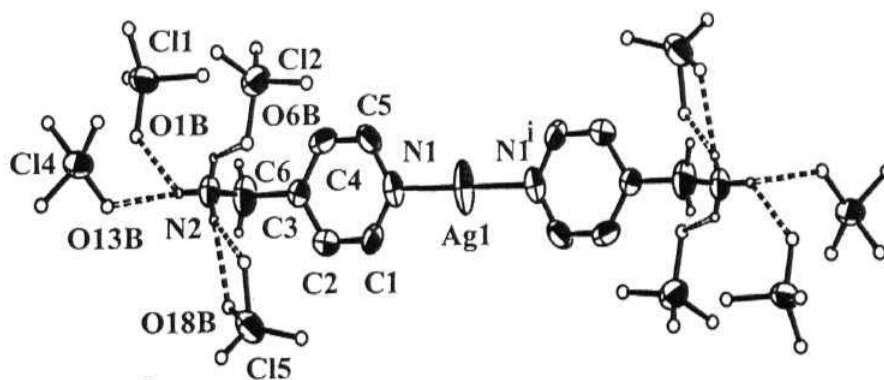
(a)
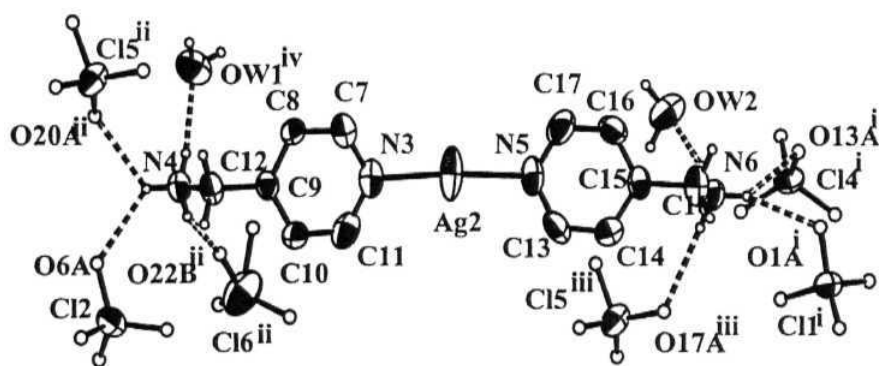
(b)

(c)

Figure 5.3 Ortep view of the molecular structures of the three different complex cations in 2 with atom labeling. Atoms are represented as 50% probability ellipsoids. Ring hydrogen atoms have been omitted for clarity. Only part of each disordered ClO_4^- ion is shown, with the disordered O atoms represented by circles. Important hydrogen bonds are shown as broken lines. Symmetry codes: in (a): (i) -x, 1 - y, z; in (b): (i) 1 - x, -1 + y, z; (ii) -x, 1 - y, -z; (iii) 1 - x, -y, -z; (iv) -1 + x, y, z; in (c): (i) -x + 1, -y + 1, -z.

Table 5.6 Hydrogen bonding in $Ag_2(4\text{-pmaH})_4(ClO_4)_6 \cdot 2H_2O$ (2).

D-H...A	d(Å)	D(A)	θ (°)	D-H...A	d(A)	D(A)	θ (°)
N2-HN21...O1B#3	2.24	2.89(2)	132	N6-HN62...OW2	1.95	2.814(8)	170
N2-HN21...O13A#3	2.32	3.002(10)	135	N6-HN63...O17A#7	2.19	3.058(13)	175
N2-HN21...O13B#3	2.38	2.93(2)	122	N6-HN63...O17B#7	2.26	3.118(16)	171
N2-HN21...O11A#4	2.62	3.328(14)	140	N8-HN81...O13B#8	2.16	2.97(2)	154
N2-HN22...O5A	2.19	3.058(11)	171	N8-HN81...O15B#8	2.25	3.00(2)	144
N2-HN22...O6B	2.32	2.93(2)	128	N8-HN81...O13A#8	2.28	3.081(11)	153
N2-HN23...O18B#5	2.10	2.92(2)	157	N8-HN81...O15A#8	2.46	3.219(14)	146
N2-HN23...O20B#5	2.35	3.16(2)	154	N8-HN82...O9B#2	1.96	2.758(18)	151
N2-HN23...O18A#5	2.53	3.33(2)	153	N8-HN82...O9A#2	2.50	3.225(12)	142
N4-HN41...O6A	2.20	2.842(11)	130	N8-HN83...OW1	2.00	2.866(9)	171
N4-HN41...O20A#5	2.23	2.844(13)	128	OW1-HW11...O23A#9	2.07(7)	2.796(17)	134(8)
N4-HN41...O20B#5	2.29	2.981(17)	137	OW1-HW11...O23B#9	2.35(6)	3.22(2)	156(8)
N4-HN41...O6B	2.34	2.973(18)	130	OW1-HW11...O21A#9	2.50(8)	3.105(18)	123(7)
N4-HN42...O22B#5	1.86	2.68(2)	155	OW1-HW12...O14A#9	2.03(7)	2.830(12)	141(7)
N4-HN42...O22A#5	2.11	2.978(14)	177	OW1-HW12...O14B#9	2.10(8)	2.87(2)	138(7)
N4-HN43...OW1#3	2.02	2.865(8)	163	OW2-HW21...O15A#2	2.58(10)	3.031(12)	111(7)
N6-HN61...O1B#6	2.10	2.91(2)	155	OW2-HW22...O24B#2	2.14(6)	2.942(19)	151(8)
N6-HN61...O1A#6	2.37	3.091(10)	140	OW2-HW22...O24A#2	2.20(7)	3.026(19)	155(8)
N6-HN61...O13A#6	2.48	3.057(13)	124	OW2-HW22...O21A#2	2.42(6)	3.178(17)	144(7)
N6-HN61...O2A#6	2.52	2.954(10)	112				

#2   -x+ 1, -y+ 1,-2   #3   x - 1, y, z   #4   x- 1, y + \,z   #5 -x, -y + \,z

#6 x + 1, y - 1, z   #7 -x + 1, -v, -z   #8   -x+ 1, -y+ 2, -z   #9   x+ 1, y, z

5.3. Conclusions

The formation of $AgHL^{2+}$ (L = 2-amp) was proposed based on solution studies.[5] Their formation from mineral acid solutions is consistent with the greater affinity of the primary amino group for H^+, and the affinity of pyridine group for Ag^+. However, the formation of this type of protonated complexes is rather delicate. The affinity of primary amino group for H^+ may lead to the formation of inorganic salts like NH_4ClO_4, as observed in case of 3. Thus it is to be understood that the crystallization conditions are very crucial factors which control the formation of complexes with such protonated ligand systems.

In both the structures, the number of potential hydrogen bond acceptor atoms is higher than the number of 'acidic' hydrogen atoms. This is also the case with $Ag(2-pmaH)_2(NO_3)_3$.[6] This leads to numerous 3-center (bifurcated - donor type) hydrogen bonds. However, the number of available acceptor atoms is limited by crystal packing constraints. In 1, 13 out of 20 ClO_4^- oxygen atoms and in 2, 9 out of 24 ClO_4^- oxygen atoms and two water oxygen atoms, are able to act as acceptors, while in $Ag(2-pmaH)_2(NO_3)_3$ only 6 out of 9 oxygen atoms are acting as acceptors. So, if the ratio of available to potential acceptor atoms is considered, in 1, (13/20) and in $Ag(2-pmaH)_2(NO_3)_3$, (6/9) it is more than 50%, while in 2, (9/24), it is less than 50%. Hence, it appears that to make best use of the hydrogen bonding interactions, the ClO_4^- oxygen atoms in 2 are disordered, which is not the case with 1 or $Ag(2-pmaH)_2(NO_3)_3$. Thus, in contrast with the usual situation, where hydrogen bonding inhibits positional disorder, all the ClO_4^- ions in 2 arc disordered. We propose that this unusual situation is a consequence of the small number of available acceptors in 2.

5.4. References

(1)   Cotton, F. A.; Wilkinson, G. *Advanced Inorganic Chemistry*; 5 ed.; John Wiley: New York, 1988, pp 1179.

(2)   Louloudi, M; Hadjiliadis, N. *Coord. Chetti. Rev.* 1994, *136*, 429.

(3)   Stucky, G. D.; Ross, F. K. *Inorg. Chem.* 1969, *8*, 2734.

(4)   Cecconi, F.; Ghilardi, C. A.; Innocenti, P.; Mealli, C; Midollini, S.; Orlandi, A. *Inorg. Chem.* **1984**, *23*, 922.

(5)   Goeminne, A. M.; Eeckhaut, Z. *J. Inorg. Nucl. Chem.* 1974, *36*, 357.

(6)   Sailaja, S.; Swarnabala, G.; Rajasekharan, M. V. *Acta Cryst.* 2001, *C57*, 1162.

(7)   Sailaja, S.; Rajasekharan, M. V. *Inorg. Chem.* 2000, *39*, 4586.

(8)   North, A. C. T.; Phillips, D. C; Mathews, F. S. *Acta Cryst.* 1968, *A24*, 351.

(9)   Sheldrick, G. M. *SHELXS-97 and SHELXL-97*; University of Gottingen: Germany, 1997.

(10)   Burnett, M. N.; Johnson, C. K. *ORTEP-III: Oak Ridge Thermal Ellipsoid Plot Program for Crystal Structure Illustrations;* Oak Ridge National Laboratory Report ORNL-6895: Tennessee, USA, 1996.

(11)   Smith, G.; Sagatys, D. S.; Campbell, C. A.; Lynch, D. E.; Kennard, C. H. L. *Aust. J. Chem.* 1990, 43, 1707.

(12)   Chen, X.-M.; Mak, T. C. W. *J. Chem. Soc, Dalton Trans.* 1991, 3253.

(13)   Smith, G.; Reddy, A. N.; Byriel, K. A.; Kennard, C. H. L. *Polyhedron* 1994, *13*, 2425.

(14) Navarro, J. A. R.; Romero, M. A.; Salas, J. M.; Faure, R.; Solans, X. *J. Chem. Soc, Dalton Trans.* 1997, 2321.

(15) Hartshorn, C. M.; Steel, P. J. *J. Chem. Soc, Dalton Trans.* **1998,** 3927.

(16) Tong, M.-L.; Zheng, S.-L.; Chen, X.-M. *Chem. Commun.* **1999,** 561.

(17) Tong, M.-L.; Zheng, S.-L.; Chen, X.-M. *Chem. - Eur. J.* **2000,** *6,* 3729.

(18) Bertelli, M.; Carlucci, L.; Ciani, G.; Proserpio, D. M.; Sironi, A. *J. Mater. Chem.* **1997,** 7, 1271.

(19) Ino, I.; Wu, L. P.; Munakata, M.; Maekawa, M.; Suenaga, Y.; Kuroda-Sowa, T.; Kitamori, Y. *Inorg. Chem.* **2000,** *39,* 2146.

(20) Ning, G. L.; Wu, L. P.; Sugimoto, K.; Munakata, M.; Kuroda-Sowa, T. *J. Chem. Soc, Dalton Trans.* 1999, 2529.

(21) Jaber, F.; Charbonnier, F.; Faure, R. *Polyhedron* **1996,** 75, 2909.

(22) Baenziger, N. C.; Fox, J. C. L.; Modak, S. L. *Acta Cryst.* **1986,** *C42*, 1505.

(23) Yamaguchi, T.; Yamazaki, F.; Ito, T. *J. Chem. Soc, Dalton Trans.* **1999,** 273.

(24) Brooks, N. R.; Blake, A. J.; Champness, N. R.; Cunningham, J. W.; Hubberstey, P.; Teat, S. J.; Wilson, C; Schroder, M. *J. Chem. Soc, Dalton Trans.* **2001,** 2530.

(25) Crabtree, S. P.; Batsanov, A. S.; Howard, J. A. K.; Kilner, M. *Polyhedron* **1998,** *1* 7,367.

(26) Swarnabala, G.; Rajasekharan, M. V. *Polyhedron* **1996,** 75, 3197.